



HAL
open science

Solutions de cellulose et matériaux hybrides/composites à base de liquides ioniques et solvants alcalins

Weiqing Liu

► **To cite this version:**

Weiqing Liu. Solutions de cellulose et matériaux hybrides/composites à base de liquides ioniques et solvants alcalins. Autre. Ecole Nationale Supérieure des Mines de Paris, 2013. Français. NNT : 2013ENMP0004 . pastel-00819908

HAL Id: pastel-00819908

<https://pastel.hal.science/pastel-00819908>

Submitted on 2 May 2013

HAL is a multi-disciplinary open access archive for the deposit and dissemination of scientific research documents, whether they are published or not. The documents may come from teaching and research institutions in France or abroad, or from public or private research centers.

L'archive ouverte pluridisciplinaire **HAL**, est destinée au dépôt et à la diffusion de documents scientifiques de niveau recherche, publiés ou non, émanant des établissements d'enseignement et de recherche français ou étrangers, des laboratoires publics ou privés.

Ecole doctorale n° 364: Sciences Fondamentales et Appliquées

Doctorat ParisTech

T H È S E

pour obtenir le grade de docteur délivré par

l'École nationale supérieure des mines de Paris

Spécialité "Sciences et Génie des Matériaux"

présentée et soutenue publiquement par

Weiqing LIU

le 18 Janvier 2013

**Cellulose solutions and hybrid/composite materials
from ionic liquid and alkaline solvents**

**Solutions de cellulose et matériaux hybrides/composites
à base de liquides ioniques et solvants alcalins**

Directeurs de thèse : **Tatiana BUDTOVA & Patrick NAVARD**

Jury

M. Jacques DESBRIERES
M. Stephen HARDING
M. Volker RIBITSCH
M. Laurent HEUX
Mme. Tatiana BUDTOVA
M. Patrick NAVARD

Professeur, IPREM, Université de Pau
Professor, Faculty of Science, University of Nottingham
Professor, Institute of Chemistry, University of Graz
Directeur de Recherche, CERMAV-CNRS
Maître de recherche, CEMEF, MINES ParisTech
Directeur de Recherche, CEMEF-CNRS

Rapporteur
Rapporteur
Examineur
Examineur
Examineur
Examineur

to my father

Acknowledgement

No doubt, such few paragraphs would never be enough to cover all the people helped me during the last three years, and would never be enough to express all my gratitude, but I'll try anyway.

Professor Patrick Navard and Dr. Tatiana Budtova, my two supervisors in CEMEF, MINES ParisTech, deserve my deepest gratitude, for their encouragement and guidance. Without their constant support and illuminating instructions, this thesis would never have reached its current form. Scientific aspects aside, they have also been very supportive during some difficult moments in my personal life, which is gratefully appreciated.

I'm also grateful to all the jury members of my thesis defense. Particularly, Professor Jacques Desbrieres from University of Pau and Professor Stephen Harding from University of Nottingham are gratefully thanked, for carefully reviewing my manuscript and providing very instructive feedbacks. My appreciation also goes to Professor Volker Ribitsch from University of Graz and Dr. Laurent Heux from CERMAV-CNRS, who agreed to serve on the committee of my thesis defense, for their valuable suggestions on my work.

Also I would like to thank the project SurFunCell, not only for the financial support enabling this research, but also for all the wonderful partners that it brought together, Uni Graz, Uni Maribor, Uni Jena, Uni Hull, TITK, Uni Utrecht, NanoMePS, Pentair, Innovia, Litija, CHT, Mondy. Among which, special thanks to team of Professor Ribitsch, including Rupert, Martin & Martin, Gerald, Victoria, Andrea, Stephen, and Tamil, for their warm welcome and generous help during my two months exchange in the University of Graz. Also much appreciation to Dr. Jens Potreck and Stefan Koel of X-Flow Pentair, for my short but quite beneficial stay in their research center, which allowed me to get a first peek into the water treatment industry.

My sincere thanks also go to all the friends and colleagues in CEMEF and the former PCP group: to Anne, Trystan, Kim, François, Thibaut, Edwige, Cyrielle, Arnauld, Georg, Lise, and Romain, for the amazing collaboration and interaction in science and in life; to Suzanne,

Gaby, Gilbert, Eric, Thierry, Francis and Roland for the technical support; to Patrick, Marie-Françoise, Françoise, Geneviève, Sylvie, and Florence for the administrative support; and to the Zhidan, Nanjiang, Ke, Zhigang, Yang, Shijia, and Yuan, for all the fun brought with the “Chinese team”.

Professor Jean-Louis Halary of ESPCI ParisTech is specially thanked. Without his suggestion and recommendation, I would have never started my thesis at CEMEF. He saw potential in me, and encouraged me to pursue further in the polymer field.

Last but not least, my gratitude goes to my mother, and Ping, the love of my life, for their constant unconditional support, and also for tolerating me.

List of abbreviations

ACC	all-cellulose composite
ALD	atomic layer deposition
AMIMBr	1-allyl-3-methylimidazolium bromide
AMIMCl	1-allyl-3-methylimidazolium chloride
BMIMAc	1-n-butyl-3-methylimidazolium acetate
BMIMCl	1-butyl-3-methylimidazolium chloride
BSDB	benzyl amine
BSE	back-scattered electron
CAB	cellulose acetate butyrate
CB	carbon black
CMC	carboxymethylcellulose
COSMO-RS	conductor-like screening model for realistic solvation
CuEn	cupri-ethylenediamine
DAPA	dimer fatty acid-based polyamides
DMAA	dimethylamylamine
DMAc	dimethylacetamide
DMF	dimethylformamide
DMIMCl	1-decyl-3-methylimidazolium chloride
DMSO	dimethylsulfoxide
DMTA	dynamic mechanical thermal analysis
DP	degree of polymerization
EDA	ethylene diamine
EMIMAc	1-ethyl-3-methylimidazolium acetate
FESEM	field emission scanning electron microscope
FTIR	Fourier transform infrared spectroscopy
HMIMCl	1-H-3-methylimidazolium chloride
HMPA	hexamethyl phosphorotriamide
HPC	hydroxypropyl cellulose
IL	ionic liquid
ISDB	iminodiacetic acid sodium salt
KSCN	potassium thiocyanate
LDPE	low density polyethylene
MFC	microfibrillated cellulose
MWCN	multi-walled carbon nanotube
NFC	nanofabricated cellulose

NMI	N-methylimidazole
NMMO	N-methylmorpholine N-oxide
NMR	nuclear magnetic resonance
PA	polyamide
PAA	poly (acrylic acid)
PAN	poly (acrylonitrile)
PCL	poly (ϵ -caprolactone)
PDADMAC	poly dimethyldiallylammonium-chloride
PEG	poly (ethylene glycol)
PFA	paraformaldehyde
PMMA	poly(methyl methacrylate)
PP	polypropylene
PVA	poly (vinyl alcohol)
PVP	poly (N-vinyl pyrrolidone)
PVPP	polyvinyl pyrrolidone
SBS	styrene butadiene styrene
SEM	scanning electron microscopy
SWCN	single-walled carbon nanotube
TBAF	tetrabutylammonium fluoride
TEAC	triethylammonium chloride
TFA	trifluoroacetic acid
TIP	titanium isopropoxide
TITK	Thüringische Institut für Textil und Kunststoff Forschung
TPS	thermoplastic starch
TTBO	titanium tetrabutyloxide
XRD	X-ray diffraction

List of symbols

$\%W$	weight loss in percentage
C	solution concentration
C^*	overlap concentration
C_0	critical concentration for gelation
C_{cell}	cellulose concentration
$C_{starch, real}$	real starch concentration in films after coagulation
$C_{starch, theo}$	theoretical starch concentration in films after coagulation
C_{ZnO}	ZnO concentration
E_a	activation energy
G'	elastic modulus
G''	viscous modulus
G_{gel}'	elastic modulus at gelation
h	gap between two plates in rheo-optical measurement
I_{ij}	current between two probes in Van der Pauw method
K	water permeability
k	rate constant for the gelation of cellulose solution with ZnO
k_H	Huggins coefficient
M_i	weight of specific component
n'	number of polymer chains involved in a junction zone
P	pressure
ρ	percolation exponent
r	radial distance of agglomerate towards the rotation axis
R	universal gas constant
$R(t)$	radius of agglomerate at time t
R_0	initial radius of agglomerate
$R_{j,mn}$	resistance calculated in Van der Pauw method
R_s	sheet resistivity
S	surface
T	temperature
T_{on}	onset temperature
t	time
t_0	gelation time of cellulose solution without ZnO
t_{gel}	gelation time
V	volume
V_i	rotation speeds of two glass plates
V_{ij}	voltage between two probes in Van der Pauw method

V_s	settling velocity of ZnO particle
We^*	dynamic Weissenberg number
W_f	final weight during the weight loss measurement
W_{ini}	initial weight during the weight loss measurement
α	fitting parameter for Carreau-Yasuda model
ε_b	elongation at breaking
η	viscosity
$[\eta]$	intrinsic viscosity
η_0	zero shear viscosity
η_{rel}	relative viscosity
η_{sol}	solution viscosity
η_{solv}	solvent viscosity
η_∞	solvent viscosity in Carreau-Yasuda model
$\eta(\dot{\gamma})$	viscosity at a certain steady shear rate
ρ	resistivity (specific resistance)
ρ_f	density of solution at room temperature
ρ_p	density of ZnO particle
σ	shear stress
σ_b	tensile strength
Φ_i	weight fractions of each component
λ	relaxation time
$\dot{\gamma}$	shear rate
$\dot{\gamma}_c$	critical shear rate for carbon black dispersion

Table of Contents

INTRODUCTION	3
CHAPTER I	13
State of the art: properties of cellulose solutions and cellulose-based hybrid materials	
CHAPTER II	71
Materials and Methods	
CHAPTER III	93
Stabilization of cellulose-NaOH-water solutions with ZnO as additive	
CHAPTER IV	117
From dissolution of unmodified waxy starch (amylopectin) in ionic liquid to homogenous starch-cellulose films with tuned morphology	
CHAPTER V	157
Dispersion of carbon black in cellulose solutions & preparation of conductive cellulose films	
CONCLUSIONS & PERSPECTIVES	191
ANNEX	197

Introduction

Background and objective of the thesis

Cellulose, as the most common organic compounds on Earth, and also the most abundant polysaccharide, is definitely an important natural resource. With the initiatives of replacing (partially) the conventional petrochemical polymers by bio-based polymers, cellulose has regained the researchers' interests in the last few decades, not only because it is renewable and biodegradable, but also due to interesting properties such as biocompatibility and chemical stability. Additionally, cellulose properties can be further enhanced by chemical/physical modification or making composites with functional fillers.

SurFunCell project supported by the European Commission was established in this context. By combining the interdisciplinary expertise of partners from both academic and industrial fields, SurFunCell was aimed at creating innovative, surface-nanostructured, cellulose-based composites with good surface functionality, improved strength, abrasion, thermal and chemical stability, hydrophilicity/hydrophobicity, as well as antimicrobial activity, UV resistance, conductivity, and barrier properties.

As one of the academic partners, the role and objective of CEMEF-ARMINES in SurFunCell project was to investigate several fundamental scientific aspects as cellulose dissolution, making cellulose-based materials from solutions, and test of new concepts as surface modification or coating at laboratory scale. We studied and will present in this manuscript the characterization and properties of both cellulose solutions in different solvents (aqueous sodium hydroxide and ionic liquid) and two types of cellulose-based hybrid materials (one with starch and the other with carbon black), which were all prepared from dissolved cellulose.

Outline of the thesis

This manuscript is divided into six chapters. Chapter I is a review of the recent research progress in the scope of this study. We start by describing the various available solvents of cellulose and the different forms of cellulose-based materials obtained from cellulose solutions. The blends and composites of cellulose with polymers (natural or synthetic) and inorganic fillers are reviewed. The emphasis in the last part is on composites of cellulose - carbon black with a description of the dispersion mechanisms of carbon black agglomerates and the preparation of conductive materials.

Chapter II is the description of the materials used in this thesis, as well as the experimental methods to both prepare and characterize the cellulose solutions and films. The rheo-optical technique used to study the dispersion process of carbon black is also described in this chapter.

Chapter III describes the role of zinc oxide (ZnO) as a stabilizer for the cellulose-NaOH-water solutions. We examined and established the correlations between the gelation time of the solutions and several parameters like cellulose concentration, ZnO concentration and temperature. The mechanism of ZnO stabilization was explained as the result of the “free-water-binder” role of ZnO. With less than 1 wt% ZnO added, the gelation of cellulose-NaOH-water solutions was delayed significantly at room temperature.

In Chapter IV, cellulose is blended with starch via the “dissolution-mixing-coagulation” route to make porous films. The dissolution of starch in common solvent (an ionic liquid) was first studied. The porous morphology of the blended films is due to the lack of interaction between cellulose and starch, and this can be tuned by varying the composition and the nature of the coagulation bath. Other properties as permeability of the obtained films were also characterized.

Chapter V is the study of a similar “dissolution-dispersion-coagulation” approach taken when we prepared cellulose-carbon black composite films. To control better the processing of carbon black-filled cellulose materials, we first investigated the mechanisms of carbon black

dispersion and measured the critical shear stresses to induce dispersion. It was found that the elasticity of cellulose solutions matrix played an important role in the dispersion process. Carbon black filled cellulose films were prepared and their electric conductivity was measured. A carbon black percolation threshold above which the material becomes conductive was identified. We proposed two methods to reduce the percolation threshold based on the assembly of two types of cellulose solutions.

Finally we summarize the major conclusions for each chapter, and propose several prospective in the last part of this manuscript.

Introduction

Contexte et objectif de l'étude

La cellulose, composé organique le plus courant et polysaccharide le plus abondant sur Terre, est une ressource naturelle très importante. Les initiatives pour remplacer totalement ou partiellement les polymères pétrochimiques conventionnels avec des bio-polymères à base de cellulose ont donc attiré l'intérêt des chercheurs ces dernières décennies, non seulement parce que la cellulose est renouvelable et biodégradable, mais aussi en raison de ses propriétés intéressantes telles que la biocompatibilité et la stabilité chimique. De plus, les propriétés de cellulose peuvent être encore améliorées par des procédés chimiques, des modifications physiques ou en préparant des composites avec des charges fonctionnelles.

Le projet SurFunCell soutenu par la Commission Européenne a été créé dans ce contexte. En combinant l'expertise interdisciplinaire de partenaires académiques et industriels, SurFunCell visait à créer des composites à base de cellulose ayant de nouvelles fonctionnalités de surface capable d'apporter une meilleure résistance à l'abrasion, une meilleure stabilité thermique et chimique, des propriétés hydrophile/hydrophobe, des propriétés antimicrobiennes, une résistance aux UV, une conductivité électrique ou des propriétés barrière.

Dans ce projet, le rôle et l'objectif du laboratoire était d'étudier plusieurs aspects fondamentaux comme la dissolution de la cellulose afin de produire des matériaux et le test de nouveaux concepts autour de la modification de surface ou des revêtements, à l'échelle du laboratoire. Nous présentons dans ce manuscrit nos travaux concernant la caractérisation de solutions de cellulose dans deux solvants différents (hydroxyde de sodium aqueux et un liquide ionique) et la préparation de deux nouveaux types de matériaux à base de cellulose (un matériau hybride cellulose-amidon et un composite cellulose-noir de carbone), qui sont tous les deux préparés à partir de ces solutions de cellulose.

Résumé du manuscrit

Ce manuscrit est divisé en six chapitres. Le chapitre I est un résumé de l'état de l'art sur les recherches récentes dans le cadre de cette étude. Nous commençons par décrire les solvants de la cellulose qui sont disponibles et les différents matériaux à base de cellulose obtenus à partir de telles solutions de cellulose. Les mélanges et les composites de cellulose avec des polymères (naturels ou synthétiques) et des charges inorganiques sont également examinés. La dernière partie de ce chapitre concerne les composites de cellulose avec du noir de carbone. Elle comprend la description des mécanismes de dispersion d'agglomérats de noir de carbone dans des polymères et des modes de préparation de matériaux conducteurs.

Le chapitre II concerne la description des matériaux utilisés dans cette étude, ainsi que les méthodes expérimentales mises en œuvre pour préparer et caractériser les solutions de cellulose et de films. La technique de rhéo-optique utilisée pour étudier la dispersion du noir de carbone est également décrite dans ce chapitre.

Le chapitre III décrit le rôle de l'oxyde de zinc (ZnO) en tant que stabilisant des solutions de cellulose dans les mélanges NaOH et eau. Nous avons examiné et établi les corrélations entre le temps de gélification des solutions et les paramètres tels que la concentration de cellulose, la concentration de ZnO et la température. Le mécanisme de stabilisation de ZnO a été expliqué comme le résultat du rôle liant de ZnO avec l'eau libre présente dans la solution. Avec moins de 1 % en masse de ZnO ajouté, la gélification des solutions cellulose-NaOH-eau est retardée de façon significative à la température ambiante.

Dans le chapitre IV, nous décrivons nos résultats concernant les mélanges de la cellulose avec l'amidon par l'intermédiaire d'une voie "dissolution-mélange-coagulation" afin de préparer des films poreux. La dissolution de l'amidon dans un solvant de la cellulose (un liquide ionique) a été étudiée préalablement à l'étude des mélanges ternaires amidon-cellulose-liquide ionique et de leur régénération sous forme de films. La morphologie poreuse de ces films est due à l'absence d'interaction entre la cellulose et l'amidon, et elle peut être ajustée par le contrôle de la composition et de la nature du bain de coagulation. Nous avons d'autre part caractérisé la perméabilité des films obtenus.

Le chapitre V est une étude effectuée en utilisant une approche "dissolution-dispersion-coagulation" semblable à celle du chapitre précédent, cette fois appliquée à la préparation de films de cellulose chargés en noir de carbone. Nous avons tout d'abord étudié les mécanismes de dispersion du noir de carbone dans les solutions de cellulose et mesuré les contraintes de cisaillement critiques pour initier la dispersion. Nous avons trouvé que l'élasticité de la matrice (solution de cellulose) joue un rôle important dans le processus de dispersion et nous avons expliqué ce phénomène. Des films de cellulose chargés en noir de carbone ont été préparés et leur conductivité électrique a été mesurée. Un seuil de percolation du noir de carbone au-dessus duquel le matériau devient conducteur a été identifié. Nous avons proposé deux méthodes afin de réduire le seuil de percolation basées sur l'assemblage de deux types de solutions de cellulose.

Le dernier chapitre est une conclusion où nous résumons nos résultats principaux et décrivons les perspectives qui en découlent.

Chapter I

State of the art:

Properties of cellulose solutions and cellulose-based hybrid materials

I. Literature review	14
I.1 Dissolution of cellulose	14
I.2 Materials formed from cellulose solutions	24
I.3 Cellulose-based hybrid materials	30
I.4 Dispersion of carbon black and conductive films	44
Reference	52

I. Literature review

The literature review in this chapter consists of four parts: in the first part, we focus on the topic of cellulose solutions, and look into the characteristics and development of different cellulose solvents, and the dissolution processes of cellulose in them. The dissolution of cellulose is not only an essential step of making cellulose materials through coagulation., but it also provides the possibility of further developments as for example surface modification. Then cellulose materials of different forms and the blends of cellulose with other materials are reviewed in the following two parts of this chapter, to shed light on making blends with cellulose solutions. Finally, we describe the dispersion of carbon black in a fluid matrix and on the formation of carbon black based conductive materials, as a background to prepare conductive cellulose films by dispersing carbon black agglomerates in cellulose solutions.

I.1 Dissolution of cellulose

It has been usually stated that cellulose is difficult to dissolve, and the available solvents for cellulose are rather limited. This is certainly true considering the very large entropy of mixing decrease due to the dissolution, compared to small molecules, as for other long chain polymers. The difficulty of cellulose dissolution is also caused by its rigidity and by its complex structure in the native cellular arrangements and sometimes by the presence of other compounds that are interacting with cellulose, including hemicellulose, lignin, etc., since cellulose is “naturally synthesized”. However, the solvents for cellulose are not fewer than the ones for common polymers as polyethylene or polypropylene. A more critical problem is that they are just not the common organic solvents being used for most other polymers.

Nevertheless, researchers have been looking for cellulose solvents intensively for decades, motivated by the need of processing it: since cellulose can not melt, dissolution becomes one major option for processing cellulose directly into fibers, films, membranes or other relatively small objects like sponges, and also for carrying out chemical derivatisation. Thus many articles have been devoted to review this topic (see, for example, [Liebert 2009]). In our work, we will only focus on three widely studied cellulose solvents: aqueous NaOH, ionic liquid and *N*-methylmorpholine *N*-oxide (NMMO) monohydrate. Aqueous NaOH is easy-to-handle

and has a low cost, ionic liquids have been demonstrated to be solvents for cellulose with high dissolving power and NMMO monohydrate is only solvent of the three that is currently used in industrial production.

Considering that cellulose solutions is the main topic in our study, we will not discuss the processing of cellulose via derivatisation, as, for example, in the viscose process; nor will we cover complexing agents of cellulose as cuoxen ($[\text{Cu}(\text{NH}_2(\text{CH}_2)_2\text{NH}_2)_2[\text{HO}]_2$) or cadoxen ($[\text{Cd}(\text{NH}_2(\text{CH}_2)_2\text{NH}_2)_2[\text{HO}]_2$), despite their application in the measurement of cellulose molar mass via intrinsic viscosity [ASTM D1795; ASTM D4243], or the cuprammonium process still used at small scale for making textile fibres.

I.1.1 Cellulose solvent: NaOH-water

NaOH-water mixtures as a cellulose solvent is a very attractive option, as the dissolution method is potentially cheap, non-polluting, and using very common chemicals that can be easily handled and recycled. The history of using NaOH-water in the processing of cellulose dates back to more than one hundred years ago, when NaOH-water was used in the viscose process to dissolve cellulose xanthate and in the mercerization process to treat cotton fabrics for improving their smoothness, dye intake, mechanical properties and dimension stability. It is important to note that mercerization is not a process of dissolution, but of swelling with complex changes in the morphology and crystalline structure of cellulose.

To our knowledge, Davidson was the first to report the dissolution of microcrystalline cellulose (hydrolyzed with strong acid) in NaOH-water, although Sobue et al. are often the ones credited and cited for this discovery. Davidson dissolved a relatively large amount of cellulose (up to 80% of the total cellulose amount due to the small molar mass of his hydrolyzed cellulose) in 10% NaOH-water at -5°C , and claimed that the solubility increases with shorter chains [Davidson 1934; Davidson 1936]. Sobue et al. built the whole cellulose-NaOH-water ternary phase diagram, and reported that cellulose can only be dissolved in a narrow range of NaOH concentrations (7% to 10%) and at rather low temperatures (-5°C to 1°C), as shown in Figure I-1 [Sobue 1939].

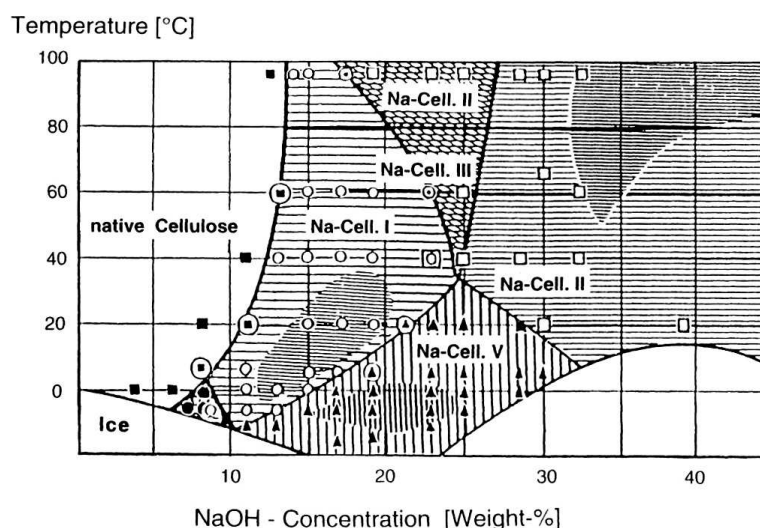


Figure I-1 Phase diagram of the cellulose/NaOH/water system, with natural ramie fibers. [Sobue 1939]

In the mid-1980s, the dissolution of cellulose in NaOH-water regained the attention of researchers. Scientists from Asahi Chemical extensively investigated the dissolution mechanism, aiming at the industrial production of cellulose fibers and films [Kamide 1984; Kamide 1987a; Kamide 1987b; Yamashiki 1988; Yamashiki 1990a; Yamashiki 1990b; Yamashiki 1990c; Yamashiki 1992; Yamada 1992; Kamide 1992; Matsui 1995; Yamane 1996a; Yamane 1996b; Yamane 1996c; Yamane 1996d]. Kamide et al. dissolved both regenerated cellulose and ball-milled amorphous cellulose in NaOH-water, and obtained rather stable solutions [Kamide 1984]. They found that the solubility «cannot be explained by only the concepts of “crystal-amorphous” or “accessible-inaccessible”» of cellulose molecules, and that the intramolecular hydrogen bonds ($O_3-H \dots O_5'$, see Figure I-2) among cellulose molecules need to be weakened to achieve a good dissolution. The lack of correlation between the solubility and non-crystalline phase was confirmed later [Kamide 1992], and the interactions between NaOH and cellulose was modelled [Yamashiki 1988], showing that the alkali structure controls the solubility of cellulose. They found, in the range of 0 to 15% NaOH-water, a maximum of 11 water molecules solvated to one NaOH molecule at very low NaOH concentration, and the number of water molecules solvated to one NaOH is reduced to 8 at a concentration of NaOH of 15%. Based on these findings, a steam-explosion treatment was used by Asahi chemists to obtain a very high solubility of pulps due to the weakened intramolecular bondings by this treatment [Yamashiki 1990a; Yamashiki 1990b]. Isogai and Atalla [Isogai 1998] succeeded in dissolving cellulose of different origins

(microcrystalline cellulose, cotton linter, bleached and unbleached kraft pulp of softwood, groundwood pulp) and with different treatments (mercerized, regenerated) in NaOH-water. The optimal procedure they proposed is freezing the cellulose solution in 8.5% NaOH at -20°C , and then thawing at room temperature while diluting with water to reach a final NaOH concentration of 5%. Stable microcrystalline cellulose solutions at room temperature and partially dissolved solutions from other samples were obtained. The authors considered the molar mass to be the key factor determining the solubility, and explained with the concept of the “coherent domains” of cellulose chains.

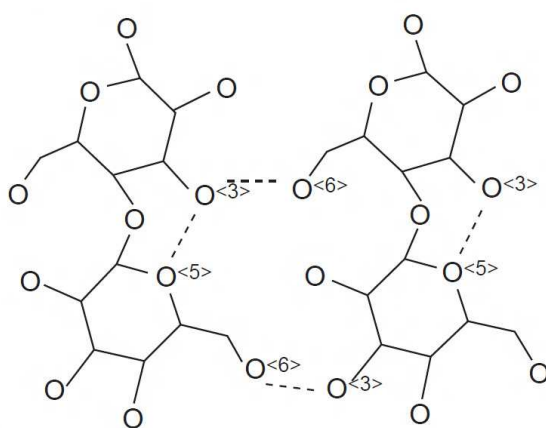


Figure I-2 Illustrated inter- and intramolecular bondings of cellulose. Reprinted with permission from [O’Sullivan 1997]. Copyright (1997) Springer.

In spite of the above successes at laboratory scale, the major drawbacks that prevent the NaOH-water dissolution process from reaching the industrial stage are: 1) the maximum concentration of cellulose dissolved is relatively low (less than 10%) [Egal 2007], and 2) the instability of cellulose-NaOH-water solution due to the gelation occurring with time and temperature increase [Roy 2003]. An additional problem is that dissolution requires rather low temperatures, from $-6/-5^{\circ}\text{C}$ to maximum 0°C . As a result, researchers have been looking for compounds to improve solubility and stabilize the cellulose-NaOH-water solution.

In fact, additives as urea, thiourea or zinc oxide have been known to improve mercerization or to help the viscose process almost from the beginning [Harrison 1928; Davidson 1937], and naturally their impacts on dissolution have also been checked. Laszkiewicz et al. found that adding thiourea improves the solubility of cellulose III in NaOH-water [Laszkiewicz 1993],

and adding 1% urea also dissolved bacterial cellulose of DP=650 [Laszkiewicz 1998]. L. Zhang's group has been looking at the dissolution of cellulose in NaOH-water with urea and thiourea, and stabilized 4%-8% cellulose solutions for preparing fibres and membranes [Zhou 2000; Zhang 2002b; Zhou 2002a; Zhou 2002b; Zhou 2004; Weng 2004; Cai 2005; Cai 2006; Cai 2007a; Cai 2007b; Cai 2008]. Urea and thiourea have been demonstrated to enhance both the solubility and the stability. They explained the function of urea as that the hydrogen bondings of cellulose (both intermolecular and intramolecular) are "disrupted" by such solvents, and the cellulose molecules are thus prevented by this "overcoat" from aggregation, as illustrated in Figure I-3 [Cai 2005]. Follow-up studies suggest that cellulose molecules in solution are both in isolated state and as aggregates, and the isolated ones tend to aggregate with higher temperature above -12°C [Cai 2008; Lu 2011a; Lue 2011]. The urea hydrates do not interact directly with cellulose [Cai 2008], but form a complex together with NaOH hydrates bonding to cellulose molecules, which provide the synergy of the anti-aggregation "overcoat" effect. This complex is also more stable at lower temperature. On the other hand, [Egal 2008] showed that NaOH and urea are not interacting. Using thiourea together with urea has been shown to further improve the dissolution based on a similar mechanism (Jin 2007; Zhang 2011; Kihlman 2011).

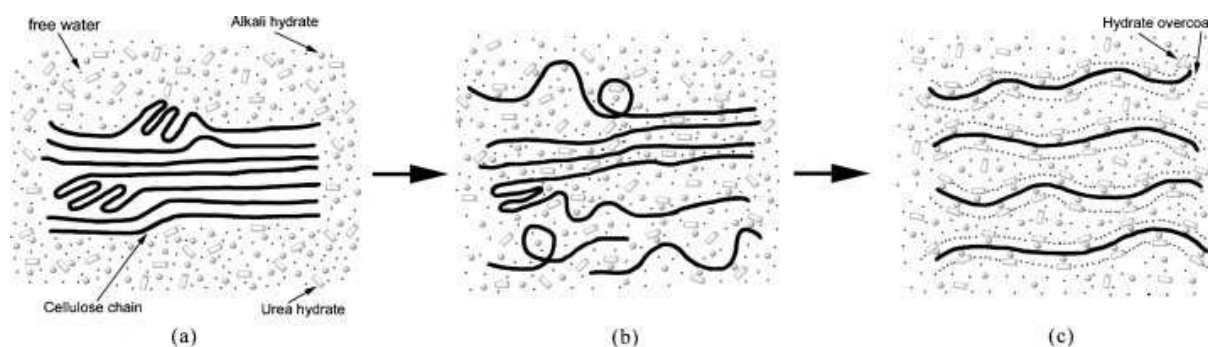


Figure I-3 The dissolution process of cellulose in LiOH/urea and NaOH/urea aqueous solutions illustrated by Cai et al.: (a) cellulose bundle in the solvent, (b) swollen cellulose in the solution, (c) transparent cellulose solution with overcoat of hydrates. Reprinted with permission from [Cai 2005]. Copyright (2005) Wiley.

Polish researchers used ZnO to facilitate the dissolution of enzymatically activated cellulose in NaOH-water with a typical formulation of 6% cellulose, 7.8% NaOH, and 0.84% ZnO [Vehvilainen 2008]. L. Zhang group also reported that the maximal cellulose dissolution is reached at 0.5% ZnO in the mixture of 7%NaOH-12%urea [Yang 2011a]. The reason for the

improved solubility was explained by the stronger hydrogen bonds between cellulose and Zn(OH)_4^{2-} as compared to hydrated NaOH. Despite the above more or less empirical studies, the function and the role of the additive, urea, thiourea and ZnO in cellulose-NaOH-water is still not well understood. As it will be shown in Chapter III, we intend to make a comprehensive investigation of the impact of ZnO on cellulose-NaOH-water dissolution and especially on its gelation-delaying effect, with the objective to prepare stabilized cellulose solutions at room temperature for either forming materials or cellulose matrix surface modification.

I.1.2 Cellulose solvent: NMMO

Of all the direct solvents of cellulose, *N*-methylmorpholine *N*-oxide (NMMO) monohydrate is the only one being currently used for the industrial production of cellulose fibers, called the Lyocell process (Lenzing, Austria) and Alceru process (Smartfiber, Germany). NMMO, when mixed with water in a certain proportion (forming a monohydrate), was patented as cellulose solvent in the late 1960s [Johnson 1969; Franks 1979; McCorsley 1979]. It is found that as in NaOH-water, cellulose can only be dissolved in a rather narrow range of temperatures and NMMO-water compositions (see Figure I-4). When water concentration is below 10%, the very high melting temperature of the solvent results in the degradation of cellulose and instability of the solution [Rosenau 2001]; whereas the mixture will no longer be cellulose solvent when the water concentration is above 25% [Cuissinat 2006]. Thus NMMO-mono-hydrate (water concentration ~ 13.3%) is used in the above mentioned industrial process.

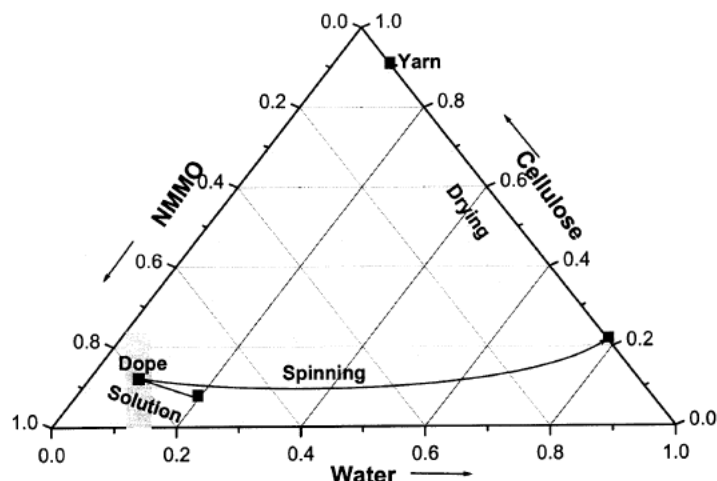


Figure I-4 Phase diagram of the ternary system NMMO/water/cellulose. Reprinted with permission from [Rosenau 2005]. Copyright (2001) Elsevier.

The major concern of NMMO-water as cellulose solvent is the thermostability of the solution. The chemical reactions accompanied with dissolution could lead to the drop of cellulose degree of polymerization, as well as NMMO degradation, and eventually reduce the recovery rate of the solvent and the properties of the fiber products [Taeger 1985; Rosenau 2001]. To evaluate the thermal activity, cellulose-NMMO can be studied with rheological, calorimetric, chromatographic and spectroscopic techniques. The onset temperature (T_{on}) of degradation is a very common indicator, obtained by plotting the deviation of pressure over time (dp/dt) vs. temperature [Rosenau 2001].

Along with some common polymer processing stabilizers, NaOH/propyl gallate system is a quite effective choice for stabilizing unmodified cellulose-NMMO solutions, by suppressing the radical formation of NMMO and thus the drop of molar mass of cellulose [Buijtenhuijs 1986]. But when the solutions are modified with additives like reactive charcoal or ion-exchange resins, new stabilizing systems become necessary, such as the one developed by Wendler et al. with iminodiacetic acid sodium salt (ISDB) and benzyl amine (BSDB) covalently bound to a styrene/divinyl benzene copolymers [Wendler 2006].

Besides the thermal stability, other parameters can also influence the quality and processing of cellulose-NMMO solutions, such as the amount of undissolved particles and the molecular weight distribution of dissolved cellulose. As a result, factors such as the origin and

pre-treatment of the cellulose, the shear flow in the mixing device, and dissolution time/temperature ratio should also be taken into consideration.

I.1.3 Ionic liquids

The major motivation driving researchers to study ionic liquids (ILs) as cellulose solvents is probably the disadvantages of other solvents (for example, other solvents could be volatile, toxic, thermally unstable, not cost-efficient, or with limited solubility). By comparison, ionic liquids look promising with tuneable properties via the choice of the cation and anion groups. They are not only efficient solvents of cellulose, but they also act as a medium for carrying out chemical modifications of cellulose. The toxicity of ionic liquids remains an open question and depends on the ion composition.

Since quaternary ammonium salts were reported to dissolve cellulose [Graenacher 1934], ILs, especially imidazolium-based ILs such as 1-butyl-3-methylimidazolium chloride (BMIMCl), 1-ethyl-3-methylimidazolium acetate (EMIMAc) and 1-allyl-3-methylimidazolium chloride (AMIMCl), as shown in Figure I-5, have been demonstrated to be powerful solvents, capable of dissolving high molecular weight cellulose to a rather high concentration (up to 20% depending on types of IL) without any pre-treatment [Swatloski 2002; Zhang 2005a; Kosan 2008].

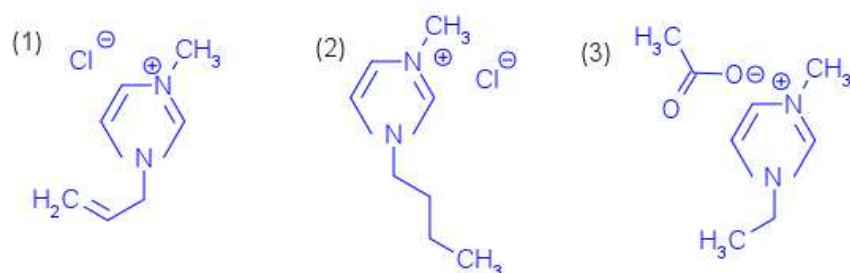


Figure I-5 Molecular structure of three ILs: 1) AMIMCl, 2) BMIMCl, and 3) EMIMAc.

Besides using ILs as reaction media to carry out homogeneous chemical modifications on cellulose, and to synthesize cellulose derivatives such as cellulose sulfates, cellulose acetates, cellulose laureates, and cellulose furoates [El Seoud 2007; Gerike 2009a, Barthel 2006,

Kohler 2007], the research on ionic liquids as cellulose solvents can be grouped into 1) the understanding and characterization of cellulose-ILs solutions, the selection of co-solvents; 2) the preparation of new cellulose materials or blends by dissolution.

Zhang et al. investigated cellulose-IL solutions by NMR and attributed the hydrogen bondings between the anhydroglucose hydroxyl groups and both the $[\text{EMIM}]^+$ and $[\text{Ac}]^-$ ions as the reason for dissolution [Zhang 2010]. Kahlen et al. screened over 2000 kinds of ILs (combining 70 cations with 30 anions) with COSMO-RS approach (Conductor-like Screening Model for Realistic Solvation) and compared their dissolving power, showing that the dissolving power is mainly determined by anions [Kahlen 2010]. In another article, molecular dynamic simulations predicted that 1-n-butyl-3-methylimidazolium acetate (BMIMAc) should be the best solvent since it has the highest capability of breaking cellulose inter- and intra-molecular hydrogen bondings [Gupta 2011].

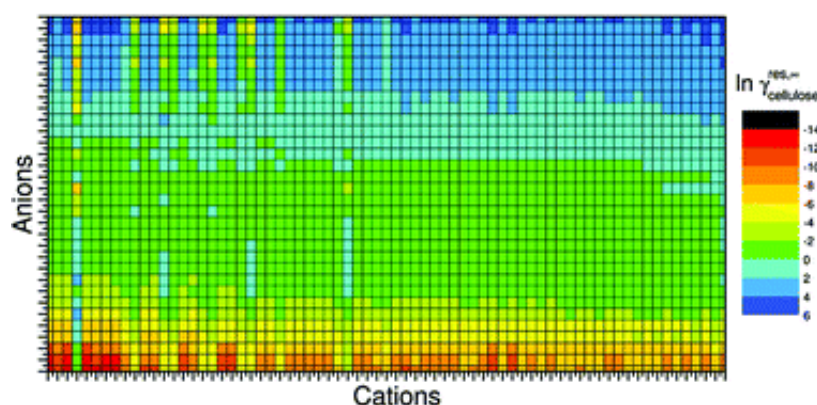


Figure I-6 Solubility map based on COSMO-RS study of cellulose in various ILs combining different cations and anions, with different colors representing the dissolving power. [Kahlen 2010]

Of course, the selection of ILs should not simply depend on the dissolving power, since the viscosities of ILs can be quite different, and usually significantly higher than conventional organic solvents. Highly viscous solvents can bring difficulty to both dissolution and the processing afterwards. Thus efforts have been devoted to the investigation of rheological properties of cellulose-ILs solutions. The shear and extensional flow properties of cellulose-IL solutions were studied as a function of cellulose concentration and temperature [Kosan 2008; Sammons 2008; Collier 2009; Haward 2012], and detailed studies on the shear rheological properties of cellulose-AMIMCl [Kuang 2008], cellulose-EMIMAc [Gerike

2009b] and cellulose-BMIMCl [Sescousse 2010a] solutions in both dilute and semi-dilute regimes have been made. With cellulose-EMIMAc solutions, hydrodynamic parameters such as intrinsic viscosity were obtained with various cellulose molar mass and in a large range of temperatures, allowing the calculation of Mark-Kuhn-Houwink constants [Gerike 2009b].

Adding co-solvent as dimethylformamide (DMF), dimethylsulfoxide (DMSO), or even water into ILs can decrease the solution viscosity without compromising the dissolving power [Gerike 2009a; Gerike 2011; Le 2012]. In fact, rheological studies of mixing DMSO with EMIMAc demonstrated that the conformation of cellulose molecules remain unchanged in both dilute and entanglement regimes. The processing of cellulose-EMIMAc solutions with DMSO, DMF and dimethylacetamide (DMA) as co-solvents for electro-spinning was also studied [Hairdelin 2012].

Another direction of the study on ILs as cellulose solvent is to prepare materials as fibres, films or aerogel-like porous materials via dissolution followed by coagulation in a non-solvent. The various types of materials prepared will be reviewed in the following sections. With the same idea, blends of cellulose with other polysaccharides can be prepared, since the latter can also be dissolved in ILs. For example, researchers dissolved starch in BMIMCl and AMIMCl [Wilpiszewska 2011], and cellulose/starch blends were obtained with BMIMCl by Kadokawa et al. [Kadokawa 2009]. We dissolved waxy corn starch in EMIMAc (Chapter IV), explored the rheological and hydrodynamic properties of the solution, blended starch with cellulose and obtained materials with various porosities,.

1.1.4 Other cellulose solvents

Other cellulose solvents have also been discovered and studied. Some will be briefly listed below.

Phosphoric acid was first reported to be able to dissolve cellulose by British Celanese in 1925 [Celanese 1925], and revisited in the 1980s [Turbak 1980]. Recently high performance cellulose fibers were produced from this solution, and demonstrated potential of being commercialized [Boerstool 2001; Northolt 2001].

McCormick group discovered the possibility of dissolving cellulose in a *N,N*-dimethylacetamide (DMAc) and LiCl mixture, and investigated the dimension and conformation of cellulose chains in this solution [McCormick 1985]. The dissolution mechanism was thought to be due to the hydrogen bondings between the cellulose hydroxyl protons and chloride ions. The mixture could dissolve up to 15% cellulose, and unlike NMMO or ionic liquids, it does not cause cellulose degradation. Matsumoto et al. found differences in the behaviors of plant cellulose and bacterial cellulose by rheological study, claiming the former being like flexible polymers and the latter being rod-like [Matsumoto 2001]. The difference was later explained by the research of Tamai et al., showing the solutions acting as a two-phase system, and the rod-like behavior could be caused by the uncompleted dissolution [Tamai 2003]. Ramos et al. found that activation of cellulose could be a precondition for the complete dissolution in this solvent [Ramos 2005a].

DMSO/tetrabutylammonium fluoride trihydrate (TBAF·3H₂O) was also developed as cellulose solvent, and used for the synthesis of cellulose derivatives [Heinze 2000; Ramos 2005b, Ostlund 2009].

Frey et al. dissolved cellulose of DP=210 without activation in ethylene diamine (EDA)/potassium thiocyanate (KSCN), and the solubility depended essentially on the solvent composition [Frey 2006].

I.2 Materials formed from cellulose solutions

I.2.1 Fibers

With NMMO as solvent, Lyocell fibers are the most successful and the only industrialized cellulose fibers fabricated from a pure cellulose solution. The process has been extensively investigated and it is well documented. Briefly, cellulose pulp is first dissolved in NMMO; then the cellulose “dope” goes through the wet-spinning process to be shaped into fibers; which are washed with diluted NMMO solution and water, before being finally dried. Fibers fabricated by Lyocell method have good properties which ensure profitability despite of the higher cost compared to the viscose process.

Cellulose solutions in NaOH-water were developed by researchers from Asahi Chemical into an industrial process making fibers with mechanical properties comparable to the viscose ones in the 1990s [Yamane 1996b; Yamane 1996c; Yamane 1996d]. The process uses steam exploded pulp pre-activated by wet pulverization dissolved in NaOH-water. Dry fibers prepared this way have a maximum tensile strength of 2 g/den (about 1.77 cN/dtex), elongation of about 20% [Yamane 1994] and Young's modulus of about 110 g/den [Yamane 1996b; Yamane 1996d]. With urea and thiourea added in the solvent system, L. Zhang group also spun cellulose fibers with tensile strength of 1 cN/dtex and elongation of about 15% (with thiourea). With ZnO as a stabilizer, Vehvilainen et al. dissolved enzyme-activated cellulose in NaOH-water, and prepared fibers with tensile strength of 1.8 cN/dtex and 15% elongation at break. The problems of the NaOH process lie in the moderate mechanical properties limited by the low cellulose solubility, and also in the need to add additives to stabilize solutions and to cool down solutions, all these factors making this process not economically attractive.

Different ionic liquids (BMIMCl, EMIMCl, BMIMAc, and EMIMAc) were used by Kosan et al. to dissolve cellulose and prepared fibers via wet-spinning [Kosan 2008]. The fibers had properties comparable with the ones prepared via Lyocell process [Kosan 2008]. The tenacity was between 44.1 cN/dtex and 53.4 cN/dtex compared to the Lyocell fibers of 43.6 cN/dtex; and the elongation was 11.2% to 15.5% compared to 16.7% for Lyocell fibers. With similar procedures, Cai et al. managed to fabricate BMIMCl-based cellulose fibers with a tenacity of 4.28 cN/dtex [Cai 2010a]. The dyeing and antifibrillation properties were demonstrated to be in the same range of Lyocell fibers. In order to optimize the spinning process, Jiang et al. looked into the impacts of the spinning speed on the mechanical properties, cellulose crystalline structure, and morphology of the final fibers, reporting that a higher spinning speed was preferable [Jiang 2012]. Quan et al. were able to prepare ultrafine cellulose fibers with minimum diameter of 500 to 800 nm via electrospinning, using BMIMCl and DMSO as a co-solvent [Quan 2009]. They found that the cellulose concentration in the IL solution is the dominant parameter for the size and morphology of obtained fibers. Freire et al. also obtained electrospun fibers of similar size (around 500 nm) with EMIMAc as solvent [Freire 2011]. To further reduce the size, the authors added the surface activated 1-decyl-3-methylimidazolium chloride (DMIMCl) to make a binary solvent mixture with EMIMAc, which lead to fibers of average diameters around 100 nm.

I.2.2 Films & Membranes

Films or membranes can be prepared from cellulose solutions by casting or spin-coating, as long as a thin layer of the solution can be obtained. The concept for processing from dissolution to coagulation is the same as that of making fibers.

L. Zhang and colleagues did intensive research during the last decades on making films or membranes from aqueous NaOH solutions of cellulose with urea or thiourea as additives. Factors as the types of coagulants, the concentrations of coagulants, the temperatures and time for the coagulation have been investigated, in order to check their impacts on the structure, morphology, permeability, and mechanical properties of the coagulated films/membranes, and also in order to find the optimized formulation and processing parameters, see Figure I-X for example [Zhang 2001; Zhou 2002; Ruan 2004; Zhang 2005b; Mao 2006; Cai 2007a]. Zinc oxide was also added to the aqueous NaOH/urea system, to further enhance the optical transmittance, solution thermal stability and tensile strength of coagulated films [Yang 2011b].

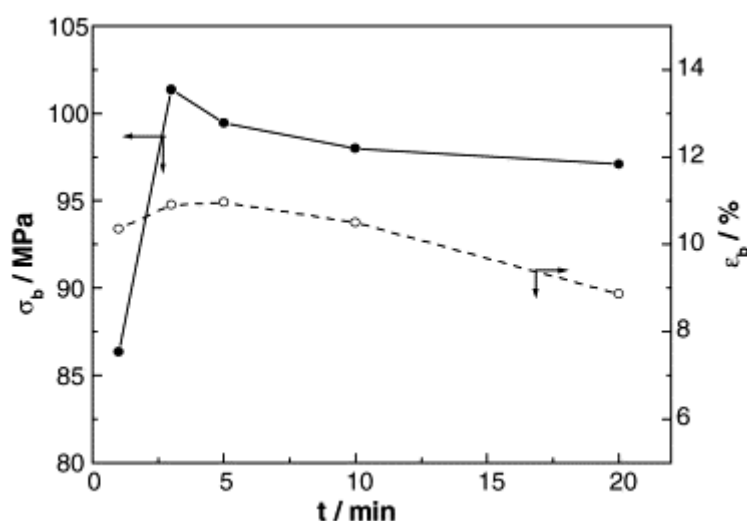


Figure I-7 Dependence of the tensile strength (σ_b) and elongation at breaking (ϵ_b) of the membranes on the coagulation time Reprinted with permission from [Ruan 2004]. Copyright (2004) Elsevier.

Turner et al. prepared enzyme-doped bioactive cellulose films primarily with BMIMCl, and different other ILs were used for the physical dispersion of enzyme [Turner 2004]. Cao et al. obtained coagulated cellulose films with both AMIMCl and EMIMAc [Cao 2010]. The ones

prepared with AMIMCl had higher tensile strength and modulus than the ones with EMIMAc. During the dissolution of cellulose with BMIMCl and preparation of coagulated films, Liu et al. added N-methylimidazole (NMI) to avoid the degradation of cellulose and the consequent drop of mechanical properties [Liu 2011c]. However, it is worth noting that dissolution time and temperature may have more significant impacts on the DP of cellulose, considering that the function of NMI proposed by the authors was to simply decrease the concentration of Cl⁻ in BMIMCl. Jin et al. added glycerol as plasticizer in the “classical” process of making cellulose films with BMIMCl, and reported that with more plasticizer and longer plasticization time, the films became less brittle, with an enhanced oxygen barrier property [Jin 2012]. Ma et al. made cellulose membranes with EMIMAc as solvent for the application as barrier layer in the ultrafiltration membranes [Ma 2011]. Although with the similar rejection ratio, the permeation flux of cellulose membranes prepared was not as high as their cellulose-chitin blend counterparts prepared in the same study, but it was still higher (4.6 times) than the control group of commercial ultrafiltration membranes PAN 10 of Sepro. Li et al. prepared nanofiltration membranes of cellulose from solutions with AMIMCl, with a similar process [Li 2011]. The obtained membranes were anti-fouling, having high water permeation flux, good stability, and a suitable molecular weight cut-off for separating medium weight organic compounds.

1.2.3 Aerogels

Based on dissolved cellulose, researchers are able to develop various cellulose aerogels or aerogel-like materials. Those materials are ultra-light, highly porous, and have lots of potential to be used as scaffolds in biomedical fields, or as insulation materials, for example. In fact, cellulose aerogels can be prepared both from dissolved cellulose (cellulose II), and also from cellulose I as bacterial cellulose or nano-/macro-fabricated cellulose. The latter is beyond the scope of this chapter, and will not be covered.

The preparation of cellulose II aerogel-like materials involves four steps: dissolution, shaping, coagulation, and drying. For the dissolution of cellulose, all of the direct cellulose solvents we cited in the above sections can be used, including aqueous NaOH [Gavillon 2008; Sescousse 2009], NMMO [Innerlohinger 2006; Liebner 2008; Liebner 2009], ionic liquids [Tsiptsias 2008; Deng 2009; Aaltonen 2009; Sescousse 2011], DMAc/LiCl [Duchemin 2010], etc.

Once dissolved, the cellulose can be coagulated directly into beads [Sescousse 2011b], or can be shaped in a mould into a three-dimensional structure either by gelation, or by solidification. Gelation happens with time and temperature in the cellulose-NaOH-water solutions when no additives are added, which enables to form a physical gel having the shape of the mould [Gavillon 2008]. The shaping can also be achieved by solidification when the solvents are NMMO monohydrate [Liebner 2008; Liebner 2009] or certain ILs as BMIMCl [Sescousse 2011a], which have very high viscosity at room temperature.

The coagulation can be performed in non-solvent as water or ethanol, and followed by either freeze-drying [Deng 2009; Duchemin 2010, for example] or supercritical CO₂ drying [Innerlohinger 2006; Liebner 2008, for example]. In the case of supercritical CO₂ drying, if the non-solvent for coagulation is water, it needs to be exchanged with a CO₂ compatible solvent, as acetone.

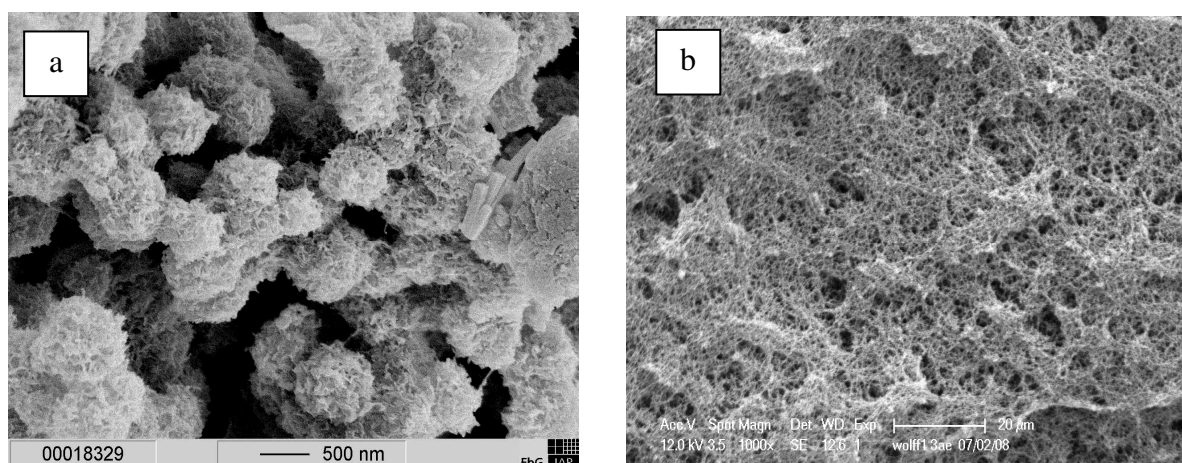


Figure I-8 “Globular”-like (a) and “Network”-like morphology of cellulose aerogels [Liebner 2009]. Reprinted with permission from [Gavillon 2008]. Copyright (2008) American Chemical Society.

Two types of morphology can be identified with cellulose aerogels, as shown in Figure I-8, and they depend largely on the procedures of preparation. “Globular”-like structures were found when liquid cellulose solutions were directly coagulated, as in molten NMMO monohydrate, or in EMIMAc. “Network”-like structures were found when the solutions were solidified, or gelled, as in the cases of NMMO at room temperature, or NaOH-water. The difference can be explained by the different phase separation processes. With the former case,

phase separation already occurs before coagulation, resulting in a free-solvent phase and cellulose-solvent bounded phase; whereas in the latter case, coagulation and phase separation happen at the same time. Density depends on the initial concentration of the cellulose solution, and can be significantly reduced when surfactant was added [Gavillon 2008].

The mechanical properties of cellulose aerogel are similar to the classical aerogel model, i.e. the Young's modulus of different cellulose aerogels (based on microcrystalline cellulose dissolved in EMIMAc or 8 wt% aqueous NaOH, and higher DP cellulose dissolved in NMMO monohydrate) was found to be correlated to the density with a power law of three [Sescousse 2011a]. The similarity can be explained by the structural defects in the cellulose aerogels appearing with the coagulation process. Although the pore size distribution of the cellulose aerogels measured with BET analysis was around 10 – 15 nm, the actual size varied from nanometers to several microns [Liebner 2009; Sescousse 2011a].

1.2.4 Hydrogels

Similar to the preparation of aerogels but without the drying step, hydrogels could also be prepared from cellulose solutions owing to the physical cross-linkings of the abundant hydroxyl groups of cellulose. In this section, hydrogels from cellulose dissolved in different solvents will be briefly reviewed. In fact, we should note that in all the appropriate literature, the cellulose hydrogels actually consist of two types of materials. The first are the “real” cellulose hydrogels formed by cross-linking of cellulose molecules. The second is coagulated cellulose forming gel-like materials, which are also called hydrogels by some researchers. The second type of materials will be specified as “hydrogel” in the following part.

Li et al. dissolved cellulose in AMIMCl, cast it into a mould, coagulated with deionised water, and obtained porous cellulose so-called “hydrogel” [Li 2009a]. The mechanical strength of the “hydrogel” was not great, but it did demonstrate good thermal stability and resistance against corrosion with acid. The researchers explored later the possibility of applying this type of “hydrogel” as diffusion matrices for gel electrophoresis applications to replace the traditional polyacrylamide gels [Lu 2011b]. With the same solvent, Hu et al. prepared and characterized “hydrogels” by doping cellulose with polyvinyl pyrrolidone (PVPP) [Hu 2010]. The mechanical properties and stability of the “hydrogel” were enhanced by PVPP, and the

swelling and release kinetics were evaluated as a function of both composition and processing for drug release applications.

The intrinsic characteristics of gelation make the aqueous NaOH system a suitable option for preparing cellulose hydrogels. Along with seeking for methods to stabilize cellulose-NaOH solutions, L. Zhang's group also investigated the hydrogels formed by gelation. As we mentioned previously, both urea and thiourea were added into the solvent system. Cai and Zhang reported that the hydrogels obtained with NaOH-urea were stable, and did not dissolve or break with heating or cooling [Cai 2006]. With NaOH-thiourea and the pre-gelation method similar to what we described in the cellulose aerogel section, Liang et al. obtained cellulose hydrogels having good mechanical properties (with stress and strain at break of 1.97 MPa and 192%) [Liang 2008]. With further investigation, Lue and Zhang found that the gelation in NaOH-thiourea is only irreversible with temperature higher than 60°C above which happens the reaction between NaOH and thiourea [Lue 2008]. The same research group demonstrated that at this temperature a relatively stable network of cellulose with a unit size of about 47 nm is formed [Weng 2004].

Saito et al. succeeded in obtaining highly transparent cellulose “hydrogels” directly by dissolution in DMAc/LiCl, PFA/DMSO, and triethylammonium chloride (TEAC)/DMSO, and then coagulation [Saito 2003]. A “hydrogel” with higher tensile strength but less transparency was also prepared by them from technical viscose solutions. Ostlund et al. dissolved cellulose in TBAF/DMSO, which lead to cellulose solutions of high viscosity or their gelation, depending on the cellulose concentration and water content in it [Ostlund 2009]. Recently, using LiCl/DMSO as cellulose solvent, Wang et al. made translucent “hydrogel” as well as porous aerogels with mesopore sizes around 10 - 60 nm [Wang 2012]. Although NMMO is another popular choice for dissolving cellulose, we do not find any published work using it to prepare cellulose hydrogel

I.3 Cellulose-based hybrid materials

We shall call as cellulose-based hybrid materials cellulose mixed with other components (mainly polymers) either in the form of blends, or with inorganic materials in the form of composites. This bring new properties and functions to the unmodified cellulose, and still

keep the intrinsic advantages of cellulose such as biodegradability, high mechanical strength, low density and cost. Two very comprehensive reviews by Nishio covered this topic, and the author pointed out that inter- and intra-molecular hydrogen bondings of polysaccharides are responsible for the miscibility in this type of hybrid materials [Nishio 2006].

I.3.1 Blends with polysaccharides

Starch:

The common objective of blending cellulose with starch is to reinforce the starch matrix. The blends are often made through the casting route with plasticizers. Psomiadou et al. blended microcrystalline cellulose with starch and prepared edible films both with or without plasticizers [Psomiadou 1996]. They reported that when films were made with higher cellulose content and without plasticizers, they had higher mechanical strength and lower permeability. But on the other hand, when water or polyol were used as a plasticizer, the permeability increased, but the mechanical and thermal performance dropped due to the plasticizing. Dufresne and Vignon reinforced the starch films with cellulose fibrils as fillers and glycerol as plasticizer [Dufresne 1998]. The thermal stability of the starch films was improved, and the water sensibility of the films was decreased. Mueller et al. also prepared similar blends with cassava starch, which turned out to be less sensible to water, but with more rigidity [Mueller 2009]. In a following study, Dufresne et al. investigated and correlated the films mechanical properties with the film composition, plasticizer and relative humidity conditions [Dufresne 2000]. Averous et al. reinforced thermoplastic starch (TPS) with leafwood cellulose fibers, demonstrating the existence of starch-cellulose interactions by Dynamic Mechanical Thermal Analysis (DMTA). These interactions lead to the improvement of the mechanical properties [Averous 2001]. Kumar and Singh additionally brought sodium benzoate into the microcrystalline cellulose-starch blended system as photo-sensitizer, and further improved the physical and mechanical properties of the blends by combining the reinforcement of microcrystalline cellulose and the photo-crosslinking of the starch matrix [Kumar 2008]. Chang et al. prepared cellulose nanoparticles of 50 to 100 nm from NaOH/urea/H₂O solution and blended them with glycerol plasticized-wheat starch, obtaining similarly better mechanical properties (tensile strength), higher thermal stability, and lower water vapour permeability [Chang 2010b].

Hybrid materials with components added to cellulose and starch were also investigated. Salgado et al. obtained ternary blends with cassava starch, sunflower proteins and cellulose fibers. The optimized formulation containing 70% starch, 20% cellulose fiber and 10% sunflower protein offered maximal resistance and largely reduced water absorption, making the composite suitable for preparing biodegradable packaging materials [Salgado 2008]. Composites with sponge-like structure were obtained by Wang et al. with starch and PVA, reinforced with cellulose nanowhiskers [Wang 2010]. Larger pores and stronger walls resulted from the repeated freeze/thaw cycles, which led to the cross-linking between starch and PVA, as well as phase-separation. Cellulose nanowhiskers improved the mechanical properties and shape stability of the material as well.

The dissolution-mixing route can also be helpful in blending starch and cellulose. Kadokawa prepared “cellulose-starch composite gel” by dissolving the two polysaccharides separately in BMIMCl, mixing these two solutions to have a homogenous mixture and coagulating the mixture in methanol. Similar fibrous blends were also obtained in acetone [Kadokawa 2009]. Although whether the blended materials can be called a gel or not is still doubtful, such process is clearly feasible and inspiring. We applied a similar process when we blended cellulose with starch, and this is presented in Chapter IV in this thesis. Builders et al. blended microcrystalline cellulose with maize starch for pharmaceutical applications as excipient [Builders 2010]. The blends showed enhanced direct compression and disintegrant properties. In this case, the cellulose was dissolved in NaOH-water, and mixed with starch dispersion in water.

Chitin:

Chitin is another type of polysaccharides with interesting properties having the potential of being exploited as artificial skin or dressing for healing wounds in biomedical applications, as sorbent of metal ions in water treatment, or for drug delivery [Kumar 2000]. The poor solubility of chitin is the major obstacle for making blends or composites via dissolution. The common route for the researchers is to find a common solvent dissolving both components.

NaOH/thiourea has been used primarily by L. Zhang's group as a common solvent to blend chitin with cellulose. They found that the morphology and mechanical properties of the blended films depend on both the composition and the regeneration bath [Zhang 2002a]. The structure, strength and thermal stability are thus tuneable, leading to more versatile

applications as functional materials. After optimizing solvent formulation and coagulation bath composition, Zhang's group prepared cellulose/chitin beads with higher surface area and better hydrophilicity compared to chitin alone, resulting in better performance in terms of lead absorption in water treatments [Zhou 2005]; as well as porous cellulose/chitin membranes, of which the porosity and permeability varied with the chitin content [Liang 2007]. Cellulose/chitin wet membranes were also prepared with similar solvents, but formed with the pre-gelation of mixed solutions instead of casting [Wu 2010]. The wet membranes showed denser structure and higher crystallinity compared to the traditional cast membranes, and had tuneable morphology, strength, and crystallinity depending both on the composition and the gelation parameters.

Due to both cellulose and chitin solubility in ionic liquids and LiCl-based solvents, they have also been used for making blends. Kadokawa and Ishikawa team succeed in using 1-allyl-3-methylimidazolium bromide (AMIMBr) and BMIMCl as common solvents to prepare blended films and hybrid gels for electrolyte applications [Takegawa 2010; Yamazaki 2010]. 1,3-dimethylamylamine (DMAA)-LiCl and DMAc-LiCl were used by Nud'ga et al. and Marsano et al. for blending cellulose with chitin and making films and fibers [Nud'ga 1999; Marsano 2002]. Marsano reported that the two components are completely miscible at 50/50 (w/w) composition, whereas Nud'ga suggested that both the solution mixture and blends structure actually change from homogenous to microheterogeneous with the concentration of any components higher than a certain limit.

Cellulose/chitin fibers can also be produced with some derivatives of chitin and cellulose, see for example [Hirano 1998; He 2009], which we will not review in this section.

Chitosan:

As a derivative of chitin, chitosan has a similar structure and properties, but a better solubility. Thus to make blends or composites with cellulose and chitosan, the researchers can either find a common solvent for both, or two different solvents for each component. The former route gives us more likely blends, whereas the latter route is more common when composites consist of matrix and coated layers are prepared.

To use a common solvent for both components seems to be a quite straightforward option. Hasegawa and Isogai group used trifluoroacetic acid (TFA) as a common solvent to dissolve

cellulose and chitosan and prepared blended films. Based on X-ray diffraction and Raman analysis, they suggested the presence of micro-phase separation between cellulose and chitosan in the blends, and it was the reduced size of cellulose “domain”, as well as the interactions at the interfacial area between cellulose and chitosan domains that improved the mechanical properties of the composites [Isogai 1992; Hasegawa 1992]. Chloral/dimethylformamide was also used by Hasegawa et al. as the common solvent to obtain cellulose/chitosan blends [Hasegawa 1994]. The mechanical performance of the blended films was higher than the calculated value by simple additive mixing rule, indicating that interactions between the two components occurred. The permeability was also increased compared to the single component films. Similar cellulose/chitosan films prepared from TFA as by Hasegawa et al. were further treated by Cai and Kim in glutaraldehyde solution to conduct crosslinking reaction between the two components in order to have an interpenetrating polymer network (IPN) for application as electro-active actuators [Cai 2009]. They found that the IPN became denser with higher chitosan contents, and evaluated the actuator performance and durability as a function of the composition.

NMMO is another choice as common solvent for blending cellulose and chitosan. Twu et al. dissolved the two components in NMMO to have a homogenous mixture, and prepared blended beads with rough surface and porous structure, which can be potentially used in odor treatment and the absorption of metal ions [Twu 2003]. The same group also obtained cellulose/chitosan films, and showed that the surface morphology and mechanical strength of the films depend on the chitosan content and the limit of phase separation of the two components. They also demonstrated that the antibacterial property due to chitosan was not significant [Shih 2009].

Ionic liquids can also dissolve both cellulose and chitosan. Sun et al. chose BMIMCl as common solvent to blend cellulose with chitosan to make composite biosorbents. They detected strong intermolecular hydrogen bonding between two components, and good performance in heavy metal ions absorption [Sun 2009]. Xiao et al. developed a binary ILs solvent system consisting of 1,3-dimethylimidazolium chloride (DMIMCl) and 1-H-3-methylimidazolium chloride (HMIMCl) [Xiao 2011]. The solvent system had relatively low viscosity, good miscibility between components, and was used to produce fibers and membranes with good mechanical properties.

Similar to the cases with chitin, Almeida et al. made cellulose/chitosan films using NaOH/thiourea as common solvent system, and claimed that the brittleness of blended films were reduced compared to pure chitosan films.

Chitosan can be dissolved in common solvents such as acetic acid, whereas cellulose is dissolved or treated in the classical cellulose solvent. Here we list a few examples using acetic acid dissolving chitosan. Nordqvist et al. prepared microfibrillated cellulose (MFC)-reinforced chitosan films which had better mechanical performance in wet state, with no difference in terms of strength in dry state [Nordqvist 2007]. The MFC was prepared separately and suspended in water, then mixed with chitosan-acetic acid solution during the process. Fernandes et al. later were inspired by this concept and obtained similar reinforced chitosan films with nanofabricated cellulose (NFC), which had improved mechanical properties in dry state, and better thermal stability [Fernandes 2010]. Li et al. prepared chitosan films with cellulose whiskers. The mechanical properties, thermal stability and water resistance of reinforced films were enhanced [Li 2009b]. Da Roz et al. prepared cellulose films dissolving in DMAc/LiCl, then oxidized the cellulose films, and deposited an ultra-thin layer of chitosan-acetic acid solution. The chitosan layer increased the surface roughness of the films, and had potential antibacterial applications [Da Roz 2010]. With acetic acid dissolved chitosan, Dogan and Hilmioglu coated the cellulose films regenerated from NMMO solution and filled with zeolite, which gave enhanced performance for the dehydration treatment of ethylene glycol [Dogan 2010a].

Cellulose:

Since the concept was first reported by Nishino et al. [Nishino 2004], all-cellulose composites (ACCs) have been investigated in recent years and showed excellent mechanical properties. Two processing routes have been used in the preparation of ACCs, a two-step method (Figure I-9-a) and a one-step method (Figure I-9-b), which were illustrated by Huber et al. in their recent reviews.

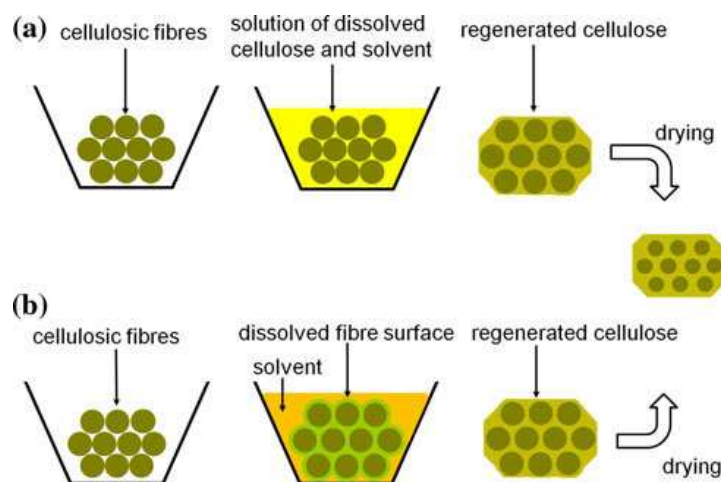


Figure I-9 Two routes for preparing all-cellulose composites. Reprinted with permission from [Huber 2012]. Copyright (2012) Elsevier.

In the two-step route [Nishino 2004; Esteves 2011], the cellulose matrix was added to the fibers in solution form, and it did not have to be the same type of cellulose as the fibers; whereas in the one-step route [Nishino 2007; Soykeabkaew 2008; Soykeabkaew 2009; Duchemin 2009; Han 2010; Gindl-Altmutter 2012; Ou 2012], the cellulose matrix came from the partial dissolved cellulose fibers. Since it involves the dissolution of cellulose, various types of cellulose solvents were exploited to prepare ACCs, including DMAc/LiCl [Nishino 2004; Nishino 2007; Soykeabkaew 2008; Soykeabkaew 2009], ionic liquids [Duchemin 2009; Gindl-Altmutter 2012; Ou 2012], NMMO [Esteves 2011], and NaOH/water system [Han 2010].

The reason for the impressive mechanical performance of the ACCs can be explained by the superior cohesion between the same or similar cellulosic matrix and reinforcing fibers but lots of research is still required to correlate the mechanical performance with the type of cellulose, the type of solvent and the processing routes.

Lignin:

Given the fact that natural fibers are very good composites made of cellulose and lignin with the presence of other components (polysaccharides, waxes, etc.), there has not been a great deal of research efforts devoted to blend unmodified cellulose with lignin. There are studies on separating those components in paper industry, see, for example, [Willauer 2000; Lateef 2009], or to blend lignin with cellulose derivatives as hydroxypropyl cellulose (HPC),

cellulose acetate butyrate (CAB), or ethyl cellulose [Glasser 1998]. In rheological studies by Glasser et al. and Collier et al., DMAc/LiCl and BMIMCl were used as common solvent to dissolve and mix cellulose and lignin [Glasser 1998; Collier 2009]. The viscosity higher than calculated with simple mixing rule and dynamic elastic modulus of the mixtures suggest certain interactions between the two components. Aaltonen and Jauhiainen reported that they prepared aerogel with low density and partially reversible compressibility with cellulose/lignin as well as cellulose/lignin/xylan, with ionic liquid BMIMCl as common solvent. However, the composition of each composite after the coagulation and solvent exchange was not specified [Aaltonen 2009]. Later Sescousse et al. used NaOH-water as common solvent, and studied the regenerated materials, which were also reported to be aerogel-like materials [Sescousse 2010b]. They attributed the porous structure to the incompatibility of the two components and the wash-out of lignin in the process of regeneration. In another attempt, Maximova et al. coated cellulose fibers with lignin by absorption, and the cellulose fibers were treated with a cationic polyelectrolyte called poly dimethyldiallylammonium-chloride (PDADMAC) in order to be bonded with the lignin [Maximova 2001]. With AMIMCl, ternary blended films of cellulose, starch and lignin were prepared by Wu et al. with good mechanical properties, transparency, and stability, but the lignin content in the films were fairly low (maximum concentration of 7.3 wt%) [Wu 2009].

Other polysaccharides:

Other polysaccharides such as pectin or carrageenan can also be blended with cellulose as mixtures. The cellulose-pectin composites have been studied to model and mimic the cell wall structure of plants, and also to improve the understanding of plant-derived products. Touzel et al. performed *in vitro* polymerization of lignin using mats of bacterial cellulose/pectin composite, concluding that pectin enhanced the dispersion of lignin in cellulose network [Touzel 2003]. Zykwiniska et al. conducted *in vitro* bindings of various pectin and cellulose microfibrils, and studied their impacts [Zykwiniska 2005]. Gu and Catchmark investigated the influence of pectin, together with xyloglucan, on the assembly process of bacterial cellulose and reported morphological changes and enhanced bindings among different cellulose fibrils [Gu and Catchmark]. Agoda-Tandjawa et al. prepared cellulose/pectin composites, and found that although the mechanical properties were determined by the cellulose network, the structure of pectin had impacts on the rigidity of the composites [Agoda-Tandjawa 2012]. Prasad et al. prepared carrageenan/cellulose composite gels with BMIMCl as common solvent,

claiming the composite gel to have better mechanical properties than hydrogel of pure carrageenan [Prasad 2009].

Cellulose derivatives are also options for blends/composites. To just name one example, using epichlorohydrin as cross-linker, Chang et al. prepared a suprasorbent hydrogel with “smart” swelling and shrinking functions with cellulose and carboxymethylcellulose (CMC), by dissolving and mixing them in NaOH-urea-water solvent system [Chang 2010a].

I.3.2 Blends with synthetic polymers

Usually with the help of proper solvent systems, cellulose can be blended with certain synthetic polymers to improve the properties of one or both components, or to bring new properties to the composite. Nishio reviewed some examples of binary blends of cellulose/synthetic polymer from a structural point of view, and listed the scale of homogenous mixing, which was estimated by combining data obtained from various techniques such as thermal transition data with dynamic mechanical analysis and spectroscopic data with solid-state NMR, given in the following Table I-1 [Nishio 2006]. We can see that in the area enclosed with dotted line, cellulose/synthetic polymers can reach a highly compatible state of mixing. In the following sections, we will review some of the examples from processing and functional points of view.

Table I-1 Scale of homogeneity for cellulose/synthetic polymer binary blends. Reprinted with permission from [Nishio 2006]. Copyright (2006) Springer.

Composition	Scale of homogenous mixing */nm						
	CELL/P4VPy ^a	MC/P4VPy ^b	MC/PVP ^b	CELL/PVA ^c	CELL/PAN ^c	CELL/PCL ^c	CELL/Ny6 ^c
CELL < 30 wt %	} <2.5	} 2.5-15	} ca. 2.7	15-39	15-35	ca. 27	} >31
CELL ≈ 50 wt %				<15-36	<15-31	ca. 27	
CELL > 70 wt %		ca. 2.5	2.7-15	1-15	4-15	>28	

Notations: CELL, cellulose; P4VPy, poly(4-vinyl pyridine); MC, methylolated cellulose; PVP, poly(N-vinyl pyrrolidone); PVA, poly(vinyl alcohol); PAN, poly(acrylonitrile); PCL, poly(ϵ -caprolactone); Ny6, nylon 6.

Polyamide (PA)

Garcia-Ramirez et al. blended and characterized cellulose with polyamide 66 (PA66) by dissolving them separately in a mixture of NMMO-phenol (80/20 w/w) [Garcia-Ramirez 1994; Garcia-Ramirez 1995]. Films and fibers were obtained by coagulation in methanol, and a two-phase system with PA reinforcing cellulose matrix was found. Despite of the immiscibility, the mechanical performance of cellulose was improved due to the strong interfacial interaction between the two components. With a gas-phase treatment of a silyl coupling agent (aminosilane), Paunikallio et al. chemically modified the surface of viscose fibers, and enhanced their adhesion with a polyamide 12 matrix, resulting in an improved strength of the composites [Paunikallio 2006]. Hablot et al. prepared renewable biocomposites by blending cellulose fibers with dimer fatty acid-based polyamides (DAPA) [Hablot 2010a; Hablot 2010b]. The mechanical performance of the blends were tested, and the hydrogen bondings between the carbonyl groups of the DAPA and the hydroxyl group of cellulose was found to increase the stiffness and thermal-mechanical stability of the blends, compared to pure DAPA.

Poly (vinyl alcohol) (PVA)

Homogenous porous hydrogels of cellulose/PVA were prepared by Chang et al. with both physical and chemical cross-linkings using aqueous NaOH-urea system as cellulose solvent. The authors characterized the structure and performance of the hydrogels and claimed that the chemical ones with epichlorohydrin as cross-linking agent had a significantly higher water uptake [Chang 2008]. Cellulose nanocrystals have been used as fillers in PVA membranes, together with poly (acrylic acid) (PAA) as cross-linking agent for PVA [Paralikal 2008]. The mechanical performance of the blend membranes was found to be best with a formulation of 10% cellulose, 10% PAA and 80% PVA. Also the water vapor barrier property was enhanced by adding cellulose nanocrystals and PAA. In the research of Tang and Liu, a cellulose nanofibrous mat was also found to remarkably reinforce PVA films [Tang 2008]. With AMIMCl, Zhang et al. prepared and characterized PVA-reinforced cellulose films. It was found that cellulose and PVA were compatible in the blend films. While the transparency of the films was maintained, a composition with good mechanical performance was found by the authors (10 wt% PVA), and the shape stability was also improved [Zhang 2012].

Poly (ethylene glycol)

Liang et al. prepared cellulose/PEG blends with solutions in dimethyl sulfoxide (DMSO)-paraformaldehyde (PFA). They found that the crystalline PEG parts in the blends did not melt to liquid state with increasing temperature, but changed to amorphous state, probably due to the strong hydrogen bonding between PEG and cellulose chains [Liang 1995]. Due to the strong hydrogen bondings, cellulose/PEG composites can be prepared in dry state with ball-milling, instead of the more convention solution route [Endo 1999]. Some potential applications have been explored by researchers. Shen and Liu blended cellulose with PEG, and found that the composites can be used in the controlled-release of drugs [Shen 2007]. Cellulose gels coagulated from aqueous NaOH-thiourea solutions were swollen in PEG, which strengthened the gel by hydrogen bondings [Liang 2008]. By surface coating with PEG, biocompatible bacterial cellulose/PEG scaffolds were obtained, and the thermal stability was demonstrated to be increased [Cai 2010b]. Cellulose-graft-PEG copolymers also have very interesting features and have been extensively studied. We will not discuss these here.

Poly (acrylonitrile) (PAN)

He et al. dissolved cellulose and PAN in DMSO-PFA solvent system, and obtained blend membranes [He 2002]. The permeability and retention of the membranes were tested as a function of the composition, and a satisfying capacity for removing creatinine and urea was obtained.

Poly (ϵ -caprolactone) (PCL)

Nishio and Manley used a DMAc/LiCl solvent system to blend cellulose with both PCL and polyamide Nylon 6 [Nishio 1990]. They reported that unlike the case of cellulose/Nylon 6, which was almost immiscible at the molecular level; amorphous cellulose could be well blended with PCL, and an optimized ratio between the interacting hydroxyl and ester groups of the two components was necessary for good miscibility. PCL nanofibers were mixed with modified or unmodified cellulose nanocrystals by Zoppe et al. They found that the mechanical properties of the PCL nanofibers were largely improved, whereas the thermo behaviour remained unchanged [Zoppe 2009]. Unmodified cellulose nanocrystals were claimed to bring better homogeneity of the morphology of the blends. Kim and White investigated and compared the interfacial adhesion and dynamic viscosity of cellulose/PCL blends with cellulose/polypropylene blends [Kim 2009]. A stronger interfacial adhesion was found with cellulose/PCL. Gea et al. used both fibrous bacterial cellulose and particulate bacterial

cellulose to reinforce the PCL matrix [Gea 2010]. They found that while the modulus of both type of composites was the same, the one reinforced with fibrous bacterial cellulose had a higher tensile strength and strain at break.

Poly (N-vinyl pyrrolidone) (PVP)

Paillet et al. blended cellulose with PVP, using NMMO-DMSO as common solvent and different coagulation baths. The blends were found to be a two-phase system due to the phase-separation of the two components [Paillet 1993]. Assymmetric porous structures were found when the blends were coagulated in a hexamethyl phosphorotriamide (HMPA)-DMSO bath due to the partial leaching out of PVP.

I.3.3 Cellulose-based composites with inorganic materials

Metal oxide:

TiO₂ is mixed with cellulose to produce films or fibers with photoactive properties, and various precursors and processing methods have been developed. Miao et al. prepared mesoporous cellulose/TiO₂ composite films with particles at nano-scale by the calcination of titanium tetrabutyloxide (TTBO) with ionic liquid (AMIMCl) dissolved cellulose [Miao 2006]. Uddin et al. coated nano-scale TiO₂ on cellulose fibers with titanium isopropoxide (TIP) using a more classical sol-gel method [Uddin 2007]. Kemell et al. succeed in making TiO₂/cellulose composite films through atomic layer deposition (ALD), with Ti(OMe)₄ as precursor [Kemell 2005].

Al₂O₃ was also used to coat cellulose fibers, but usually further modified with organofunctional groups with Al-O-Si bonds, so to facilitate metal ion absorption [Alfaya 1999; Lazarin 2000].

L. Zhang's group investigated Fe₂O₃/cellulose nanocomposites, and prepared magnetic fibers and films via in situ synthesis of Fe₂O₃, based on regenerated cellulose from NaOH/urea solutions [Liu 2008; Liu 2011b].

SnO₂-coated cellulose films were prepared by Mahadeva and Kim with liquid phase deposition technique. The composite films were further functionalized with enzyme -- glucose

oxidase by physical absorption, which was linked with SnO₂ with covalent bondings. The films were found to be effective glucose sensor for biomedical applications [Mahadeva 2011]. Ye et al. embedded ZnO nanocrystallites on cellulose nanofibers with electrospinning/solvothermal techniques. The composite obtained had both the photocatalytic capacity of ZnO nanocrystallites and the stability and mechanical properties of cellulose fibers [Ye 2011]. John et al. also conducted the coating of cellulose films with ZnO nanoparticles by controlled hydrolysis of a Zn(II)-amine complex. This method was considered by the authors to be very practical, since it did not require the use of binders or calcination processes as in most cases [John 2011].

Silica:

Sequeira et al. made cellulose/silica composites via sol-gel process, and obtained materials with better thermal stability, water resistibility, mechanical strength, as well as satisfying thermal insulating capacity [Sequeira 2009]. Jin et al. fabricated cellulose/mesoporous silica composite films. The composite films became less rigid, and their water and oxygen permeability could be adjusted by varying the films composition [Jin 2010]. Composite fibers of cellulose/silica were also obtained by Jia et al. synthesizing in ethanol/water with tetraethoxysilane as precursor, using the pre-dissolved cellulose in DMAc/LiCl [Jia 2011].

Clay:

Gawryla et al. used freeze-drying technique to prepare nanocomposite aerogel from cellulose whiskers and montmorillonite. The three-dimensional structure formed between the two components reduced the fragility of the aerogels of single component [Gawryla 2009]. Delhom et al. developed cellulose/montmorillonite nanocomposites, showing improved flame-retardancy and mechanical strength [Delhom 2010]. Liu et al. brought montmorillonite platelets together with nanofibrillated cellulose (NFC) to form multilayered nanopaper [Liu 2011a]. NFC provided excellent mechanical performance to the nanocomposite, allowing a higher loading of clay, which brought fire retardancy and gas barrier functions without compromising the ductility of the composite. Later chitosan was added by the same researchers to the nanocomposite to further enhance the toughness of the nanocomposite [Liu 2012a]. Perotti et al. coated bacterial cellulose with laponite clay claimed to have increased the Young modulus and tensile strength, but decreased the strain at break [Perotti 2011]. However, the thermal stability of the composite was only slightly improved in this case.

Carbon black and carbon nanotube:

Cellulose-based composites filled with carbon black has been rather scarce, probably due to the aggregation of carbon black, and the excellent properties of similar materials – carbon nanotubes. Li and Sun proposed to dye cellulose fabrics directly with carbon black nanoparticles [Li 2005]. Though certain colorfastness had been demonstrated with this method, the results were still not satisfying considering the surface aggregation of carbon black and vulnerability when washed with soap. Voigt et al. prepared laminated composite with cellulose and melamine-formaldehyde, then added carbon black for conductivity [Voigt 2005]. The researchers also found that carbon black and cellulose formed a network which increased the elastic modulus of the composites at low carbon black loading.

On the other hand, the research on cellulose/carbon nanotube composites has been more intensive. Yun and Kim mixed 0.1 wt% multi-walled carbon nanotube (MWCN) with DMAc/LiCl dissolved cellulose, and obtained electro-active paper with satisfying actuator performance [Yun 2007]. MWCN of 8.32 wt% was used by Fugetsu et al. to prepare conductive cellulose papers, which showed shielding capacity for electromagnetic interference (EMI) [Fugetsu 2008]. The EMI shielding effectiveness was investigated for this kind of composite cellulose papers with a rather large range of MWCN concentration (0.5-16.7 wt%) by Imai et al., in order to find the optimum formulation [Imai 2010]. Cellulose/MWCN fibers were obtained by Zhang et al., with AMIMCl as both cellulose solvent and suspending medium in the process [Zhang 2007]. The composite fibers were claimed to be potential precursor for the production of cellulose-based carbon fibers. Imidazolium ionic liquids as EMIMAc, 1-butyl-3-methylimidazolium acetate (BMIMAc) were also used by researchers to dissolve cellulose and mix it with MWCN or single-walled carbon nanotube (SWCN) for making conductive composites for applications as electrode or cell sensor [Rahatekar 2009; Wan 2010]. Kim et al. prepared cellulose/SWCN nanocomposite films with NMMO as cellulose solvent, and achieved satisfying conductivity [Kim 2010].

Zeolite:

Vu et al. deposited zeolite onto pre-treated cellulose fibers, and investigated related parameters as reaction time/temperature, fiber pre-treatment and ratio of each component for the preparation process [Vu 2002]. They obtained stable cellulose/zeolite fibers resistant against washing. Dogan and Hilmioglu first prepared zeolite-filled cellulose membranes regenerated from NMMO solutions. The membranes were thermally and chemically stable,

and could be used for the dehydration of glycerol [Dogan 2010a]. The performance of the composite membranes was further enhanced by coating the zeolite with chitosan [Dogan 2010b].

Apatite:

Yoshida et al. synthesized cellulose/carbonate apatite composite materials for bone substitution using poly (ϵ -caprolactone) as plasticizer [Yoshida 2005]. The composite was able to form bondings with bone, stable in simulated body fluid, and had low Young modulus value. Cellulose-hydroxyapatite composite fibers were also obtained based on Lyocell process by Hofmann et al. for bone-related medical applications [Hofmann 2008]. With higher apatite loading, the composite fibers had lower tensile strength and maximum strain at dry state, but higher strain at wet state.

I.4 Dispersion of carbon black and conductive films

The research on conductive polymers has been driven by the numerous applications as electromagnetic interference shielding, static electricity dissipation, sensor materials, and heating elements (in textile). Bringing carbon black into cellulose films is one of the solutions to prepare conductive cellulose-based composites, which could combine the advantages of both components, including the chemical and thermal resistance, the processability and the abundance of cellulose as well as the low cost and conductivity of this common filler.

Two topics will be reviewed in the following sections: 1) the dispersion of carbon black agglomerates in cellulose solutions; 2) the percolation threshold of carbon black in composites. Both a good dispersion and an appropriate loading of carbon black are essential for our aim of preparing conductive cellulose-carbon black composite films using ionic liquid.

I.4.1 Dispersion of carbon black in fluids

The dispersion of fillers in a suspending fluid is the process in which the size of fillers will be reduced. A single filler particle is split into several smaller ones. It is important not to confuse dispersion with distribution, which is the process scattering all the filler particles and

dispersed fragments in the suspending fluid [Manas 1989]. Thus the quality of a suspension is controlled by both the dispersion, when it is applicable, and the distribution. A blend can have a good dispersion, where all fillers are broken into many tiny pieces, but a bad distribution if all these particles are located in some specific areas. The contrary can also happen, with filler not being fully broken, but with all the large pieces homogeneously distributed in the suspending medium.

Not all fillers can be dispersed. The most popular case is when fillers are formed, on purpose, of smaller particles that are agglomerated. A flow field will break apart these agglomerates and if the flow is correctly calculated, these tiny broken particles will distribute all over the suspending medium. Important technological cases are the dispersion of pharmaceutical tablets [Sheen 1991; Serajuddin 1999; Brouwers 2009] and of carbon black or silica in reinforced elastomers [Cotten 1984]. In the latter case, carbon black or silica agglomerates of a few tens of micrometers are first prepared. With such sizes, the agglomerates can be easily handled without danger. They are then mixed with an elastomer (e.g. styrene-butadiene rubber or natural rubber) in a mixing equipment (usually an internal mixer) and after certain time of mixing, nanometer-size carbon black or silica particles are distributed all over the matrix, followed by a phase of curing. Such morphology is known to drastically reinforce elastomers [Heinrich 2002].

Mechanisms of agglomerate dispersion have been studied for a long time, owing to the practical importance of this process. Numerous papers have been devoted to the study of dispersion in internal mixers, since it is the major preparation method. The difficulty is that it is not possible to observe how dispersion occurs, and the studies must rely on interrupted experiments during which the mixture is removed from the mixer and studied. It is from such studies that the classical BIT (Black Incorporation Time) parameter was found. BIT is measured from the power dissipated during mixing and corresponds to the time needed to attain the second power dissipation peak, where most (not all) authors are considering that carbon black is well dispersed, i.e. that all micron-size particles broke down to nanometer-size ones [Cotton 1984]. Despite of the practical importance of such result, it is still difficult to identify the mechanisms by which agglomerates reduce their sizes. However, observation of the size changes of carbon black extracted from internal mixers showed that two mechanisms are at stake during dispersion, rupture and erosion [Bolen 1958, Shiga 1985]. Rupture is a sudden phenomenon by which agglomerate is broken into two or more pieces. Erosion is a

gradual phenomenon by which individual, very small fragments are detached from the surface of the agglomerate.

Another approach for studying dispersion is rheology, since the viscoelastic response of a suspension depends on its state of dispersion [Metzner 1985]. Again, such a method is not telling much about the dispersion mechanisms. Rheo-optical tools being able to combine flow and optical observations must be used to observe how an agglomerate particle breaks under the action of shear stresses. Observations have been conducted both in Newtonian [Rwei 1990, Rwei 1991, Bohin 1996] and in viscoelastic matrices, but in this latter case, only the variation of viscosity was considered [Astruc 2001, Collin 2004, Collin 2005].

A critical parameter influencing greatly the way agglomerates break is the degree of infiltration of the matrix inside the agglomerate. The first one to study this phenomenon was Bohin et al. [Bohin 1996] who built a model describing the infiltration of spherical agglomerate by a Newtonian matrix, taking surface tension, geometry of pores and viscosity of the matrix into account. It has also been observed that infiltration kinetics was higher when increasing shear rate in viscoelastic matrices [Collin 2005]. Changes in dispersion kinetics and/or mechanisms of silica agglomerates dispersion in viscoelastic matrices as a function of infiltration have been observed [Roux 2008, Boyle 2005]. Partially infiltrated silica agglomerates are easier to disperse due to the detachment of the rather thick infiltrated layer, which accelerates erosion [Bohin 1996]. But this phenomenon is reversed when the infiltration is important, since in this case, surface tension inside the infiltrated agglomerate is resisting dispersion [Yamada 1997]. Mechanisms other than erosion and rupture have also been studied, like collision [Seyvet 2000], decohesion (cavitation leading to the detachment of fragments) [Astruc 2001], disintegration (explosive destruction of the agglomerate) and cleavage (deformation of a fully penetrated agglomerate like the deformation of a viscous drop) [Roux 2008].

Dispersion occurs when the hydrodynamic forces acting on the flowing agglomerate exceed the cohesion force. Both these two forces have been the subject of numerous studies, with the most advanced ones considering some complex structural morphologies of the agglomerates [Rumpf 1962; Sonntag 1987, Horwatt 1992a; Horwatt 1992b; Thornton 2004; Harada 2006; Zaccone 2009; Weiler 2010]. The hydrodynamic aspects have been approached by simplified models considering forces around a sphere flowing in a Newtonian fluid [Bagster 1974].

Rupture appears when a critical hydrodynamic stress is achieved. The rupture of carbon black agglomerates was observed by rheo-optics above a critical stress proportional to $\eta\dot{\gamma}$ [Rwei 1991] (where η is viscosity and $\dot{\gamma}$ is the shear rate) when the agglomerates are not infiltrated. They ascribed rupture to defects in the structure of the agglomerates. In the case of erosion of carbon black immersed in a viscoelastic matrix [Collin 2005], the evolution of the eroded volume as a function of time follows:

$$\frac{R_0^3 - R(t)^3}{R_0^3} = C \times \dot{\gamma}t \quad (\text{I-1})$$

where C is a constant, R_0 is the initial radius of the agglomerate, $R(t)$ the radius at time t and $\dot{\gamma}$ the applied shear rate. The eroded volume depends on the amount of shear deformation.

However, despite the sophistication of some of the experiments and approaches, there is always a lack of data supporting the impact of the elasticity of the suspended matrix, which is the case in our study in Chapter V, on the carbon black dispersion in cellulose solutions.

I.4.2 Percolation threshold of carbon black (CB) and conductivity

The conductivity of insulating polymer/conductive filler composites varies generally as a function of the filler concentration. In fact, a drastic increase of conductivity (several orders of magnitude) can be observed when the loading of fillers is above a critical value, at which point the fillers will form an “infinite” network capable of transferring electrons in the non-conductive polymer matrix. This phenomenon is percolation, and the critical value is called percolation threshold. Once the loading is well above the percolation threshold, the conductivity will level off and reach a plateau. Such dependence can be illustrated as in Figure I-10.

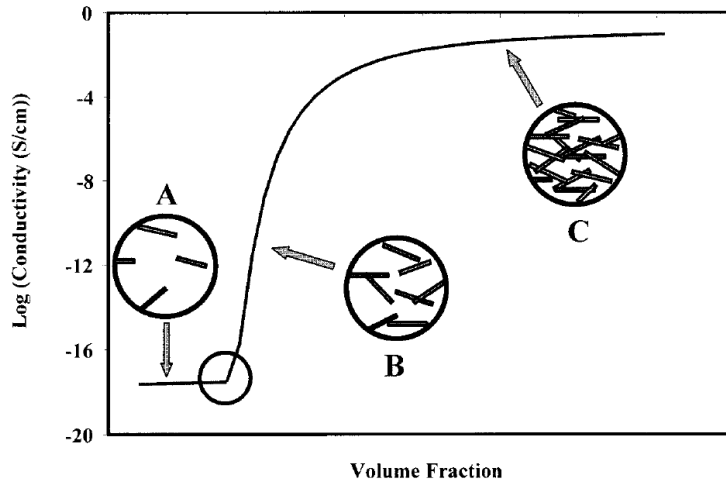


Figure I-10 Specific conductivity as a function of filler volume fraction, and illustrated morphology of filler dispersion at different loadings, with (A) low filler loading, (B) percolation threshold, and (C) high filler loading. Reprinted with permission from [Clingerman 2003]. Copyright (2003) Wiley.

Various models have been proposed by researchers. In a very detailed review by F. Lux, those models were grouped into four types: statistical, thermodynamic, geometrical and structure-oriented ones [Lux 1993]. Among those models, a basic, yet widely used, statistical model was the one proposed by Kirkpatrick and Zallen [Kirkpatrick 1973; Zallen 1983]. In this model, the particles of certain shape are distributed statistically on a regular and finite lattice, and a significant increase of the conductivity is a result of the continuous network formed by particles contacting each other. The estimation of percolation threshold with this classical model was 0.15 [Scher 1970]. Another calculation made by Powell gives the percolation threshold for random packed hard sphere of same size to be 0.183, both in terms of volume fraction [Powell 1979]. A power law relation between the conductivity and the volume fraction of the filler was also proposed in equation I-1:

$$\sigma = \sigma_0 (\phi - \phi_c)^\alpha \quad (\text{I-1})$$

where the composite conductivity σ depends on the constant σ_0 (with value close to the filler conductivity), the difference of filler volume fraction ϕ and percolation threshold ϕ_c , and also the coefficient α , which should theoretically only depend on the dimension of the network.

The experimental values of percolation threshold for composites with different carbon black powders vary in a much larger range than in the theoretical calculation, for example, less than 0.5% for epoxy resin [Schueler 1997], 5% for polypropylene [Yu 2005], about 9% for polyethylene [Hindermann-Bischoff 2001; Yu 2005], and 20 wt% for polyurethane [Li 2000]. These discrepancies can be explained by several factors. In the theoretical prediction, the fillers were considered to be same-sized spheres uniformly and randomly dispersed in the matrix; whereas in practice, the carbon black agglomerates are usually dispersed into smaller units which tend to aggregate. The aggregates are neither spherical nor of same size. Studies of rod-like fillers of different size and different aspect ratios demonstrate that the percolation threshold vary with those two parameters ([Otten 2011]; [Chatterjee 2012], for example), which can shed some light on the polydisperse anisotropy of carbon black aggregates. Another reason is that contrary to the theoretical model, the carbon black particles do not have to contact with each other to be conductive, and electrons can jump over an insulating gap between two neighbouring carbon black particles by quantum tunnelling effect [Sichel 1982]. As a result, a smaller amount of carbon black is necessary.

As we said, efforts have been devoted to reduce the percolation threshold. One approach is to reduce the size of dispersed carbon black. This approach has been proven effective in numerous experimental studies and numerical simulations, see the research of Horibe and Schwartz, for example [Horibe 2005; Schwartz 2000]. Jing and Zhao explained this phenomenon by the reduced distance between particles with decreased particle size, which is in favour of the quantum tunnelling effect and conductivity [Jing 2000]. Also it is worth noting that the decrease of size does not improve the maximum achievable conductivity, as shown in Figure I-11 [Untereker 2009]. The authors explained that the maximum achievable conductivity is only determined by the contact electrical impedance of the particles, but is not size-dependent.

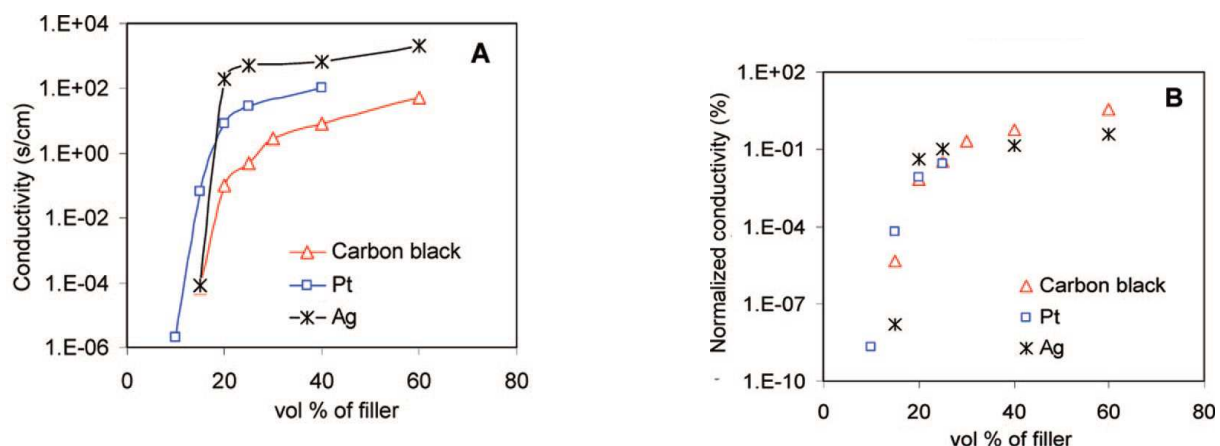


Figure I-11 (a) Conductivity of polymer/filler composites as functions of filler loadings. (b) Composite conductivity normalized to that of the bulk fillers as functions of filler loadings. Reprinted with permission from [Untereker 2009]. Copyright (2009) American Chemical Society.

Different processing methods, other than the traditional “melt and mix”, have also been used to reduce the percolation threshold. Li et al. prepared polystyrene/carbon black composite with in-situ polymerization of styrene [Li 2003]. With this method, the carbon black agglomerates were penetrated by low-molecular-weight monomers, facilitating the formation of carbon black network at lower loading. Moriarty et al. first stabilized carbon black with gum Arabic in aqueous suspension with latex particles, and then obtained latex/carbon black composites with drying [Moriarty 2011]. The percolation threshold was reduced with larger latex particle size. This process is illustrated as Figure I-12.

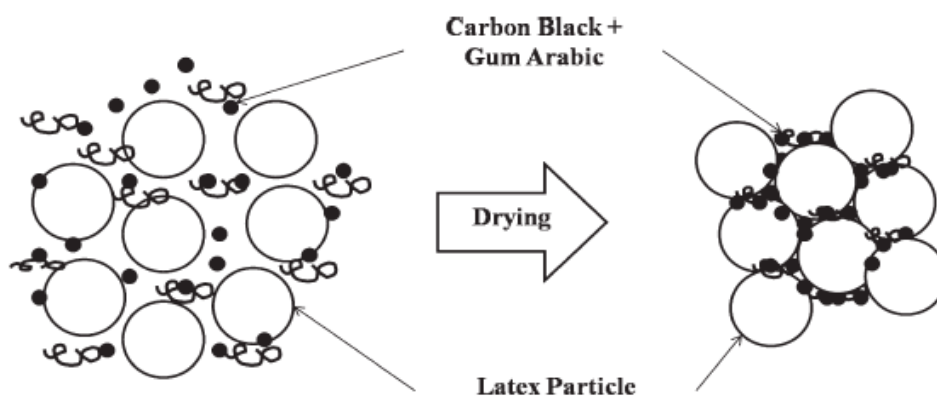


Figure I-12 Stabilization of carbon black by gum Arabic among latex particles, and the network formed after drying. Reprinted with permission from [Moriarty 2011],. Copyright (2011) Wiley.

Mixing carbon black with incompatible polymer blends was also proposed and studied. The different affinity of carbon black with different polymer components results in a selective localization of carbon black in the blends. Carbon black aggregates would distribute either at the interface of the two polymers or preferably in one phase. In the latter case, a double percolation is necessary for the composite to be conductive, which means that not only the CB needs to be above the percolation threshold, but also the polymer phase in which CB locates needs to be percolated too. In both scenarios, the heterogeneous distribution of CB reduces the percolation threshold. Sumita et al. demonstrated this concept nicely by blending every two components of PP, LDPE and PMMA, predicting the localization of CB with interfacial tension, and measuring the reduced percolation threshold [Sumita 1991]. In another example, Al-Saleh and Sundararaj shifted the distribution of CB in PP/PS blends from the PS phase to the interfacial region of the two by adding SBS block polymers, and reduced the percolation threshold by 40% [Al-Saleh 2008].

Inspired by the incompatible polymer blends composites, one of our preliminary approaches in the preparation of cellulose/CB composites was to mix cellulose of different chain lengths, and try to reduce the CB loading from the “immiscibility” of the two types of cellulose.

Reference

- [Aaltonen 2009] Aaltonen, O., & Jauhiainen, O. (2009). The preparation of lignocellulosic aerogels from ionic liquid solutions. *Carbohydrate Polymers*, 75(1), 125-129.
- [Agoda 2012] Agoda-Tandjawa, G., Durand, S., Gaillard, C., Garnier, C., & Doublier, J. L. (2012). Properties of cellulose/pectins composites: Implication for structural and mechanical properties of cell wall. *Carbohydrate Polymers*, 90(2), 1081-1091.
- [Alfaya 1999] Alfaya, R. V. S., & Gushikem, Y. (1999). Aluminium oxide coated cellulose fibers modified with n-propylpyridinium chloride silsesquioxane polymer: Preparation, characterization, and adsorption of some metal halides from ethanol solution. *Journal of Colloid and Interface Science*, 213(2), 438-444.
- [Al-Saleh 2008] Al-Saleh, M. H., & Sundararaj, U. (2008). An innovative method to reduce percolation threshold of carbon black filled immiscible polymer blends. *Composites Part a-Applied Science and Manufacturing*, 39(2), 284-293.
- [ASTM D1795] ASTM Standard D1795. (2007). Standard Test Method for Intrinsic Viscosity of Cellulose. ASTM International, West Conshohocken, PA, doi: 10.1520/d1795-96r07e01, www.astm.org.
- [ASTM D4243] ASTM Standard D4243. (2009). Standard Test Method for Measurement of Average Viscometric Degree of Polymerization of New and Aged Electrical Papers and Boards. ASTM International, West Conshohocken, PA, doi: 10.1520/d4243-99r09, www.astm.org.
- [Astruc 2001] Astruc, M. (2001). Etude rhéo-optique de la morphologie de mélanges concentrés de polymères immiscibles et de polymères chargés en noir de carbone. Thèse de doctorat. Ecole des Mines de Paris, Sophia-Antipolis.
- [Averous 2001] Averous, L., Fringant, C., & Moro, L. (2001). Plasticized starch-cellulose interactions in polysaccharide composites. *Polymer*, 42(15), 6565-6572.
- [Bagster 1974] Bagster, D. F., & Tomi, D. (1974). The stresses within a sphere in simple flow fields. *Chemical Engineering Science*, 29, 1773-1783.
- [Barthel 2006] Barthel, S., & Heinze, T. (2006). Acylation and carbanilation of cellulose in ionic liquids. *Green Chemistry*, 8(3), 301-306.
- [Boerstoel 2001] Boerstoel, H., Maatman, H., Westerink, J. B., & Koenders, B. M. (2001). Liquid crystalline solutions of cellulose in phosphoric acid. *Polymer*, 42(17), 7371-7379.
- [Bohin 1996] Bohin, F., Manas-Zloczower, I., & Feke, D. L. (1996). Kinetics of dispersion for sparse agglomerates in simple shear flows: Application to silica agglomerates in silicone polymers. *Chemical Engineering Science*, 51(23), 5193-5204.
- [Bolen 1958] Bolen, W. R., & Colwell, R. E. (1958). Intensive mixing. *Society of Plastics Engineers Journal*, 14(8), 24-28.
- [Boyle 2005] Boyle, J. F., Manas-Zloczower, I., & Feke, D. L. (2005). Hydrodynamic analysis of the mechanisms of agglomerate dispersion. *Powder Technology*, 153(2), 127-133.
- [Brouwers 2009] Brouwers, J., Brewster, M. E., & Augustijns, P. (2009). Supersaturating Drug Delivery Systems: The Answer to Solubility-Limited Oral Bioavailability? *Journal of Pharmaceutical Sciences*, 98(8), 2549-2572.
- [Buijtenhuijs 1986] Buijtenhuijs, F. A., Abbas, M., & Witteveen, A. J. (1986). The degradation and stabilization of cellulose dissolved in *N*-methylmorpholine-*N*-oxide (NMMO). *Papier*, 40(12), 615-619.
- [Builders 2010] Builders, P. F., Bonaventure, A. M., Tiwalade, A., Okpako, L. C., & Attama, A. A. (2010).

Novel multifunctional pharmaceutical excipients derived from microcrystalline cellulose-starch microparticulate composites prepared by compatibilized reactive polymer blending. *International Journal of Pharmaceutics*, 388(1-2), 159-167.

[Cai 2007a] Cai, J., Wang, L. X., & Zhang, L. N. (2007a). Influence of coagulation temperature on pore size and properties of cellulose membranes prepared from NaOH-urea aqueous solution. *Cellulose*, 14(3), 205-215.

[Cai 2005] Cai, J., & Zhang, L. (2005). Rapid dissolution of cellulose in LiOH/Urea and NaOH/Urea aqueous solutions. *Macromolecular Bioscience*, 5(6), 539-548.

[Cai 2006] Cai, J., & Zhang, L. (2006). Unique gelation behavior of cellulose in NaOH/Urea aqueous solution. *Biomacromolecules*, 7(1), 183-189.

[Cai 2008] Cai, J., Zhang, L., Liu, S. L., Liu, Y. T., Xu, X. J., Chen, X. M., Chu, B., Guo, X. L., Xu, J., Cheng, H., Han, C. C., & Kuga, S. (2008). Dynamic Self-Assembly Induced Rapid Dissolution of Cellulose at Low Temperatures. *Macromolecules*, 41(23), 9345-9351.

[Cai 2007b] Cai, J., Zhang, L. N., Zhou, J. P., Qi, H. S., Chen, H., Kondo, T., Chen, X. M., & Chu, B. (2007b). Multifilament fibers based on dissolution of cellulose in NaOH/urea aqueous solution: Structure and properties. *Advanced Materials*, 19(6), 821-825.

[Cai 2010a] Cai, T., Zhang, H., Guo, Q., Shao, H., & Hu, X. (2010a). Structure and Properties of Cellulose Fibers from Ionic Liquids. *Journal of Applied Polymer Science*, 115(2), 1047-1053.

[Cai 2009] Cai, Z., & Kim, J. (2009). Cellulose-Chitosan Interpenetrating Polymer Network for Electro-Active Paper Actuator. *Journal of Applied Polymer Science*, 114(1), 288-297.

[Cai 2010b] Cai, Z., & Kim, J. (2010b). Bacterial cellulose/poly(ethylene glycol) composite: characterization and first evaluation of biocompatibility. *Cellulose*, 17(1), 83-91.

[Cao 2010] Cao, Y., Li, H. Q., Zhang, Y., Zhang, J., & He, J. S. (2010). Structure and Properties of Novel Regenerated Cellulose Films Prepared from Cornhusk Cellulose in Room Temperature Ionic Liquids. *Journal of Applied Polymer Science*, 116(1), 547-554.

[Celanese 1925] British Celanese. (1925). GB Patent 263810.

[Chang 2010a] Chang, C. Y., Duan, B., Cai, J., & Zhang, L. N. (2010a). Superabsorbent hydrogels based on cellulose for smart swelling and controllable delivery. *European Polymer Journal*, 46(1), 92-100.

[Chang 2009] Chang, C. Y., Lue, A., & Zhang, L. (2008). Effects of crosslinking methods on structure and properties of cellulose/PVA hydrogels. *Macromolecular Chemistry and Physics*, 209(12), 1266-1273.

[Chang 2010b] Chang, P. R., Jian, R., Zheng, P., Yu, J., & Ma, X. (2010b). Preparation and properties of glycerol plasticized-starch (GPS)/cellulose nanoparticle (CN) composites. *Carbohydrate Polymers*, 79(2), 301-305.

[Chatterjee 2012] Chatterjee, A. P. (2012). A Remark Concerning Percolation Thresholds in Polydisperse Systems of Finite-Diameter Rods. *Journal of Statistical Physics*, 146(1), 244-248.

[Clingerman 2003] Clingerman, M. L., Weber, E. H., King, J. A., & Schulz, K. H. (2003). Development of an additive equation for predicting the electrical conductivity of carbon-filled composites. *Journal of Applied Polymer Science*, 88(9), 2280-2299.

[Collier 2009] Collier, J. R., Watson, J. L., Collier, B. J., & Petrovan, S. (2009). Rheology of 1-Butyl-3-Methylimidazolium Chloride Cellulose Solutions. II. Solution Character and Preparation. *Journal of Applied Polymer Science*, 111(2), 1019-1027.

[Collin 2004] Collin, V. (2004). Etude rhéo-optique des mécanismes de dispersion du noir de carbone dans des élastomères. Thèse de doctorat. Ecole des Mines de Paris, Sophia-Antipolis.

- [Collin 2005] Collin, V., & Peuvrel-Disdier, E. (2005). Dispersion mechanisms of carbon black in an elastomer matrix. *Elastomery*, 9, 9-15.
- [Cotten 1984] Cotten, G. R. (1984). Mixing of carbon-black with rubber. 1. Measurement of dispersion rate by changes in mixing torque. *Rubber Chemistry and Technology*, 57(1), 118-133.
- [Cuissinat 2006] Cuissinat, C., & Navard, P. (2006). Swelling and dissolution of cellulose Part 1: Free floating cotton and wood fibres in N-methylmorpholine-N-oxide-water mixtures. *Macromolecular Symposia*, 244, 1-18.
- [Da Roz 2010] Da Roz, A. L., Leite, F. L., Pereira, L. V., Nascente, P. A. P., Zucolotto, V., Oliveira, O. N., & Carvalho, A. J. F. (2010). Adsorption of chitosan on spin-coated cellulose films. *Carbohydrate Polymers*, 80(1), 65-70.
- [Davidson 1934] Davidson, G. F. (1934). The dissolution of chemically modified cotton cellulose in alkaline solutions. Part I: In solutions of NaOH, particularly at T°C below the normal. *Journal of Textile Industry*, 25, 174-196.
- [Davidson 1936] Davidson, G. F. (1936). The dissolution of chemically modified cotton cellulose in alkaline solutions. Part II: A comparison of the solvent action of solutions of Lithium, Sodium, Potassium and tetramethylammonium hydroxides. *Journal of Textile Industry*, 27, 112-130.
- [Davidson 1937] Davidson, G. F. (1937). The dissolution of chemically modified cotton cellulose in alkaline solutions. Part III: In solutions of Sodium and Potassium hydroxyde containing dissolved Zinc, Beryllium and Aluminium oxides. *Journal of Textile Industry*, 28, 27-44.
- [Delhom 2010] Delhom, C. D., White-Ghoorahoo, L. A., & Pang, S. S. (2010). Development and characterization of cellulose/clay nanocomposites. *Composites Part B-Engineering*, 41(6), 475-481.
- [Deng 2009] Deng, M., Zhou, Q., Du, A., van Kasteren, J., & Wang, Y. (2009). Preparation of nanoporous cellulose foams from cellulose-ionic liquid solutions. *Materials Letters*, 63(21), 1851-1854.
- [Dogan 2010a] Dogan, H., & Hilmioglu, N. D. (2010a). Chitosan coated zeolite filled regenerated cellulose membrane for dehydration of ethylene glycol/water mixtures by pervaporation. *Desalination*, 258(1-3), 120-127.
- [Dogan 2010b] Dogan, H., & Hilmioglu, N. D. (2010b). Zeolite-filled regenerated cellulose membranes for pervaporative dehydration of glycerol. *Vacuum*, 84(9), 1123-1132.
- [Duchemin 2009] Duchemin, B. J. C., Mathew, A. P., & Oksman, K. (2009). All-cellulose composites by partial dissolution in the ionic liquid 1-butyl-3-methylimidazolium chloride. *Composites Part a-Applied Science and Manufacturing*, 40(12), 2031-2037.
- [Duchemin 2010] Duchemin, B. J. C., Staiger, M. P., Tucker, N., & Newman, R. H. (2010). Aerocellulose Based on All-Cellulose Composites. *Journal of Applied Polymer Science*, 115(1), 216-221.
- [Dufresne 2000] Dufresne, A., Dupeyre, D., & Vignon, M. R. (2000). Cellulose microfibrils from potato tuber cells: Processing and characterization of starch-cellulose microfibril composites. *Journal of Applied Polymer Science*, 76(14), 2080-2092.
- [Dufresne 1998] Dufresne, A., & Vignon, M. R. (1998). Improvement of starch film performances using cellulose microfibrils. *Macromolecules*, 31(8), 2693-2696.
- [Egal 2007] Egal, M., Budtova, T., & Navard, P. (2007). Structure of aqueous solutions of microcrystalline cellulose/sodium hydroxide below 0°C and the limit of cellulose dissolution. *Biomacromolecules*, 8(7), 2282-2287.
- [Egal 2008] Egal, M., Budtova, T., & Navard, P. (2008). The dissolution of microcrystalline cellulose in sodium hydroxide-urea aqueous solutions. *Cellulose*, 15(3), 361-370.

- [El Seoud 2007] El Seoud, O. A., Koschella, A., Fidale, L. C., Dorn, S., & Heinze, T. (2007). Applications of ionic liquids in carbohydrate chemistry: A window of opportunities. *Biomacromolecules*, 8(9), 2629-2647.
- [Endo 1999] Endo, T., Kitagawa, R., Zhang, F., Hirotsu, T., & Hosokawa, J. (1999). Mechano-chemical preparation of novel cellulose-poly(ethylene glycol) composite. *Chemistry Letters*(11), 1155-1156.
- Esteves Magalhaes, W. L., Cao, X., Ramires, M. A., & Lucia, L. A. (2011). Novel all-cellulose composite displaying aligned cellulose nanofibers reinforced with cellulose nanocrystals. *Tappi Journal*, 10(4),19-25.
- [Fernandes 2010] Fernandes, S. C. M., Freire, C. S. R., Silvestre, A. J. D., Pascoal Neto, C., Gandini, A., Berglund, L. A., & Salmen, L. (2010). Transparent chitosan films reinforced with a high content of nanofibrillated cellulose. *Carbohydrate Polymers*, 81(2), 394-401.
- [Franks 1979] Franks, N. A., & Varga, J. K. (1979). Process for making precipitated cellulose. US Patent 4,145,532.
- [Freire 2011] Freire, M. G., Teles, A. R. R., Ferreira, R. A. S., Carlos, L. D., Lopes-da-Silva, J. A., & Coutinho, J. A. P. (2011). Electrospun nanosized cellulose fibers using ionic liquids at room temperature. *Green Chemistry*, 13(11), 3173-3180.
- [Frey 2006] Frey, M. W., Li, L., Xiao, M., & Gould, T. (2006). Dissolution of cellulose in ethylene diamine/salt solvent systems. *Cellulose*, 13(2), 147-155.
- [Fugetsu 2008] Fugetsu, B., Sano, E., Sunada, M., Sambongi, Y., Shibuya, T., Wang, X. S., & Hiraki, T. (2008). Electrical conductivity and electromagnetic interference shielding efficiency of carbon nanotube/cellulose composite paper. *Carbon*, 46(9), 1256-1258.
- [Garcia-Ramirez 1994] Garcia-Ramirez, M., Cavaille, J. Y., Dupeyre, D., & Peguy, A. (1994). Cellulose-polyamide-66 blends. 1. Processing and characterization. *Journal of Polymer Science Part B-Polymer Physics*, 32(8), 1437-1448.
- [Garcia-Ramirez 1995] Garcia-Ramirez, M., Cavaille, J. Y., Dufresne, A., & Tekely, P. (1995). Cellulose-polyamide-66 blends. 2. Mechanical-behavior. *Journal of Polymer Science Part B-Polymer Physics*, 33(15), 2109-2124.
- [Gavillon 2008] Gavillon, R., & Budtova, T. (2008). Aerocellulose: New highly porous cellulose prepared from cellulose-NaOH aqueous solutions. *Biomacromolecules*, 9(1), 269-277.
- [Gawryla 2009] Gawryla, M. D., van den Berg, O., Weder, C., & Schiraldi, D. A. (2009). Clay aerogel/cellulose whisker nanocomposites: a nanoscale wattle and daub. *Journal of Materials Chemistry*, 19(15), 2118-2124.
- [Gea 2010] Gea, S., Reynolds, C. T., Roohpur, N., Soykeabkaew, N., Wirjosentono, B., Bilotti, E., & Peijs, T. (2010). Biodegradable Composites Based on Poly(epsilon-Caprolactone) and Bacterial Cellulose as a Reinforcing Agent. *Journal of Biobased Materials and Bioenergy*, 4(4), 384-390.
- [Gericke 2011] Gericke, M., Liebert, T., El Seoud, O. A., & Heinze, T. (2011). Tailored Media for Homogeneous Cellulose Chemistry: Ionic Liquid/Co-Solvent Mixtures. *Macromolecular Materials and Engineering*, 296(6), 483-493.
- [Gericke 2009a] Gericke, M., Liebert, T., & Heinze, T. (2009a). Interaction of Ionic Liquids with Polysaccharides, 8-Synthesis of Cellulose Sulfates Suitable for Polyelectrolyte Complex Formation. *Macromolecular Bioscience*, 9(4), 343-353.
- [Gericke 2009b] Gericke, M., Schlufte, K., Liebert, T., Heinze, T., & Budtova, T. (2009b). Rheological Properties of Cellulose/Ionic Liquid Solutions: From Dilute to Concentrated States. *Biomacromolecules*, 10(5), 1188-1194.

- [Gindl-Altmutter 2012] Gindl-Altmutter, W., Keckes, J., Plackner, J., Liebner, F., Englund, K., & Laborie, M. P. (2012). All-cellulose composites prepared from flax and lyocell fibres compared to epoxy-matrix composites. *Composites Science and Technology*, 72(11), 1304-1309.
- [Glasser 1998] Glasser, W. G., Rials, T. G., Kelley, S. S., & Dave, V. (1998). Studies of the molecular interactions between cellulose and lignin as a model for the hierarchical structure of wood. In: Heinze, T. J., & Glasser, W. G. (eds) Cellulose derivatives. Modification, characterization and nanostructures. ACS Symposium series 688, Chapter 19. Orlando, pp 265–282.
- [Graenacher 1934] Graenacher, C. (1934). Cellulose Solution. U.S. Patent 1,943,176.
- [Gupta 2011] Gupta, K. M., Hu, Z., & Jiang, J. (2011). Mechanistic understanding of interactions between cellulose and ionic liquids: A molecular simulation study. *Polymer*, 52(25), 363-366.
- [Hablot 2010a] Hablot, E., Matadi, R., Ahzi, S., & Averous, L. (2010a). Renewable biocomposites of dimer fatty acid-based polyamides with cellulose fibres: Thermal, physical and mechanical properties. *Composites Science and Technology*, 70(3), 504-509.
- [Hablot 2010b] Hablot, E., Matadi, R., Ahzi, S., Vaudemond, R., Ruch, D., & Averous, L. (2010b). Yield behaviour of renewable biocomposites of dimer fatty acid-based polyamides with cellulose fibres. *Composites Science and Technology*, 70(3), 525-529.
- [Han 2010] Han, D., & Yan, L. (2010). Preparation of all-cellulose composite by selective dissolving of cellulose surface in PEG/NaOH aqueous solution. *Carbohydrate Polymers*, 79(3).
- [Harada 2006] Harada, S., Tanaka, R., Nogami, H., & Sawada, M. (2006). Dependence of fragmentation behavior of colloidal aggregates on their fractal structure. *Journal of Colloid and Interface Science*, 301(1), 123-129.
- [Hardelin 2012] Hardelin, L., Thunberg, J., Perzon, E., Westman, G., Walkenstrom, P., & Gatenholm, P. (2012). Electrospinning of cellulose nanofibers from ionic liquids: The effect of different cosolvents. *Journal of Applied Polymer Science*, 125(3).
- [Harrison 1928] Harrison, W. (1928). Manufacture of carbohydrate derivatives. US Patent 1,684, 732.
- [Hasegawa 1994] Hasegawa, M., Isogai, A., Kuga, S., & Onabe, F. (1994). Preparation of cellulose chitosan blend film using chloral dimethylformamide. *Polymer*, 35(5), 983-987.
- [Hasegawa 1992] Hasegawa, M., Isogai, A., Onabe, F., Usuda, M., & Atalla, R. H. (1992). Characterization of cellulose chitosan blend films. *Journal of Applied Polymer Science*, 45(11), 1873-1879.
- [Haward 2102] Haward, S. J., Sharma, V., Butts, C. P., McKinley, G. H., & Rahatekar, S. S. (2012). Shear and Extensional Rheology of Cellulose/Ionic Liquid Solutions. *Biomacromolecules*, 13(5), 1688-1699.
- [He 2009] He, C. J., Ma, B. M., & Sun, J. F. (2009). The Preparation and Properties of Cellulose/Chitin Blend Filaments. *Journal of Applied Polymer Science*, 113(5), 2777-2784.
- [He 2002] He, C. J., Pang, F. J., & Wang, Q. R. (2002). Properties of cellulose/PAN blend membrane. *Journal of Applied Polymer Science*, 83(14), 3105-3111.
- [Heinrich 2002] Heinrich, G., Kluppel, M., & Vilgis, T. A. (2002). Reinforcement of elastomers. *Current Opinion in Solid State & Materials Science*, 6(3), 195-203.
- [Heinze 2000] Heinze, T., Dicke, R., Koschella, A., Kull, A. H., Klohr, E. A., & Koch, W. (2000). Effective preparation of cellulose derivatives in a new simple cellulose solvent. *Macromolecular Chemistry and Physics*, 201(6), 627-631.
- [Hindermann 2001] Hindermann-Bischoff, M., & Ehrburger-Dolle, F. (2001). Electrical conductivity of carbon black-polyethylene composites - Experimental evidence of the change of cluster connectivity in the PTC effect. *Carbon*, 39(3), 375-382.

- [Hirana 1998] Hirano, S., Usutani, A., Yoshikawa, M., & Midorikawa, T. (1998). Fiber preparation of N-acylchitosan and its cellulose blend by spinning their aqueous xanthate solutions. *Carbohydrate Polymers*, 37(3), 311-313.
- [Hofmann 2008] Hofmann, I., Haas, D., Eckert, A., Ruf, H., Firgo, H., Muller, F. A., & Greil, P. (2008). Mechanical properties of cellulose-apatite composite fibres for biomedical applications. *Advances in Applied Ceramics*, 107(5), 293-297.
- [Horibe 2005] Horibe, H., Kamimura, T., & Yoshida, K. (2005). Electrical conductivity of polymer composites filled with carbon black. *Japanese Journal of Applied Physics Part 1-Regular Papers Brief Communications & Review Papers*, 44(4A), 2025-2029.
- [Horwatt 1992a] Horwatt, S. W., Feke, D. L., & Manas-Zloczower, I. (1992a). The influence of structural heterogeneities on the cohesivity and breakup of agglomerates in simple shear-flow. *Powder Technology*, 72(2), 113-119.
- [Horwatt 1992b] Horwatt, S. W., Manas-Zloczower, I., & Feke, D. L. (1992b). Dispersion behaviour of heterogeneous agglomerates at supercritical stresses. *Chemical Engineering Science*, 47(8), 1849-1855.
- [Hu 2010] Hu, X. Y., Hu, K., Zeng, L. L., Zhao, M. M., & Huang, H. H. (2010). Hydrogels prepared from pineapple peel cellulose using ionic liquid and their characterization and primary sodium salicylate release study. *Carbohydrate Polymers*, 82(1), 62-68.
- [Huber 2012] Huber, T., Muessig, J., Curnow, O., Pang, S., Bickerton, S., & Staiger, M. P. (2012). A critical review of all-cellulose composites. *Journal of Materials Science*, 47(3), 1171-1186.
- [Imai 2010] Imai, M., Akiyama, K., Tanaka, T., & Sano, E. (2010). Highly strong and conductive carbon nanotube/cellulose composite paper. *Composites Science and Technology*, 70(10), 1564-1570.
- [Innerlohinger 2006] Innerlohinger, J., Weber, H. K., & Kraft, G. (2006). Aerocellulose: Aerogels and aerogel-like materials made from cellulose. *Macromolecular Symposia*, 244.
- [Isogai 1992] Isogai, A., & Atalla, R. H. (1992). Preparation of cellulose-chitosan polymer blends. *Carbohydrate Polymers*, 19(1), 25-28.
- [Isogai 1998] Isogai, A., & Atalla, R. H. (1998). Dissolution of cellulose in aqueous NaOH solutions. *Cellulose*, 5(4), 309-319.
- [Jia 2011] Jia, N., Li, S. M., Ma, M. G., Zhu, J. F., & Sun, R. C. (2011). Synthesis and characterization of cellulose-silica composite fiber in ethanol/water mixed solvents. *Bioresources*, 6(2), 1186-1195.
- [Jiang 2012] Jiang, G. S., Yuan, Y., Wang, B. C., Yin, X. M., Mukuze, K. S., Huang, W. F., Zhang, Y. M., & Wang, H. P. (2012). Analysis of regenerated cellulose fibers with ionic liquids as a solvent as spinning speed is increased. *Cellulose*, 19(4), 1075-1083.
- [Jin 2007] Jin, H., Zha, C., & Gu, L. (2007). Direct dissolution of cellulose in NaOH/thiourea/urea aqueous solution. *Carbohydrate Research*, 342(6), 851-858.
- [Jin 2010] Jin, Z. W., Wang, S., Wang, J. Q., & Xu, M. (2010). The Fabrication and Characterization of Cellulose/Mesoporous Silica Composites Packaging Films with Adjustable Permeability by NMMO Technology. *Polymer-Plastics Technology and Engineering*, 49(13), 1371-1377.
- [Jin 2012] Jin, Z. W., Wang, S., Wang, J. Q., & Zhao, M. X. (2012). Effects of plasticization conditions on the structures and properties of cellulose packaging films from ionic liquid BMIMCl. *Journal of Applied Polymer Science*, 125(1), 704-709.
- [Jing 2000] Jing, X., Zhao, W., & Lan, L. (2000). The effect of particle size on electric conducting percolation threshold in polymer/conducting particle composites. *Journal of Materials Science Letters*, 19(5),

377-379.

[John 2011] John, A., Ko, H. U., Kim, D. G., & Kim, J. (2011). Preparation of cellulose-ZnO hybrid films by a wet chemical method and their characterization. *Cellulose*, 18(3), 675-680.

[Johnson 1969] Johnson, D. L. (1969). Compounds dissolved in cyclic amine oxides. US Patent 3,447,939.

[Kadokawa 2009] Kadokawa, J.-i., Murakami, M.-a., Takegawa, A., & Kaneko, Y. (2009). Preparation of cellulose-starch composite gel and fibrous material from a mixture of the polysaccharides in ionic liquid. *Carbohydrate Polymers*, 75(1), 180-183.

[Kahlen 2010] Kahlen, J., Masuch, K., & Leonhard, K. (2010). Modelling cellulose solubilities in ionic liquids using COSMO-RS. *Green Chemistry*, 12(12), 2172-2181.

[Kamide 1992] Kamide, K., Okajima, K., & Kowsaka, K. (1992). Dissolution of natural cellulose into aqueous alkali solution - role of super-molecular structure of cellulose. *Polymer Journal*, 24(1), 71-96.

[Kamide 1984] Kamide, K., Okajima, K., Matsui, T., & Kowsaka, K. (1984). Study on the solubility of cellulose in aqueous alkali solution by deuteration IR and C-13 NMR. *Polymer Journal*, 16(12), 857-866.

[Kamide 1987a] Kamide, K., & Saito, M. (1987a). Cellulose and cellulose derivatives – recent advances in physical-chemistry. *Advances in Polymer Science*, 83, 1-56.

[Kamide 1987b] Kamide, K., Saito, M., & Kowsaka, K. (1987b). Temperature-dependence of limiting viscosity number and radius of gyration for cellulose dissolved in aqueous 8-percent sodium-hydroxide solution. *Polymer Journal*, 19(10), 1173-1181.

[Kemell 2005] Kemell, M., Pore, V., Ritala, M., Leskela, M., & Linden, M. (2005). Atomic layer deposition in nanometer-level replication of cellulosic substances and preparation of photocatalytic TiO₂/cellulose composites. *Journal of the American Chemical Society*, 127(41), 14178-14179.

[Kihlman 2011] Kihlman, M., Wallberg, O., Stigsson, L., & Germgard, U. (2011). Dissolution of dissolving pulp in alkaline solvents after steam explosion pretreatments. *Holzforchung*, 65(4), 613-617.

[Kim 2010] Kim, D.-H., Park, S.-Y., Kim, J., & Park, M. (2010). Preparation and Properties of the Single-Walled Carbon Nanotube/Cellulose Nanocomposites Using N-methylmorpholine-N-oxide Monohydrate. *Journal of Applied Polymer Science*, 117(6), 3588-3594.

[Kim 2009] Kim, K. J., & White, J. L. (2009). Relationship Between Interfacial Adhesion and Viscosity of Cellulose Fiber Filled Polypropylene and Poly(epsilon-caprolactone): A Review. *Composite Interfaces*, 16(7-9), 583-598.

[Kirkpatrick 1973] Kirkpatrick, S. (1973). Percolation and Conduction. *Reviews of Modern Physics*, 45(4), 574-588.

[Koehler 2007] Koehler, S., & Heinze, T. (2007). Efficient synthesis of cellulose furoates in 1-N-butyl-3-methylimidazolium chloride. *Cellulose*, 14(5), 489-495.

[Kosan 2008] Kosan, B., Michels, C., & Meister, F. (2008). Dissolution and forming of cellulose with ionic liquids. *Cellulose*, 15(1), 59-66.

[Kuang 2008] Kuang, Q.-L., Zhao, J.-C., Niu, Y.-H., Zhang, J., & Wang, Z.-G. (2008). Celluloses in an ionic liquid: the rheological properties of the solutions spanning the dilute and semidilute regimes. *Journal of Physical Chemistry B*, 112(33), 10234-10240.

[Kumar 2008] Kumar, A. P., & Singh, R. P. (2008). Biocomposites of cellulose reinforced starch: Improvement of properties by photo-induced crosslinking. *Bioresource Technology*, 99(18), 8803-8809.

[Kumar 2000] Kumar, M. (2000). A review of chitin and chitosan applications. *Reactive & Functional Polymers*, 46(1), 1-27.

[Laszkiewicz 1998] Laszkiewicz, B. (1998). Solubility of bacterial cellulose and its structural properties. *Journal of Applied Polymer Science*, 67(11), 1871-1876.

[Laszkiewicz 1993] Laszkiewicz, B., & Cuculo, J. A. (1993). SOLUBILITY OF CELLULOSE-III IN SODIUM-HYDROXIDE SOLUTION. *Journal of Applied Polymer Science*, 50(1), 27-34.

[Lateef 2009] Lateef, H., Grimes, S., Kewcharoenwong, P., & Feinberg, B. (2009). Separation and recovery of cellulose and lignin using ionic liquids: a process for recovery from paper-based waste. *Journal of Chemical Technology and Biotechnology*, 84(12), 1818-1827.

[Lazarin 2000] Lazarin, A. M., Gushikem, Y., & de Castro, S. C. (2000). Cellulose aluminium oxide coated with organofunctional groups containing nitrogen donor atoms. *Journal of Materials Chemistry*, 10(11), 2526-2531.

[Le 2012] Le, K. A., Sescousse, R., & Budtova, T. (2012). Influence of water on cellulose-EMIMAc solution properties: a viscometric study. *Cellulose*, 19(1), 45-54.

[Li 2005] Li, D. P., & Sun, G. (2005). Direct coloration of cellulose with carbon black nanoparticles. *Abstracts of Papers of the American Chemical Society*, 229, U282-U282.

[Li 2000] Li, F. K., Qi, L. Y., Yang, J. P., Xu, M., Luo, X. L., & Ma, D. Z. (2000). Polyurethane/conducting carbon black composites: Structure, electric conductivity, strain recovery behavior; and their relationships. *Journal of Applied Polymer Science*, 75(1), 68-77.

[Li 2003] Li, J. R., Xu, J. R., Zhang, M. Q., & Rong, M. Z. (2003). Carbon black/polystyrene composites as candidates for gas sensing materials. *Carbon*, 41(12), 2353-2360.

[Li 2009a] Li, L., Lin, Z. B., Yang, X., Wan, Z. Z., & Cui, S. X. (2009a). A novel cellulose hydrogel prepared from its ionic liquid solution. *Chinese Science Bulletin*, 54(9), 1622-1625.

[Li 2009b] Li, Q., Zhou, J. P., & Zhang, L. N. (2009b). Structure and Properties of the Nanocomposite Films of Chitosan Reinforced with Cellulose Whiskers. *Journal of Polymer Science Part B-Polymer Physics*, 47(11), 1069-1077.

[Li 2011] Li, X. L., Zhu, L. P., Zhu, B. K., & Xu, Y. Y. (2011). High-flux and anti-fouling cellulose nanofiltration membranes prepared via phase inversion with ionic liquid as solvent. *Separation and Purification Technology*, 83, 66-73.

[Liang 2008] Liang, S. M., Wu, J. J., Tian, H. F., Zhang, L. N., & Xu, J. (2008). High-Strength Cellulose/Poly(ethylene glycol) Gels. *Chemosuschem*, 1(6), 558-563.

[Liang 2007] Liang, S. M., Zhang, L., & Xu, H. (2007). Morphology and permeability of cellulose/chitin blend membranes. *Journal of Membrane Science*, 287(1), 19-28.

[Liang 1995] Liang, X. H., Guo, Y. Q., Gu, L. Z., & Ding, E. Y. (1995). Crystalline-amorphous phase-transition of a poly(ethylene glycol) cellulose blend. *Macromolecules*, 28(19), 6551-6555.

[Liebert 2009] Liebert, T. (2009). Cellulose Solvents - Remarkable History, Bright Future. *Cellulose Solvents: for Analysis, Shaping and Chemical Modification*, 1033.

[Liebner 2009] Liebner, F., Haimer, E., Potthast, A., Loidl, D., Tschegg, S., Neouze, M.-A., Wendland, M., & Rosenau, T. (2009). Cellulosic aerogels as ultra-lightweight materials. Part 2: Synthesis and properties. *Holzforchung*, 63(1), 3-11.

[Liebner 2008] Liebner, F., Potthast, A., Rosenau, T., Haimer, E., & Wendland, M. (2008). Cellulose aerogels: Highly porous, ultra-lightweight materials. *Holzforchung*, 62(2), 129-135.

[Liu 2012a] Liu, A. D., & Berglund, L. A. (2012). Clay nanopaper composites of nacre-like structure based on montmorillonite and cellulose nanofibers-Improvements due to chitosan addition. *Carbohydrate*

Polymers, 87(1), 53-60.

[Liu 2011a] Liu, A. D., Walther, A., Ikkala, O., Belova, L., & Berglund, L. A. (2011a). Clay Nanopaper with Tough Cellulose Nanofiber Matrix for Fire Retardancy and Gas Barrier Functions. *Biomacromolecules*, 12(3), 633-641.

[Liu 2008] Liu, S. L., Zhang, L., Zhou, J. P., & Wu, R. X. (2008). Structure and properties of cellulose/Fe₂O₃ nanocomposite fibers spun via an effective pathway. *Journal of Physical Chemistry C*, 112(12), 4538-4544.

[Liu 2011b] Liu, S. L., Zhou, J. P., & Zhang, L. N. (2011b). In situ synthesis of plate-like Fe₂O₃ nanoparticles in porous cellulose films with obvious magnetic anisotropy. *Cellulose*, 18(3), 663-673.

[Liu 2011c] Liu, Z., Wang, H., Li, Z. X., Lu, X. M., Zhang, X. P., Zhang, S. J., & Zhou, K. B. (2011c). Characterization of the regenerated cellulose films in ionic liquids and rheological properties of the solutions. *Materials Chemistry and Physics*, 128(1-2), 220-227.

[Lu 2011a] Lu, A., Liu, Y., Zhang, L., & Potthast, A. (2011a). Investigation on Metastable Solution of Cellulose Dissolved in NaOH/Urea Aqueous System at Low Temperature. *Journal of Physical Chemistry B*, 115(44), 12801-12808.

[Lu 2011b] Lu, X. W., Li, L., Lin, Z. B., & Cui, S. X. (2011b). Formation mechanism of ionic liquid-reconstituted cellulose hydrogels and their application in gel electrophoresis. *Acta Polymerica Sinica*(9), 1026-1032.

[Lue 2011] Lue, A., Liu, Y., Zhang, L., & Potthast, A. (2011). Light scattering study on the dynamic behaviour of cellulose inclusion complex in LiOH/urea aqueous solution. *Polymer*, 52(17), 3857-3864.

[Lue 2008] Lue, A., & Zhang, L. (2008). Investigation of the scaling law on cellulose solution prepared at low temperature. *Journal of Physical Chemistry B*, 112(15), 4488-4495.

[Lux 1993] Lux, F. (1993). Models proposed to explain the electrical-conductivity of mixtures made of conductive and insulating materials. *Journal of Materials Science*, 28(2), 285-301.

[Ma 2011] Ma, H. Y., Hsiao, B. S., & Chu, B. (2011). Thin-film nanofibrous composite membranes containing cellulose or chitin barrier layers fabricated by ionic liquids. *Polymer*, 52(12), 2594-2599.

[Mahadeva 2011] Mahadeva, S. K., & Kim, J. (2011). Conductometric glucose biosensor made with cellulose and tin oxide hybrid nanocomposite. *Sensors and Actuators B-Chemical*, 157(1), 177-182.

[Manas-Zloczower 1989] Manas-Zloczower, I., & Feke, D. L. (1989). Analysis of agglomerate rupture in linear flow-fluids. *International Polymer Processing*, 4(1), 185.

[Mao 2006] Mao, Y., Zhou, J. P., Cai, J., & Zhang, L. N. (2006). Effects of coagulants on porous structure of membranes prepared from cellulose in NaOH/urea aqueous solution. *Journal of Membrane Science*, 279(1-2), 246-255.

[Marsano 2002] Marsano, E., Conio, G., Martino, R., Turturro, A., & Bianchi, E. (2002). Fibers based on cellulose-chitin blends. *Journal of Applied Polymer Science*, 83(9), 1825-1831.

[Matsui 1995] Matsui, T., Sano, T., Yamane, C., Kamide, K., & Okajima, K. (1995). Structure and morphology of cellulose films coagulated from novel cellulose/aqueous sodium-hydroxide solutions by using aqueous sulfuric-acid with various concentrations. *Polymer Journal*, 27(8), 797-812.

[Matsumoto 2001] Matsumoto, T., Tatsumi, D., Tamai, N., & Takaki, T. (2001). Solution properties of celluloses from different biological origins in LiCl center dot DMAc. *Cellulose*, 8(4), 275-282.

[Maximova 2001] Maximova, N., Osterberg, M., Koljonen, K., & Stenius, P. (2001). Lignin adsorption on cellulose fibre surfaces: Effect on surface chemistry, surface morphology and paper strength. *Cellulose*, 8(2), 113-125.

- [McCormick 1985] McCormick, C. L., Callais, P. A., & Hutchinson, B. H. (1985). Solution studies of cellulose in lithium-chloride and N,N-dimethylacetamide. *Macromolecules*, 18(12), 2394-2401.
- [McCorsley 1979] McCorsley III, C. C., & Varga, J. K. (1979). A "Process for making a precursor of a solution of cellulose". US Patent 4142913.
- [Metzner 1985] Metzner, A. B. (1985). Rheology of suspensions in polymeric liquids. *Journal of Rheology*, 29(6), 739-775.
- [Miao 2006] Miao, S., Miao, Z., Liu, Z., Han, B., Zhang, H., & Zhang, J. (2006). Synthesis of mesoporous TiO₂ films in ionic liquid dissolving cellulose. *Microporous and Mesoporous Materials*, 95(1-3), 26-30.
- [Moriarty 2011] Moriarty, G. P., Whittemore, J. H., Sun, K. A., Rawlins, J. W., & Grunlan, J. C. (2011). Influence of Polymer Particle Size on the Percolation Threshold of Electrically Conductive Latex-Based Composites. *Journal of Polymer Science Part B-Polymer Physics*, 49(21), 1547-1554.
- [Mueller 2009] Mueller, C. M. O., Laurindo, J. B., & Yamashita, F. (2009). Effect of cellulose fibers on the crystallinity and mechanical properties of starch-based films at different relative humidity values. *Carbohydrate Polymers*, 77(2), 293-299.
- [Nishino 2007] Nishino, T., & Arimoto, N. (2007). All-cellulose composite prepared by selective dissolving of fiber surface. *Biomacromolecules*, 8(9), 2712-2716.
- [Nishino 2004] Nishino, T., Matsuda, I., & Hirao, K. (2004). All-cellulose composite. *Macromolecules*, 37(20), 7683-7687.
- [Nishio 1990] Nishio, Y., & Manley, R. S. (1990). Blends of cellulose with Nylon-6 and poly(epsilon-caprolactone) prepared by a solution-coagulation methods. *Polymer Engineering and Science*, 30(2), 71-82.
- [Nishio 2006] Nishio, Y. (2006). Material functionalization of cellulose and related polysaccharides via diverse microcompositions. *Advanced Polymer Science*, 205, 97-151.
- [Nordqvist 2007] Nordqvist, D., Idermark, J., & Hedenqvist, M. S. (2007). Enhancement of the wet properties of transparent chitosan-acetic-acid-salt films using microfibrillated cellulose. *Biomacromolecules*, 8(8), 2398-2403.
- [Northolt 2001] Northolt, M. G., Boerstael, H., Maatman, H., Huisman, R., Veurink, J., & Elzerman, H. (2001). The structure and properties of cellulose fibres spun from an anisotropic phosphoric acid solution. *Polymer*, 42(19), 8249-8264.
- [Nud'ga 1999] Nud'ga, L. A., Petrova, V. A., Bochek, A. M., Kalyuzhnaya, L. M., Alekseev, V. L., Evmenenko, G. A., & Pretropavlovskii, G. A. (1999). Structure of chitin-cellulose mixtures in solution and in the solid state. *Vysokomolekulyarnye Soedineniya Seriya A & Seriya B*, 41(11), 1786-1792.
- [Ostlund 2009a] Ostlund, A., Lundberg, D., Nordstierna, L., Holmberg, K., & Nyden, M. (2009a). Dissolution and Gelation of Cellulose in TBAF/DMSO Solutions: The Roles of Fluoride Ions and Water. *Biomacromolecules*, 10(9), 2401-2407.
- [O'sullivan 1997] O'sullivan, A. C. (1997). Cellulose: the structure slowly unravels. *Cellulose*, 4(3), 173-207.
- [Otten 2011] Otten, R. H. J., & van der Schoot, P. (2011). Connectivity percolation of polydisperse anisotropic nanofillers. *Journal of Chemical Physics*, 134(9), 094902.
- [Ou 2012] Ou, R., Xie, Y., Shen, X., Yuan, F., Wang, H., & Wang, Q. (2012). Solid biopolymer electrolytes based on all-cellulose composites prepared by partially dissolving cellulose fibers in the ionic liquid 1-butyl-3-methylimidazolium chloride. *Journal of Materials Science*, 47(16), 5978-5986.

- [Paillet 1993] Paillet, M., Cavaille, J. Y., Desbrieres, J., Dupeyre, D., & Peguy, A. (1993). Cellulose-poly(vinyl pyrrolidone) blends studied by scanning electron-microscopy and dynamic mechanical measurements. *Colloid and Polymer Science*, 271(4), 311-321.
- [Paralikara 2008] Paralikara, S. A., Simonsen, J., & Lombardi, J. (2008). Poly(vinyl alcohol)/cellulose nanocrystal barrier membranes. *Journal of Membrane Science*, 320(1-2), 248-258.
- [Paunikallio 2006] Paunikallio, T., Suvanto, M., & Pakkanen, T. T. (2006). Viscose fiber/polyamide 12 composites: Novel gas-phase method for the modification of cellulose fibers with an aminosilane coupling agent. *Journal of Applied Polymer Science*, 102(5), 4478-4483.
- [Perotti 2011] Perotti, G. F., Barud, H. S., Messaddeq, Y., Ribeiro, S. J. L., & Constantino, V. R. L. (2011). Bacterial cellulose-laponite clay nanocomposites. *Polymer*, 52(1), 157-163.
- [Powell 1979] Powell, M. J. (1979). Site percolation in randomly packed spheres. *Physical Review B*, 20(10), 4194-4198.
- [Prasad 2009] Prasad, K., Kaneko, Y., & Kadokawa, J. (2009). Novel Gelling Systems of kappa-, iota- and lambda-Carrageenans and their Composite Gels with Cellulose Using Ionic Liquid. *Macromolecular Bioscience*, 9(4), 376-382.
- [Psomiadou 1996] Psomiadou, E., Arvanitoyannis, I., & Yamamoto, N. (1996). Edible films made from natural resources; Microcrystalline cellulose (MCC), methylcellulose (MC) and corn starch and polyols .2. *Carbohydrate Polymers*, 31(4), 193-204.
- [Quan 2010] Quan, S. L., Kang, S. G., & Chin, I. J. (2010). Characterization of cellulose fibers electrospun using ionic liquid. *Cellulose*, 17(2), 223-230.
- [Rahatekar 2009] Rahatekar, S. S., Rasheed, A., Jain, R., Zammarano, M., Koziol, K. K., Windle, A. H., Gilman, J. W., & Kumar, S. (2009). Solution spinning of cellulose carbon nanotube composites using room temperature ionic liquids. *Polymer*, 50(19), 4577-4583.
- [Ramos 2005a] Ramos, L. A., Assaf, J. M., El Seoud, O. A., & Frollini, E. (2005a). Influence of the supramolecular structure and physicochemical properties of cellulose on its dissolution in a lithium chloride/N,N-dimethylacetamide solvent system. *Biomacromolecules*, 6(5), 2638-2647.
- [Ramos 2005b] Ramos, L. A., Frollini, E., & Heinze, T. (2005b). Carboxymethylation of cellulose in the new solvent dimethyl sulfoxide/tetrabutylammonium fluoride. *Carbohydrate Polymers*, 60(2), 259-267.
- [Rosenau 2001] Rosenau, T., Potthast, A., Sixta, H., & Kosma, P. (2001). The chemistry of side reactions and byproduct formation in the system NMMO/cellulose (Lyocell process). *Progress in Polymer Science*, 26(9), 1763-1837.
- [Roux 2008] Roux, C. (2008). Etude rhéo-optique des mécanismes de dispersion de la silice dans des élastomères. Thèse de doctorat. Ecole des Mines de Paris, Sophia-Antipolis.
- [Roy 2003] Roy, C., Budtova, T., & Navard, P. (2003). Rheological properties and gelation of aqueous cellulose-NaOH solutions. *Biomacromolecules*, 4(2), 259-264.
- [Ruan 2004] Ruan, D., Zhang, L. N., Mao, Y., Zeng, M., & Li, X. B. (2004). Microporous membranes prepared from cellulose in NaOH/thiourea aqueous solution. *Journal of Membrane Science*, 241(2), 265-274.
- [Rumpf 1962] Rumpf, H. (1962). The strength of granules and agglomerates, in: Knepper, W.A. (Ed.), *Agglomeration*. Interscience (New York); pp. 379-418.
- [Rwei 1991] Rwei, S. P., Horwatt, S. W., Manas-Zloczower, I., & Feke, D. L. (1991). Observation and analysis of carbon-black agglomerates dispersion in simple shear flows. *International Polymer Processing*, 6(2), 98-102.

- [Rwei 1990] Rwei, S. P., Manas-Zloczower, I., & Feke, D. L. (1990). Observation of carbon-black agglomerate dispersion in simple shear flows. *Polymer Engineering and Science*, 30(12), 701-706.
- [Saito 2003] Saito, H., Sakurai, A., Sakakibara, M., & Saga, H. (2003). Preparation and properties of transparent cellulose hydrogels. *Journal of Applied Polymer Science*, 90(11), 3020-3025.
- [Salgado 2008] Salgado, P. R., Schmidt, V. C., Ortiz, S. E. M., Mauri, A. N., & Laurindo, J. B. (2008). Biodegradable foams based on cassava starch, sunflower proteins and cellulose fibers obtained by a baking process. *Journal of Food Engineering*, 85(3), 435-443.
- [Sammons 2008] Sammons, R. J., Collier, J. R., Rials, T. G., & Petrovan, S. (2008). Rheology of 1-butyl-3-methylimidazolium chloride cellulose solutions. I. Shear rheology. *Journal of Applied Polymer Science*, 110(2), 1175-1181.
- [Scher 1970] Scher, H., & Zallen, R. (1970). Critical density in percolation processes. *Journal of Chemical Physics*, 53(9), 3759-3761.
- [Schueler 1997] Schueler, R., Petermann, J., Schulte, K., & Wentzel, H. P. (1997). Agglomeration and electrical percolation behavior of carbon black dispersed in epoxy resin. *Journal of Applied Polymer Science*, 63(13), 1741-1746.
- [Schwartz 2000] Schwartz, G., Cervený, S., & Marzocca, A. J. (2000). A numerical simulation of the electrical resistivity of carbon black filled rubber. *Polymer*, 41(17), 6589-6595.
- [Sequeira 2009] Sequeira, S., Evtuguin, D. V., & Portugal, I. (2009). Preparation and Properties of Cellulose/Silica Hybrid Composites. *Polymer Composites*, 30(9), 1275-1282.
- [Serajuddin 1999] Serajuddin, A. T. M. (1999). Solid dispersion of poorly water-soluble drugs: Early promises, subsequent problems, and recent breakthroughs. *Journal of Pharmaceutical Sciences*, 88(10), 1058-1066.
- [Sescousse 2009] Sescousse, R., & Budtova, T. (2009). Influence of processing parameters on regeneration kinetics and morphology of porous cellulose from cellulose-NaOH-water solutions. *Cellulose*, 16(3), 417-426.
- [Sescousse 2011a] Sescousse, R., Gavillon, R., & Budtova, T. (2011a). Aerocellulose from cellulose-ionic liquid solutions: Preparation, properties and comparison with cellulose-NaOH and cellulose-NMMO routes. *Carbohydrate Polymers*, 83(4), 1766-1774.
- [Sescousse 2011b] Sescousse, R., Gavillon, R., & Budtova, T. (2011b). Wet and dry highly porous cellulose beads from cellulose-NaOH-water solutions: influence of the preparation conditions on beads shape and encapsulation of inorganic particles. *Journal of Materials Science*, 46(3), 759-765.
- [Sescousse 2010a] Sescousse, R., Le, K. A., Ries, M. E., & Budtova, T. (2010a). Viscosity of Cellulose-Imidazolium-Based Ionic Liquid Solutions. *Journal of Physical Chemistry B*, 114(21), 7222-7228.
- [Sescousse 2010b] Sescousse, R., Smacchia, A., & Budtova, T. (2010b). Influence of lignin on cellulose-NaOH-water mixtures properties and on Aerocellulose morphology. *Cellulose*, 17(6), 1137-1146.
- [Seyvet 2000] Seyvet, O., & Navard, P. (2000). Collision-induced dispersion of agglomerate suspensions in a shear flow. *Journal of Applied Polymer Science*, 78(5), 1130-1133.
- [Sheen 1991] Sheen, P. C., Kim, S. I., Petillo, J. J., & Serajuddin, A. T. M. (1991). Bioavailability of a poorly water-soluble drug from tablet and solid dispersion in humans. *Journal of Pharmaceutical Sciences*, 80(7), 712-714.
- [Shen 2007] Shen, Q., & Liu, D. S. (2007). Cellulose/poly(ethylene glycol) blend and its controllable drug release behaviors in vitro. *Carbohydrate Polymers*, 69(2), 293-298.
- [Shiga 1985] Shiga, S., & Furuta, M. (1985). Processability of electron-paramagnetic-res in an internal

- mixer. 2. Morphological-changes of carbon-black agglomerates during mixing. *Rubber Chemistry and Technology*, 58(1), 1-22.
- [Shih 2009] Shih, C.-M., Shieh, Y.-T., & Twu, Y.-K. (2009). Preparation and characterization of cellulose/chitosan blend films. *Carbohydrate Polymers*, 78(1), 169-174.
- [Sichel 1982] Sichel, E. K., Gittleman, J. I., & Sheng, P. (1982). Electrical-properties of carbon-polymer composites. *Journal of Electronic Materials*, 11(4), 699-747.
- [Sores 2005] Soares, R. M. D., Lima, A. M. F., Oliveira, R. V. B., Pires, A. T. N., & Soldi, V. (2005). Thermal degradation of biodegradable edible films based on xanthan and starches from different sources. *Polymer Degradation and Stability*, 90(3), 449-454.
- [Sobue 1939] Sobue, H., Kiessig, H., & Hess, K. (1939). The cellulose-sodium hydroxide-water system as a function of the temperature. *Zeitschrift für Physikalische Chemie B*, 43, 309-328.
- [Sonntag 1987] Sonntag, R. C., & Russel, W. B. (1987). Structural and breakup of flocs subjected to fluid stresses. 2. Theory. *Journal of Colloid and Interface Science*, 115(2), 378-389.
- [Soykeabkaew 2008] Soykeabkaew, N., Arimoto, N., Nishino, T., & Peijs, T. (2008). All-cellulose composites by surface selective dissolution of aligned ligno-cellulosic fibres. *Composites Science and Technology*, 68(10-11), 2201-2207.
- [Soykeabkaew 2009] Soykeabkaew, N., Nishino, T., & Peijs, T. (2009). All-cellulose composites of regenerated cellulose fibres by surface selective dissolution. *Composites Part A-Applied Science and Manufacturing*, 40(4), 321-328.
- [Sumita 1991] Sumita, M., Sakata, K., Asai, S., Miyasaka, K., & Nakagawa, H. (1991). Dispersion of fillers and the electrical-conductivity of polymer blends filled with carbon-black. *Polymer Bulletin*, 25(2), 265-271.
- [Sun 2009] Sun, X. Q., Peng, B., Ji, Y., Chen, J., & Li, D. Q. (2009). Chitosan(Chitin)/Cellulose Composite Biosorbents Prepared Using Ionic Liquid for Heavy Metal Ions Adsorption. *Aiche Journal*, 55(8), 2062-2069.
- [Swatloski 2002] Swatloski, R. P., Spear, S. K., Holbrey, J. D., & Rogers, R. D. (2002). Dissolution of cellulose with ionic liquids. *Journal of the American Chemical Society*, 124(18), 4974-4975.
- [Taeger 1985] Taeger, E., Franz, H., Mertel, H., Schleicher, H., Lang, H., & Lukanoff, B. (1985). *Formeln, Fasern, Fertigware*, 4, 14-22.
- [Takegawa 2010] Takegawa, A., Murakami, M., Kaneko, Y., & Kadokawa, J. (2010). Preparation of chitin/cellulose composite gels and films with ionic liquids. *Carbohydrate Polymers*, 79(1), 85-90.
- [Tamai 2003] Tamai, N., Aono, H., Tatsumi, D., & Matsumoto, T. (2003). Differences in rheological properties of solutions of plant and bacterial cellulose in LiCl/N,N-dimethylacetamide. *Journal of the Society of Rheology Japan*, 31(3), 119-130.
- [Tang 2008] Tang, C. Y., & Liu, H. Q. (2008). Cellulose nanofiber reinforced poly(vinyl alcohol) composite film with high visible light transmittance. *Composites Part A-Applied Science and Manufacturing*, 39(10), 1638-1643.
- [Thornton 2004] Thornton, C., & Liu, L. F. (2004). How do agglomerates break? *Powder Technology*, 143, 110-116.
- [Touzel 2003] Touzel, J. P., Chabbert, B., Monties, B., Debeire, P., & Cathala, B. (2003). Synthesis and characterization of dehydrogenation polymers in *Gluconacetobacter xylinus* cellulose and cellulose/pectin composite. *Journal of Agricultural and Food Chemistry*, 51(4), 981-986.
- [Tsiptsias 2008] Tsiptsias, C., Stefopoulos, A., Kokkinomalis, I., Papadopoulou, L., & Panayiotou, C. (2008). Development of micro- and nano-porous composite materials by processing cellulose with ionic

liquids and supercritical CO₂). *Green Chemistry*, 10(9), 965-971.

[Turbak 1980] Turbak, A. F., Hammer, R. B., Davies, R. E., & Hergert, H. L. (1980). Cellulose solvents. *Chemtech*, 10(1), 51-57.

[Turner 2004] Turner, M. B., Spear, S. K., Holbrey, J. D., & Rogers, R. D. (2004). Production of bioactive cellulose films reconstituted from ionic liquids. *Biomacromolecules*, 5(4), 1379-1384.

[Twu 2003] Twu, Y. K., Huang, H. I., Chang, S. Y., & Wang, S. L. (2003). Preparation and sorption activity of chitosan/cellulose blend beads. *Carbohydrate Polymers*, 54(4), 425-430.

[Uddin 2007] Uddin, M. J., Cesano, F., Bonino, F., Bordiga, S., Spoto, G., Scarano, D., & Zecchina, A. (2007). Photoactive TiO₂ films on cellulose fibres: synthesis and characterization. *Journal of Photochemistry and Photobiology a-Chemistry*, 189(2-3), 286-294.

[Untereker 2009] Untereker, D., Lyu, S., Schley, J., Martinez, G., & Lohstreter, L. (2009). Maximum Conductivity of Packed Nanoparticles and Their Polymer Composites. *Acs Applied Materials & Interfaces*, 1(1), 97-101.

[Vehvilainen 2008] Vehvilainen, M., Kamppuri, T., Rom, M., Janicki, J., Ciechanska, D., Gronqvist, S., Siika-Aho, M., Christoffersson, K. E., & Nousiainen, P. (2008). Effect of wet spinning parameters on the properties of novel cellulosic fibres. *Cellulose*, 15(5), 671-680.

[Voigt 2005] Voigt, B., Rouxel, D., McQueen, D. H., & Rychwalski, R. W. (2005). Organization of carbon black in laminates of cellulose and melamine-formaldehyde. *Polymer Composites*, 26(2), 144-151.

[Vu 2002] Vu, D., Marquez, M., & Larsen, G. (2002). A facile method to deposit zeolites Y and L onto cellulose fibers. *Microporous and Mesoporous Materials*, 55(1), 93-101.

[Wan 2010] Wan, J., Yan, X., Ding, J. J., & Ren, R. (2010). A simple method for preparing biocompatible composite of cellulose and carbon nanotubes for the cell sensor. *Sensors and Actuators B-Chemical*, 146(1), 221-225.

[Wang 2010] Wang, Y., Chang, C., & Zhang, L. (2010). Effects of Freezing/Thawing Cycles and Cellulose Nanowhiskers on Structure and Properties of Biocompatible Starch/PVA Sponges. *Macromolecular Materials and Engineering*, 295(2), 137-145.

[Wnag 2012] Wang, Z. G., Liu, S. L., Matsumoto, Y., & Kuga, S. (2012). Cellulose gel and aerogel from LiCl/DMSO solution. *Cellulose*, 19(2), 393-399.

[Weiler 2010] Weiler, C., Wolkenhauer, M., Trunk, M., & Langguth, P. (2010). New model describing the total dispersion of dry powder agglomerates. *Powder Technology*, 203(2), 248-253.

[Wendler 2006] Wendler, F., Graness, G., Buttner, R., Meister, F., & Heinze, T. (2006). A novel polymeric stabilizing system for modified lyocell solutions. *Journal of Polymer Science Part B-Polymer Physics*, 44(12), 1702-1713.

[Weng 2004] Weng, L. H., Zhang, L. N., Ruan, D., Shi, L. H., & Xu, J. (2004). Thermal gelation of cellulose in a NaOH/thiourea aqueous solution. *Langmuir*, 20(6), 2086-2093.

[Willauer 2000] Willauer, H. D., Huddleston, J. G., Li, M., & Rogers, R. D. (2000). Investigation of aqueous biphasic systems for the separation of lignins from cellulose in the paper pulping process. *Journal of Chromatography B*, 743(1-2), 127-135.

[Wilpiszewska 2011] Wilpiszewska, K., & Spychaj, T. (2011). Ionic liquids: Media for starch dissolution, plasticization and modification. *Carbohydrate Polymers*, 86(2), 424-428.

[Wu 2009] Wu, R.-L., Wang, X.-L., Li, F., Li, H.-Z., & Wang, Y.-Z. (2009). Green composite films prepared from cellulose, starch and lignin in room-temperature ionic liquid. *Bioresource Technology*, 100(9), 2569-2574.

[Wu 2010] Wu, J. J., Liang, S. M., Dai, H. J., Zhang, X. Y., Yu, X. L., Cai, Y. L., Zheng, L. N., Wen, N., Jiang, B., & Xu, J. (2010). Structure and properties of cellulose/chitin blended hydrogel membranes fabricated via a solution pre-gelation technique. *Carbohydrate Polymers*, 79(3), 677-684.

[Xiao 2011] Xiao, W. J., Chen, Q., Wu, Y., Wu, T. H., & Dai, L. Z. (2011). Dissolution and blending of chitosan using 1,3-dimethylimidazolium chloride and 1-H-3-methylimidazolium chloride binary ionic liquid solvent. *Carbohydrate Polymers*, 83(1), 233-238.

[Yamada 1992] Yamada, H., Kowsaka, K., Matsui, T., Okajima, K., & Kamide, K. (1992). Nuclear magnetic study on the dissolution of natural and regenerated celluloses into aqueous alkali solution. *Cellulose Chemistry and Technology*, 26(2), 141-150.

[Yamada 1997] Yamada, H., Manas-Zloczower, I., & Feke, D. L. (1997). Influence of matrix infiltration on the dispersion kinetics of carbon black agglomerates. *Powder Technology*, 92(2), 163-169.

[Yamane 1994] Yamane, C., Saito, M., Kowsaka, K., Kataoka, N., Sagara, K., & Kamide, K. (1994). New cellulosic filament yarn spun from cellulose / aq NaOH solution. Proceedings of '94 Cellulose R&D, 1st Annual Meeting of the Cellulose Society of Japan (Cellulose Society of Japan, ed.) Tokyo, pp 183-188.

[Yamane 1996a] Yamane, C., Saito, M., & Okajima, K. (1996a). Industrial preparation method of cellulose-alkali dope with high solubility. *Sen-I Gakkaishi*, 52(6).

[Yamane 1996b] Yamane, C., Saito, M., & Okajima, K. (1996b). New spinning process of cellulose filament production from alkali soluble cellulose dope-net process: Production of new cellulosic filament spun from cellulose/aqueous NaOH solution .4. *Sen-I Gakkaishi*, 52(7), 378-384.

[Yamane 1996c] Yamane, C., Saito, M., & Okajima, K. (1996c). Specification of alkali soluble pulp suitable for new cellulosic filament production. *Sen-I Gakkaishi*, 52(6), 310-317.

[Yamane 1996d] Yamane, C., Saito, M., & Okajima, K. (1996d). Spinning of alkali soluble cellulose-caustic soda solution system using sulfuric acid as coagulant: Production of new cellulosic filament spun from cellulose/aqueous NaOH solution .3. *Sen-I Gakkaishi*, 52(7), 369-377.

[Yamashiki 1988] Yamashiki, T., Kamide, K., Okajima, K., Kowsaka, K., Matsui, T., & Fukase, H. (1988). Some characteristic features of dilute aqueous alkali solutions of specific alkali concentration (2.5 mol^{-1}) which possess maximum solubility power against cellulose. *Polymer Journal*, 20(6), 447-457.

[Yamashiki 1992] Yamashiki, T., Matsui, T., Kowsaka, K., Saitoh, M., Okajima, K., & Kamide, K. (1992). New class of cellulose fiber spun from the novel solution of cellulose by wet spinning methods. *Journal of Applied Polymer Science*, 44(4), 691-698.

[Yamashiki 1990a] Yamashiki, T., Matsui, T., Saitoh, M., Okajima, K., & Kamide, K. (1990a). Characterization of cellulose treated by the steam explosion methods. 1. Influence of cellulose resources on changes in morphology, degree of polymerization, solubility and solid structure. *British Polymer Journal*, 22(1), 73-83.

[Yamashiki 1990b] Yamashiki, T., Matsui, T., Saitoh, M., Okajima, K., & Kamide, K. (1990b). Characterization of cellulose treated by the steam explosion method. 2. Effect of treatment conditions on changes in morphology, degree of polymerization, solubility in aqueous sodium-hydroxide and supermolecular structure of soft wood pulp during steam explosion. *British Polymer Journal*, 22(2), 121-128.

[Yamashiki 1990c] Yamashiki, T., Saitoh, M., Yasuda, K., Okajima, K., & Kamide, K. (1990c). Cellulose fiber spun from gelatinized cellulose aqueous sodium-hydroxide system by the wet-spinning methods. *Cellulose Chemistry and Technology*, 24(2), 237-249.

[Yamazaki 2010] Yamazaki, S., Takegawa, A., Kaneko, Y., Kadokawa, J.-i., Yamagata, M., & Ishikawa, M. (2010). High/low temperature operation of electric double layer capacitor utilizing acidic cellulose-chitin hybrid gel electrolyte. *Journal of Power Sources*, 195(18), 6245-6249.

- [Yang 2011a] Yang, Q., Qi, H., Lue, A., Hu, K., Cheng, G., & Zhang, L. (2011a). Role of sodium zincate on cellulose dissolution in NaOH/urea aqueous solution at low temperature. *Carbohydrate Polymers*, 83(3), 1185-1191.
- [Yang 2011b] Yang, Q. L., Qin, X. Z., & Zhang, L. N. (2011b). Properties of cellulose films prepared from NaOH/urea/zincate aqueous solution at low temperature. *Cellulose*, 18(3), 681-688.
- [Ye 2011] Ye, S. H., Zhang, D., Liu, H. Q., & Zhou, J. P. (2011). ZnO Nanocrystallites/Cellulose Hybrid Nanofibers Fabricated by Electrospinning and Solvothermal Techniques and Their Photocatalytic Activity. *Journal of Applied Polymer Science*, 121(3), 1757-1764.
- [Yoshida 2005] Yoshida, A., Miyazaki, T., Ishida, E., & Ashizuka, M. (2005). Preparation of cellulose-carbonate apatite composites through mechanochemical reaction. *Bioceramics*, Vol 17, 284-286, 855-858.
- [Yu 2005] Yu, J., Zhang, L. Q., Rogunova, M., Summers, J., & Hiltner, A. (2005). Conductivity of polyolefins filled with high-structure carbon black. *Journal of Applied Polymer Science*, 98(4), 1799-1805.
- [Yun 2007] Yun, S., & Kim, J. (2007). A bending electro-active paper actuator made by mixing multi-walled carbon nanotubes and cellulose. *Smart Materials & Structures*, 16(4), 1471-1476.
- [Zaccone 2009] Zaccone, A., Soos, M., Lattuada, M., Wu, H., Baebler, M. U., & Morbidelli, M. (2009). Breakup of dense colloidal aggregates under hydrodynamic stresses. *Physical Review E*, 79(6), 061401.
- [Zallen 1983] Zallen, R. (1983). *The Physics of Amorphous Solids*; Wiley: New York; Chapter 4.
- [Zhang 2007] Zhang, H., Wang, Z. G., Zhang, Z. N., Wu, J., Zhang, J., & He, H. S. (2007). Regenerated-cellulose/multiwalled-carbon-nanotube composite fibers with enhanced mechanical properties prepared with the ionic liquid 1-allyl-3-methylimidazolium chloride. *Advanced Materials*, 19(5), 698-.
- [Zhang 2005a] Zhang, H., Wu, J., Zhang, J., & He, J. S. (2005a). 1-Allyl-3-methylimidazolium chloride room temperature ionic liquid: A new and powerful nonderivatizing solvent for cellulose. *Macromolecules*, 38(20), 8272-8277.
- [Zhang 2010] Zhang, J., Zhang, H., Wu, J., Zhang, J., He, J., & Xiang, J. (2010). NMR spectroscopic studies of cellobiose solvation in EmimAc aimed to understand the dissolution mechanism of cellulose in ionic liquids. *Physical Chemistry Chemical Physics*, 12(8), 1941-1947.
- [Zhang 2005b] Zhang, L., Mao, Y., Zhou, J. P., & Cai, J. (2005b). Effects of coagulation conditions on the properties of regenerated cellulose films prepared in NaOH/urea aqueous solution. *Industrial & Engineering Chemistry Research*, 44(3), 522-529.
- [Zhang 2002a] Zhang, L. N., Guo, J., & Du, Y. M. (2002a). Morphology and properties of cellulose/chitin blends membranes from NaOH/thiourea aqueous solution. *Journal of Applied Polymer Science*, 86(8), 2025-2032.
- [Zhang 2002b] Zhang, L. N., Ruan, D., & Gao, S. J. (2002b). Dissolution and regeneration of cellulose in NaOH/thiourea aqueous solution. *Journal of Polymer Science Part B-Polymer Physics*, 40(14), 1521-1529.
- [Zhang 2001] Zhang, L. N., Ruan, D., & Zhou, J. P. (2001). Structure and properties of regenerated cellulose films prepared from cotton linters in NaOH/Urea aqueous solution. *Industrial & Engineering Chemistry Research*, 40(25), 5923-5928.
- [Zhang 2011] Zhang, S., Li, F.-X., & Yu, J.-Y. (2011). Kinetics of cellulose regeneration from cellulose-NaOH/thiourea/H₂O system. *Cellulose Chemistry and Technology*, 45(9-10), 593-604.
- [Zhang 2012] Zhang, X. M., Zhu, J., & Liu, X. Q. (2012). Preparation and characterization of regenerated cellulose blend films containing high amount of poly(vinyl alcohol) (PVA) in ionic liquid. *Macromolecular Research*, 20(7), 703-708.

- [Zhou 2005] Zhou, D., Zhang, L., & Guo, S. L. (2005). Mechanisms of lead biosorption on cellulose/chitin beads. *Water Research*, 39(16), 3755-3762.
- [Zhou 2002] Zhou, J. P., Zhang, L., Cai, J., & Shu, H. (2002). Cellulose microporous membranes prepared from NaOH/urea aqueous solution. *Journal of Membrane Science*, 210(1), 77-90.
- [Zhou 2000] Zhou, J. P., & Zhang, L. N. (2000). Solubility of cellulose in NaOH urea aqueous solution. *Polymer Journal*, 32(10), 866-870.
- [Zhou 2004] Zhou, J. P., Zhang, L. N., & Cai, J. (2004). Behavior of cellulose in NaOH/urea aqueous solution characterized by light scattering and viscometry. *Journal of Polymer Science Part B-Polymer Physics*, 42(2), 347-353.
- [Zhou 2002] Zhou, J. P., Zhang, L. N., Shu, H., & Chen, F. G. (2002). Regenerated cellulose films from NaOH/urea aqueous solution by coagulating with sulfuric acid. *Journal of Macromolecular Science-Physics*, B41(1), 1-15.
- [Zoppe 2009] Zoppe, J. O., Peresin, M. S., Habibi, Y., Venditti, R. A., & Rojas, O. J. (2009). Reinforcing Poly(epsilon-caprolactone) Nanofibers with Cellulose Nanocrystals. *Acs Applied Materials & Interfaces*, 1(9), 1996-2004.
- [Zykwinska 2005] Zykwinska, A. W., Ralet, M. C. J., Garnier, C. D., & Thibault, J. F. J. (2005). Evidence for in vitro binding of pectin side chains to cellulose. *Plant Physiology*, 139(1), 397-407.

Chapter II

Materials and Methods

I Materials	72
I.1 Cellulose	72
I.2 Starch	73
I.3 Hydroxypropylcellulose	73
I.4 Sodium hydroxide	73
I.5 Zinc oxide	73
I.6 Ionic liquid	74
I.7 Carbon black	74
I.8 Polyisobutylene	75
II Methods	76
II.1 Dissolution of cellulose and starch	76
II.2 Making films via dissolution-coagulation process	78
II.3 Characterization	82
II.4 Analysis of agglomerate dispersion by rheo-optical technique	87
References	90

I Materials

I.1 Cellulose

In this work, we used the following four types of native cellulose. They have different origins and molecular weights, as described in the next sections.

I.1.1 Avicel

Avicel[®] PH-101 microcrystalline cellulose was from Sigma-Aldrich. It is a purified, partially depolymerized α -cellulose, with a mean degree of polymerization (DP) of 180. For Avicel and also the following cellulose samples, DP was calculated following the equation proposed by Evans and Wallis, who used cupri-ethylenediamine (CuEn) as the cellulose solvent [Evans 1989]: $DP=1.65 [\eta]/\text{ml.g}^{-1}$. The intrinsic viscosity was measured for each samples according to ISO 5351/1B, and the details will be given in Section II.3.1.

I.1.2 VFC

VFC cellulose from Buckeye is a pine wood pulp obtained after vapor hydrolysis treatment, with cooking in sodium sulfite and soda solution. It has a degree of crystallinity of 46%, and a higher molar mass than the microcrystalline cellulose (DP=440).

I.1.3 Cotton

Cotton was kindly provided by Thuringische Institut für Textil und Kunststoff Forschung (TITK), Germany (DP=710).

I.1.4 Bacterial cellulose

It was provided by Research Centre for Medical Technology and Biotechnology GmbH, Geranienweg 7, D-99947 Bad Langensalza, Germany (DP=1700).

I.1.5 Spruce pulp

We also used 11 wt% spruce pulp cellulose which was dissolved in *N*-methylmorpholine *N*-oxide (NMMO) monohydrate concentration. The solution was provided by TITK.

I.2 Starch

Unmodified waxy corn starch was purchased from Sigma-Aldrich. It is amylose-free, and contains only the larger and more branched macromolecule, amylopectin. It was chosen to facilitate the analysis and exclude the influence of starch composition. The waxy starch will also be mentioned as “starch” or “amylopectin” in the following. It was dried before use in vacuum oven at 50°C for 1 hour to remove water residues.

I.3 Hydroxypropylcellulose

Hydroxypropylcellulose (KluCELTM) was from Ashland, with Mw = 80000 (type E) and Mw = 370000 (type G). The molecular weights are given by the manufacturer. Aqueous HPC solutions were prepared by direct dissolution in distilled water with stirring for 24 hours.

I.4 Sodium Hydroxide

Sodium hydroxide (NaOH) in pellets was supplied by Merck, with purity higher than 97%.

I.5 Zinc Oxide

Zinc oxide (ZnO) powder (particles with the size of several microns) of 99.9% purity was from Sigma-Aldrich.

I.6 Ionic liquid

1-ethyl-3-methylimidazolium acetate (EMIMAc) of purity $\geq 90\%$ was from BASF. The molecular structure is shown in Figure IV-1. A fresh bottle of EMIMAc was used as received without further purification.

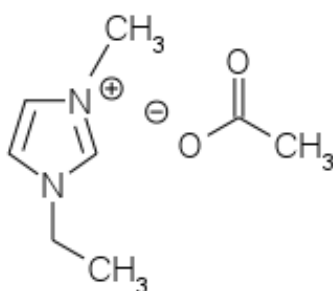


Figure II-1 Molecular structure of 1-ethyl-3-methylimidazolium acetate (EMIMAc).

I.7 Carbon black

Carbon black (Printex[®] L) was from Evonik. It was dried in vacuum oven at 50°C for 2 hours before use. Since experiments were performed on single agglomerates, a 50-micrometer meshed sieve was used to select the agglomerates to be studied by rheo-optics.

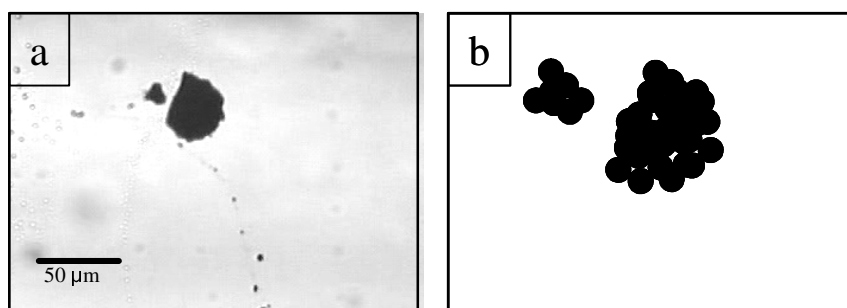


Figure II-2 Optical microscopy image and schematic illustration of sieved carbon black agglomerates.

I.8 Polyisobutylene

Two samples of polyisobutylene (PIB) from Exxon were used, Parapol 1300 ($M_w=1300$) and Parapol 2225 ($M_w=2225$).

II Methods

II.1 Dissolution of cellulose and starch

II.1.1 Cellulose dissolution in aqueous sodium hydroxide solutions

Cellulose (Avicel) solutions in NaOH-water were prepared following the standard procedure [Egal 2007; Egal 2008]:

- 1) An aqueous solution of NaOH (18%~20% of NaOH) was cooled to -6°C. ZnO was added into this solution when applicable.
- 2) Cellulose was dried in a vacuum at 50 °C for 1 hour to remove water residues, and then swollen by distilled water at 5°C for 1 hour.
- 3) We mixed NaOH solution (with or without ZnO) and swollen cellulose/water with an overhead mixer at 800 rpm for 2 hours in a -6°C to obtain the cellulose solutions of various cellulose and ZnO concentrations in 8%NaOH-water.
- 4) Solutions were stored in refrigerator at 5°C and studied within one day to avoid aging.

Different concentrations of components in cellulose solutions will be noted as X%cellulose-Y%NaOH-Z%ZnO-water, in which X% is the weight concentration of cellulose, calculated as:

$$X \% = 100 \times M_{\text{cell}} / (M_{\text{cell}} + M_{\text{water}} + M_{\text{NaOH}} + M_{\text{ZnO}}) \quad (\text{II-1})$$

where M_i is the weight of each component. Y and Z% are the weight concentrations of NaOH and ZnO, respectively, in solvent only, calculated as:

$$Y \% = 100 \times M_{\text{NaOH}} / (M_{\text{water}} + M_{\text{NaOH}} + M_{\text{ZnO}}) \quad (\text{II-2})$$

$$Z \% = 100 \times M_{\text{ZnO}} / (M_{\text{water}} + M_{\text{NaOH}} + M_{\text{ZnO}}) \quad (\text{II-3})$$

The concentration of NaOH in the final solution was fixed to 8%, and the concentration of ZnO was varied from 0 to 1.5%. For the calculation of intrinsic viscosity, we use cellulose concentration in g/cm^3 . In the first approximation $\text{g/cm}^3 = \text{g/g}$ as far as solvent density is less than 1.1 g/cm^3 .

For intrinsic viscosity measurements, 2% cellulose solutions were prepared as described above, and then diluted with the corresponding solvent to have a starting solution of 0.5% cellulose. Solutions were not filtered in order not to lose micron-size non-dissolved ZnO particles and thus change ZnO concentration. The presence of 0.7% ZnO in 8%NaOH-water with some non-dissolved particles does not change solvent viscosity within the experimental error (for example, kinematic viscosity at 25°C of 8%NaOH-water was $1.32 \text{ mm}^2/\text{s}$ and of 8%NaOH-0.7%ZnO-water was $1.33 \text{ mm}^2/\text{s}$).

II.1.2 Cellulose dissolution in ionic liquid

Except for optical microscope observations, cellulose or starch solutions in EMIMAc of different concentrations (in wt%) were prepared by mixing cellulose or starch and IL in a sealed reaction vessel at 80°C for 24 ~ 48 hours to ensure complete dissolution. The reaction vessel was filled with nitrogen during the dissolution process. Cellulose-starch-EMIMAc mixtures were prepared by mixing ready solutions in various proportions and stirring under the same condition for additional 8 hours.

II.1.3 Cellulose solutions with carbon black

Cellulose solutions in IL were mixed with carbon black using a Thermo Scientific HAAKE MiniLab II micro compounder with counter-rotating twin screws. About 6g of solution with a certain amount of carbon black according to the desired CB concentration was added into compounder at the same time, following a sequence of roughly half of the solution, CB, the other half of the solution to make sure all the CB can be dispersed instead of being left on the inside of the compounder. Then they were mixed at 250 rpm and 30°C for 45 minutes. Then the temperature was raised to 80°C for another 15 minutes before the mixture was collected and stored for later use.

II.2 Making films via dissolution-coagulation process

II.2.1 Cellulose and cellulose-starch films

Films from cellulose-EMIMAc solutions and cellulose-starch-EMIMAc mixtures (Figure II-3) were prepared via dissolution-mixing-coagulation route. Few milliliters of solution or mixture was placed on a Petri dish and a thin layer was obtained using a spin-coater SPIN150-NPP (SPS, the Netherlands) at 300 – 400 rpm for 120s. The polymer was then coagulated in distilled water or in ethanol followed by washing in successive baths at room temperature until a stable conductivity of the bath. Bath volume was 10 times higher than solution volume, thus theoretically all EMIMAc was washed out. The wet films obtained were either freeze-dried in liquid nitrogen to be used for SEM observation, or dried between two clipped glass slides in vacuum oven at 70°C for 24 hours for XRD and FTIR tests. Because it was not possible to obtain pure starch films without a plasticizer when coagulated in water, to perform FTIR and XRD analysis starch was simply precipitated in ethanol, washed repeatedly and then dried in the same conditions as described above.

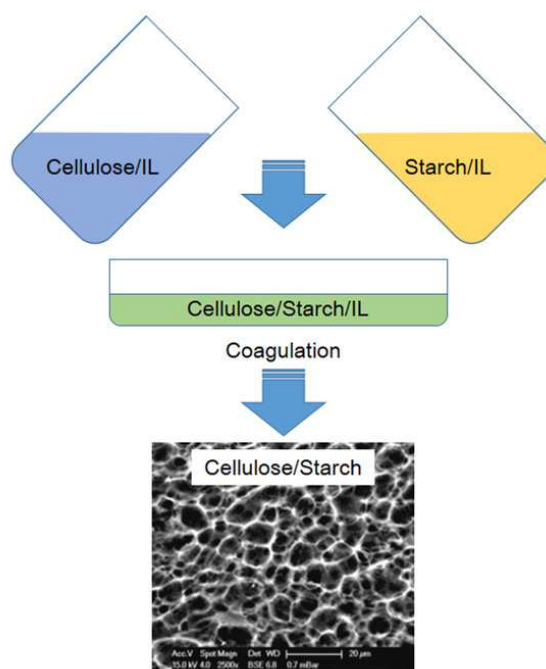


Figure II-3 Process of preparing cellulose/starch blended films.

II.2.3 Cellulose (Avicel)/cellulose (VFC)/carbon black composite films

We tried two methods to make cellulose (Avicel)/cellulose (VFC)/carbon black films. With the first approach, a three-layered sample was made (Figure II-5): we spin-coated solutions of Avicel-EMIMAc-carbon black solution, then VFC-EMIMAc solution (without carbon black) was put on the top of Avicel-EMIMAc layer and spin-coated and finally Avicel-EMIMAc-carbon black solution droplet was placed on the top of VFC-EMIMAc layer and spin-coated. The sample obtained was coagulated in water so as to have 3-layered films as shown in the following figure. The films after coagulation were homogenous, and no separation between the layers was observed.

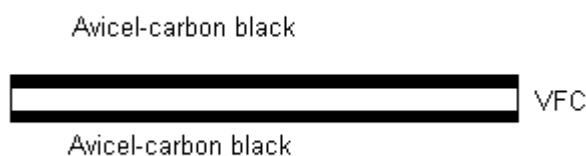


Figure II-5 Illustration of the 3-layered Avicel-VFC-carbon black composite films.

In the other method, we mixed the Avicel-EMIMAc-carbon black solution and the VFC solution in the micro compounder gently for a short time (50 rpm for 5mins), as shown in Figure II-6, hoping to have a binary structure, and then spin-coated to have cellulose A/cellulose-B/carbon black films.

In both cases, 15 wt% Avicel-EMIMAc solution and 12 wt% VFC-EMIMAc were chosen, for their similar viscosity but quite different degree of polymerization.

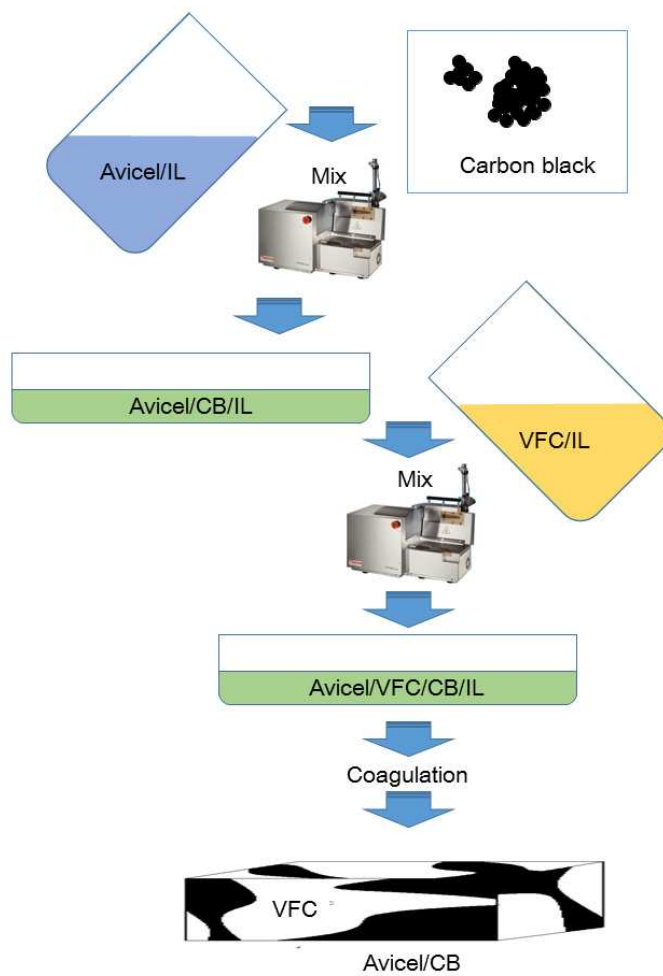


Figure II-6 Process of preparing “binary” Avicel-VFC-carbon black composite films.

II.3 Characterization

II.3.1 Viscometry

Intrinsic viscosities of cellulose in NaOH-water solutions with or without additive were measured with a Lauda PVS-1 (Lauda, Germany) Ubbelohde type viscometer with capillary tube 53110/I (Schott AG, Germany). The viscometer was placed in a thermally controlled water bath at least 15 minutes before measurement. The system is equipped with an automatic dosing device (Dosimat 765, Metrohm, Switzerland) to control sample concentration by sequential dilution. A magnetic stirrer was used for concentration homogenization at each dilution. For each concentration, one pre-measurement and three measurements were performed. The mean flow time was recorded and the reduced viscosity was calculated by software automatically. The temperature was varied from 5°C to 30°C with a 5°C increment. The intrinsic viscosity values obtained are within 5% experimental error.

For the estimation of DP, the intrinsic viscosity values of various types of cellulose were also measured according to ISO 5351/1B (determination of the intrinsic viscosity of pulp in a dilute cupri-ethylenediamine (CuEn) solution). The flow times of 0.5 mol/L CuEn and different types of cellulose/CuEn solutions with concentrations from 0.003 to 0.005 g/ml were measured at 25°C with the same capillary tube.

II.3.2 Rheology

For most of the samples in our study, including different types of cellulose or starch solutions in EMIMAc, aqueous HPC solution and polyisobutylene, rheological measurements were performed on the Bohlin GeminiTM 150 rheometer (Malvern Instruments, UK) with a Peltier temperature control system. Measuring system was cone-plate geometry with either 4° angle, 40 mm diameter or 2° angle, 60 mm diameter.

In steady state, viscosity was recorded as a function of shear rate at a constant temperature. Each shear rate sweep was repeated at various temperatures. With the dynamic mode, elastic modulus (G') and viscous modulus (G'') were measured at different temperatures as a function of time with constant frequency and stress (to study gelation time), or as a function

of frequency with constant stress (to study viscoelastic property). The usual testing temperature interval was between 10°C to 80°C with 10°C increment, if not specified. A solvent trap covering the measuring cell and wrapped with Parafilm® (Pechiney Plastic Packaging, US) was used to prevent water evaporation/absorption. Additionally, due to the hygroscopicity of EMIMAc, silicone oil (DC 200, Sigma–Aldrich) was placed around the edge of the cone to prevent water absorption during some measurements. The silicone oil is not miscible with cellulose or starch solutions and had a much lower viscosity ($\eta_{20^\circ\text{C}} = 9.5$ mPa.s), thus it did not perturb the measurements.

For 11% cellulose in NMMO, the measurements were performed on a MCR 302 rheometer (Anton Paar, Austria) with CTD 450 convection heating systems for temperature control. A cone-plate system of 25mm and 2° is used. Shear rates were varied from 0.005 s⁻¹ to 20 s⁻¹ for steady state viscosity measurements, and frequencies were varied from 0.1 Hz to 10 Hz for visco-elastic measurements. Temperature was fixed at 90°C.

II.3.3 Optical microscope for starch dissolution/gelatinization observation

Optical microscope (Leica, Germany) was used to observe the initial morphology of materials as ZnO and carbon black, and also to compare the behavior of starch granules in EMIMAc, water and EMIMAc/water mixtures (in wt%). In the latter case, dry starch was dispersed in each solvent to reach 5 wt%, and then stirred for 10 minutes at room temperature to obtain a homogenous dispersion. Within this duration the granules remained intact. One drop of sample was placed between two glass slides, quickly heated to 40°C and then heated from 40°C to 100°C at 5°C/min using Linkam hot stage with Peltier plate for temperature control. Photos of 500X magnification were taken with Archimedes software at every 2°C during the heating. Each experiment was repeated two-three times; the difference in dissolution/gelatinization temperature for the same system from one experiment to another was 2-3°C.

II.3.4 X-ray diffraction

X-ray diffraction (XRD) was performed on X'Pert PRO (PANalytical, Netherlands) with the following conditions: Cu K α = 1.5406 Å, operating at 30mA and 40kV, and 2 θ varied from 6° to 50°. Samples for X-ray diffraction were initial polysaccharides (Avicel microcrystalline cellulose and waxy corn starch granules), dry coagulated cellulose and starch and cellulose-starch films prepared via wet casting.

II.3.5 Fourier transform infrared spectroscopy

Fourier transformed infrared spectroscopy (FTIR) was performed with a PerkinElmer SpectrumTM One spectrometer in the range of 4000 to 400 cm⁻¹ with 8 scans. The resolution was 4 cm⁻¹. The samples studied were the same as described in the previous section. About 150 mg sample was milled and mixed with 1mg KBr and transformed into pellets.

II.3.6 Scanning electron microscopy

Two scanning electron microscopes (SEMs) were used to investigate the morphology of film samples. A PHILIPS XL30 SEM was set in environmental mode, with a back-scattered electron (BSE) detector, and the acceleration voltage at 15 KV. Samples were placed on a Peltier device at -8°C, and the pressure was maintained at 0.4 - 1.0 mbar in the vacuum chamber. Before being placed in the measuring chamber, all wet films underwent freeze-dried treatment: they were frozen in liquid nitrogen and immediately transferred to the vacuum chamber; as a result the liquid in the pores (water or ethanol) was sublimated. This treatment preserved the three-dimensional morphology of the wet films.

We also used a Carl Zeiss SUPRATM 40 field emission scanning electron microscope (FESEM) to investigate the morphology and the dispersion of carbon black in the composite films. The cellulose-carbon black composite samples, both from EMIMAc solution and NMMO solution, were coagulated in water, dried in vacuum oven, and then sputter-coated with gold/palladium.

II.3.7 Weight loss during coagulation

In order to estimate material weight loss from films during coagulation due to starch (amylopectin) partial leaching-out caused by its dissolution in water, the total weight of polymer in the film was compared with the weight known from the preparation, W_{ini} . Films were dried in a vacuum oven at 70°C for 24 hours, their weight W_f was measured and weight loss $W\%$ calculated as follows:

$$W\% = 100\% \times (W_{ini} - W_f) / W_{ini} \quad (\text{II-4})$$

II.3.8 Permeability measurements

Water permeability of wet films was evaluated using experimental set-up of X-Flow (Enschede, the Netherlands). A round film of diameter 74 mm was placed into the measuring chamber. The permeability, K , was calculated according to Equation II-5, in which V is the volume of permeate in L, t is flow time in hour, P is applied pressure in bar, and S is the film surface in m^2 . The measurements were carried out with pressure from 1 to 6 bar at room temperature.

$$K = \frac{V}{t \times P \times S} \quad (\text{II-5})$$

II.3.9 Resistivity measurements

The sheet resistance (R_s , Ω/sq) of composite films was measured with the Van der Pauw method [Van 1958], of which the principle will be detailed in Chapter V. The experimental set-up was in the ELECTRO laboratory of Centre de Recherche sur l'Hétéro-Epitaxie (CRHEA), and as shown in Figure II-7 and Figure II-8, and the measurements was carried out with kind help of Dr. Yvon Cordier of CRHEA, France. Films samples were cut into size of about 1 cm^2 , and the thickness was measured with a micrometer for calculating specific

resistance. The currents applied for more conductive films were 10^{-3} A, 10^{-4} A, and 10^{-5} A, and the sheet resistance was the average of the three measurements; the currents applied for films with high resistivity were 10^{-7} A, in order to obtain a more reliable result. The set-up is as following:

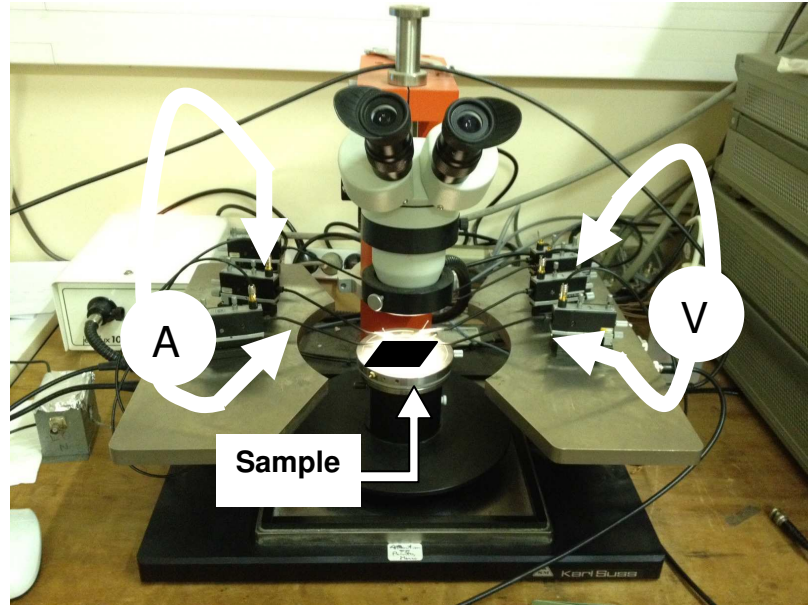


Figure II-7 Experimental set-up of resistivity measurement with Van de Pauw 4-points method by ELECTRO lab of CRHEA, France. The four arrows marked “A” and “V” indicate the four probes used. Measurements of the current between two neighboring probes and the voltage between the other two were carried out, and then rotated among the four probes, see Chapter V.

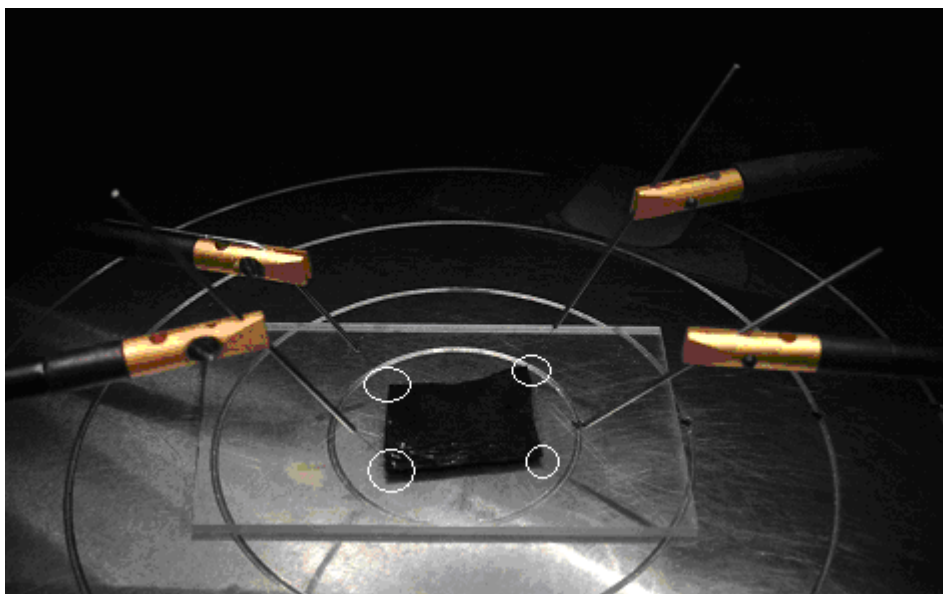


Figure II-8 Measuring part of the Van de Pauw 4-points device: the four probing needles were placed right on the corner of the cellulose-carbon black film sample, as shown in the circles on the figure. The device was set up by ELECTRO lab of CRHEA, France.

Once the sheet resistance (in ohm/sq) has been measured, resistivity (specific resistance, ρ , in ohm.m) could then be calculated knowing the thickness of the films. All measurements were performed at room temperature and without humidity control. Since all the films were dried sufficiently and measured immediately after being taken out from sealed bags, we can ignore the influence of temperature and humidity on resistivity here.

II.4 Analysis of agglomerate dispersion by rheo-optical technique

A counter-rotating rheo-optical device was used for analyzing the dispersion process of carbon black agglomerates under shear. It consists of two flat glass plates rotating in opposite directions, each plate being independently controllable in rotation speed. The shear rate $\dot{\gamma}$ at the position within the two plates where a single carbon black agglomerate particle is positioned (Figure II-9) is given by:

$$\dot{\gamma} = \frac{(V_1 + V_2)r}{h} \quad (\text{II-6})$$

where V_1 and V_2 are the rotation speeds of the two glass plates, in rad/s, r is the radial distance of the agglomerate towards the rotation axis, and h is the gap between the two glass plates

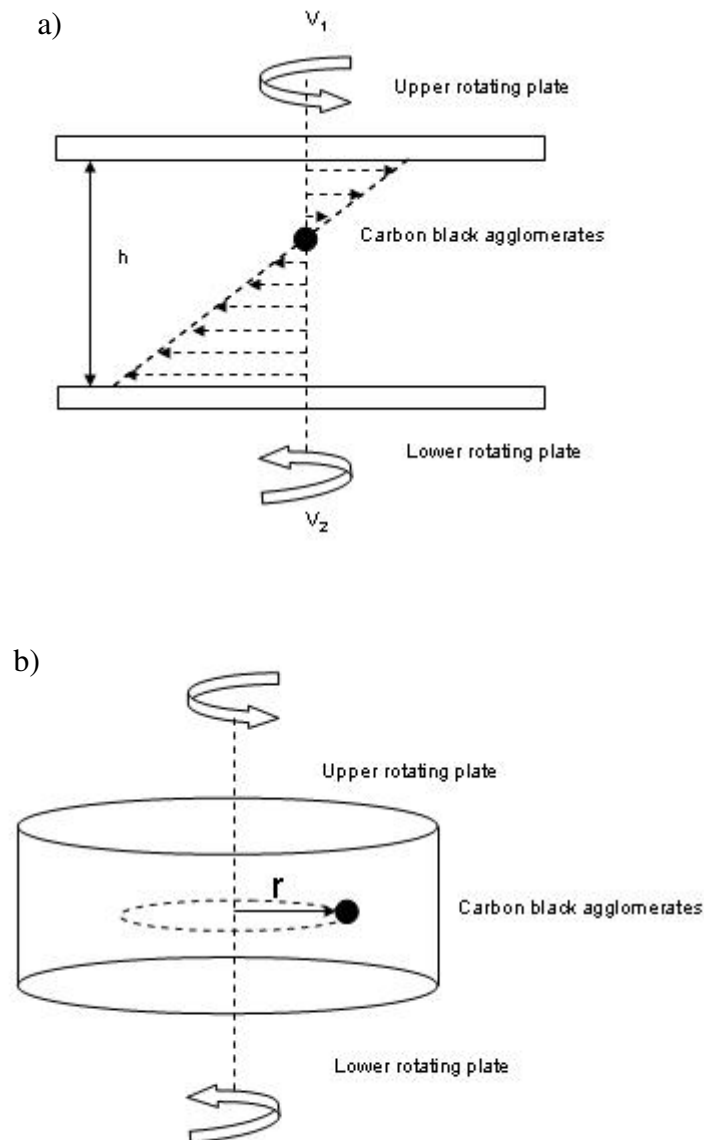


Figure II-9 Schematic illustration of the counter rotating optical device with a carbon black agglomerate particle placed in its suspending medium. The optical observations are performed from above the upper plate.

It has to be remembered that this is not the effective shear stress applied to the agglomerate [Bagster 1974]. This issue will be discussed in the Results and Discussion Part (page

167-171). Due to the counter-rotation of the two glass plates, carbon black agglomerates could be maintained in the laboratory framework, allowing them to be observed in real time during shear with a Metallux 3 (Leitz) optical microscope in transmission mode, fitted with an analogical JVC TK-C1481EG camera at 25 frames per second, a Sony RDR-HX710 DVD video recorder, and a frame code generator (Sony FCG-700), which enable the precise analysis of the change of agglomerate size in time, at a given shear rate.

For each measurement, 2-3 ml of the suspending fluid (cellulose-EMIMAc solution) was placed between the two glass plates. A few carbon black agglomerates were added with the help of a needle tip. Observations can be made for shear rates in the range of 0 to 15-20 s⁻¹. Above about 20 s⁻¹ it is extremely difficult to maintain a single agglomerate in the field of view.

The temperature was maintained at 20°C for all the measurements, except for the measurements with 14% VFC cellulose/EMIMAc solutions, which were also carried out at 30°C, 40°C and 50°C and for the NMMO-based solution where the temperature was kept at 90°C. The temperature was controlled with an external thermal bath.

References

- [Bagster 1974] Bagster, D. F., Tomi, D. (1974). The stresses within a sphere in simple flow fields, *Chemical Engineering Science*, 29(8), 1773-1783.
- [Egal 2007] Egal, M., Budtova, T., & Navard, P. (2007). Structure of aqueous solutions of microcrystalline cellulose-sodium hydroxide below 0°C and the limit of cellulose dissolution. *Biomacromolecules*, 8(7), 2282-2287.
- [Egal 2008] Egal, M., Budtova, T., & Navard, P. (2008). The dissolution of microcrystalline cellulose in sodium hydroxide-urea aqueous solutions. *Cellulose*, 15(3), 361-370.
- [Evans 1989] Evans, R., & Wallis, A. F. A. (1989) Cellulose molecular weights determined by viscometry. *Journal of Applied Polymer Science*, 37(8), 2331-2340.
- [Van 1958] Van der Pauw, L. J. (1958). A method of measuring specific resistivity and Hall effect of discs of arbitrary shape. *Philips Research Reports* 13, 1–9.

Chapter III

Stabilization of cellulose-NaOH-water solutions with ZnO as additive

I. Introduction	94
II. Results and discussion	95
II.1 Solubility of ZnO in cellulose-NaOH-water solutions	95
II.2 Dilute solutions: Intrinsic viscosity	97
II.3 Semi-dilute solutions: gelation	99
III. Conclusions	111
References	112

I. Introduction

As reviewed in the first chapter, the most essential drawback that limits the application of cellulose-NaOH-water solutions is the phenomenon of gelation. In such cellulose solutions, gelation occurs with increasing time and temperature [Roy 2003]. Gelation can sometimes be helpful in certain applications, such as the preparation of cellulose aerogels [Gavillon 2008], but most likely being harmful for cellulose processing and making films and fibres. Thus it seems indispensable to us to search for a stabilizer for the cellulose-NaOH solutions, which prevents or at least delays the gelation, if we want to apply the solutions in, for example, the surface modifications of cellulose matrices.

Zinc oxide was chosen to be an additive to be used for delaying gelation, and the improved stability was supposed to be caused by the stronger hydrogen bonds between cellulose and Zn(OH)_4^{2-} as compared with cellulose-NaOH. Due to the lack of literature data, we aim to shed more light on the physical mechanisms, as well as the related parameters of such gelation-delaying effect, with a comprehensive viscometric and rheological study of cellulose-NaOH-water solutions with and without zinc oxide as additive.

We will look into both dilute and semi-dilute solutions, to see not only the influence of zinc oxide on the behavior of dissolved cellulose macromolecules, but also try to quantitatively correlate parameters such as cellulose concentration, zinc oxide concentration and temperature with the actual gelation-delaying time. We eventually hope to be able to provide a guideline for the practical processing and operation with such stabilized solutions.

II. Results and discussion

In this chapter, Avicel[®] PH-101 microcrystalline cellulose was dissolved in aqueous sodium hydroxide solutions with or without zinc oxide. The materials and standard dissolutions procedures are described in Chapter II. Avicel was chosen since pulp fiber of high DP cannot be fully dissolved in NaOH-water systems, including NaOH-water-ZnO [Cuissinat 2006]. The use of Avicel excludes also any influence of other-than-cellulose components that are present in cellulose fibers originating from plant cell walls.

An Ubbelohde type viscometer was used to study dilute solutions, and a Bohlin rheometer to investigate the dynamic rheological properties and gelation.

II.1 Solubility of ZnO in cellulose-NaOH-water solutions

It should be noted first that values of solution pH strongly influence ZnO solubility [Liu 1998]. It was shown that ZnO is practically insoluble in water (solubility below 10^{-6} g/L), and becomes more soluble in strong acidic or basic media [Liu 1998]. In our work, the preparation of solutions is started by making 18-20%NaOH-water (pH \approx 14.7) and adding the desired amount of ZnO. At this pH, ZnO can be dissolved up to 27 g/L [Liu 1998]. The pH of the final cellulose solutions is 14.3, with which ZnO solubility decreases to about 4 g/L. Thus the saturation of ZnO can be reached in the final solutions containing cellulose with the initial ZnO concentration above 5 g/L (0.5 wt%), and part of ZnO is then in suspended state. To check for the presence of suspended ZnO particles in solution, cellulose-8%NaOH-water with two ZnO concentrations were observed by optical microscopy (Figure III-1).

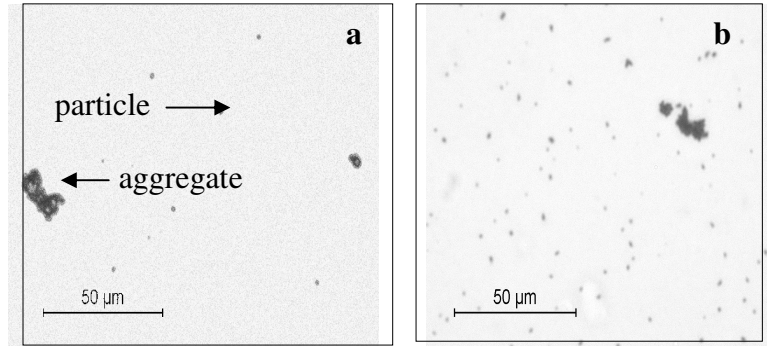


Figure III-1 Optical microscope images of (a) 4%Avicel-8%NaOH-0.7%ZnO-water and (b) 4%Avicel-8%NaOH-1.5%ZnO-water, observed shortly after the preparation at room temperature. Reprinted with permission from [Liu 2011]. Copyright (2011) Springer.

The dispersion of undissolved ZnO was homogenous, with two-size populations, i.e. ZnO particles of about 1 μm and a few aggregates of about 10-20 μm . The sedimentation time of suspended ZnO particles was roughly estimated for two solutions of different cellulose concentrations with Stokes' law (Equation III-1):

$$V_s = \frac{2}{9} \frac{\rho_p - \rho_f}{\eta} gR^2 \quad \text{(III-1)}$$

where V_s is the settling velocity of particles, $\rho_f \approx 1.1 \text{ g/cm}^3$ is the density of solution at room temperature which slightly varies depending on cellulose concentration, $\rho_p = 5.606 \text{ g/cm}^3$ is the density of ZnO particles [Hu 1992], $\eta = 0.15 \text{ Pa}\cdot\text{s}$ and $0.5 \text{ Pa}\cdot\text{s}$ are the viscosities of freshly prepared 4% cellulose-8%NaOH-water solution and 6%cellulose-8%NaOH-water at 5°C, respectively, and R is the radius of particles. The sedimentation times in a beaker of 20 cm in height are from about 8 hours to 28 hours for larger aggregates, and from about one month to four months for smaller particles, for 4% and 6% cellulose solutions, respectively. For gelation experiments this time-dependent sedimentation can be neglected as far as solution viscosity strongly increases during the measurement.

However, in case of storing solutions in refrigerator where gelation is extremely slow, sedimentation of ZnO particles were observed for 1.2% and 1.5% ZnO after several days. Thus we limited ZnO concentration to 1.5% to strongly limit particle sedimentation and most of the experiments, especially for dilute solutions, were performed for 0.7 wt%ZnO, where there is only a very small fraction of undissolved ZnO.

II.2 Dilute solutions: Intrinsic viscosity

II.2.1 Determination of the intrinsic viscosity

The intrinsic viscosity $[\eta]$ is an important parameter for polymer solutions. It depends on the size of cellulose macromolecules when dissolved in aqueous NaOH solutions, and may vary with the presence of ZnO. $[\eta]$ is usually calculated with the classical Huggins equation (Equation III-2):

$$\frac{\eta_{rel} - 1}{c} = [\eta] + k_H [\eta]^2 c \quad (\text{III-2})$$

where the relative viscosity $\eta_{rel} = \eta_{sol}/\eta_{solv}$, η_{sol} and η_{solv} are the solution and solvent viscosity, respectively, k_H is the Huggins coefficient, and the polymer concentration c is expressed in mass per volume units. The values of $[\eta]$ are deduced if we plot $(\eta_{rel}-1)/c$ vs. c , and extrapolate the line to $c=0$. We obtained the values of $[\eta]$, as demonstrated in Figure III-2, for cellulose dissolved in 8% NaOH-water solutions without or with 0.7% ZnO at two different temperatures.

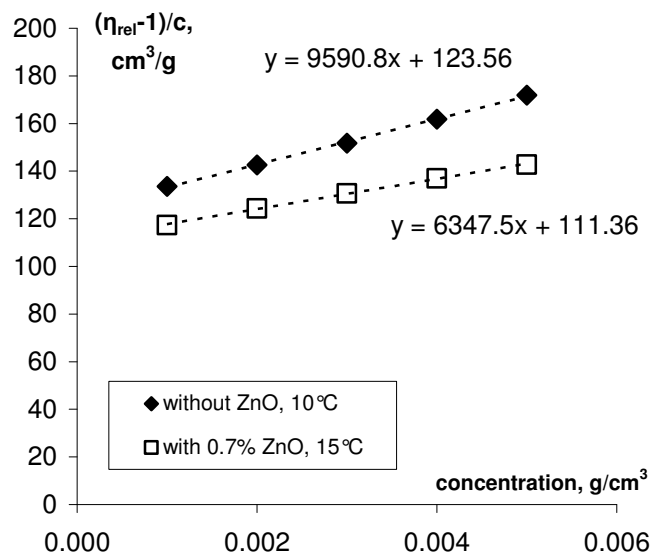


Figure III-2 Extrapolation of Huggins equation to obtain intrinsic viscosity of cellulose in 8%NaOH-water solutions without or with 0.7% ZnO, at 10°C and 15°C.

II.2.2 Influence of ZnO on cellulose intrinsic viscosity in 8%NaOH-water

With the Huggins approach, we calculated the cellulose intrinsic viscosity, $[\eta]$, in 8%NaOH-water with 0.7%ZnO and without ZnO at different temperatures, and found the temperature dependence given in Figure III-3. A steady decrease of the intrinsic viscosity with increasing temperature was observed for both cases, with and without ZnO, and is consistent with the results already reported for cellulose of another molecular weight dissolved in 8% NaOH-water [Egal 2006] and in 9% NaOH-water [Roy 2003] without any additive. The drop of $[\eta]$ signifies that the thermodynamic quality of solvent decreases with temperature. The mechanism of this phenomenon is thought to be as follows: during the dissolution process, the NaOH hydrates break intra-chain hydrogen bonds between cellulose macromolecules and link to cellulose chains. It was shown that at least four NaOH per one anhydroglucose unit are needed to dissolve cellulose [Egal 2007]. We assume that there is an unstable equilibrium between NaOH hydrates bound to cellulose chains. When temperature is raised, cellulose-cellulose interactions become more favored compared to cellulose-NaOH interactions leading to the shrinkage of cellulose coils in dilute solution and decrease of intrinsic viscosity. In semi-dilute solution, this leads to the inter-chain connection of cellulose coils, and eventually gelation happens.

The presence of ZnO did not bring any noticeable change to the intrinsic viscosity of cellulose. As it will be shown in the following, when 0.7%ZnO is mixed with 8%NaOH-water, only part of ZnO is dissolved. The unaffected value of $[\eta]$ indicates that neither dissolved nor suspended ZnO influences the conformation and behavior of cellulose chains at molecular level in dilute region. Similar results were reported when thiourea was added into cellulose-NaOH-water solution, giving the same intrinsic viscosity up to a thiourea content of 0.75M [Zhang 2002].

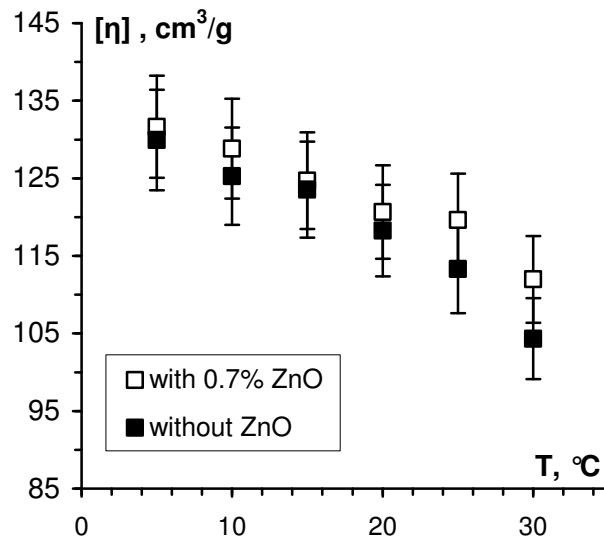


Figure III-3 Intrinsic viscosity of cellulose-8%NaOH-water solutions without or with 0.7% ZnO, from 5°C to 30°C; with error bars of 5%. Reprinted with permission from [Liu 2011]. Copyright (2011) Springer.

II.3 Semi-dilute solutions: gelation

II.3.1 Determination of the gelation time

When gelation happens, the polymers chains are cross-linked at macroscopic level by either chemical bonds (covalent bonds) or weaker physical bonds (hydrogen bonding or Van der Waals forces, etc.) to form an infinite network, resulting in either chemical gels or physical gels. In our case, the gelation of cellulose-NaOH-water solution is thermally-induced and irreversible. The traditional Winter and Chambon [Winter 1986] approach, which was proposed for the chemical gel, does not seem to be perfectly applicable in our case, since the gelation in cellulose solutions is due to the hydrogen bonds among cellulose, and it is also coupled with micro-phase separation process. Nevertheless, it still makes sense to use oscillatory rheological measurements to track the elastic modulus (G') and viscous modulus (G'') with time. As shown in Figure III-4a and Fig III-4b, the cellulose solutions were in liquid state at the beginning of the tests, having a large G'' compared to G' . When gelation happened (Figure III-4a) the sample became more elastic with $G' > G''$. We ascribe the time when the measured G' value intercepts the G'' value as the gelation time t_{gel} (Figure III-4a). Also in some cases shown in Figure III-4b, curves of G' and G'' stayed parallel and did not

cross after considerable measurement time. We are then only able to state that if gelation ever occurs, it takes longer than three days which is a maximal reasonable duration of a rheological experiment.

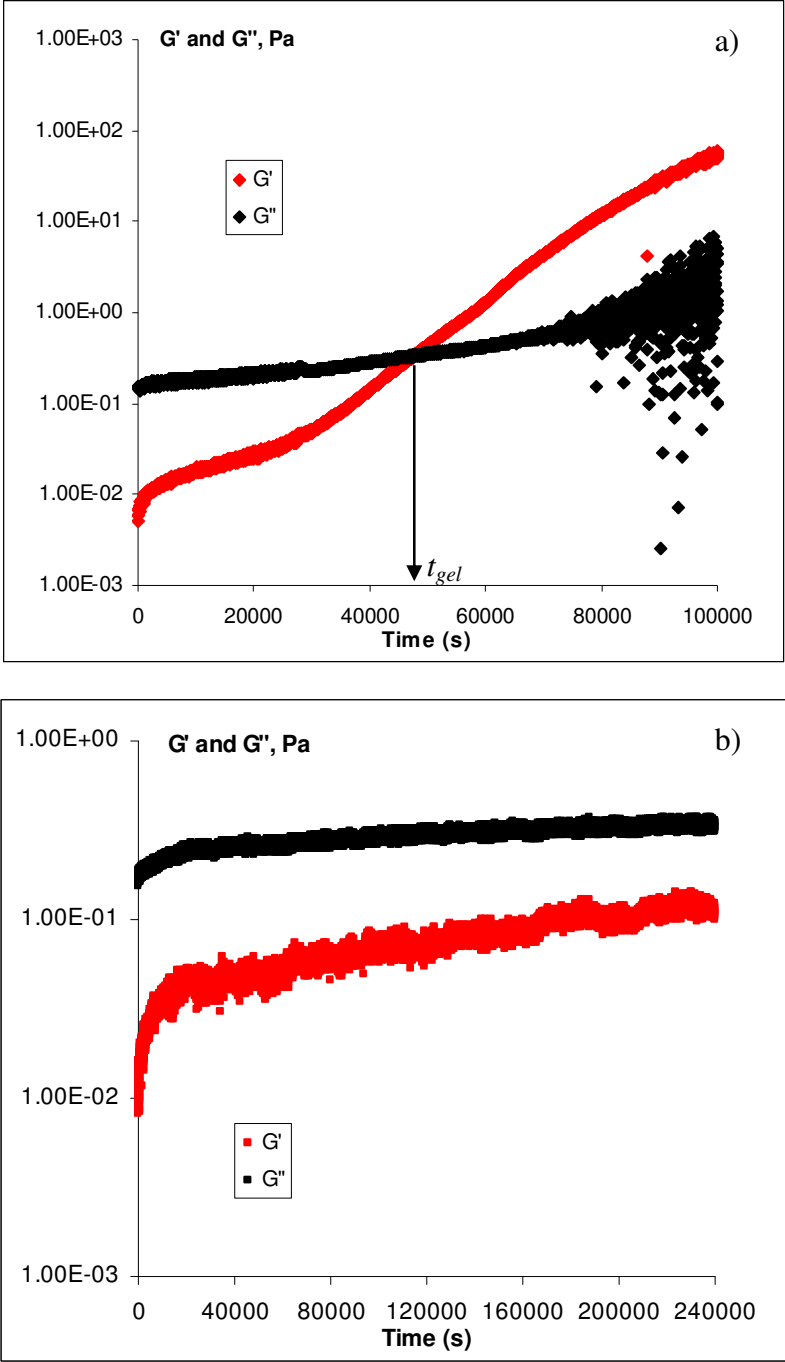


Figure III-4 G' and G'' measured as a function of time for 6%cellulose-8%NaOH-water at 15°C with a) 0.7% ZnO and b) 1.5% ZnO.

II.3.2 Overall results on the delay of gelation

The results on gelation time of cellulose-8%NaOH-water solutions at temperatures from -5° to 50°C at various cellulose and ZnO concentrations are summarized in Table III-1. An example of gelation time as a function of solution temperature for two cellulose concentrations is given in Figure III-5. The results obtained clearly show that gelation is significantly delayed in the presence of ZnO: for example, a 6%cellulose solution at 20°C is gelling in 15 minutes in only 8%NaOH-water and in 36 hours if 1.5%ZnO is added. The results presented in Table III-1 also show that gelation time depends on solution temperature and cellulose and ZnO concentrations. In the following we shall analyze the influence of each parameter, one after another, on the gelation time.

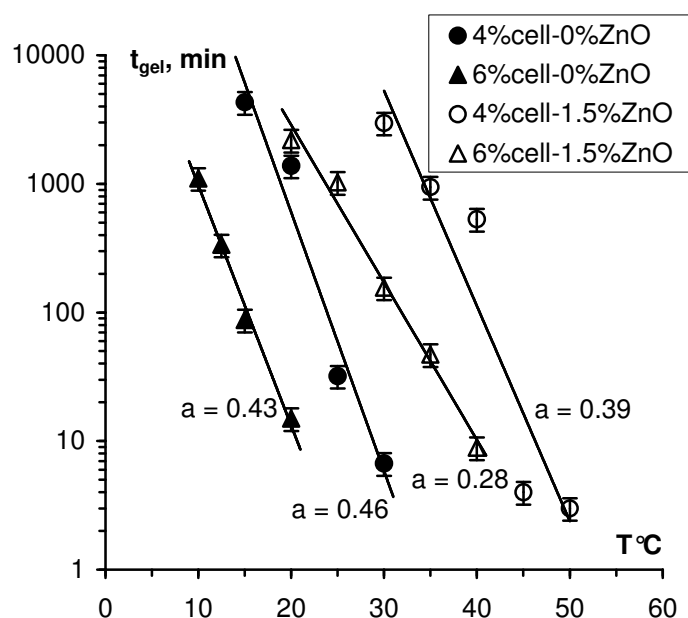


Figure III-5 Gelation times of 4% and 6% cellulose-8%NaOH-water solutions, without and with ZnO added, at different temperatures. Lines are exponential approximations according to Equation III-3. The error bars are of 20%. Reprinted with permission from [Liu 2011]. Copyright (2011) Springer.

Table III-1 Gelation times of cellulose-8%NaOH-water solutions at different temperatures and concentrations of ZnO. Adapted with permission from [Liu 2011]. Copyright (2011) Springer.

T°C	Gelation times, min				
	4%cellulose-8%NaOH		6%cellulose-8%NaOH		
	0%ZnO	0.7%ZnO	0%ZnO	0.7%ZnO	1.5%ZnO
-5	>5 days	>3 days			
0	>2 days	>2 days			
5	>2 days		> 2days		
10			1106	>2 days	
12.5			336		
15	4320		88	791	>2 days
17				452	
20	1384		15		2190
22.5				185	
25	32			74	1032
30	6.7	2980		7.7	156
35		946			47
40		532			8.9
45		4			
50		3			

II.3.3 Influence of temperature on gelation

Special attention was paid to studying the gelation time of cellulose solutions at low temperatures, around -5° - $+5^{\circ}\text{C}$. The reason was to check if a sudden decrease of gelation time with temperature decrease below -0°C , reported for cellulose-7%NaOH-12%urea system, is reproduced for our solutions [Cai 2006]. These exceptionally long experiments, from 3 to 5 days, were performed on 4%cellulose solutions (see Table III-1). In no case did we observe any decrease of gelation time with temperature decrease. According to our previous observations, gelation cannot be studied below -5°C since water in 8%NaOH-water may start crystallizing at this temperature: the end of water melting peak was recorded at -6° - -4°C when solutions were heated from -60°C to room temperature [Egal 2007].

The thermally-induced gelation of cellulose-NaOH solutions can be explained as follows. As shown for dilute solutions, solvent thermodynamic quality decreases with temperature increase. This leads to cellulose chains association via inter- and intra-chain interactions. In dilute solutions below polymer overlap concentration, the coils contract. Above the overlap concentration, gelation occurs via intra-chain interactions. The higher the temperature is, the quicker is the gelation. As already suggested in literature [Roy 2003; Gavillon 2008], at given cellulose concentration, gelation time is exponentially temperature-dependent (Equation III-3):

$$t_{gel} = Dexp(-aT) \quad \text{(III-3)}$$

where D and a are adjustable parameters. Examples of the exponential approximations of gelation time versus temperature are shown in Figure III-5. In the range of cellulose and ZnO concentrations studied, the exponent coefficient a varies from 0.28 to 0.46. Similar results were obtained for the same microcrystalline cellulose dissolved in 7.6%NaOH-water ($a = 0.35$) [Gavillon 2008] and in 9%NaOH-water ($a = 0.4$) [Roy 2003].

II.3.4 Influence of cellulose concentration on gelation

Increasing polymer concentration facilitates gelation, since chains are closer to each other, allowing an easier formation of a network. The influence of cellulose concentration on gelation time is given in Figure III-6. The inverse of t_{gel} as a function of cellulose concentration C_{cell} presents in a double logarithmic plot showing that there is a power law relation between these two parameters.

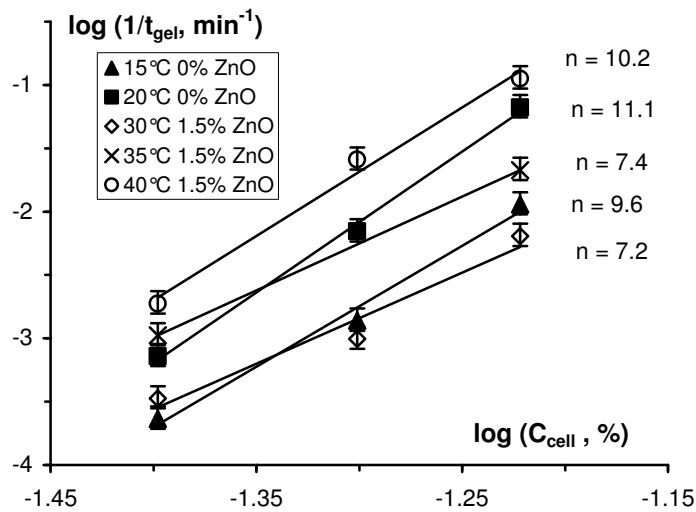


Figure III-6 Double logarithmic plot of $1/t_{gel}$ versus cellulose concentration, with and without ZnO added, at five different temperatures. Lines are power law approximations according to Equation III-5. Reprinted with permission from [Liu 2011]. Copyright (2011) Springer.

A power law dependence of gelation time on carrageenan concentration was suggested by Ross-Murphy [Ross-Murphy 1991]:

$$t_{gel} \approx \frac{K}{[(C/C_0)^{n'} - 1]^p} \quad (\text{III-4})$$

where C_0 is the critical concentration above which gelation could happen, n' is the number of polymer chains involved in a junction zone (assumed to be 2), K is a rate constant and p is a percolation exponent estimated to be around 2. An analogy between carrageenan gels and cellulose gels seems to be worth looking at. For cellulose solutions, the overlap concentration C^* , which could be considered as critical concentration for gelation, is around 1%, depending

on temperature (see Figure III-3). C^* of the same microcrystalline Avicel cellulose in 9%NaOH-water was reported to be 0.83% below 20°C and 1.25% at 40°C [Roy 2003]. Considering these values, Equation III-4 can be simplified as follows:

$$t_{gel} \approx \frac{k}{C_{cell}^n} \quad \text{(III-5)}$$

where k is a rate constant and n is a kinetic exponent. There is a good fit between the above model and the experimental data, as shows Figure III-6. The exponent n is related to the gelation kinetics as well as to the organization of the junction zones in gel. From Figure III-6, the values of n are more or less constant (within the experimental errors) and equal to 9 ± 2 , with or without ZnO. Although the gelation kinetics and the detailed description of the junction zones are not possible at this stage of investigations, we can conclude that they are not strongly influenced by the addition of ZnO.

An increase of cellulose concentration strengthened the gel, as expected. The dependence of G_{gel}' at get point (i.e. when $G' = G''$) as a function of cellulose concentration is shown in Figure III-7. A strong power law correlation between G_{gel}' and C_{cell} , $G' \sim C_{cell}^u$ is observed with the scaling exponents u varying from 2 to 3.6. A similar dependence was reported for Avicel and other types of cellulose with the scaling constant varying from 3 to 4 [Zhang 2002]. Such strong power law concentration dependence is not typical for gelling polysaccharides: for example, the Young modulus of gelled agarose or k-carrageenan is square-concentration dependent [Nijenhuis 1997]. Gelation of cellulose-NaOH-water solutions is a complex process coupled with a micro-phase separation. Network defects such as loose ends and loops are not participating to gel mechanical strength. The number of cellulose-cellulose bonds in each junction point may also vary with cellulose concentration.

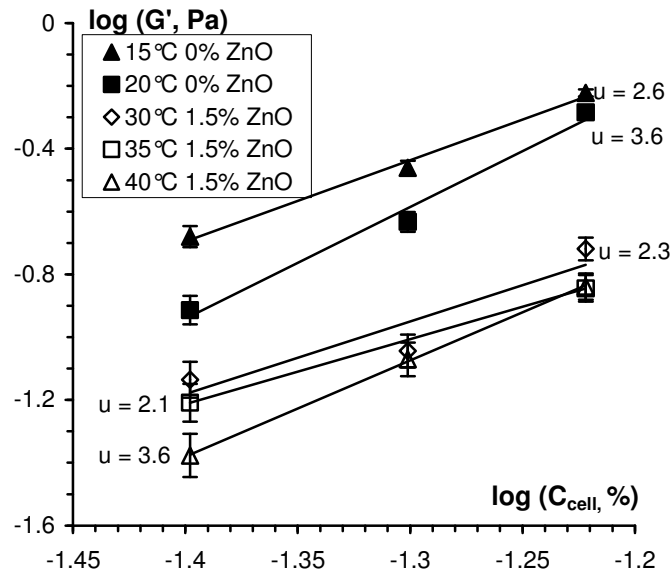


Figure III-7 Double logarithmic plot of elastic modulus G' at gel point versus cellulose concentration, with or without ZnO added, at five different temperatures. Lines are power law approximations $G' \sim C_{cell}^u$. Reprinted with permission from [Liu 2011]. Copyright (2011) Springer.

II.3.5 Influence of ZnO concentration on gelation

Table III-1 shows that the increase of ZnO concentration delays gelation. We measured the gelation time of 6%cellulose-8%NaOH-water at various ZnO content, 0%, 0.7% and 1.5% from 10°C to 45°C. The results are presented in Figure III-8a. A master plot can be obtained by shifting two data sets, for 0.7% and 1.5% ZnO, towards the one without ZnO (Figure III-8b). The same shape of the initial curves indicates that despite ZnO efficiency in delaying gelation, the increase in ZnO concentration does not change gelation kinetics.

Gelation time was studied as a function of ZnO concentration, C_{ZnO} , at fixed temperature and cellulose concentration. Figure III-9 shows results for $T = 40^\circ\text{C}$ and $C_{cell} = 4\%$. Gelation time exponentially increases with ZnO concentration and can be described by the following equation in the studied ZnO concentration range:

$$t_{gel} = t_0 + B \times C_{ZnO}^m \quad (\text{III-6})$$

where t_0 is the gelation time at $C_{ZnO} = 0$, B is a constant and m is an exponent indicating the influence of ZnO. For 4%Avicel-8%NaOH-water solutions at 40°C we have $t_0 \approx 0$ (almost immediate gelation without ZnO) and the least square approximation gives $B = 119.2$ and $m = 3.53$ when C_{ZnO} is expressed in wt% and gelation time in minutes.

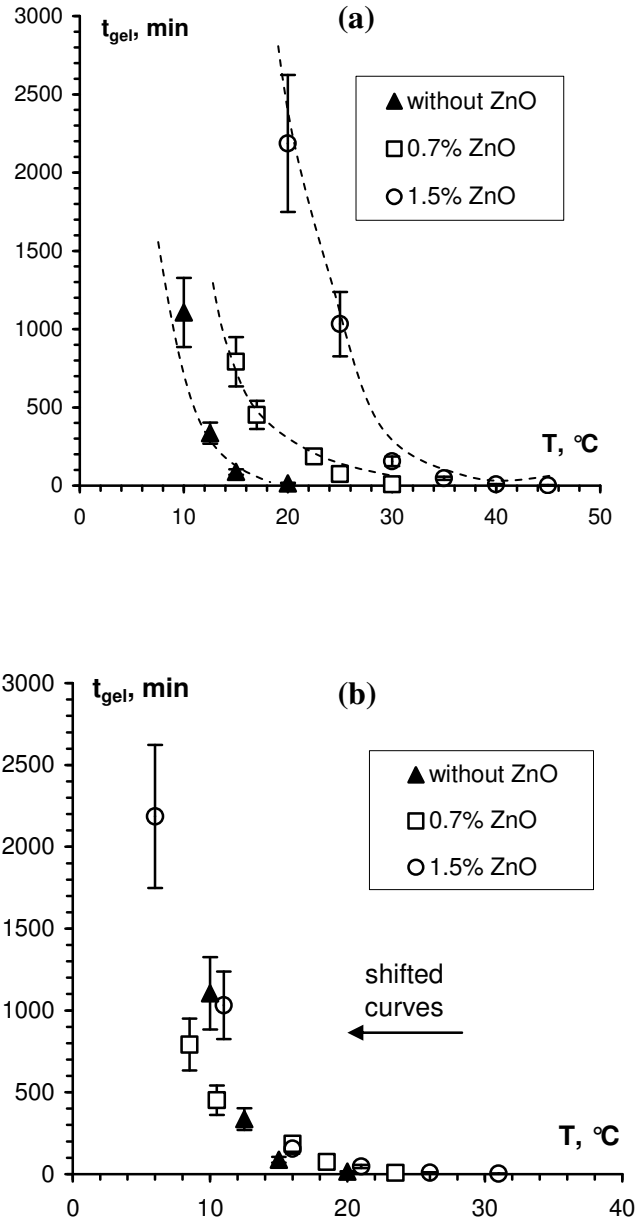


Figure III-8 Gelation time versus temperature for 6%cellulose-8%NaOH-water solutions with 0%, 0.7% and 1.5% ZnO: a) initial data, b) shifted towards 0%ZnO by 6.5°C for 0.7% ZnO and by 14°C for 1.5% ZnO. The lines are given to guide the eye. Reprinted with permission from [Liu 2011]. Copyright (2011) Springer.

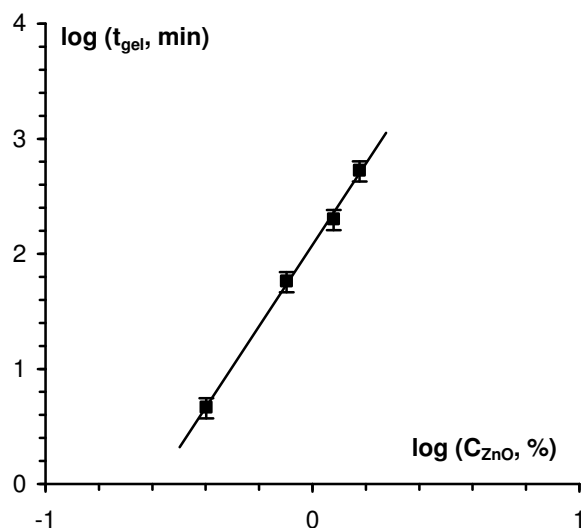


Figure III-9 Double logarithmic plot of gelation time versus ZnO concentration for 4% Avicel-8% NaOH-water solutions at $T = 40^\circ\text{C}$. The solid line is power law approximation according to Equation III-6 with $t_0 \approx 0$ for this temperature. Reprinted with permission from [Liu 2011]. Copyright (2011) Springer.

II.3.6 Role of ZnO as gelation delayer

Summarizing the results obtained from the influence of ZnO on cellulose-NaOH-water solution properties, the following three major facts can be listed:

- 1) ZnO is quite efficient in delaying gelation of cellulose solutions;
- 2) ZnO does not have much influence on either gelation kinetic order or the junction zones in cellulose gels;
- 3) ZnO does not change the properties of cellulose at the molecular level and does not improve the thermodynamic property of solvent towards cellulose.

Correlating the facts mentioned above with the results obtained on the role of urea as a stabilizer for cellulose-NaOH-water solutions [Egal 2008], we can speculate about the role of ZnO in the stabilization of cellulose-NaOH-water solutions. It was demonstrated that to dissolve cellulose, at least four NaOH molecules per one anhydroglucose unit are needed [Egal 2007]; NaOH hydrates are breaking cellulose intra-chain hydrogen bonds and linking to cellulose chains. The same is valid for cellulose-NaOH-water solutions containing urea [Egal

2008]. Cellulose-NaOH-water solutions are not stable; cellulose chains tend to aggregate, leading to gelation. When ZnO is suspended in NaOH-water solutions, a “network” of tiny particles is formed. The surface of particles is hydrolyzed and a layer of hydroxide is formed ($\equiv\text{Zn-OH}$) attracting water molecules. When dissolved, Zn(OH)_3^- and Zn(OH)_4^{2-} ions are formed [Reichle 1975; Degen 2000] that also trap water. Thus ZnO may play the role of a water “binder”, decreasing strongly the amount of free water around the cellulose chains that may drive chain aggregation. ZnO stabilizes the solution by keeping water far from the cellulose chains, as urea does [Egal 2008]. This could explain why ZnO only delays the gelation but does not change cellulose dissolution, solvent quality and gelation kinetics in NaOH-water solutions.

II.3.7 Semi-empirical model to estimate gelation times

As shown in sections II.3.3-II.3.5 of this chapter, the gelation time of cellulose solution in NaOH-ZnO-water is influenced by temperature and cellulose and ZnO concentrations. Combining Equation III-3, III-5 and III-6, an equation correlating gelation time with these three variables can be built:

$$t_{gel} = \left(\frac{A}{C_{Avicel}^n} + B \cdot C_{ZnO}^m \right) e^{-aT} \quad \text{(III-7)}$$

where the exponents n and m in the power-law concentration dependences are the arithmetic mean values of the corresponding exponents obtained for all data according to Equation III-5 and Equation III-6 ($n = 9$ and $m = 3.5$, see sections II.3.4 and II.3.5), constant a is the mean value of a -constants (Equation III-3) obtained for all data ($a = 0.35$, see section II.3.3) and A and B are fit parameters found with the least square approximation. The comparison between the calculated values of t_{gel} according to Equation III-7 and experimental data is shown in Figure III-10. The semi-empirical model suggested fits reasonably well the experimental values, allowing making an approximate estimation of gelation time of cellulose (Avicel) solutions as a function of temperature and cellulose and ZnO concentrations.

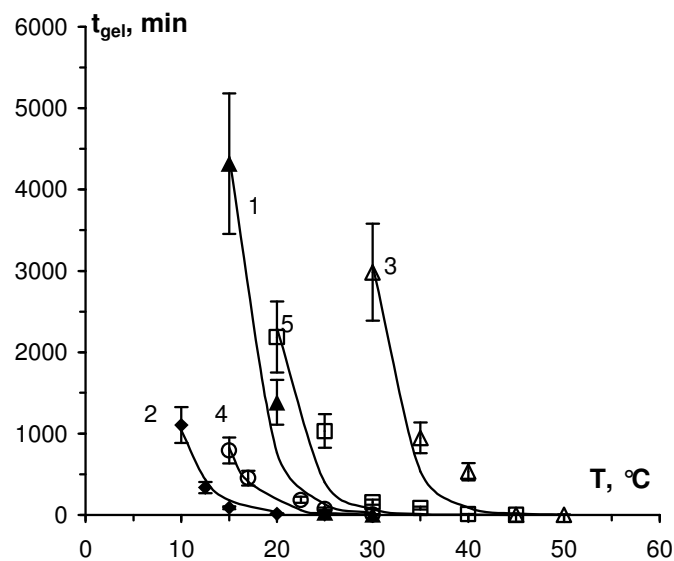


Figure III-10 Estimated (solid lines) and experimental (points) gelation times as a function of temperature for solutions of different cellulose and ZnO concentrations. Filled points: solutions without ZnO 4%cellulose-8%NaOH (1) and 6%cellulose-8%NaOH (2); open points: with ZnO 4%cellulose-8%NaOH-1.5%ZnO (3), 6%cellulose-8%NaOH-0.7%ZnO (4) and 6%cellulose-8%NaOH-1.5%ZnO (5). Reprinted with permission from [Liu 2011]. Copyright (2011) Springer.

III. Conclusions

In this chapter, we confirmed that ZnO plays a role of stabilizer against gelation in cellulose-NaOH-water solutions. The influence of ZnO on the properties of cellulose-8%NaOH-water solutions in dilute and semi-dilute state was investigated in details at various temperatures and cellulose and ZnO concentrations. The gelation-delaying effect is a power-law function of ZnO concentration despite that ZnO is both in dissolved and in suspended state above a certain concentration. The fact that *suspended* ZnO is a good stabilizer explains why it does not influence cellulose properties on the molecular level both in dilute solutions (intrinsic viscosity and solvent thermodynamic quality) and in semi-dilute state (gelation kinetics and composition of junction zones). We suggest that the physical mechanism of gelation delaying effect of ZnO is due to its role as free water “binder” via formation of hydrates (in dissolved state) and hydroxides (on particles surface). We also obtain a semi-empirical model predicting gelation time as a function of Avicel concentration, ZnO concentration and temperature. With ZnO as an additive, cellulose-NaOH-water solutions can be stabilized at room temperature, and potentially be used in the surface modification of cellulose-based materials.

References

- [Cai 2006] Cai, J., & Zhang, L. (2006). Unique gelation behavior of cellulose in NaOH/urea aqueous solution. *Biomacromolecules*, 7(1), 183-189.
- [Cuissinat 2006] Cuissinat, C., & Navard, P. (2006). Swelling and dissolution of cellulose Part II: Free floating cotton and wood fibres in NaOH-water-additives systems. *Macromolecular Symposia*, 244, 19-30.
- [Degen 2000] Degen, A., & Kosec, M. (2000). Effect of pH and impurities on the surface charge of zinc oxide in aqueous solution. *Journal of the European Ceramic Society*, 20(6), 667-673.
- [Egal 2006] Egal, M. (2006). Structure and properties of cellulose/NaOH aqueous solutions, gels and regenerated objects. Thèse de doctorat, Ecole Nationale Supérieure des Mines de Paris.
- [Egal 2007] Egal, M., Budtova, T., & Navard, P. (2007). Structure of aqueous solutions of microcrystalline cellulose/sodium hydroxide below 0 degrees C and the limit of cellulose dissolution. *Biomacromolecules*, 8(7), 2282-2287.
- [Egal 2008] Egal, M., Budtova, T., & Navard, P. (2008). The dissolution of microcrystalline cellulose in sodium hydroxide-urea aqueous solutions. *Cellulose*, 15(3), 361-370.
- [Gavillon 2008] Gavillon, R., & Budtova, T. (2008). Aerocellulose: New highly porous cellulose prepared from cellulose-NaOH aqueous solutions. *Biomacromolecules*, 9(1), 269-277.
- [Hu 1992] Hu, J. H., & Gordon, R. G. (1992). Textured aluminium-doped zinc-oxide thin-films from atmospheric-pressure chemical-vapor deposition. *Journal of Applied Physics*, 71(2), 880-890.

[Liu 1998] Liu, Y., & Piron, D. L. (1998). Study of tin cementation in alkaline solution. *Journal of the Electrochemical Society*, 145(1), 186-190.

[Liu 2011] Liu, W., Budtova, T., & Navard, P. (2011). Influence of ZnO on the properties of dilute and semi-dilute cellulose-NaOH-water solutions. *Cellulose*, 18(4), 911-920.

[Nijenhuis 1997] Nijenhuis, K. (1997). *Thermoreversible networks: viscoelastic properties and structure of gels*. Advances in Polymer Science 130, Springer.

[Reichle 1975] Reichle, R. A., McCurdy, K. G., & Hepler, L. G. (1975). Zinc hydroxide – solubility product and hydroxy-complex stability-constants from 12.5-75 °C. *Canadian Journal of Chemistry-Revue Canadienne De Chimie*, 53(24), 3841-3845.

[Ross-Murphy 1991] Ross-Murphy, S. B. (1991). Concentration dependence of gelation time. In: Dickinson E (ed) *Food Polymers, Gels and Colloids*. Royal Society of Chemistry, Cambridge, pp 357-368.

[Roy 2003] Roy, C., Budtova, T., & Navard, P. (2003). Rheological properties and gelation of aqueous cellulose-NaOH solutions. *Biomacromolecules*, 4(2), 259-264.

[Wikes 2001] Wilkes, A. G. (2001). The viscose process. In: Woodings C (ed) *Regenerated cellulose fibres*. Woodhead Publishing, Cambridge, pp 37-61.

[Winter 1986] Winter, H. H., & Chambon, F. (1986). Analysis of linear viscoelasticity of a cross-linking polymer at the gel point. *Journal of Rheology*, 30(2), 367-382.

[Zhang 2002] Zhang, L. N., Ruan, D., & Gao, S. J. (2002). Dissolution and regeneration of cellulose in NaOH/thiourea aqueous solution. *Journal of Polymer Science Part B-Polymer Physics*, 40(14), 1521-1529.

Chapter IV

From dissolution of unmodified waxy starch (amylopectin) in ionic liquid to homogenous starch-cellulose films with tuned morphology

I. Introduction	118
II. Results and discussion	120
II.1 Dissolution/gelatinisation process of waxy starch	120
II.2. Rheological proprieties of starch solution in EMIMAc	125
II.3 Rheological properties of starch-cellulose-EMIMAc	132
II.4 Properties of starch-cellulose films	137
III. Conclusions	148
References	150

I. Introduction

One important application for cellulose is to make films and membranes [Zhang 1995; Ruan 2004; Mao 2006; Cai 2007; Miyamoto 2009], which are biocompatible and of high chemical stability. If we want to bring extra functionalities and to vary the material properties and morphology to the cellulosic films and membranes, one solution is to blend them with other components, including starch and its various derivatives, which opens new routes for making multifunctional films, membranes and templates for food, pharmaceutical, biomedical and water treatment applications.

A common route to prepare such blended cellulose-starch films or membranes is what is called the “dissolution-mixing-coagulation” process. In this process, cellulose and starch are first dissolved in a common solvent separately, then mixed together, and finally coagulated in a non-solvent to obtain the films or the membranes. EMIMAc was chosen as such a common solvent, as we detailed in Chapter II, due to its low vapour pressure, high thermal stability and a relatively low viscosity at room temperature, which enables cellulose and starch dissolution by simple heating and stirring.

Since the information about the dissolution of starch in EMIMAc is rather scarce, we start by investigating the fundamental background on solution and hydrodynamic properties of starch-ionic liquid solutions, as well as starch-cellulose-ionic liquid mixtures. First we used optical microscope to monitor starch granules dissolution in EMIMAc, and we compared this process with starch gelatinization in water. Then we examined the rheological properties of both dilute and semi-dilute starch-EMIMAc solutions. Using the Carreau-Yasuda model, we obtained zero-shear rate viscosities at various temperatures and starch concentrations and use them to build viscosity-concentration dependences. This work allows us to determine starch intrinsic viscosity at different temperatures, to compare the trend obtained with the one known for cellulose dissolved in EMIMAc, and also to calculate starch activation energy, showing that it is power-law dependent on starch concentration. A similar rheological study of cellulose-starch-EMIMAc mixtures of various compositions and at different temperatures was also performed. We checked if the mixing rule can be applied and if there are any special interactions between two polysaccharides in solution.

Once we have a fully understanding of solutions/mixtures, we prepared blended starch/cellulose films via the dissolution-mixing-coagulation process. Films were obtained, thoroughly characterized with FTIR, XRD, SEM and tested for water permeability, in order to understand structure-properties relationships. Cellulose films prepared with the same method were also studied for comparison.

II. Results and discussion

The starch that we chose here is unmodified waxy corn starch, since it is essentially pure amylopectin, and can simplify the understanding and interpretation of the results obtained. The materials used, including Avicel cellulose, waxy corn starch, and EMIMAc, are described previously. Details on the solution characterization and film characterization can also be found in Chapter II.

II.1 Dissolution/gelatinisation process of waxy starch in EMIMAc, water and EMIMAc/water

The goal of this part is to qualitatively analyse the behaviour of starch granules in ionic liquid and compare with the known starch-in-water gelatinisation process. Only one heating rate, 5°C/min, was used to qualitatively demonstrate the difference of starch behaviour in EMIMAc versus water.

The evolution of 5% starch dry granules dispersed in EMIMAc under heating from 40°C is shown in Figure IV-1 for some representative temperatures. For comparison, the same process in water is demonstrated in Figure IV-2. In EMIMAc, starch dissolution gradually proceeds with time and temperature. Solvent penetrates granule, making outer layer slightly swollen (and thus transparent). However, most of the granules kept their initial shape up to 80°C. Above 80°C quick dissolution occurs (Figure IV-1d) and less and less granules can be seen, up to complete visual disappearance at 100°C after a few minutes of storage at this temperature. Total (visual) dissolution time in these conditions was about 16 minutes. A similar behaviour was observed for normal maize starch (23% amylose content) in 78%NMMO-22%water system [Koganti 2011]. Starch dissolution in EMIMAc also occurs at room temperature but kinetics is very slow. Such dissolution process is clearly very different from starch gelatinization in water, see Figure IV-2. In water, waxy corn starch granules first swell with temperature increase and then burst around 65°-70°C (Figure IV-2b) under heating conditions. While there is a large amount of liquid around dissolving starch granules in

EMIMAc (Figure IV-1, b-e), in water granules are highly swelling absorbing almost all water around (Figure IV-2, a-b). The viscosities of these systems are thus very different.

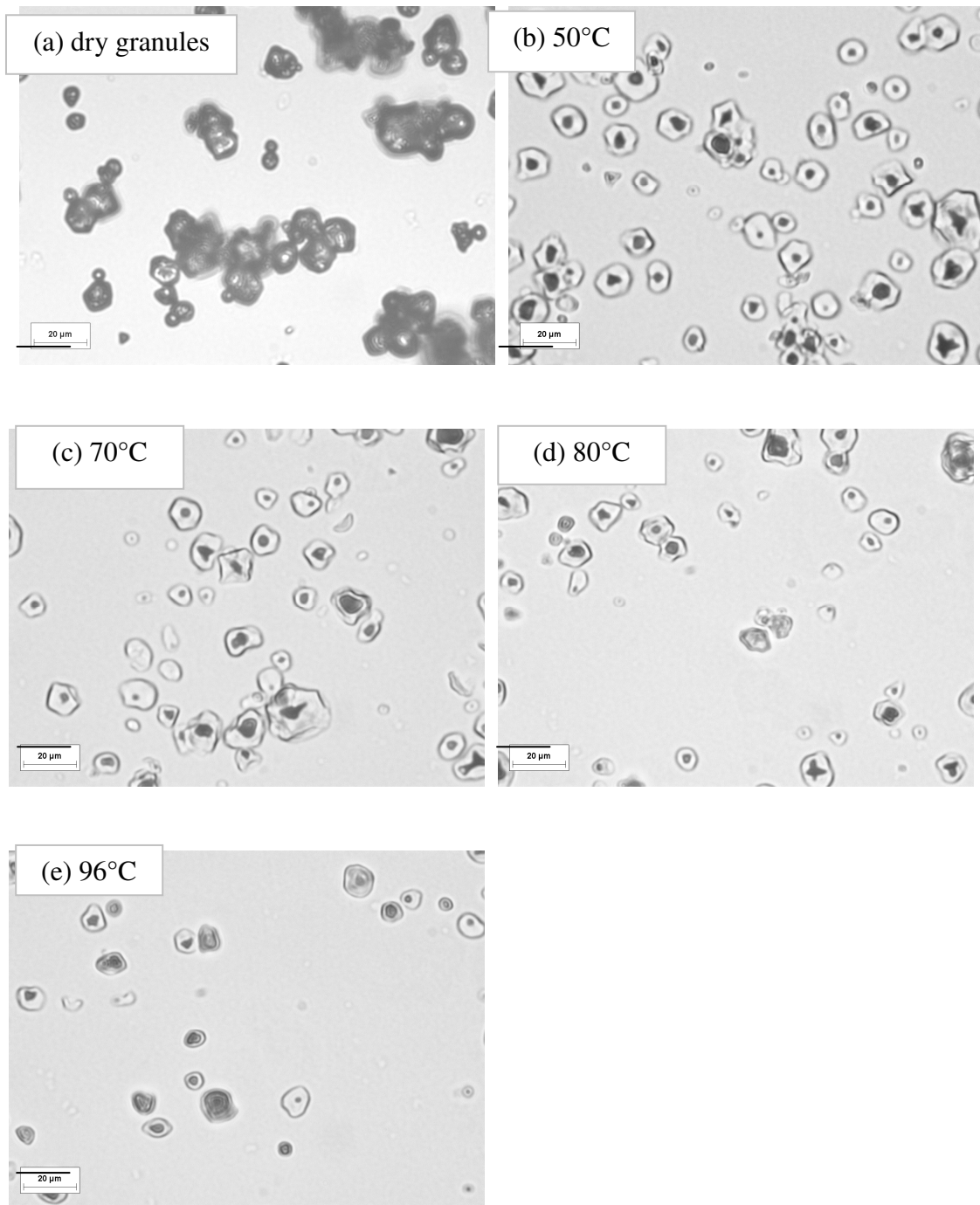


Figure IV-1 Evolution of waxy corn starch granules in EMIMAc during heating. The scale in all optical micrographs is 20 μm . Reprinted with permission from [Liu 2012a]. Copyright (2012) Elsevier.

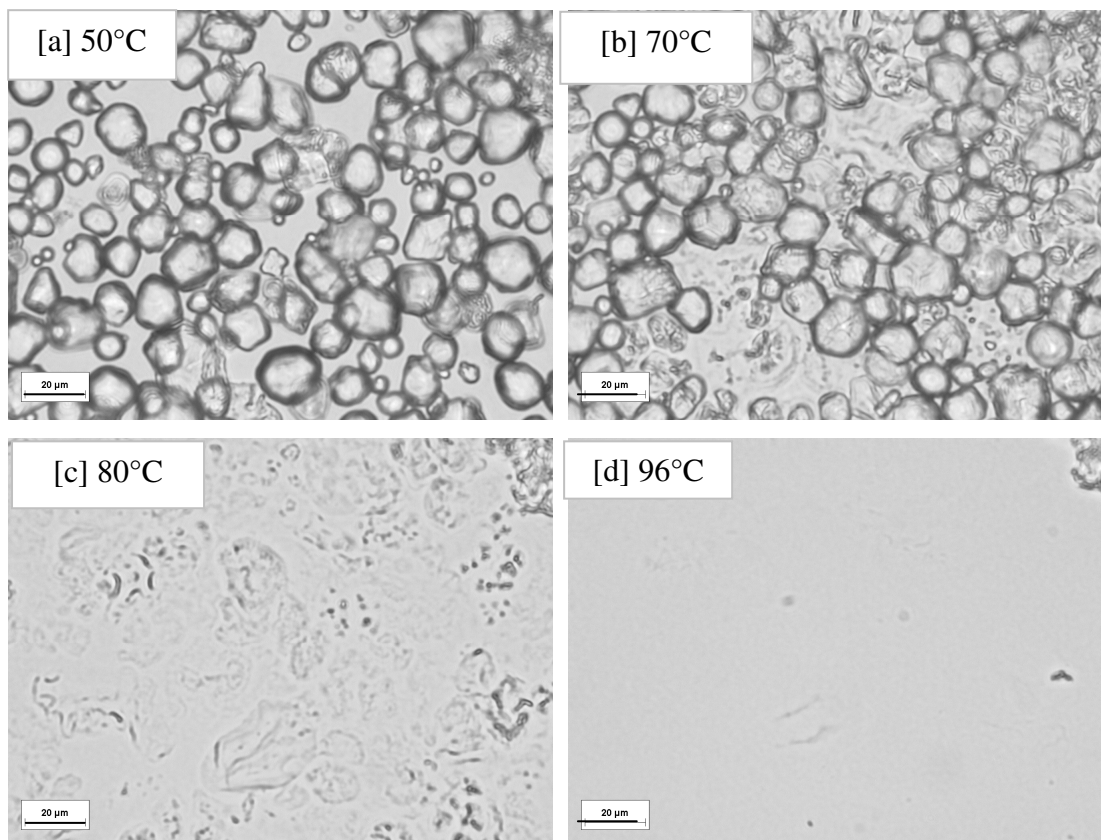


Figure IV-2 Swelling and burst of waxy corn starch in water at different temperatures. The scale in all optical micrographs is 20 μm . Reprinted with permission from [Liu 2012a]. Copyright (2012) Elsevier.

It was interesting to check what type of behaviour, dissolution or gelatinisation, “dominates” in a mixed solvent, EMIMAc-water. Here again, only qualitative conclusions were made based on granule evolution monitored with optical microscopy. Three solvent mixtures were prepared, with 25, 50 and 75wt% of EMIMAc, the rest being water. We found that dissolution similar to the one in pure EMIMAc occurs for 75%EMIMAc-25%water system (Figure IV-3) and gelatinization was detected for 25%-75% (Figure IV-4) and 50%-50% EMIMAc-water. The characteristic temperatures of the beginning and the end of gelatinisation or dissolution, and the total time needed to dissolve granules as depicted from optical micrographs, are shown in Table 1. The availability of water molecules can be one of the factors controlling gelatinisation vs. dissolution, however, several other factors such as the interactions between EMIMAc and water should also be taken into account.

The presence of water in EMIMAc strongly accelerates the dissolution as compared with pure EMIMAc (Table IV-1): for example, in 75%EMIMAc-25%water the dissolution is visually

completed at 78°C in 8 minutes vs. 16 min in pure EMIMAc. Several reasons can be given to explain this. Water, being much less bulky than EMIMAc, penetrates the granule first, swells the outer layer and facilitates ionic liquid penetration and starch dissolution. The viscosity of “new solvent”, 75%EMIMAc-25%water, is much lower than the one of pure EMIMAc, as shown in a recent article of Le and co-workers [Le 2012]. The decrease in solvent viscosity increases polymer diffusion coefficient and allows quicker homogenisation of the whole system and thus quicker dissolution. Finally, EMIMAc and water are interacting [Le 2012] and EMIMAc-water may become a more powerful solvent than pure EMIMAc. While the last reason is a speculation, the first two can indeed explain the acceleration of starch dissolution in the presence of water. When the major component in EMIMAc-water mixture is water (25% EMIMAc-75% water system, Figure IV-4), gelatinisation process occurs: granules first swell and then start bursting at 75-77°C. Surprisingly, this temperature is almost ten degrees higher than the equivalent one in water; gelatinisation is “delayed” as compared with pure water. The dissolution in 25%EMIMAc-75%water is visually completed at 100°C. To interpret this result the interactions between EMIMAc and water should be first understood.

What can be concluded from this qualitative study is:

- 1) Starch dissolution in EMIMAc proceeds in time with very low swelling of granules, with temperature increase speeding up the dissolution.
- 2) The presence of water up to 50% strongly accelerates dissolution.

Table IV-1. Parameters characterising dissolution and gelatinisation of waxy starch in EMIMAc, water and EMIMAc-water mixtures. Adapted with permission from [Liu 2012b]. Copyright (2012) Elsevier.

	Beginning of dissolution or gelatinization, °C	Temperature of complete dissolution, °C	Total dissolution or gelatinisation time, min
100% EMIMAc	75 – 80	100	16
75%EMIMAc-25%water	54 – 56	76 – 78	8
50%EMIMAc -50% water	54 – 56	76 – 78	8
25%EMIMAc-75%water	75 - 77	100	12
100% water	65 – 70	95-100	12

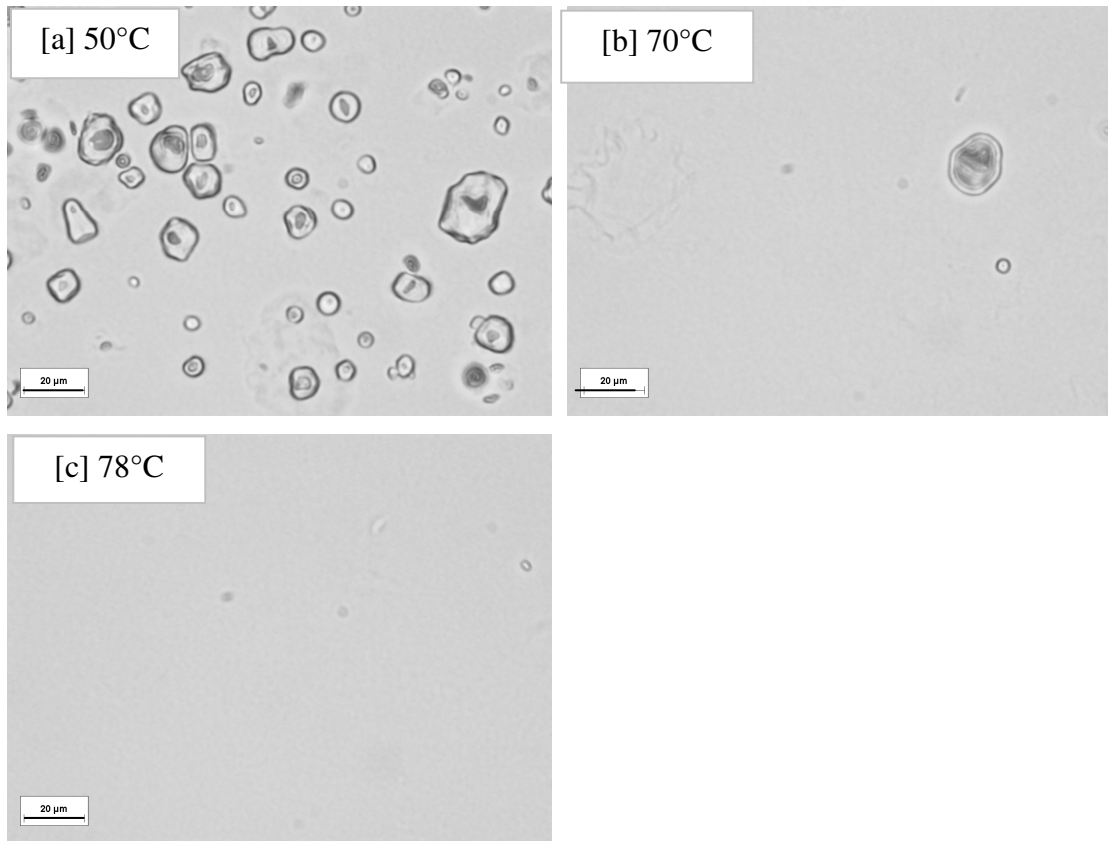


Figure IV-3 Behaviour of waxy corn starch granules in 75%EMIMAc-25%water at different temperatures. Reprinted with permission from [Liu 2012a]. Copyright (2012) Elsevier.

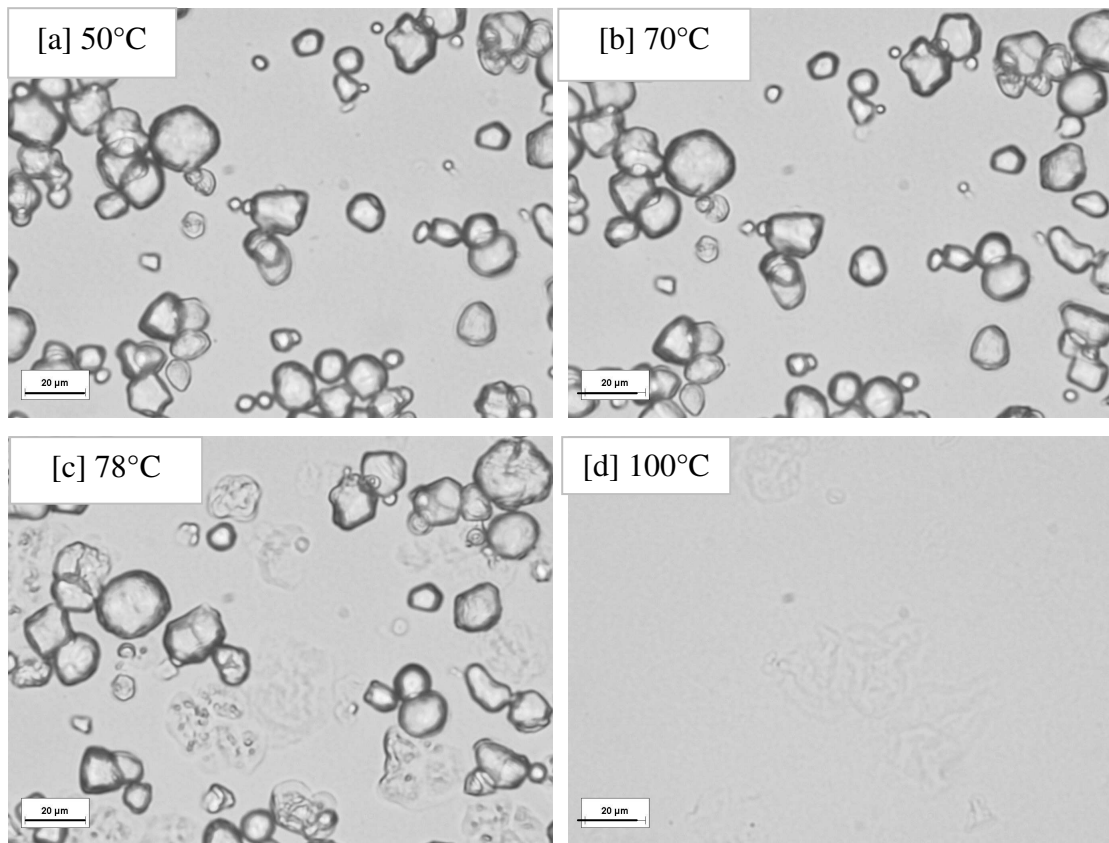


Figure IV-4 Swelling and bursting of waxy corn starch granules in 25%EMIMAc-75%water at different temperatures. Reprinted with permission from [Liu 2012a]. Copyright (2012) Elsevier.

II.2. Rheological proprieties of waxy starch solution in EMIMAc

II.2.1 Flow curves

The examples of steady state viscosity of starch-EMIMAc solutions at various concentrations and temperatures are presented in Figure IV-5. At high polymer concentrations the flow is shear-thinning. Such behaviour is different from microcrystalline cellulose-EMIMAc solution which was found to be Newtonian over several shear rate decades [Gericke 2009] and can be explained by higher molecular weight of amylopectin. The shear-thinning behaviour of amylopectin has also been reported in other solvents as water, DMSO and NMMO [De Vasconcelos 2001; Koganti 2011].

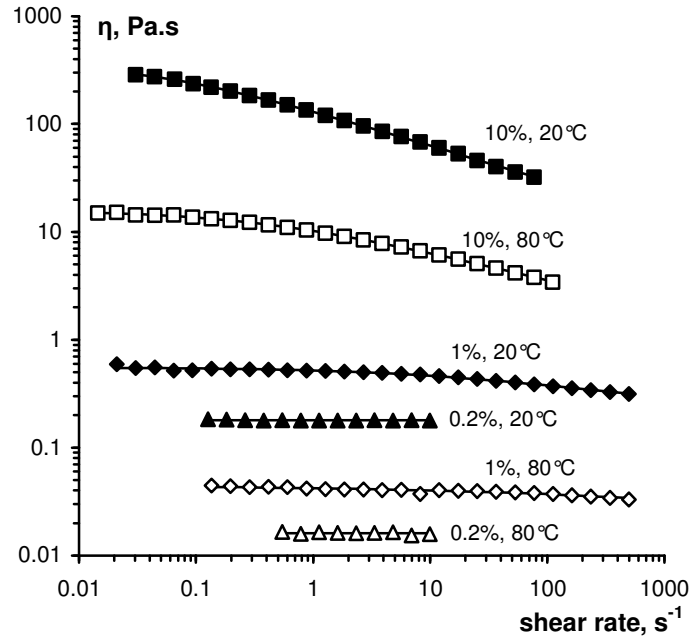


Figure IV-5 Viscosity-shear rate dependence for starch-EMIMAc solutions of various concentrations at different temperatures. Lines are approximations calculated according to Equation IV-1. Reprinted with permission from [Liu 2012a]. Copyright (2012) Elsevier.

In order to perform further analysis of starch-EMIMAc solutions on the molecular level, zero-shear rate viscosities, η_0 , were determined for each polymer concentration and temperature. The values of η_0 were obtained by fitting the flow curves with the Carreau-Yasuda model according to Equation IV-1 [Yasuda 1981]:

$$\frac{\eta(\dot{\gamma}) - \eta_{\infty}}{\eta_0 - \eta_{\infty}} = \left[1 + (\lambda \dot{\gamma})^{\alpha} \right]^{\frac{m-1}{\alpha}} \quad (\text{IV-1})$$

where $\eta(\dot{\gamma})$ is viscosity measured at a certain steady shear rate, η_{∞} is solvent viscosity, λ is the relaxation time, m is power law index and α is the fitting parameter. Solid lines in Figure IV-5 show that calculated viscosity-shear rate dependences are fitting well the experimental data. Contrary to starch-water pastes, amylopectin-EMIMAc solutions behave like a classical polymer solution allowing further analysis of macromolecule hydrodynamic properties.

II.2.2 Viscosity-concentration dependence, intrinsic viscosity and overlap concentration

The examples of zero-shear rate viscosity as a function of polymer concentration for amylopectin-EMIMAc solutions at four selected temperatures are shown in Figure IV-6. In dilute region, the viscosity increases linearly with starch concentration. Once in the semi-dilute region, we found the classical power law viscosity-concentration dependence for polymer solutions:

$$\eta_0 \sim C^n \quad (\text{IV-2})$$

The power law coefficient n decreases from 2.84 to 2.53 when temperature increased from 20°C to 100°C, as demonstrated in Figure IV-7. The values of n are in the same range as for other polysaccharides in EMIMAc and also for amylopectin in other solvents [Yang 2006; Gericke 2009; Sescousse 2010]; however, the influence of temperature on amylopectin macromolecules is much less pronounced as compared with cellulose dissolved in the same solvent [Gericke 2009; Sescousse 2010]. A possible reason could be that the radius of gyration of cellulose, which is a major factor in controlling the increase of viscosity with concentration, is decreasing much quicker with temperature than amylopectin, due to its branched topology. This is also reflected in Fig IV-8.

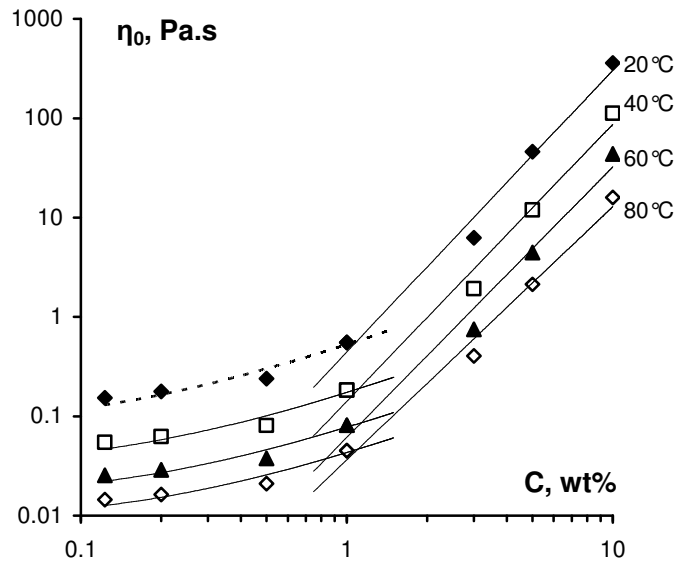


Figure IV-6 Zero-shear rate viscosity vs. concentration for amylopectin-EMIMAc solutions at different temperatures. Dashed lines are linear dependence for dilute solutions, solid lines correspond to power-law approximation (Equation IV-2) calculated above the overlap concentrations. Reprinted with permission from [Liu 2012a]. Copyright (2012) Elsevier.

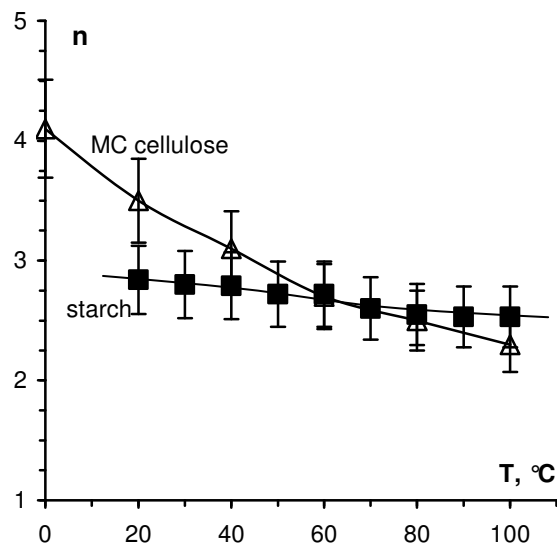


Figure IV-7 Power law coefficient from Equation IV-2 as a function of temperature for semi-dilute starch-EMIMAc solutions, with error bars of 10%. Data for microcrystalline cellulose (DP = 300) are taken from reference [Gericke 2009]. Lines are to guide the eye. Reprinted with permission from [Liu 2012a]. Copyright (2012) Elsevier.

Polymer intrinsic viscosity, $[\eta]$, is an important parameter which reflects the size of the macromolecule in a given solvent at a certain temperature. Usually $[\eta]$ is obtained from solution dilution with the solvent in Ubbelohde capillary viscometer. The procedure then consists in plotting $(\eta_{rel} - 1)/C$ vs. C and deducing $[\eta]$ as limiting value at $C = 0$, where relative viscosity $\eta_{rel} = \eta_{sol}/\eta_{solv}$, η_{sol} and η_{solv} are solution and solvent viscosity, respectively, and polymer concentration C is expressed in mass per volume units. In order to recalculate amylopectin concentration in g/cm^3 , we used solvent (EMIMAc) density equal to $1.1 \text{ g}/\text{cm}^3$ which is a mean value between 1.08 at 90°C and $1.12 \text{ g}/\text{cm}^3$ at 20°C [Sescousse 2010]. This small variation of density with temperature can be neglected in the calculation of the intrinsic viscosity in the view of all other accumulated errors.

In the case studied here it was not possible to perform measurements in a capillary Ubbelohde viscometer, because EMIMAc is too viscous and too hygroscopic to be studied in contact with the air. Thus we used solution and solvent zero-shear rate viscosities obtained from the flow curves as described above at various starch concentrations and solution temperatures. We applied Wolf approach [Wolf 2007; Eckelt 2011] to calculate amylopectin intrinsic viscosity as far as data presented in the classical Huggins plot, $(\eta_{rel} - 1)/C$ vs C , were somewhat scattered and do not allow an adequate $[\eta]$ determination. Briefly, the Wolf approach consists in the calculation of the limiting slope of $\ln(\eta_{rel})$ vs C which, according to phenomenological considerations, is identical to the intrinsic viscosity [Wolf 2007]. Indeed, both the Huggins and the Wolf approaches gave the same cellulose intrinsic viscosity values for cellulose dissolved in NMMO monohydrate [Eckelt 2011].

Amylopectin intrinsic viscosity as a function of temperature is shown in Figure IV-8. It slightly decreases with increasing temperature. The trend obtained can again be compared with $[\eta]$ of microcrystalline cellulose (DP 300) in EMIMAc as a function of temperature [Gericke 2009]. Figure IV-8 shows that cellulose macromolecule is much more sensitive to temperature as compared with amylopectin; however, for both polysaccharides temperature increase leads to solvent (EMIMAc) thermodynamic quality decrease. Considering the fact that amylopectin is a branched, high molecular weight polymer, and its intrinsic viscosity is close to the one of microcrystalline cellulose at room temperature, we can assume that amylopectin has a very compact conformation, probably solvent impenetrable, like oblate ellipsoid in water and in DMSO [Callaghan 1985]. Amylopectin is thus much less affected by

temperature as compared with cellulose, a linear polymer which can more easily vary conformations as a reaction to external conditions.

Another proof that amylopectin conformation in EMIMAc is similar to the one in water can be deduced from the analysis of the overlap concentration, C^* , which can be determined as the inverse value of $[\eta]$. C^* of amylopectin in EMIMAc varies from 0.8 to 1 wt% for temperatures from 20° to 100°C. The value of about 1 wt% could be roughly guessed from the viscosity-concentration dependence (Figure IV-6). Our value of C^* of amylopectin in EMIMAc is in the same range as the $C^* = 0.9$ wt% of waxy starch in water at 25°C as reported by Ring and co-workers [Ring 1987] and higher than the $C^* = 0.46$ wt% in 0.5M NaOH-water at 25°C obtained by Yang and co-workers [Yang 2006]. This means that 0.5M NaOH-water is thermodynamically better solvent for amylopectin than EMIMAc. It should be noted that the comparison of the exact values of overlap concentrations cited above should be taken with care as far as they were obtained with different methods: in 0.5M NaOH it was with light scattering technique, in water with Ubbelohde viscometer and in EMIMAc (this case) with viscosity measured with rotational rheometer. As far as amylopectin C^* values in water and in EMIMAc are practically the same (0.9 and 0.8, respectively), this confirms that amylopectin conformation in EMIMAc is similar to the one in water.

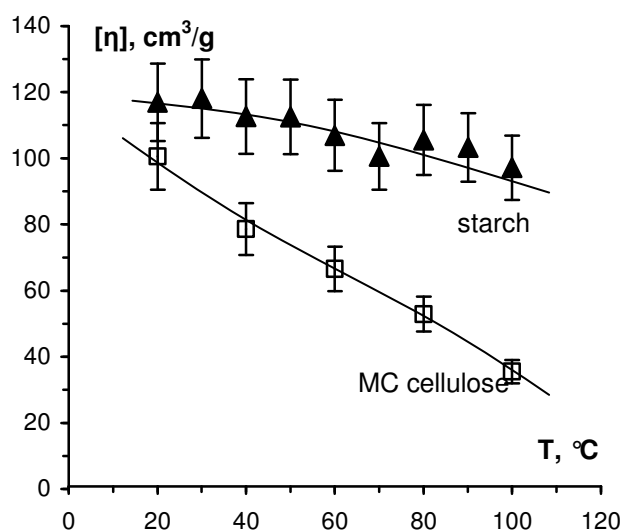


Figure IV-8 Intrinsic viscosity of amylopectin and MC cellulose in EMIMAc as a function of temperature, with error bars of 10%. Data on cellulose are taken from [Gericke 2009]. Lines are to guide the eye. Reprinted with permission from [Liu 2012a]. Copyright (2012) Elsevier.

II.2.3 Viscosity-temperature dependence and activation energy

The viscosity-temperature dependence of amylopectin-EMIMAc solution was analyzed with the classical Arrhenius approach: $\eta \sim \exp(E_a/RT)$, where E_a is the activation energy, R is the universal gas constant and T is temperature in K. The values of $\ln\eta_0$ plotted as a function of the inverse temperature are shown in Figure IV-9. The experimental dependence of $\ln\eta_0$ vs $1/RT$ can be considered linear within the experimental errors (standard deviation $R^2 > 0.985$) despite the fact that data for EMIMAc and low-concentrated solutions have a slightly concave shape. This has also been observed for cellulose solutions in EMIMAc and in BMIMCl and is due to the unique behaviour of the ionic liquids [Gericke 2009; Sescousse 2010].

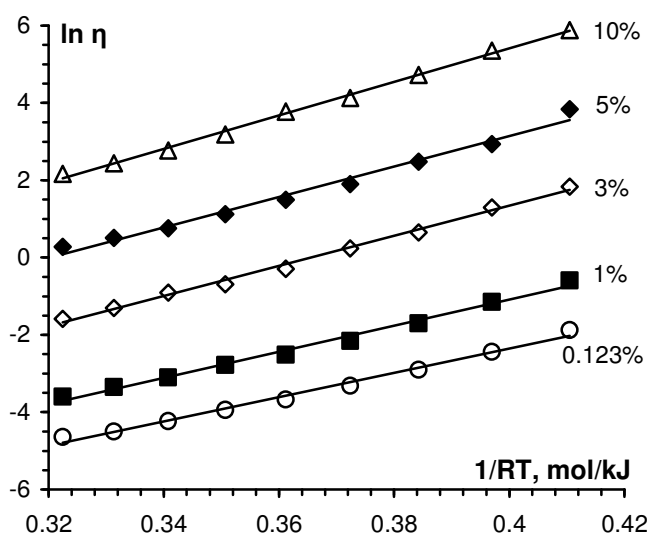


Figure IV-9 Arrhenius plots for starch-EMIMAc solutions at different concentrations; error bars are smaller than or equal to the point size. Reprinted with permission from [Liu 2012a]. Copyright (2012) Elsevier.

The values of E_a obtained are comparable with the ones of microcrystalline cellulose dissolved in EMIMAc [Gericke 2009] as well as with amylose dissolved in BMIMCl [Horinaka 2011]. The activation energy increases with polymer concentration increase, as shows Figure IV-10. A power law correlation between solution activation energy and polymer concentration C was suggested for cellulose-ionic liquid solutions [Sescousse 2010]: $E_a = E_a(0) + pC^x$, where $E_a(0)$ is solvent activation energy and p and x are adjustable constants. A far as at

low polymer concentrations E_a vs. C can be approximated by a straight line (see inset Figure IV-10), we suggest a more general correlation:

$$E_a = E_a(0) + aC + bC^x \quad (\text{IV-3})$$

Indeed, at $C < C^*$ E_a vs. C is linear; and at $C > C^*$, the least square approximation gives $a = 0$, $b = 49.5$ and $x = 0.61$, see line in Figure IV-10. The result obtained shows that activation energy-polymer concentration power law dependence works well for polysaccharides dissolved in ionic liquids.

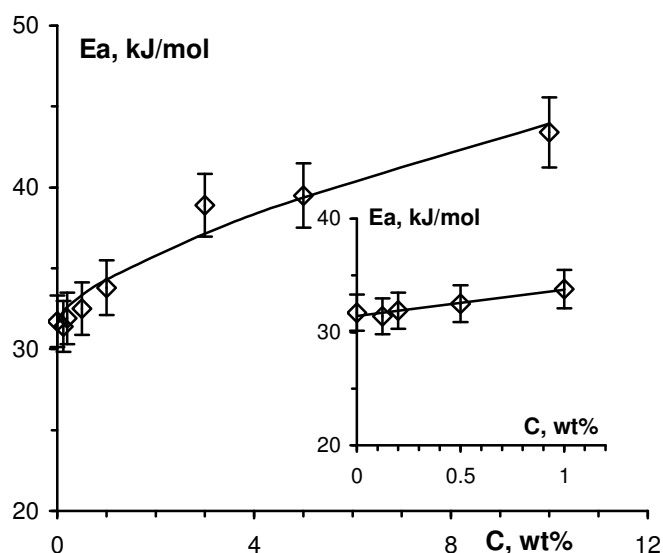


Figure IV-10 Activation energy of starch-EMIMAc solutions at different concentrations: symbols are experimental data with 10% error bars; solid line is calculated according to Equation IV-3. Inset: the same data below the overlap concentration, line is a linear approximation. Reprinted with permission from [Liu 2012a]. Copyright (2012) Elsevier.

II.3 Rheological properties of starch-cellulose-EMIMAc mixtures

In the previous section we looked into the rheological properties of amylopectin starch dissolved in EMIMAc. On the other hand, a detailed study and discussion of microcrystalline cellulose-EMIMAc solution properties in dilute and semi-dilute regimes (flow, viscosity-concentration dependence, intrinsic viscosity as a function of temperature, etc.) have

been reported in literatures [Gericke 2009; Sescousse 2010]. In this part we will discuss the rheological properties of starch-cellulose-EMIMAc mixtures briefly.

An example of the flow of 1:1 = cellulose:starch mixtures in EMIMAc with total polymer concentration 5% at different temperatures is shown in Figure IV-11. Mixtures were shear thinning; the viscosity-shear rate dependence was successfully fitted with Equation IV-1 (solid lines in Figure IV-11). A comparison of the flow of the initial components with their mixtures, at a fixed temperature, is given in Figure IV-12. It seems that mixture is behaving simply as a “sum” of the components, with the relaxation times corresponding to the ones of each individual polymer. This is the first indication that there are no specific interactions between two polymers.

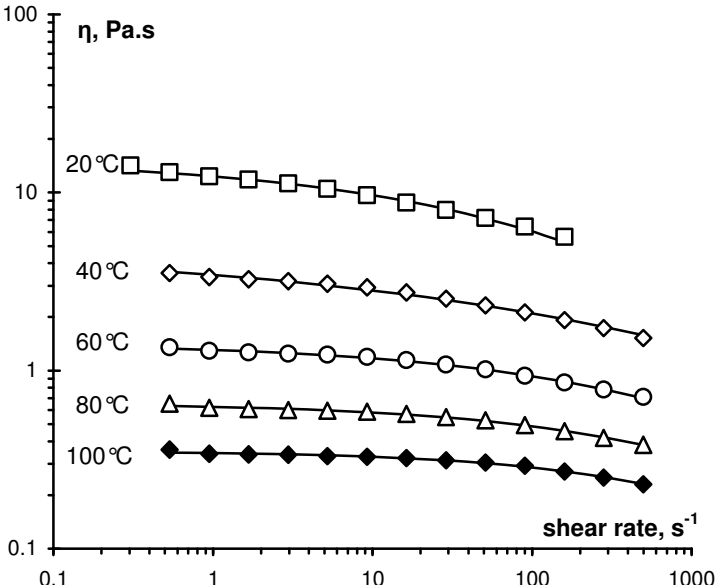


Figure IV-11 Viscosity-shear rate dependence for 1:1 = cellulose:starch mixture, total polymer concentration 5%, at different temperatures. Solid lines are the best fits to Equation IV-1. Reprinted with permission from [Liu 2012b]. Copyright (2012) Elsevier.

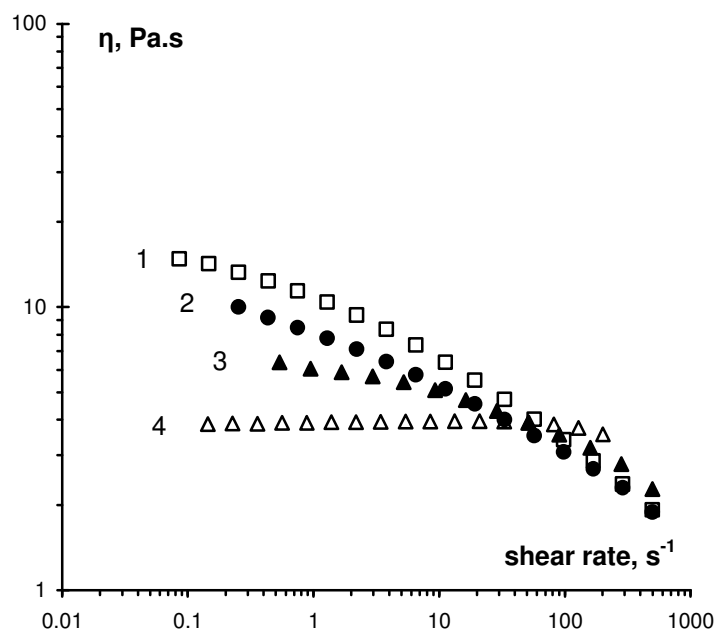


Figure IV-12 Viscosity-shear rate dependence of 5% starch-EMIMAc (1), 5% cellulose-EMIMAc (4) and their mixtures starch: cellulose = 4:1 (2) and 1:1 (3) at 30°C. Reprinted with permission from [Liu 2012b]. Copyright (2012) Elsevier.

In order to check, in the first approximation, if there are any special interactions between different mixed macromolecules, a simple mixing rule was applied for zero shear rate viscosities. Because polymer concentration in the mixture is above the overlap concentration of each polymer (for amylopectin it varies from 0.8 wt% to 1 wt% [Liu 2012a] and for cellulose from ~1 wt% to ~2 wt% [Gericke 2009; Lovell 2010] for temperatures from 20° to 100°C, respectively), a log-additive dependence was used:

$$\ln \eta_{mix} = \Phi_1 \ln \eta_1 + \Phi_2 \ln \eta_2 \quad (\text{IV-4})$$

where η_{mix} is the calculated viscosity, Φ_1 and Φ_2 are the weight fractions of each component in the mixture with $\Phi_1 + \Phi_2 = 1$, and η_1 and η_2 are the viscosities of each component at $\Phi_1 = 1$ and $\Phi_2 = 1$, respectively. Roughly, the comparison between the experimental and calculated viscosity allows concluding on the formation of new structures in solution. If experimental values of viscosity are lower than the calculated ones, this should indicate that new “compact” systems (interpolymer complexes) are formed. If the experimental viscosities are higher than the calculated ones, the components are making “loose gel-like” or “branched” structures with loops and dangling ends.

The experimental and calculated values of mixture zero shear rate viscosity as a function of composition (here, as a function of cellulose weight fraction Φ_{cell}) at different temperatures from 20°C to 100°C is shown in Figure IV-13. With the increase of cellulose concentration in the mixture, the viscosity smoothly decreases, as far as cellulose-EMIMAc solution zero shear rate viscosity is lower than the one of starch-EMIMAc. The calculated additive viscosity coincides with the experimental values indicating that there are no special interactions leading to the formation of any new cellulose-amylopectin structures. These two polysaccharides coexist in the common solvent without any phase separation as far as total polymer concentration used, 5%, is far from the limit of their dissolution in ionic liquid: the maximum solubility is not reported in literature for these polymers, but it is known that it is possible to dissolve cellulose up to 20% in EMIMAc [Biswas 2006; Kosan 2008], and corn starch up to 15% in 1-butyl-3-methylimidazolium chloride, as well as 19% amylose can be dissolved in 1-allyl-3-methyl imidazole formate [Zhang 2005; Fukaya 2006]. Cellulose-starch mixtures of 10wt% total polymer concentration that we prepared for making films were also not phase separating. As it will be shown in the following sections, cellulose and starch phase separate when coagulated in a non-solvent.

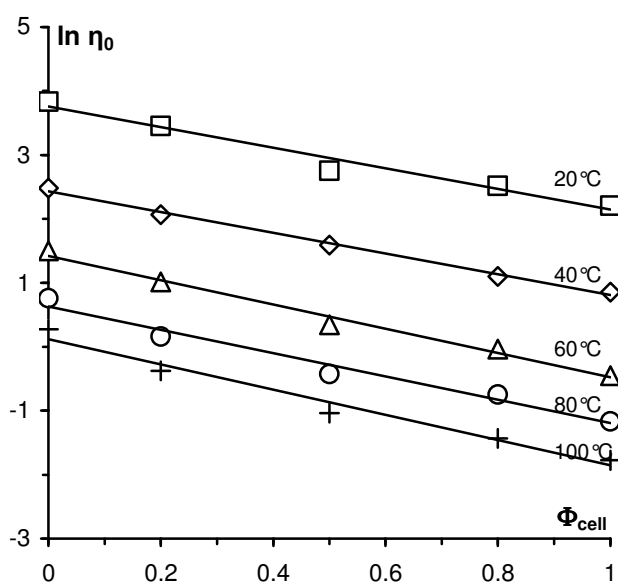


Figure IV-13 Viscosity vs. mixture composition at different temperatures; total polymer concentration is 5%. Symbols are experimental data; lines are calculated according to Equation IV-1. Reprinted with permission from [Liu 2012b]. Copyright (2012) Elsevier.

Zero-shear rate viscosity-temperature dependence of mixtures is presented as an Arrhenius plot in Figure IV-14 where T is the temperature in K and R the universal gas constant. The experimental dependences of $\ln \eta_0$ vs. $1/RT$ can be considered as linear (with a reasonable standard deviation of 0.985), despite a slightly concave shape. The non-linear dependence of $\ln \eta_0$ on $1/RT$ is due to EMIMAc specific temperature behaviour as demonstrated in refs [Gericke 2009; Lovell 2010] for cellulose-EMIMAc solutions. Vogel-Fulcher-Tamman (VFT) approach has been shown to fit better the experimental data; however, here, in the first approximation, we shall use the classical Arrhenius approach $\eta \sim \exp(E_a/RT)$, where E_a is the activation energy.

The values and the dependence of the activation energy on mixture composition are shown in Figure IV-15. Within the experimental errors, E_a linearly varies as a function of mixture composition, which is another indirect proof of the absence of any special interactions between the components.

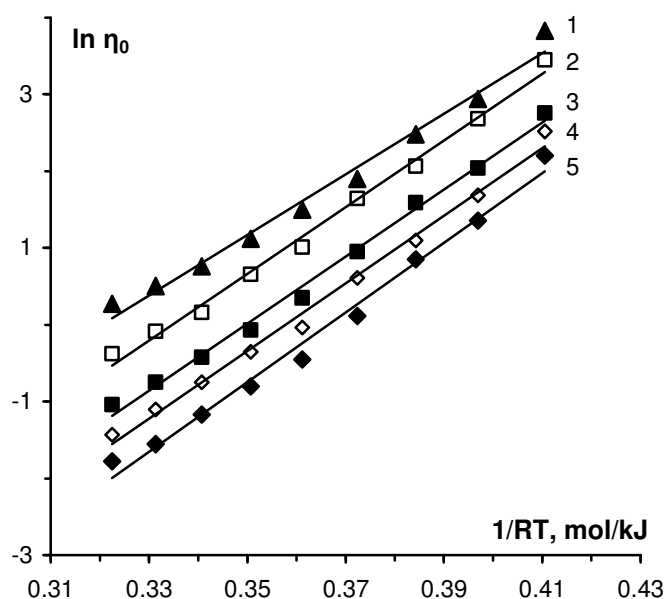


Figure IV-14 Mixture zero-shear rate viscosity as a function of inverse temperature for various compositions, with total polymer concentration 5%: 5%starch-EMIMAc (1), 4:1=starch:cellulose (2), 1:1=starch:cellulose (3), 1:4=starch:cellulose (4) and 5%cellulose-EMIMAc (5). Lines are Arrhenius linear fits. Reprinted with permission from [Liu 2012b]. Copyright (2012) Elsevier.

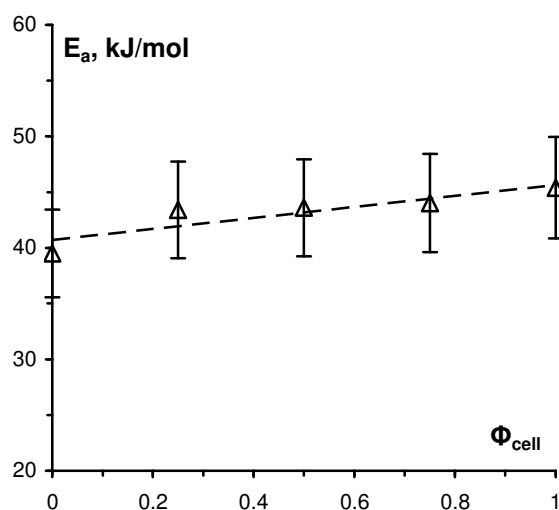


Figure IV-15 Activation energy of starch-cellulose-EMIMAc mixtures as a function of composition. Total polymer concentration is 5 %. Dashed line is a linear fit. Reprinted with permission from [Liu 2012b]. Copyright (2012) Elsevier.

II.4 Properties of starch-cellulose films

II.4.1 FTIR

In order to conclude on the absence of any new chemical bonds formed between cellulose and amylopectin mixed and coagulated from a common solvent, FTIR spectra of the initial components, their coagulated counterparts, and films made from the mixture were recorded.

First, FTIR spectra of native and coagulated cellulose (Figure IV-16) were compared. During the dissolution-coagulation process (transformation of cellulose I to cellulose II), the ionic liquid broke the hydrogen bonds of cellulose molecules, and increased the content of free hydroxyl group, resulting in the shift of the O-H stretching peak from 3374cm^{-1} to 3408cm^{-1} . The peak of C-O-C antisymmetrical stretching was also relocated from 1170cm^{-1} to 1158cm^{-1} . C-H stretching peak was also affected and slightly shifted (from 2900cm^{-1} to 2892cm^{-1}), also CH_2 scissoring peak was shifted from 1432cm^{-1} to 1420cm^{-1} , indicating the split of intramolecular hydrogen bond concerning O at C_6 . The C-OH skeletal vibration peak at 1112cm^{-1} was masked due to the strong band at 1068cm^{-1} on the spectra of coagulated cellulose. The above changes of the peaks are consistent with the results reported for the FTIR

spectra of native and coagulated cellulose from other solvents, such as NaOH/thiourea [Zhang 2005], AMIMCl [Zhang 2005] and BMIMCl [Lan 2011]. As suggested by Nelson and O'Connor [Nelson 1964], the intensity ratio of C-H bending peak at 1376cm^{-1} and C-H stretching peak at 2900cm^{-1} is linearly proportional to the crystallinity of cellulose. In our case, this ratio varied from 0.61 to 0.41 for native and coagulated cellulose, respectively, indicating a decrease of crystallinity from cellulose I to cellulose II. This trend was also confirmed by the XRD analysis as described in the Section II.4.2.

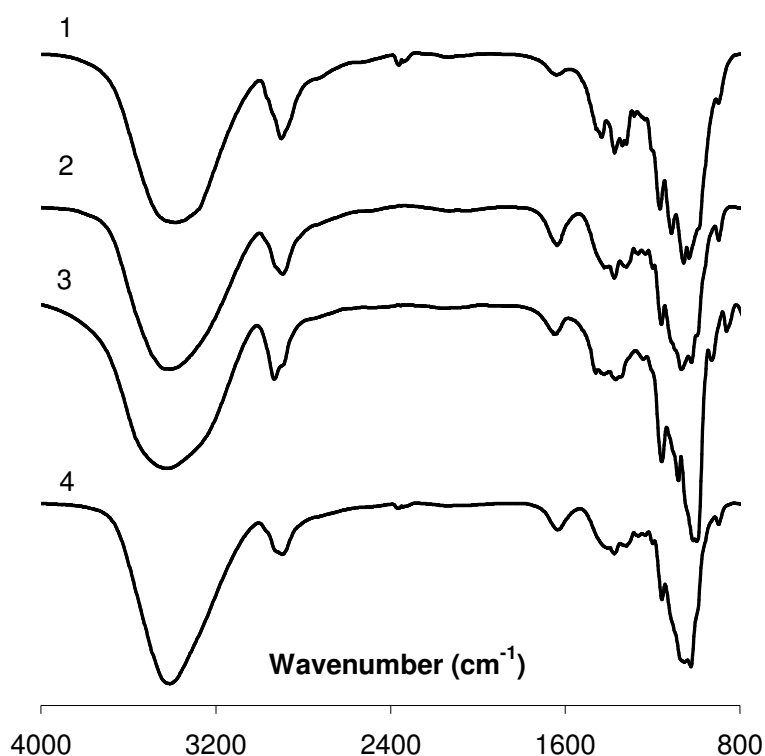


Figure IV-16 FTIR spectra of native microcrystalline cellulose (1), coagulated cellulose (2), native amylopectin (3) and 1:1 = cellulose: starch film (4), the spectrum of coagulated amylopectin was not shown to avoid overloading the graph, it was identical to native amylopectin within the experimental errors. Reprinted with permission from [Liu 2012b]. Copyright (2012) Elsevier.

The spectra of native and coagulated amylopectin were practically identical within the experimental errors: characteristic triplet peaks were at 1158cm^{-1} , 1082cm^{-1} , and 1014cm^{-1} as reported in ref [Zou 2012]. FTIR spectra of the blends were a superposition of the spectra of neat components. As far as both are very similar, the conclusion that can be made is that the

two component are strongly phase separated in the coagulated state and that when mixed in a common solvent, no new strong bonds between amylopectin and cellulose were formed.

II.4.2 X-ray diffraction

Figure IV-17 shows the XRD spectra of the initial and coagulated polysaccharides, and of their blend 1:1 = cellulose:starch obtained from coagulated in water 7.5%cellulose-7.5%starch-EMIMAc solution (total polymer concentration in solution 15%). Microcrystalline cellulose (Figure IV-17, spectrum 1) shows classical diffraction peaks characteristic of cellulose I at $2\theta=14.8^\circ$, 16.3° , and 22.6° [Zhang 2002; Zhang 2005; Sun 2009]. After the dissolution in EMIMAc and coagulation, cellulose II crystals show three characteristic diffraction peaks at $2\theta=12.1^\circ$, 19.8° , and 22.0° (Figure IV-17, 2), also previously reported for cellulose dissolved in EMIMAc [Sun 2009]. The smaller area under diffraction peaks of coagulated cellulose compared to the native one indicates a lower crystallinity after dissolution and coagulation, as expected.

Films made from dissolved amylopectin without a plasticizer are known to be completely amorphous [Rindlav-Westling 1998; Myllarinen 2000], which is confirmed by the spectrum of coagulated starch (Figure IV-17, 4). The spectrum of cellulose:starch = 1:1 film (Figure IV-17, 5) is a superposition of the spectra of neat coagulated polymers and reflects an amorphous structure. Two characteristic diffraction peaks of cellulose II at 19.8° and 22.0° are “hidden” under the amorphous halo of coagulated starch.

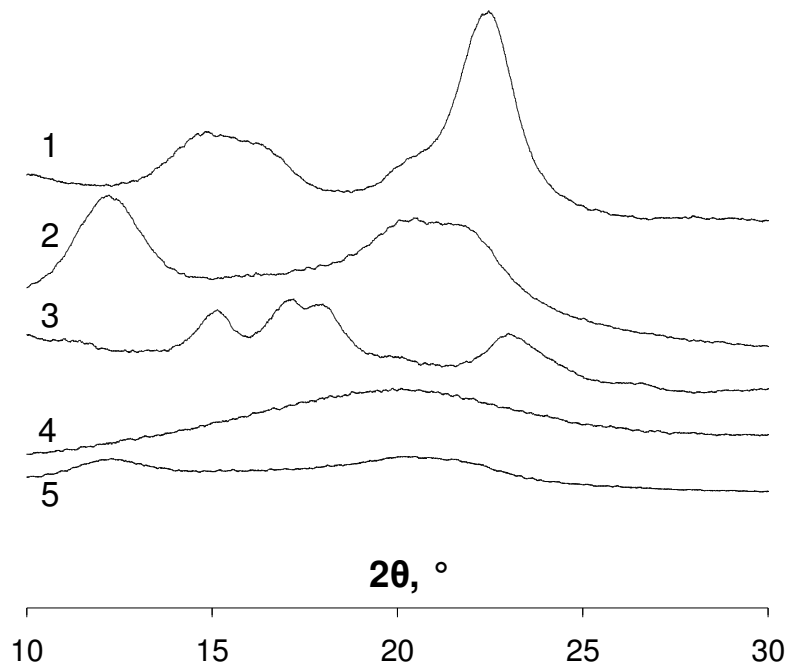


Figure IV-17 XRD spectra of native microcrystalline cellulose (1), cellulose II (2), native amylopectin (3), coagulated amylopectin (4) and 1:1 = cellulose: starch film (5). Reprinted with permission from [Liu 2012b]. Copyright (2012) Elsevier.

II.4.3 Loss of starch during coagulation and washing

When coagulated in water or in ethanol from solution in ionic liquid, starch becomes amorphous, forms flocks and precipitates, but does not make a 3D network structure as coagulated cellulose does. Amylopectin becomes partially soluble in water. A similar phenomenon, i.e. fast dispersion in water of amylopectin films prepared via starch gelatinization-dissolution in water with subsequent drying, has been reported [Myllarinen 2000]. Thus it is very difficult, if impossible, to make amylopectin films via wet casting from EMIMAc. The mechanical properties of cellulose-amylopectin wet films with high starch content are also poor. In the following we shall thus focus on films made from cellulose-starch mixtures with cellulose being in the major phase.

We assume that when the dissolved in EMIMAc cellulose-starch mixtures were coagulated in water, amylopectin partially leached out because of its solubility in water and the absence of

“cohesion” between cellulose and starch molecules. If coagulating starch-cellulose mixtures in ethanol, amylopectin should be trapped in cellulose network. The hypothesis of amylopectin leaching out during coagulation and washing in water was checked by measuring material weight loss, as described in Section I.2.8. Figure IV-18 shows the weight loss $W\%$ as a function of the theoretical starch concentration in the film, $C_{\text{starch, theor}}$, supposing total material conservation. The same measurement was performed for films obtained in ethanol coagulation bath.

The loss of starch during coagulation in water was confirmed: for example, about 35% of amylopectin was leached from 1:1 = cellulose:starch mixture. As a result, the starch concentration in the dry film was about 30% instead of 50%. The inset of Figure IV-18 shows real starch concentration in the film, $C_{\text{starch, real}}$, recalculated considering the weight loss, as a function of the theoretical starch concentration in the film. When coagulating in ethanol, starch was not leaching out and thus real starch concentration in the film coincides with the bisector of $C_{\text{starch, real}}$ vs $C_{\text{starch, theor}}$ which corresponds to no weight loss. We may expect that depending on the type of coagulation bath and mixture composition, films with various morphologies and porosities can be prepared. This will be discussed in the next section.

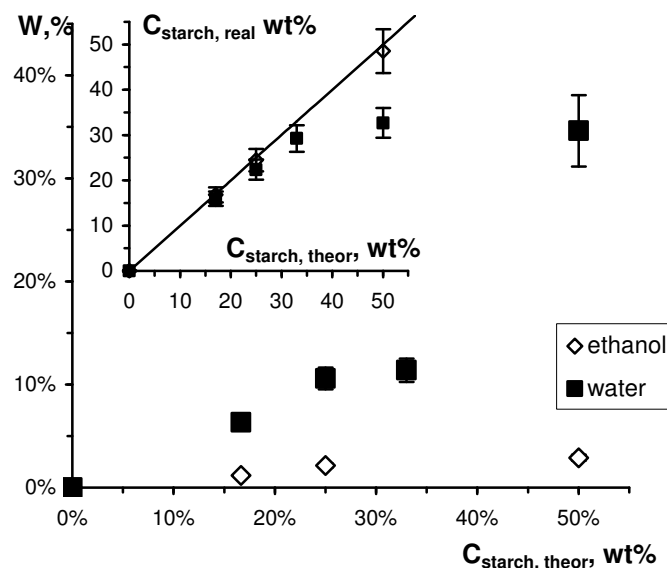


Figure IV-18 Starch weight loss as a function of the theoretical starch concentration in the film. Inset: real starch concentration in the film versus theoretical starch concentration. See more details in the text. Reprinted with permission from [Liu 2012b]. Copyright (2012) Elsevier.

II.4.4 Films morphology as probed with the scanning electron microscope

Cellulose films and films obtained from cellulose-starch blends coagulated in water (Figure IV-19, 20) and in ethanol (Figure IV-21, 22) were analyzed by SEM. Three compositions were selected: 100% cellulose (“a” images in Figure IV-19, 20, 21, 22), cellulose:starch = 2:1 (“b” images) and 1:1 (“c” images). The initial total polymer concentration in EMIMAc was 10%. The morphologies of surfaces (Figure IV-19 and 21) and cross-sections (Figure IV-20 and 22) of freeze-dried wet (never dried) films are compared and discussed below.

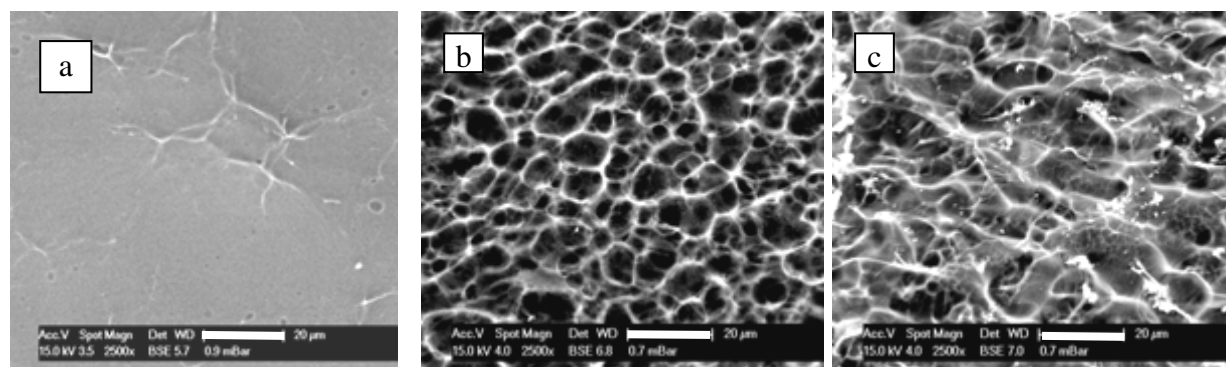


Figure IV-19 SEM images of film surfaces prepared from cellulose (a), cellulose:starch = 2:1 (b), and 1:1 (c) mixtures coagulated in water. The initial polymer concentration in EMIMAc was 10%. The scale bar is 20 μm [Liu 2012b].

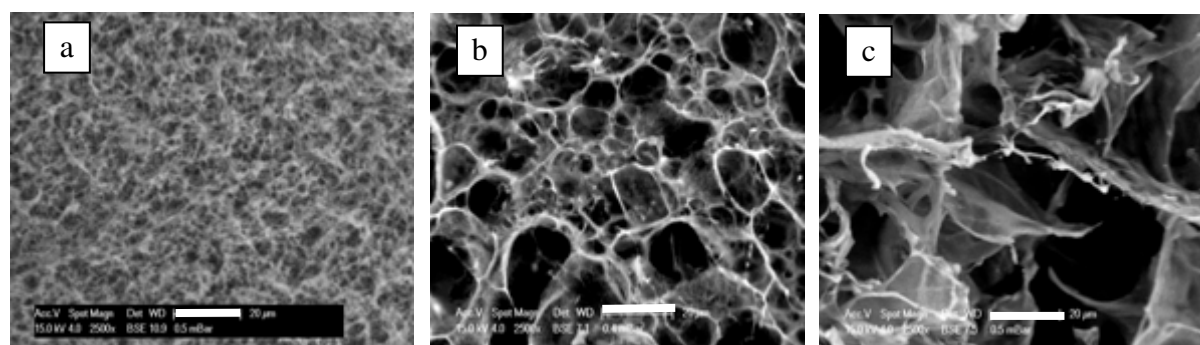


Figure IV-20 Cross-section of the same films as in Figure IV-19. Reprinted with permission from [Liu 2012b]. Copyright (2012) Elsevier.

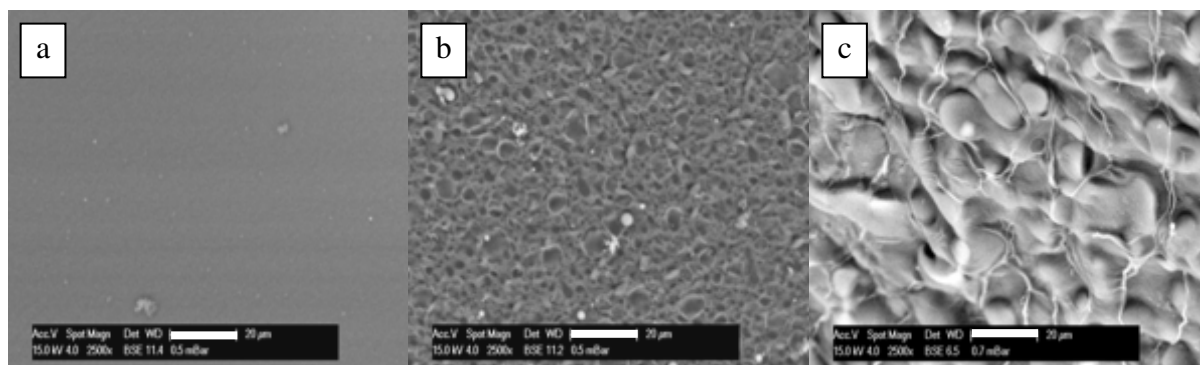


Figure IV-21 SEM images of film surfaces prepared from cellulose (a), cellulose:starch = 2:1 (b), and 1:1 (c) mixtures coagulated in ethanol. The initial polymer concentration in EMIMAc was 10%. The scale bar is 20 μm . Reprinted with permission from [Liu 2012b]. Copyright (2012) Elsevier.

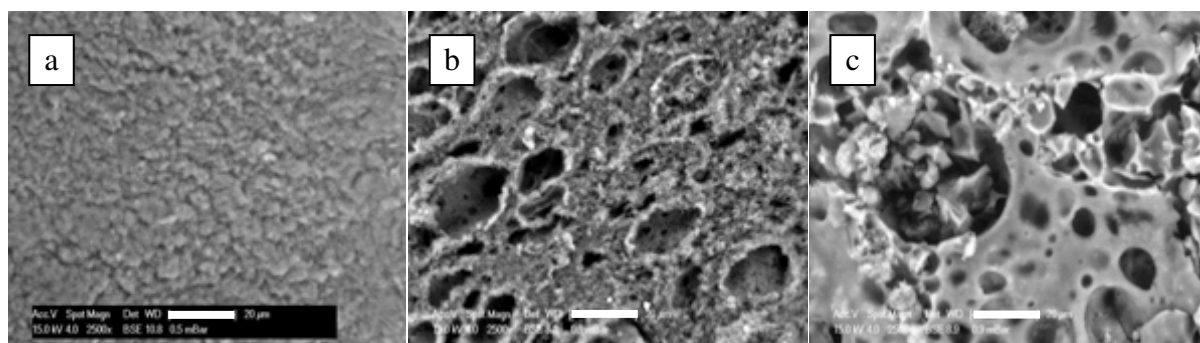


Figure IV-22 Cross-section of the same films as in Figure IV-21. Reprinted with permission from [Liu 2012b]. Copyright (2012) Elsevier.

The first striking difference between cellulose and cellulose-starch films observed for all series of samples is the increased heterogeneity, roughness and porosity of films made from mixtures, seen both for surface and cross-section (compare all “a” images corresponding to cellulose films on Figure IV-19 to Figure IV-22 with “b” and “c” images corresponding to hybrid films). Amylopectin and cellulose coexist when dissolved in EMIMAc, but phase separate during coagulation, with cellulose making a 3D network and starch being trapped in it or partially washed out (when coagulated in water). This is one of the reasons of the heterogeneous morphology of cellulose-starch films.

Another significant difference between cellulose and cellulose-starch films is the influence of coagulation bath, water versus ethanol, on sample morphology. For coagulated cellulose films,

the morphology of water-coagulated films is similar to the ones coagulated in ethanol (compare Figure IV-19a vs. 21a and 20a vs. 22a). On the contrary, cellulose-starch films coagulated in water are of much higher porosity as compared with the ones coagulated in ethanol; this is valid for both surface and cross-section observations (for example, compare Figure IV-19b vs. 21b, 20b vs. 22b). As demonstrated in the previous section, amylopectin is leaching out into water during coagulation and washing. This creates large pores and channels seen on the surface and even larger pores seen on the cross-section. Samples obtained via coagulation in water are of open porosity.

With the increase of starch content in the mixture (“b” images for 2:1= cellulose:starch mixtures vs “c” images for 1:1 mixtures), larger amount of starch is “lost” when coagulated in water (see Figure IV-18). A similar trend was observed for films prepared from solutions with total polysaccharides concentration of 15% (not shown). Pores in 1:1 = cellulose:starch films are thus larger than in the one of 2:1 = cellulose:starch films (see Figure IV-20 b vs. c). In reality, starch concentration in these films is 33% instead of 50% (1:1 mixture) and 29% instead of 33% (2:1 mixture) because of amylopectin leaching out during coagulation and washing in water.

The surface of cellulose and cellulose-starch films obtained by coagulation in water and in ethanol is quite dense and smooth (Figure IV-19a and 21a). The formation of such a rather dense skin is known for cellulose dissolved in other solvents, for example, in N-methylmorpholine-N-oxide monohydrate and coagulated from hot fluids [Fink 2001]. This morphology may result from the increase of cellulose concentration stimulated by rapid solvent depletion on the surface of the sample during coagulation. Similar observations were reported for cellulose membranes regenerated from cuoxam [Zhang 1995]. The cross-section of wet cellulose films displays a rather homogeneous porous structure, with pore size of about few microns for cellulose coagulated in water (Figure IV-20a) and smaller pores for cellulose coagulated in ethanol (Figure IV-22a).

Surprisingly, a denser core and a porous skin have been reported for wet cellulose films made from the dissolution in alkali solvents [Mao 2006; Zhou 2002]. The difference could be due to the fact that in NaOH-based solvent cellulose is gelling with time and temperature, this process being accompanied by a micro-phase separation. Cellulose solutions in ionic liquid and in NMMO monohydrate are stable when not in contact with water vapors. The

mechanisms of cellulose coagulation from alkali solvents and from ionic liquid or NMMO are thus different, which was already reported for cellulose aerogel-like materials prepared by dissolution in these three solvents [Sescousse 2011].

II.4.5 Permeability

Water permeability of wet (never dried) cellulose and cellulose-starch films was measured using a set-up described in Section I.2.9. As far as the permeability of cellulose and cellulose-starch films obtained from EMIMAc wet-casting had never been reported, we shall first present our experimental findings, and then compare them with known results for cellulose films made from other solvents.

First, the influence of the pressure imposed on the water permeability of films was investigated. An example for a film prepared from cellulose dissolved in EMIMAc and coagulated in water is shown in Figure IV-23. The film was subjected to several cycles of consecutively step-wise increasing pressure: first from 1 to 6 bars, then immediately from 2 to 6 bars and again 2 bars. Then there was a 45 minutes interval for the film to relax before the permeability at 2 bars was measured again. Permeability dropped with increasing pressure and did not fully recover when a new cycle was started immediately (Figure IV-23). The decrease of permeability is most probably due to the flexibility of walls of the 3D network of coagulated cellulose, making the overall sample rather soft and compressible. The loss of permeability turned out to be partially reversible: it was recovered after a 45 minutes relaxation between the last two tests.

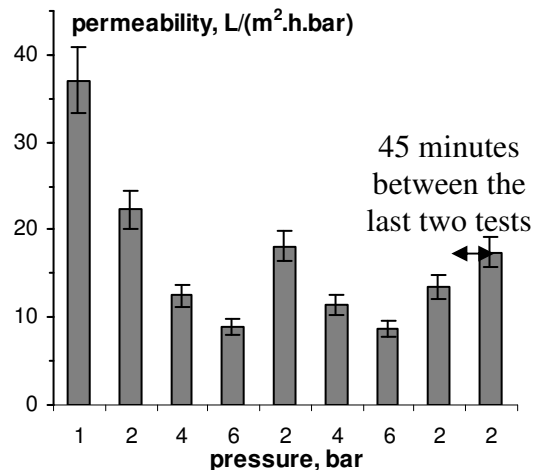


Figure IV-23 Permeability of cellulose films coagulated from 10% cellulose-EMIMAc solution in water, with 20% errors. See more details in the text. Reprinted with permission from [Liu 2012b]. Copyright (2012) Elsevier.

In order to exclude the influence of film compressibility, the permeability of films of different compositions prepared in different conditions (coagulation in ethanol and in water) was performed at the same fixed applied pressure. Figure IV-24 shows the results for cellulose coagulated in water and in ethanol, and for 3:1 = cellulose-starch films coagulated in ethanol. In all samples the total polymer concentration in solution was 10%. The permeability of cellulose film coagulated in water is twice lower than the one coagulated in ethanol, at any pressure studied. A similar result, 30 versus 150 L.m⁻².s⁻¹.bar⁻¹, was reported for cellulose films prepared via dissolution in NaOH-urea-water [Mao 2006]. For this alkali solvent, the size of the pores in films coagulated in ethanol is almost twice higher than the size when coagulated in water, which can be the reason of higher permeability. In general, the permeability of our cellulose films prepared via dissolution in EMIMAc followed by coagulation in water or ethanol falls in the same range as the values previously reported for cellulose dissolved in alkali solvents and coagulated in various aqueous solutions, from 10 to 80 L.m⁻².s⁻¹.bar⁻¹ [Zhang 2001; Ruan 2004; Zhang 1995]. The permeability of cellulose films from EMIMAc, coagulated in water and equilibrated under pressure (4-6 bar) is very similar to the conventional ultrafiltration membranes prepared from cellulose dissolved in cuprammonium (10-15 L.m⁻².s⁻¹.bar⁻¹, [Abe 2003]). When coagulated in ethanol, the permeability of cellulose films from ionic liquid is close to the one made from cellulose dissolved in NMMO (70-80 L.m⁻².s⁻¹.bar⁻¹, [Abe 2002]).

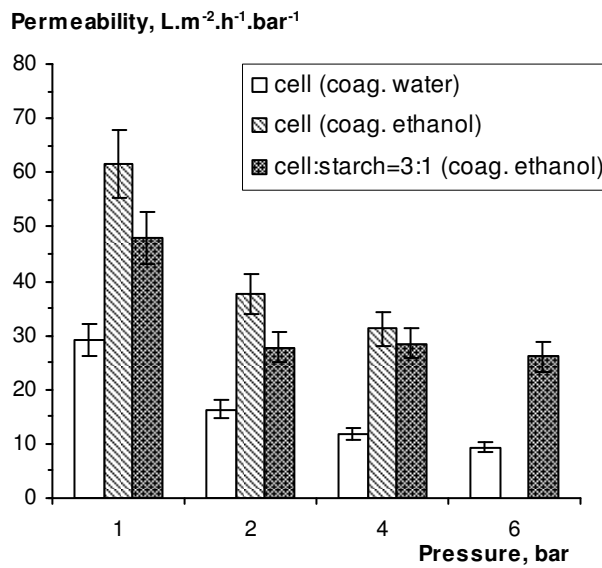


Figure IV-24 Permeability of cellulose film coagulated in water and ethanol and of hybrid film based on 3:1=cellulose:starch coagulated in ethanol, with 20% errors. Total polymer concentration in EMIMAc solution was 10%. Reprinted with permission from [Liu 2012b]. Copyright (2012) Elsevier.

The permeability of cellulose-starch films coagulated in ethanol decreases with the increase of applied pressure from 1 to 2 bars, similar to what was obtained for cellulose films (Figure IV-24). This is not surprising since the major phase forming the film is cellulose, which is “pressure-sensitive”. However, further pressure increase does not decrease cellulose-starch film permeability: at 2, 4 and 6 bars it is practically the same, contrary to a continuous permeability decrease for cellulose films. Starch, being blocked in cellulose matrix, is “reinforcing” it. The permeability of cellulose-starch films coagulated in ethanol is slightly lower than that of their counterpart, cellulose coagulated in ethanol, despite the presence of some rather large pores in hybrid films (see Figure IV-22 “a” versus “b” and “c”). The reason can be again the same: starch is located in the pores in coagulated cellulose and thus the permeability is decreased.

III. Conclusions

Dissolution of waxy corn starch in 1-ethyl-3-methylimidazolium acetate (EMIMAc) was qualitatively studied and compared with gelatinisation process in water. The rheological properties of starch–EMIMAc solutions were investigated in dilute and semi-dilute regions, from 0.1 to 10 wt% over temperature range from 20°C to 100°C. The values of zero shear viscosity, obtained by applying Carreau–Yasuda model to shear-thinning flow curves, were plotted as a function of polymer concentration. Power law exponents in viscosity-concentration dependence in semi-dilute region were compared with the ones reported previously for microcrystalline cellulose. Intrinsic viscosity was obtained as a function of temperature and compared with the one of microcrystalline cellulose. Starch was found to be much less temperature sensitive than cellulose. Amylopectin overlap concentration in EMIMAc was compared with the one in water and 0.5 M NaOH–water. Based on these comparisons, it was suggested that starch conformation in EMIMAc is similar to the one in water (compact ellipsoid). The activation energy was calculated for starch–EMIMAc solutions and demonstrated to obey power-law concentration dependence.

Then cellulose was mixed with starch in EMIMAc. The properties of mixtures in the liquid state (flow, viscosity, miscibility) and of films obtained by wet casting were investigated. No obvious phase separation in mixtures was observed even at high polymer concentration studied (up to 10 wt%). Mixture zero-shear rate viscosity plotted as a function of composition followed a mixing law, allowing concluding, in first approximation, on the absence of any special interactions between the components. Hybrid films from corn starch-cellulose mixtures were obtained by coagulation in water and in ethanol. FT-IR analysis of dry films confirmed the absence of any new bonds formed between the components, and XRD showed a significant decrease of crystallinity. When coagulated in ethanol, starch was trapped in a 3D cellulose network while when coagulated in water, starch was partially leached out, creating pores and channels. The morphology of freeze-dried wet films showed that pore size can be tuned by altering mixture composition and varying coagulation bath. Wet film water permeability was from 10 to 60 L.m⁻².s⁻¹.bar⁻¹.

The results obtained demonstrate the possibility of mixing two of the most abundant polysaccharides (cellulose and starch) in a common solvent, ionic liquid, in a large range of

concentrations and compositions, and making materials with tuned morphology. This opens new ways of making multifunctional films, separation devices and templates with controlled properties.

References

- [Abe 2002] Abe, Y., & Mochizuki, A. (2002). Hemodialysis membrane prepared from cellulose/N-methylmorpholine-N-oxide solution. I. Effect of membrane preparation conditions on its permeation characteristics. *Journal of Applied Polymer Science*, 84(12), 2302-2307.
- [Abe 2003] Abe, Y., & Mochizuki, A. (2003). Hemodialysis membrane prepared from cellulose/N-methylmorpholine-N-oxide solution. II. Comparative studies on the permeation characteristics of membranes prepared from N-methylmorpholine-N-oxide and cuprammonium solutions. *Journal of Applied Polymer Science*, 89(2), 333-339.
- [Biswas 2006] Biswas, A., Shogren, R. L., Stevenson, D. G., Willett, J. L., & Bhowmik, P. K. (2006). Ionic liquids as solvents for biopolymers: Acylation of starch and zein protein. *Carbohydrate Polymers*, 66(4), 546-550.
- [Cai 2007] Cai, J., Wang, L. X., & Zhang, L. N. (2007). Influence of coagulation temperature on pore size and properties of cellulose membranes prepared from NaOH-urea aqueous solution. *Cellulose*, 14(3), 205-215.
- [Callaghan 1985] Callaghan, P.T., & Lelievre, J. (1985). The size and shape of amylopectin: a study using pulsed-field gradient nuclear magnetic resonance. *Biopolymers* 24, 441-460.
- [De Vasconcelos 2011] De Vasconcelos, C. L., Pereira, M. R., & Fonseca, J. L. C. (2001). Solvent composition and rheology of starch-DMSO-water solutions. *Journal of Applied Polymer Science*, 80(8), 1285-1290.
- [Eckelt 2011] Eckelt, J., Knopf, A., Roder, T., Weber, H. K., Sixta, H., & Wolf, B. A. (2011). Viscosity-molecular weight relationship for cellulose solutions in either NMMO monohydrate or cuen. *Journal of Applied Polymer Science*, 119(2), 670-676.
- [Fink 2001] Fink, H. P., Weigel, P., Purz, H. J., & Ganster, J. (2001). Structure formation

of regenerated cellulose materials from NMMO-solutions. *Progress in Polymer Science*, 26(9), 1473-1524.

[Fukaya 2006] Fukaya, Y., Sugimoto, A., & Ohno, H. (2005). Superior solubility of polysaccharides in low viscosity, polar, and halogen-free 1, 3-dialkylimidazolium formates. *Biomacromolecules*, 7(12), 3295-3297.

[Gericke 2009] Gericke, M., Schlufte, K., Liebert, T., Heinze, T., & Budtova, T. (2009). Rheological Properties of Cellulose/Ionic Liquid Solutions: From Dilute to Concentrated States. *Biomacromolecules*, 10(5), 1188-1194.

[Horinaka 2011] Horinaka, J.-i., Yasuda, R., & Takigawa, T. (2011). Entanglement Properties of Cellulose and Amylose in an Ionic Liquid. *Journal of Polymer Science Part B-Polymer Physics*, 49(13), 961-965.

[Koganti 2011] Koganti, N., Mitchell, J. R., Ibbett, R. N., & Foster, T. J. (2011). Solvent Effects on Starch Dissolution and Gelatinization. *Biomacromolecules*, 12(8), 2888-2893.

[Kosan 2008] Kosan, B., Michels, C., & Meister, F. (2008). Dissolution and forming of cellulose with ionic liquids. *Cellulose* 15(1), 59-66.

[Lan 2011] Lan, W., Liu, C.-F., Yue, F.-X., Sun, R.-C., & Kennedy, J. F. (2011). Ultrasound-assisted dissolution of cellulose in ionic liquid. *Carbohydrate Polymers*, 86(2), 672-677.

[Le 2012] Le, K. A., Sescousse, R., & Budtova, T. Influence of water on cellulose-EMIMAc solution properties: a viscometric study, *Cellulose*, 19(1), 45-54.

[Liu 2012a] Liu, W., Budtova, T. (2012). Dissolution of unmodified waxy starch in ionic liquid and solution rheological properties. *Carbohydrate Polymers*, [10.1016/j.carbpol.2012.01.090](https://doi.org/10.1016/j.carbpol.2012.01.090).

[Liu 2012b] Liu, W., Budtova, T. (2012). Ionic liquid: A powerful solvent for homogeneous starch/cellulose mixing and making films with tuned morphology. *Polymer*,

53(25), 5779-5787.

[Lovell 2010] Lovell, C. S., Walker, A., Damion, R. A., Radhi, A., Tanner, S. F., Budtova, T., & Ries, M. E. (2010). Influence of Cellulose on Ion Diffusivity in 1-Ethyl-3-Methyl-Imidazolium Acetate Cellulose Solutions. *Biomacromolecules*, 11(11), 2927-2935.

[Mao 2006] Mao, Y., Zhou, J. P., Cai, J., & Zhang, L. N. (2006). Effects of coagulants on porous structure of membranes prepared from cellulose in NaOH/urea aqueous solution. *Journal of Membrane Science*, 279(1-2), 246-255.

[Miyamoto 2009] Miyamoto, H., Yamane, C., Seguchi, M., & Okajima, K. (2009). Structure and Properties of Cellulose-Starch Blend Films Regenerated from Aqueous Sodium Hydroxide Solution. *Food Science and Technology Research*, 15(4), 403-412.

[Myllarinen 2000] Myllarinen, P., Buleon, A., Lahtinen, R., & Forssell, P. (2002). The crystallinity of amylose and amylopectin films. *Carbohydrate Polymers*, 48(1), 41-48.

[Nelson 1964] Nelson, M., O'Connor, R. (1964). Relation of certain infrared bands to cellulose crystallinity and crystal lattice type. Part II. A new infrared ratio for estimation of crystallinity in celluloses I and II. *Journal of Applied Polymer Science* 8(3), 1325-1341.

[Rindlav-Westling 1998] Rindlav-Westling, A., Stading, M., Hermansson, A. M., & Gatenholm, P. (1998). Structure, mechanical and barrier properties of amylose and amylopectin films. *Carbohydrate Polymers*, 36(2-3), 217-224.

[Ring 1987] Ring, S. G., Colonna, P., Ianson, K. J., Kalichevsky, M. T., Miles, M. J., Morris, V. J., & Orford, P. D. (1987). The gelation and crystallization of amylopectin. *Carbohydrate Research*, 162(2), 277-293.

[Ruan 2004] Ruan, D., Zhang, L. N., Mao, Y., Zeng, M., & Li, X. B. (2004). Microporous membranes prepared from cellulose in NaOH/thiourea aqueous solution. *Journal of Membrane Science*, 241(2), 265-274.

[Sescousse 2010] Sescousse, R., Le, K. A., Ries, M. E., & Budtova, T. (2010). Viscosity of Cellulose-Imidazolium-Based Ionic Liquid Solutions. *Journal of Physical Chemistry B*, *114*(21), 7222-7228.

[Sescousse 2011] Sescousse, R., Gavillon, R., & Budtova, T. (2011). Aerocellulose from cellulose-ionic liquid solutions: Preparation, properties and comparison with cellulose-NaOH and cellulose-NMMO routes. *Carbohydrate Polymers*, *83*(4), 1766-1774.

[Sun 2009] Sun, N., Rahman, M., Qin, Y., Maxim, M. L., Rodriguez, H., & Rogers, R. D. (2009). Complete dissolution and partial delignification of wood in the ionic liquid 1-ethyl-3-methylimidazolium acetate. *Green Chemistry*, *11*(5), 646-655.

[Wolf 2007] Wolf, B. A. (2007). Polyelectrolytes revisited: Reliable determination of intrinsic viscosities. *Macromolecular Rapid Communications*, *28*(2), 164-170.

[Yang 2006] Yang, C., Meng, B., Liu, X., Chen, M., Hua, Y., & Ni, Z. (2006). Dynamics of amylopectin in semidilute aqueous solution. *Polymer*, *47*(23), 8044-8052.

[Yasuda 1981] Yasuda, K., Armstrong, R. C., & Cohen, R. E. (1981). Shear flow properties of concentrated solutions of linear and branched polystyrenes. *Rheologica Acta*, *20*(2), 163-178.

[Zhang 1995] Zhang, L. N., Yang, G., & Xiao, L. (1995). BLEND MEMBRANES OF CELLULOSE CUOXAM/CASEIN. *Journal of Membrane Science*, *103*(1-2), 65-71.

[Zhang 2001] Zhang, L. N., Ruan, D., & Zhou, J. P. (2001). Structure and properties of regenerated cellulose films prepared from cotton linters in NaOH/Urea aqueous solution. *Industrial & Engineering Chemistry Research*, *40*(25), 5923-5928.

[Zhang 2002] Zhang, L. N., Ruan, D., & Gao, S. J. (2002). Dissolution and regeneration of cellulose in NaOH/thiourea aqueous solution. *Journal of Polymer Science Part B-Polymer Physics*, *40*(14), 1521-1529.

[Zhang 2005] Zhang, H., Wu, J., Zhang, J., & He, J. S. (2005).

1-Allyl-3-methylimidazolium Chloride Room Temperature Ionic Liquid: A New and Powerful Nonderivatizing Solvent for Cellulose. *Macromolecules* 38(20), 8272-8277.

[Zhou 2002] Zhou, J. P., Zhang, L., Cai, J., & Shu, H. (2002). Cellulose microporous membranes prepared from NaOH/urea aqueous solution. *Journal of Membrane Science*, 210(1), 77-90.

[Zou 2012] Zou, W., Yu, L., Liu, X., Chen, L., Zhang, X., Qiao, D., & Zhang, R. (2012). Effects of amylose/amylopectin ratio on starch-based superabsorbent polymers. *Carbohydrate Polymers*, 87(2), 1583-1588.

Chapter V

Dispersion of carbon black in cellulose solutions & preparation of conductive cellulose films

I. Introduction	158
II. Results and discussion	160
II.1 Dispersion of carbon black in cellulose solutions	160
II.2 Preparation of conductive cellulose films	172
III. Conclusions	184
References	186

I. Introduction

Driven by the various potential applications mentioned in the first chapter, such as EMI shielding components, biosensors, or electrodes, the goal of this part of our study is to prepare conductive cellulose-based composite films filled with carbon black (CB). Similar to the cellulose/starch blends described in Chapter IV, we also took the “dissolution-coagulation” approach when we prepared the composite films. As the cellulose solvent, we used ionic liquid (EMIMAc) and NMMO monohydrate to dissolve cellulose, for their effectiveness and dissolving power. The only difference is that we replaced the step of mixing cellulose and starch solutions by the step of dispersing carbon black agglomerates in the cellulose solution. We divided this chapter into two parts: in the first part we looked into the mechanisms of the dispersion of carbon black agglomerates, and in the second part we focused on the properties of the composite films obtained by mixing CB and cellulose such as conductivity, percolation threshold, etc.

A good dispersion and a good distribution of the fillers are the prerequisites for making composites with satisfying properties. Due to its practical importance, the mechanisms of carbon black agglomerate dispersion have been examined intensively in the past, as reviewed in Chapter I. However, whatever techniques or polymer matrix used by the researchers, the impacts of the visco-elastic characteristic of the matrix were never thoroughly discussed. Elasticity, among other parameters as agglomerate size or infiltration time, can play an important role in the way stress is generated. Most polymers, all elastomers and of course cellulose solutions can be non-Newtonian and highly elastic. As already done in our group, and real-time microscopic observations of the dispersion process. We studied how the different levels of matrix elasticity changed the carbon black dispersion, and how the critical shear stress of agglomerate rupture was influenced by matrix elasticity. Some solutions or fluids other than cellulose solutions were also used, not only to provide a large range of dispersing matrix elasticity, but also to check if the correlation between elasticity and dispersion is also valid for fluids other than cellulose solutions. The results of this study gave guidelines for the selecting the processing parameters.

Once the dispersion of CB in cellulose solutions was understood, we optimized the processing, prepared cellulose-CB composite films, and measured their conductivity with different CB

loadings in order to identify the percolation threshold. In order to have a better processability and mechanical properties, we went further in order to try reducing the percolation threshold and the CB loading. With idea of taking advantages from the “immiscibility” of the different types of cellulose in a common solvent, two routes involving celluloses with different DP were explored. One was to coat conductive layers onto the non-conductive layer, and the other is inspired by the “double percolation” concept in the cases of CB filled polymer blends.

II. Results and discussion

II.1 Dispersion of carbon black agglomerates in cellulose solutions

The basic experiment we conducted was to place an agglomerate particle under a shear flow between two transparent rotating plates, increase the shear rate, and observe with the microscope of the rheo-optical device, which was described in Chapter II, at which critical shear rate (defined by Equation II-6 in Chapter II) this agglomerate particle broke. Knowing this critical shear rate, it was possible to calculate the stress as

$$\sigma = \eta(\dot{\gamma}_c) \dot{\gamma}_c \quad (\text{V-1})$$

where $\dot{\gamma}_c$ is the critical shear rate for dispersion and $\eta(\dot{\gamma}_c)$ is the solution viscosity at this critical shear rate.

The stress defined by Equation V-1 is not the stress that is acting around the agglomerate particle, but the stress present at the same location if there would be no agglomerate particle. To calculate the stress (Equation V-1), the viscosity must be known. And since, as we will see, elasticity is playing an important role, the full visco-elastic characterization of the suspending fluids is needed.

II.1.1 Rheological study of the suspending media

We performed a full visco-elastic characterization of four types of cellulose-EMIMAc solutions, a cellulose-NMMO monohydrate solution, two types of aqueous hydroxypropylcellulose (HPC) solutions and two PIB of different molar mass. The data obtained enabled us to make the analysis of dispersion mechanisms reported in the next sections.

Viscosity:

For most samples, the viscosity at the shear rates where dispersion occurred was easily measurable (see some examples with cellulose solutions with different flow properties in

which carbon black was dispersed on Figure V-1). However, for certain solutions, we had to extrapolate the viscosity to shear rates higher than the measuring limit of the instrument, using the Carreau-Yasuda model (Equation IV-1), which was proven effective in Chapter IV:

$$\frac{\dot{\eta}(\dot{\gamma}) - \eta_{\infty}}{\eta_0 - \eta_{\infty}} = \left[1 + (\lambda \dot{\gamma})^{\alpha} \right]^{\frac{m-1}{\alpha}} \quad (\text{IV-1})$$

where $\dot{\eta}(\dot{\gamma})$ is viscosity measured at a certain steady shear rate, η_{∞} is solvent viscosity, λ is the relaxation time, m is power law index and α is a fitting parameter.

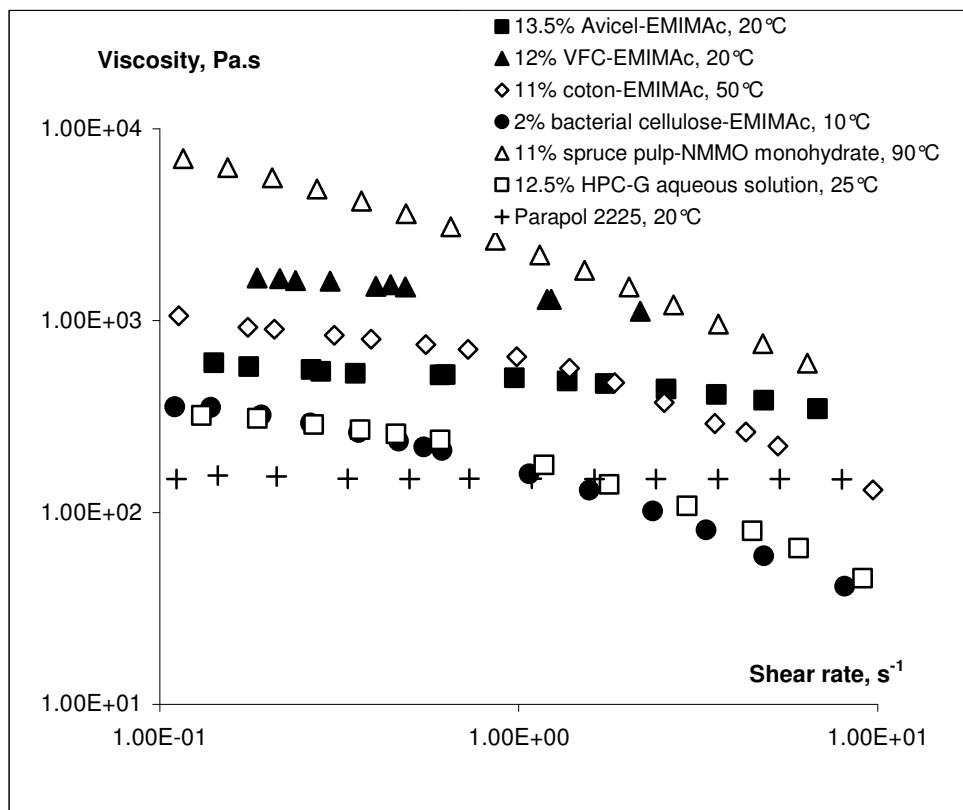


Figure V-1 Viscosity as a function of shear rate for some samples measured at different temperatures.

In certain cases, the solution viscosity at 20°C, which is the temperature at which the carbon black agglomerates were mostly dispersed, was too high to be accurately measured over the whole shear rate range. In this case, the viscosities of the same solution were measured at several temperatures higher than 20°C with 10°C intervals. As far as viscosity followed Arrhenius law, as the case of starch-EMIMAc solutions in section II.2.3 of chapter IV, it was

possible to extrapolate down to room temperature the viscosity value from the plot of $\ln(\eta)$ as a function of the inverse of absolute temperature. All the cellulose solutions in both EMIMAc and NMMO monohydrate, as well as the aqueous HPC solutions are more or less shear-thinning, while the two PIB are Newtonian fluid.

Elasticity:

The elasticity of cellulose solutions was characterized by two parameters: the elastic modulus of solutions (G') at an arbitrary frequency of 0.1Hz and what we called the dynamic Weissenberg number (We^*) at the same arbitrary frequency fixed at 0.1 Hz, defined in Equation V-2:

$$We^* = G'(\omega)/G''(\omega) \tag{V-2}$$

where $G'(\omega)$ and $G''(\omega)$ are the elastic and viscous modulus at the same specified arbitrary frequency, respectively. The higher these two parameters are, the more elastic the fluid is and the more elastic compared to viscous the fluid is. The elasticity of the cellulose solutions is related to both the cellulose concentration and the molar mass of cellulose. As expected, the solutions became more elastic when increasing concentration, with a rather sharp influence at high cellulose concentrations when entanglements are playing a major role (e.g. a 15% Avicel/EMIMAc is much more elastic than a 12% Avicel/EMIMAc solutions). As also expected, the solutions are more elastic when the dissolved cellulose has a higher degree of polymerization (DP) (VFC pulp of DP=440 gave a solution more elastic than Avicel microcrystalline cellulose of DP=180 at the same concentration). Table V-1 gives some representative values of G' and G'/G'' for the samples we measured. For example, the cellulose-NMMO monohydrate solution was very elastic; the Avicel cellulose solutions in EMIMAc and aqueous HPC solutions were less elastic, whereas the two PIB tested did not have elasticity at all in the range of shear rates used.

Table V-1 Parameters representing the elastic moduli (G') and dynamic Weissenberg number (G'/G'') measured at 0.1 Hz for some samples.

Samples	G' , Pa	G'/G''
12% Avicel-EMIMAc	14	0.09
12% VFC-EMIMAc	217	0.27
5% cotton-EMIMAc	195	0.72
4% bacterial cellulose-EMIMAc	73	0.54
11% spruce pulp cellulose-NMMO monohydrate, 90°C	1 140	0.88
Parapol 1300	0.04	0.00054
Parapol 2225	1.5	0.0058
12.5% G-HPC-water, 25°C	78	0.43
40% E-HPC-water, 25°C	48	0.19

II.1.2 Relations between rheological characteristics of the suspending medium, critical shear stress and dispersion mechanism

The dispersion of individual carbon black agglomerate was studied in all the suspending fluids, concentrations and temperatures described in Table V-2. When increasing the shear rate, and thus the macroscopic shear stress calculated by Equation V-1, agglomerates started to desagglomerate by one of the two main mechanisms, rupture or erosion, as illustrated on Figure V-2. It is worth noting that we classified the dispersion mechanisms in different matrix into either rupture or erosion, depending on which mechanism was firstly observed at the critical shear rate. In fact, this is a rather simplified description, since the dispersion process can be quite complex, and for example, during the erosion process, we could still observe the breakdown of relatively large pieces which could look similar to rupture.

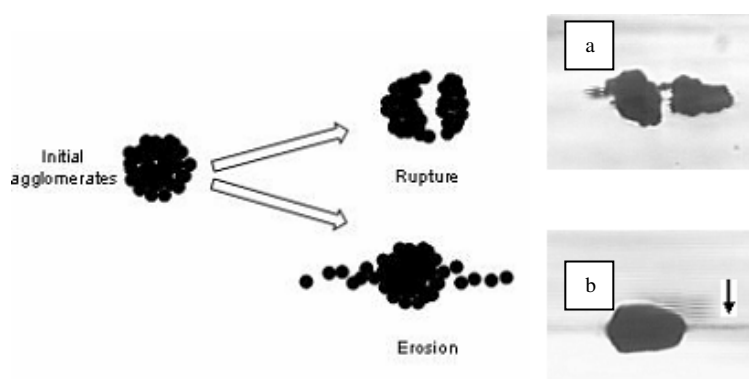


Figure V-2 Two mechanisms of carbon black agglomerates dispersion in a) 9% cotton-EMIMAc by rupture where the agglomerate is broken into two pieces and b) in 14.2%

Avicel-EMIMAc by erosion, where the arrow points on the long black trace of carbon black nanoparticles that are detached from the agglomerate.

In each fluid at 20°C, and for 14% VFC-EMIMAc solution at various temperatures, two parameters were recorded, first the type of mechanism, and second at which critical macroscopic shear stress this dispersion is starting. These two parameters are given in Table V-2.

Table V-2 Critical macroscopic shear stress (calculated from equation 3) and dispersion mechanism for carbon black agglomerates in all dispersion media tested for dispersion.

Samples	DP	Critical shear stress, Pa, with errors of $\pm 25\%$	Mechanism
Parapol 1300		576	erosion
Parapol 2225		1100	erosion
12% Avicel		865	erosion
13.5% Avicel		1450	erosion
14.2% Avicel	180	1630	erosion
14.5% Avicel		1730	erosion
14.8% Avicel		1820	erosion
15% Avicel		2860	erosion
12.6% VFC-a			1770
12% VFC		2160	erosion
14% VFC 50°C		3410	erosion
14% VFC 40°C	440	5170	erosion
14% VFC 30°C		11300	erosion/rupture
13% VFC		13370	erosion/rupture
12.6% VFC-b		16970	rupture
14% VFC		25450	rupture
4% bacterial cellulose	1700	560	erosion
10% Avicel-0.67% bacterial cellulose		1180	erosion
5% cotton		1310	erosion
7% cotton	710	800	erosion
9% cotton		4550	erosion/rupture
12.5% G-HPC/water		734	erosion
40% E-HPC/water		1830	erosion
11% spruce pulp cellulose-NMMO monohydrate		1830	erosion

Cellulose was dissolved in EMIMAc except the cases explicitly mentioned. Except for VFC-EMIMAc solutions, all experiments were performed at 20°C.

From Table 2, we can see that except for three suspending media being at the erosion-rupture transition, the mechanisms of dispersion were well identified, being either erosion or rupture. The erosion dispersion mechanism happened at a lower macroscopic critical shear stress than the rupture dispersion mechanism, in agreement with what has been reported for agglomerate dispersion in literature [Rwei 1990, Boudimbou 2011]. The major and striking result shown in Table V-2 is that the critical macroscopic shear stress is a function of the suspending medium. If erosion or ruptures are processes mainly controlled by some cohesion parameter of agglomerates for erosion and certain structural defects for rupture, the critical shear stress should be a constant for erosion and for rupture, independent on the fluid that is applying the hydrodynamic stress. Table V-2 shows that this critical stress is varying over a considerable range, from 600 to 13000 Pa for erosion and 4500 to 25000 Pa for rupture. There are three aspects that must be considered to interpret these results and which could play a role on the critical macroscopic stress value: the infiltration of matrix fluid, the size of the agglomerate, and the elasticity of the solution.

II.1.3 Potential influence of fluid infiltration inside the agglomerates

As mentioned, if matrix fluid (solvent alone or cellulose plus solvent or even cellulose itself) penetrates inside the pores of an agglomerate, it is increasing its erosion kinetics when agglomerates are not fully infiltrated [Bohin 1996] due to the detachment of large infiltration layers (sort of mixture between erosion and rupture), and this is also changing the critical stress [Roux 2008]. Contrary to agglomerates that are becoming transparent when infiltrated like silica, and for which it is easy to see infiltration, it is not possible to see if a carbon black agglomerate has been penetrated or not. For carbon black, only indirect evidences of infiltration can be obtained, like a difference in dispersion kinetics and critical stress. Polyisobutylene Parapol 1300 and 12% Avicel-EMIMAc were chosen to check the impact of the infiltration of matrix fluids because of their low elasticity, in order to eliminate any possible influence of elasticity on the measured values of critical shear stress. Carbon black agglomerates were placed in these two fluids for different waiting times in order for infiltration, if any, to occur, and then sheared up to dispersion. The values of critical macroscopic shear stress shown in Table V-3 indicate that time has no influence on the critical stress. This shows that either there was no infiltration or that infiltration had a very low effect (variations of critical shear rates within the measurement errors). It can be concluded that the infiltration of suspending fluids is

not significant enough to have an influence on dispersion, or at least not during the scale of time (hours) we are performing experiments. Two points must be noted. First is that the waiting time we used for checking infiltration was much higher than the time used in rheo-optical dispersion time (usually less than 30 minutes). Second, in Table V-3, the longest waiting time was 3 hours in the case of 12% Avicel-EMIMAc since the solution is very hygroscopic. Above this time, water was starting to penetrate inside the solution.

Table V-3 Critical shear rate and stress for carbon black agglomerate in Parapol 1300 with infiltration time varied from 0 to 24 hours and in 12% Avicel-EMIMAc solution with infiltration time varied from 0 to 3 hours.

	Infiltration time (hour)	Critical shear rate (s^{-1})	Critical shear stress (Pa), with errors of $\pm 25\%$
Parapol	0	4.55	683
	16	3.96	594
	24	4.48	672
Avicel	0	1.86	724
	3	2.45	914

II.1.4 Influence of size of agglomerates

A second factor that is known to influence the critical stress for dispersion is the size of the agglomerate [Collin 2004, Shiga 1985, Leblanc 1996]. In the present case, the agglomerate shape is not considered [Seyvet 2001] and its radius is calculated as the geometric mean value of the three dimensions of each agglomerate. Due to the sieving procedure, the size range is relatively small, between 33 and 63 μm , which limit the potential effect of agglomerate size which is usually seen on much larger size differences [Collin 2004, Roux 2008]. The values of the critical shear stresses divided by elastic modulus (to eliminate the effect of elasticity) in different matrix fluids (12% - 15% Avicel-EMIMAc solution and 12% - 14% VFC-EMIMAc solution, both at 20°C) is independent of initial radius R_0 of the agglomerates, most probably due to the small range of sizes used in this study, implying that agglomerate size is not a factor able to explain the variation of critical macroscopic stresses reported in Table V-2.

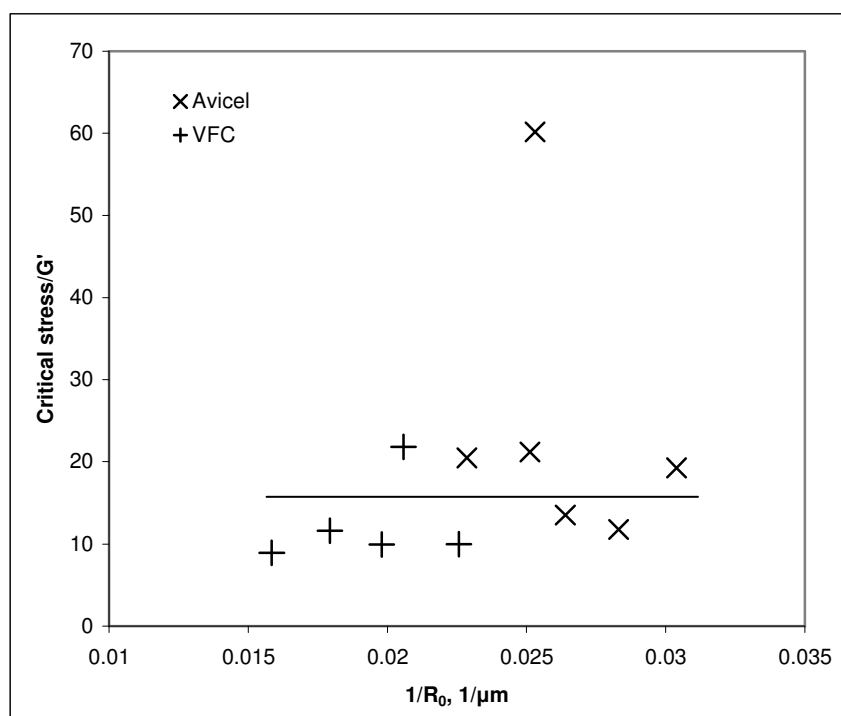


Figure V-3 Reduced critical macroscopic shear stress divided by G' as a function of the inverse of agglomerate radius, for carbon black agglomerate dispersion in 12% - 15% Avicel-EMIMAc solution and 12% - 14% VFC-EMIMAc solution at 20°C. One point (12% Avicel) is clearly out of the range with a much higher critical stress most probably due to a different structure of this agglomerate (more compact for example).

II.1.5 Influence of elasticity on dispersion

The third potential factor able to explain the dependence of critical shear stress for dispersion on the suspending medium is the fact that the critical macroscopic stress is calculated in a very crude way. It is estimated as the stress of a non elastic fluid at the position where the agglomerate is flowing, but without the actual presence of the agglomerate. This is probably a good approximation of the stress acting on an agglomerate in a Newtonian fluid, and perfectly suitable to make comparison between different such fluids when the agglomerate size is not varied too much. But if the fluids are elastic, the real local stress acting on the agglomerate can be very much influenced by the elasticity of the fluid influencing stress distribution around the particle.

Due to the technological importance of suspension rheology, the behavior of a sphere in a shear flow has been intensively studied. If the description of the flow of a sphere in a Newtonian viscous fluid has a classical analytic solution, it is not the case when the fluid is either non-Newtonian or viscoelastic, where only numerical simulation can give access to the stress distribution around the sphere. A first experiment showing the profound effect of elasticity on stress distribution and values is the measurement of the rotation period of a sphere submitted to a steady shear flow. Compared to the Newtonian case, the period of rotation increases with the elasticity of the fluid, in agreement with numerical simulations which show that the maximal local stress increases and shifts its location when the fluid is elastic [Astruc 2003; Snijkers 2009; Snijkers 2011]. From maximum stress location at 45° of the flow direction and in the shear plane for the Newtonian case, the maximum stress location move to other angles depending on elasticity. The classical hypothesis for performing simulations (incompressible fluid, negligible inertial and gravitational forces, no-slip condition at the boundary, and torque-free particle) are valid in the case of the flow of carbon black agglomerates such as studied here. Aside from the fact that visco-elastic fluids have time-dependant properties, this class of fluids is also building normal stresses which are absent in Newtonian fluids. It is the existence, magnitude and location of these normal stresses that are drastically changing the behavior of a sphere flowing in a visco-elastic fluid. Numerical simulations in 2D suggest that the higher the elasticity is, the higher are the local compressive stresses and the lower are the local extensional stresses acting on the particle [Snick 2011]. An example adapted from the Master thesis of Maxime Snick [Snick 2011] is given on Figure V-4.

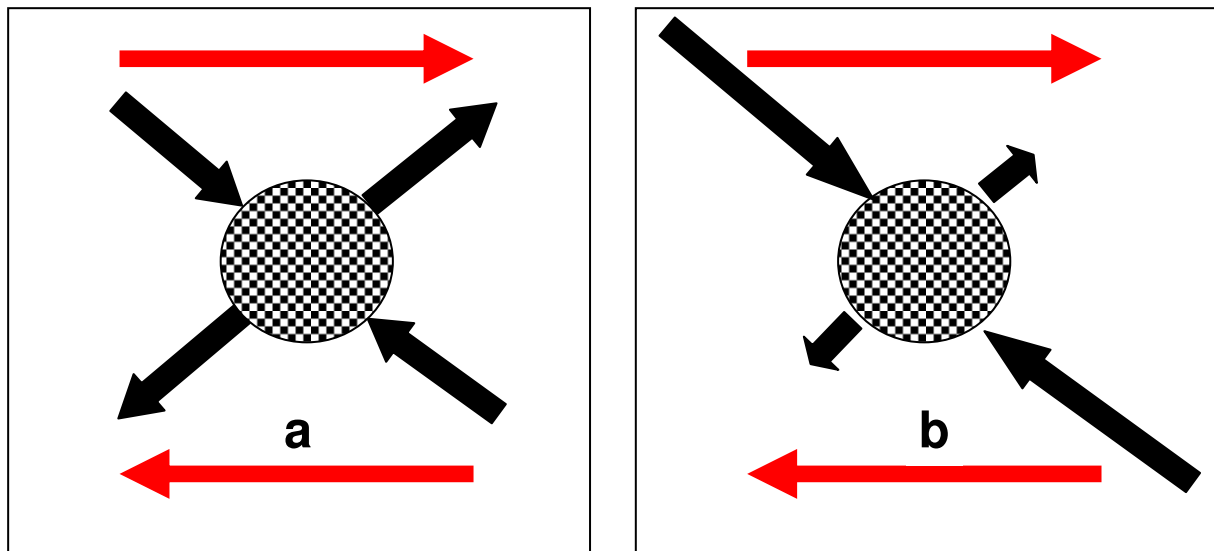


Figure V-4 Magnitude of the stresses acting on a flowing sphere in (a) a Newtonian fluid and (b) an elastic fluid (adapted from the Master thesis of Maxime Snick [Snick 2011]). The length of the arrows is proportional to the magnitude of the stress and the direction specifies if the stress is compressive or extensional.

If the simulation is applicable to our case, the change of stress distribution due to elasticity around the agglomerate has two important consequences. First, the dominant stresses are the strong compressive stresses, which compress the suspended agglomerate rather than disperse it, contrary to the extensional stresses that are acting to disperse agglomerates. Second, with the same macroscopic shear stress, the extensional stresses are lower in viscoelastic fluids than in Newtonian fluids. These two effects are both independently resulting in more difficulties to disperse agglomerates when the elasticity of the matrix fluid is increased. This implies that it will be necessary to impose a larger macroscopic stress (as measured from Equation V-1) to achieve the same critical local stress for dispersion.

Since we have an estimation of the elasticity of all fluids used at the macroscopic shear rate where dispersion occurs, it is possible to plot this critical macroscopic shear rate as a function of elasticity parameters. Figure V-5 and Figure V-6 show that there is a strong correlation between the critical shear stress for initiating dispersion (rupture or erosion) and the elastic modulus of the suspending fluids (note that we did not use all the cases of Table V-2 since many are falling in the same low elasticity region). A higher critical macroscopic shear stress will be needed when carbon black agglomerates are dispersed in a more elastic fluid. If we extrapolate the stress versus modulus to a zero value of modulus, it gives 837 Pa. Physically it

means that the dispersion of carbon black agglomerates in a completely non-elastic fluid would occur at a critical shear stress of 837 Pa. It is in the same range of the critical shear stress measured in Parapol 1300 (575Pa), which is basically a non-elastic fluid. The same results are found if we take the dynamic Weissenberg number ($We^* = G'/G''$) to characterize the elasticity of the fluids. The critical stress necessary for either erosion or rupture also increased with higher We^* ; but there seems to be a difference between erosion and rupture, with a leveling-off in the rupture region. Extrapolation to zero elasticity gives a critical shear stress of 612 Pa, which is consistent with the two values reported above. Increasing temperature of cellulose solutions decreases G' . We checked that temperature has no effect on the correlation between critical shear rate for dispersion and elasticity, as shown in Figure V-7.

The more elastic the matrix fluid is, the higher the macroscopic shear rate is needed for dispersing a given agglomerate. Elasticity has a negative effect on filler dispersion.

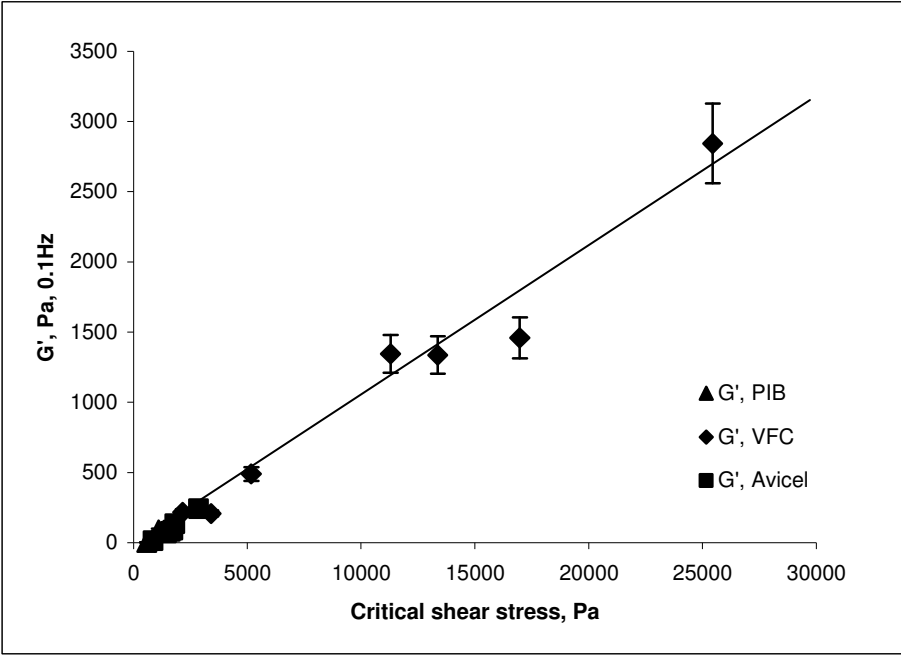


Figure V-5 Critical macroscopic shear stress of carbon black agglomerates in cellulose solutions of various concentrations and PIB versus elastic modulus, at 20°C.

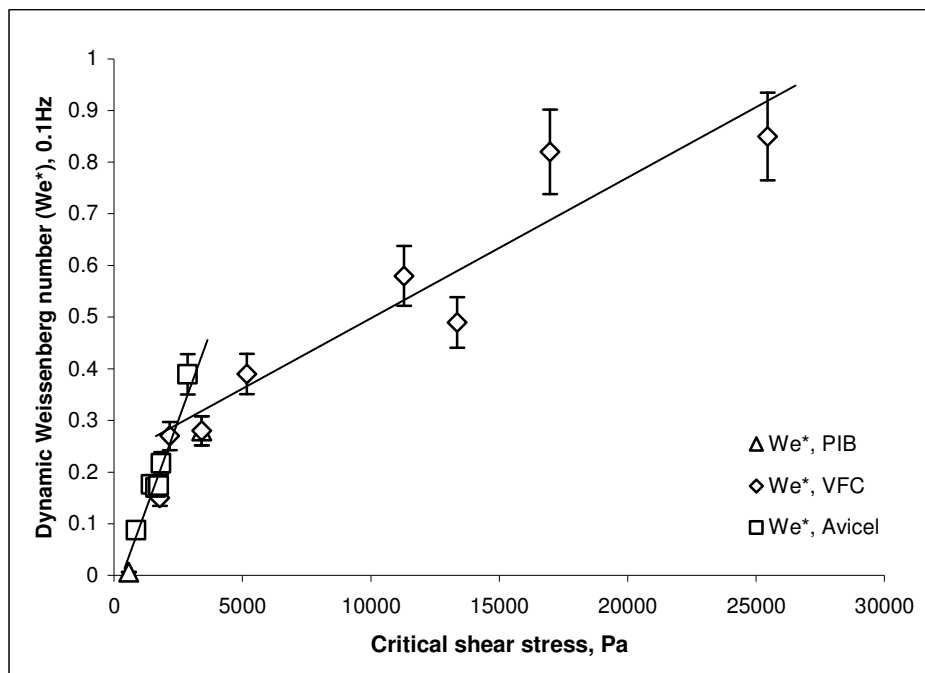


Figure V-6 Critical macroscopic shear stress of carbon black agglomerates in cellulose solutions of various concentrations and PIB versus dynamic Weissenberg number, at 20°C.

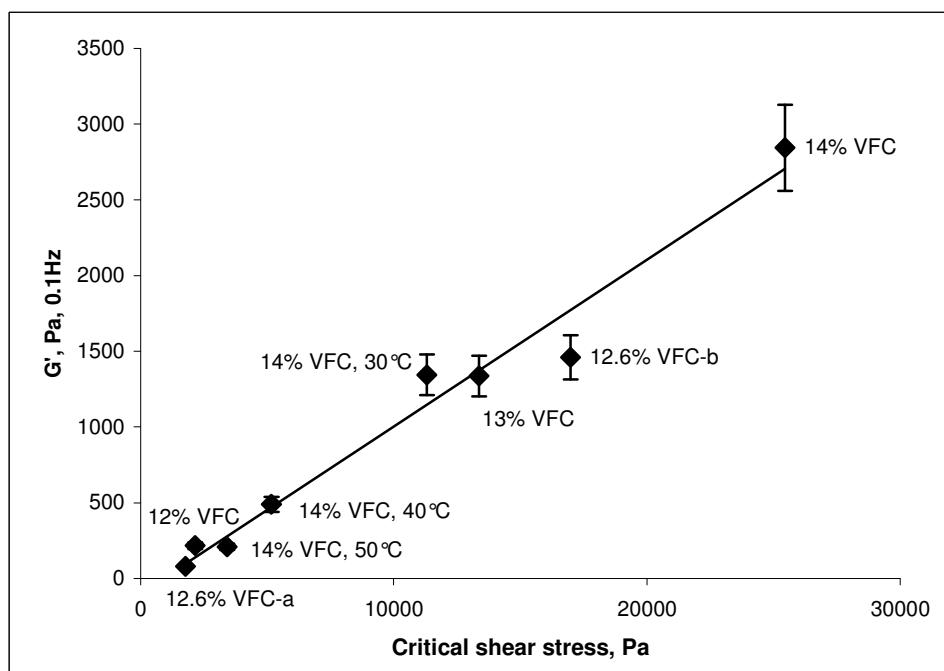


Figure V-7 Critical macroscopic shear stress of carbon black agglomerates in 12% - 14% VFC cellulose solutions versus elastic modulus, at 20°C, 30°C, 40°C and 50°C.

II.2 Preparation of conductive cellulose films

II.2.1 Morphology of carbon black dispersion

We prepared the composites using a counter rotating twin-screw micro-compounder to disperse carbon black in 15% Avicel-EMMIMAc solution. To reach a good dispersion, we must have inside the compounder shear stresses exceeding the critical shear stress necessary for the carbon black agglomerates to disperse into much smaller aggregates.

According to our study with the counter-rotating rheo-optical device, a macroscopic critical shear stress of roughly 3000 Pa is needed for the 15% Avicel-EMIMAc used as the dispersion matrix. Taken into account the viscosity of 15% Avicel-EMIMAc solution at 30°C, we estimated that carbon black agglomerates start to disperse with shear rate above 3.5 s⁻¹.

We do not know the precise shear rate that we can achieve inside the conical counter-rotating twin-screw compounder. We used a crude estimation of the magnitude of the shear rate we can obtain with this device. As shown in the following Figure V-8, we focus on one single carbon black agglomerate between the two screws. The radius of each screw is r , and the distance between the thread of one screw and the cylinder part of the other one is h . The speed of the two screw is $\omega = 250$ rpm. Simply taking the movement of the two screws as a Couette flow, the shear rate $\dot{\gamma}$ can then be calculated as:

$$\dot{\gamma} = \frac{2\pi r * 250}{60 * h} \quad (V-3)$$

We measured $r=5$ mm and $h=1$ mm which give a shear rate of about 130 s⁻¹, which is much larger than the needed critical shear rate of 3.5 s⁻¹. Here we made the calculation with the viscosity of pure cellulose-EMIMAc solution while in reality, viscosity of the medium is increasing strongly with dispersion, which is also increasing the effective applied shear stress at a given rotation speed of the two screws.

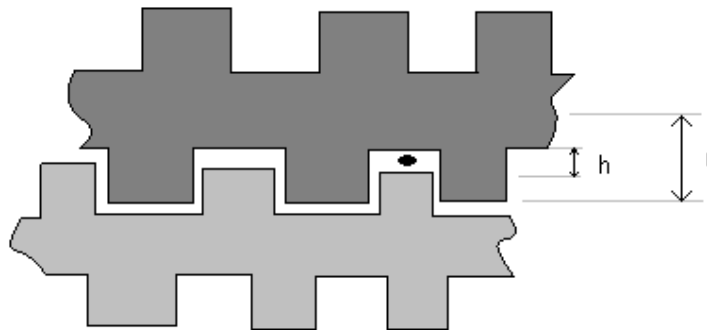


Figure V-8 Structure of conical counter-rotating twin-screw compounder and schematic illustration of one single agglomerate located between the two screws.

To confirm whether we can obtain a good dispersion with the micro-compounder and the parameters as mentioned, we observed the prepared composite film morphology with scanning electron microscopy (SEM), and compared it to a similar composite prepared by our partner TITK (9% spruce pulp-9% CB-NMMO monohydrate), as shown in Figure V-9. For cellulose-carbon black composites based on cellulose-EMIMAc solution we dissolved 15% Avicel into EMIMAc, mixed 10wt% carbon black with the total mass of cellulose solution inside the micro-compounder, and prepared composite films with a spin-coater. The other sample was 9% spruce pulp cellulose-9% carbon black-NMMO solution prepared with a regular internal mixer by TITK. Films were cut into small pieces, and regenerated in water to have cellulose-carbon black composites. Both composites (EMIMAc and NMMO) were dried, and sputter-coated with gold/palladium for SEM observations.

As we can see from Figure V-9, the morphology of both composites is rather similar. Carbon black were dispersed into aggregates of about 100nm or less, and homogenously distributed in the cellulose matrix. In short, we can consider that our procedure of dispersing carbon black in cellulose solution with the micro-compounder gives morphology results similar to the industrial procedure used by TITK. In the following part, all composite films with different carbon black loading will be prepared following the same procedure.

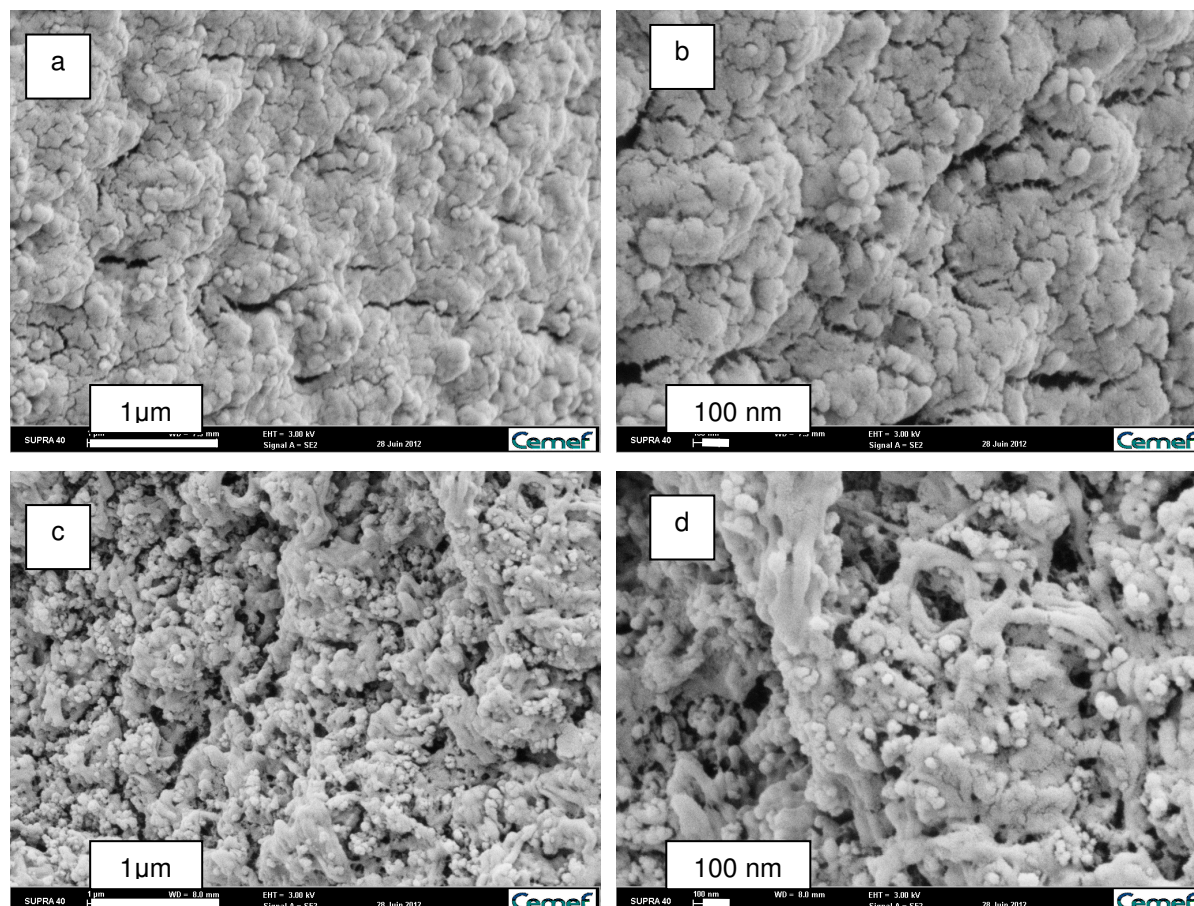


Figure V-9 SEM images of cellulose-CB composite samples coagulated from a) and b) 15% Avicel-10%CB-EMAMAc; c) and d) 9% spruce pulp-9% CB-NMMO monohydrate. Scales are as indicated on the images.

II.2.2 Impact of carbon black loading on conductivity

To investigate the impact of carbon black concentration on the resistivity/conductivity of composite films, we prepared composite films with different carbon black loadings from 0% to 45.5% by weight, and measured their sheet resistance with Van der Pauw method.

Van der Pauw method is a technique developed in 1950's to measure the resistivity of approximately two-dimensional samples, such as sheets, films or membranes, and is also largely applied in the semiconductor industry. With this method, as illustrated in Figure V-10, currents of both directions were applied on the two probes at 1 and 3 (I_{13}), and the voltages between the other two probes at 2 and 4 were measured according (equation V₂₄).

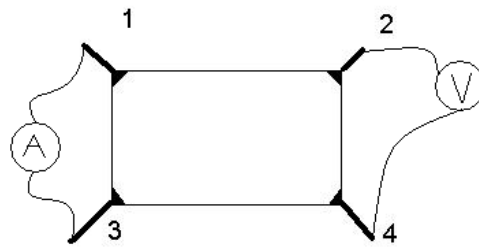


Figure V-10 Schematic illustration of 4-point Van der Pauw method for measuring sheet resistivity.

With Ohm's law, we can calculate the resistance $R_{13,24}$. Similarly the currents and voltages were applied and measured by rotating the four probes for measuring $R_{24,13}$, $R_{12,34}$, $R_{34,12}$. Then R_s can be calculated with the following equation as:

$$e^{-\pi(R_{12,34}+R_{34,12})/2R_s} + e^{-\pi(R_{13,24}+R_{24,13})/2R_s} = 1 \quad (\text{V-4})$$

Once the sheet resistance was measured, resistivity (specific resistance, ρ) can be calculated by:

$$\rho = R_s \times d \quad (\text{V-5})$$

where d is the thickness of the composite films.

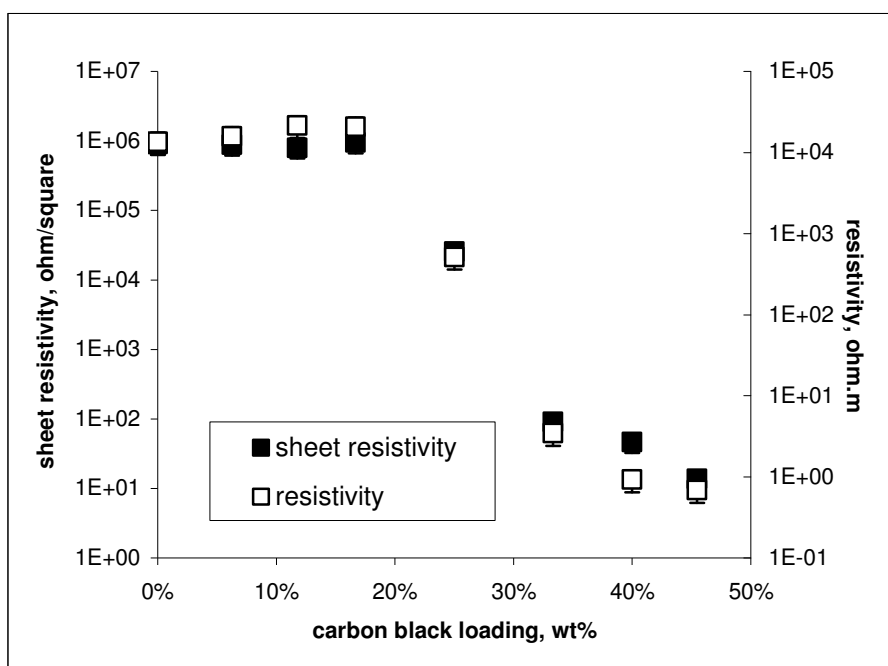


Figure V-11 Sheet resistivity (ohm/square) and resistivity (ohm.m) as a function of carbon black loading (wt %) for the prepared cellulose-CB composite films. Error bars are 30%.

In Figure V-11, we plotted the measured sheet resistivity and the calculated resistivity as a function of carbon black loading in composite films. Clearly higher is carbon black concentration in the composite films, the more conductive the films become. Also we can find that the resistivity falls sharply when the composite films had carbon black content above 20%, and stabilize when carbon black loading is above 40%, leading to the conclusion that the percolation threshold in our case is roughly above 20% by weight. It is not straightforward to estimate the density of carbon black agglomerate when they are dispersed since we do not know if the density of the small aggregate is the same of the agglomerate, and thus difficult to calculate the volume fraction.

This value of a percolation threshold of 20% by weight is also confirmed when making conductive cellulose fibers from cellulose-carbon black-NMMO mixtures in the laboratory of TITK. The lowest resistivity achieved on the composite films with carbon black above the percolation threshold is around 1 ohm.m, which is in the same range or slightly lower as reported in literature for conductive composites of carbon black filled polymers or carbon nanotube filled cellulose [Yuan 2010; Rahatekar 2009; Untereker 2009]. Thus composite

films with enough carbon black loadings are conductive, and suitable for potential applications.

Another aspect to note is that when we decreased the carbon black loading from 16.7% to the blank samples of pure cellulose films without carbon black, the resistivity is more or less constant. The values of the resistivity without or with a low amount of CB which is around 10^4 ohm.m are much lower than for normal non-conductive unmodified cellulose materials [Voigt 2005; Kim 2010] and other polymer films/membranes [Al-Saleh 2008; Yu 2005]. This may be due to a slight lack of humidity control during the tests, but it is more likely to be caused by some residual ionic liquid EMIMAc in the coagulated films. During our dissolution-mixing-coagulation process with cellulose films preparation, we found that it is rather difficult, if not impossible, to exchange all EMIMAc molecules with water during the coagulation. Thus once the films were prepared, a small fraction of ions from EMIMAc remained in the films and could bring an extra conductivity. At lower carbon black loading, such an effect is very important and the resistivity/conductivity of the films is dominated by the residual EMIMAc while with higher carbon black loadings, the impact of EMIMAc ignores negligible.

II.2.3 Attempts to reduce the carbon black loading in conductive films

As we mentioned in the Chapter I, the reduction of the carbon black loading without decreasing the conductivity is a major interest in the research of polymer/CB blends, since better processability and mechanical performance can be obtained. To this end, we did some preliminary research by blending carbon black with two types of cellulose. The two types of cellulose with quite different DP used were: Avicel with a DP of 170 and VFC with a DP of 400. More detailed information on these celluloses is given in Chapter II.

The basic idea here is to take advantage of the difference between the two types of cellulose. Due to the quite different chain length, Avicel and VFC will not be immediately miscible once the solutions of the two cellulose samples are mixed. The interpenetration of the two types of cellulose chains takes time. An analogy can be made between this case and the cases of two immiscible polymers blending with CB described in Chapter I section II.4.2. When two immiscible polymers are blended with carbon black, due to the different affinity and

interfacial energy, CB can be localized either in the interfacial region of the two polymers, or in one preferred polymer phase (double percolation). Either scenario provides the possibility of reducing CB loading at the percolation threshold of the composite.

We started with a simple concept of coating the non-conductive cellulose films with two conductive layers of cellulose blended with carbon black. If the conductive layers can stay conductive in the 3-layered composite films, the total carbon black loading will be decreased.

Three-layered cellulose-carbon black composite:

The structure and preparation of the three-layered composite films has been described in Chapter II. Briefly, it consists of one non-conductive VFC cellulose layer, coated with two conductive Avicel cellulose-CB layers on both sides, as illustrated in Figure V-12a.

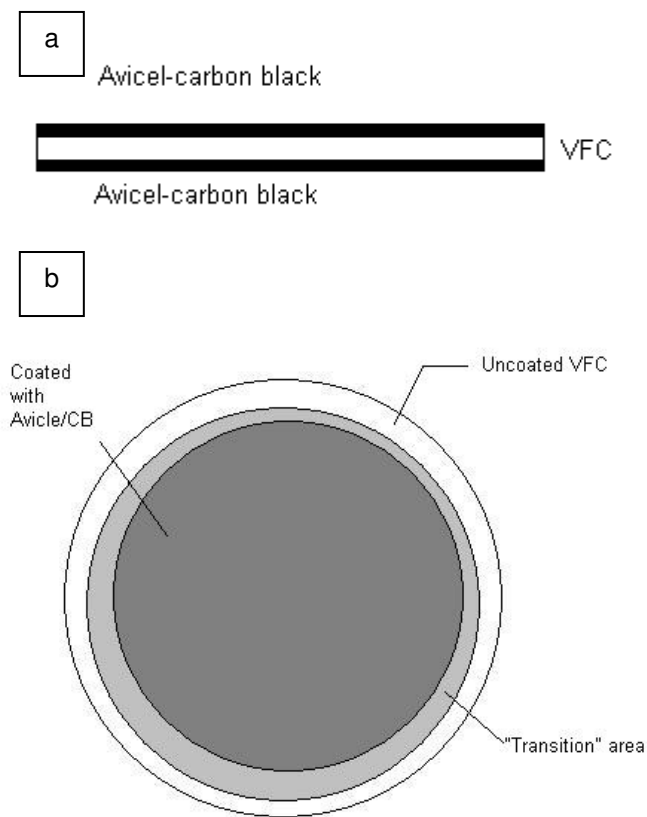


Figure V-12 Schematic illustration of three-layered cellulose-CB films, with a) view from the side, and b) view from the top.

Because we prepared the three-layered films with spin-coating technique, the three layers were deposited in sequence before being coagulated in water bath, there are two concerns from the processing point of view, (1) the homogeneity of the composite film and (2) the

adhesion between each layer. The problem of homogeneity is illustrated as V-12b, and may bring inconsistency to the conductivity results. Actually, with SEM images we can spot clearly three different regions due to the more or less inhomogeneous coating: the region covered with Avicel/CB, the region of VFC cellulose not covered with Avicel/CB, and the “transition” area between the two (Figure V-13a, b and c). The difference is also confirmed by the results of the conductivity tests, and will be specified in the following part. No decohesion of the three layers was found visually both after the coagulation or after drying, but standard peel testing should be made for a more precise evaluation. We can also notice that “layered” films are more “twisted” after drying as compared with rather flat composite films prepared by the other mixing route with only two cellulose solutions mixed (“mix” route) (Figure V-14).

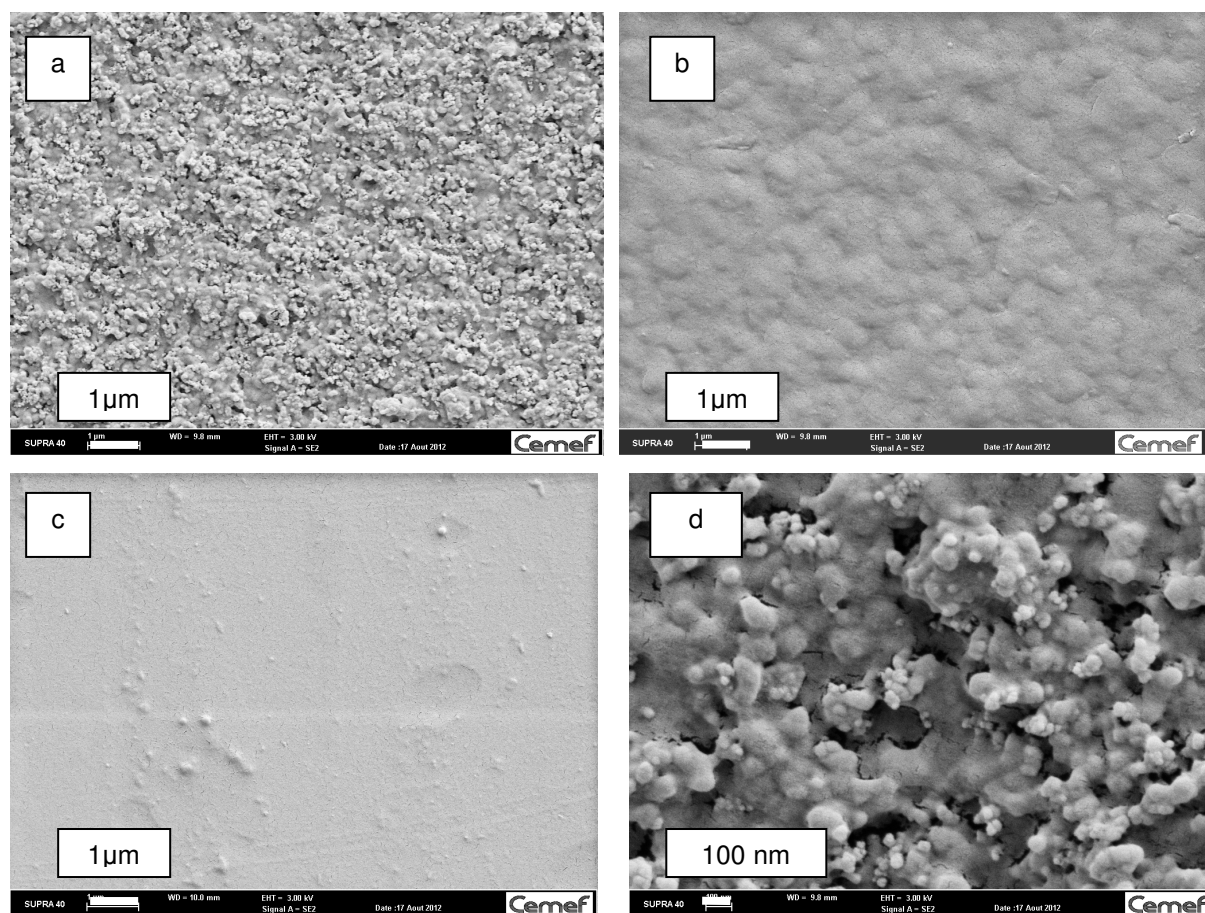


Figure V-13 SEM images of three-layered cellulose-CB composite films with a) and d) on the coated part with Avicel-CB, b) on the “transition” part, and c) on the uncoated VFC part. Scales are as indicated on the images.

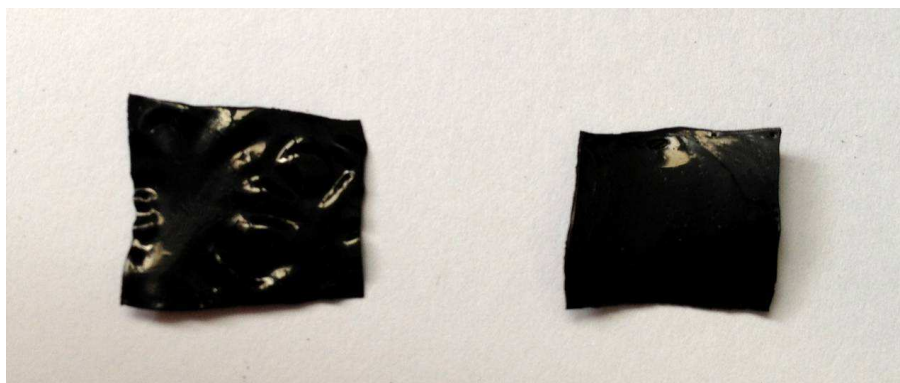


Figure V-14 Two cellulose-CB composite film samples after drying. On the left “three-layer” route, and on the right the “mix” route.

We observed the surface morphology and measured the conductivity/resistivity for the three layered composite films. As shown in Figure V-13d, we found a dispersion of carbon black at the scale of around 100 nm or less and a good distribution on the part of films coated with Avicel/CB. This is also consistent with what we observed on the pure Avicel films blended with carbon black in the section II.2.1 of this chapter.

The values of conductivity/resistivity for the three-layered composite films we prepared was measured and added on to Figure V-11, as shown in the Figure V-15. We used 12 wt% VFC-EMIMAc solution and 15 wt% Avicel-10 wt% CB-EMIMAc mixture, and the weight ratio of the 12% and 15% solution was 1.5 to 1. We can calculate that the carbon black loading in the final composite films is about 23.3 wt%, compared to the carbon black loading of 40 wt% if the 15 wt% Avicel-10 wt% CB-EMIMAc mixture was directly coagulated.

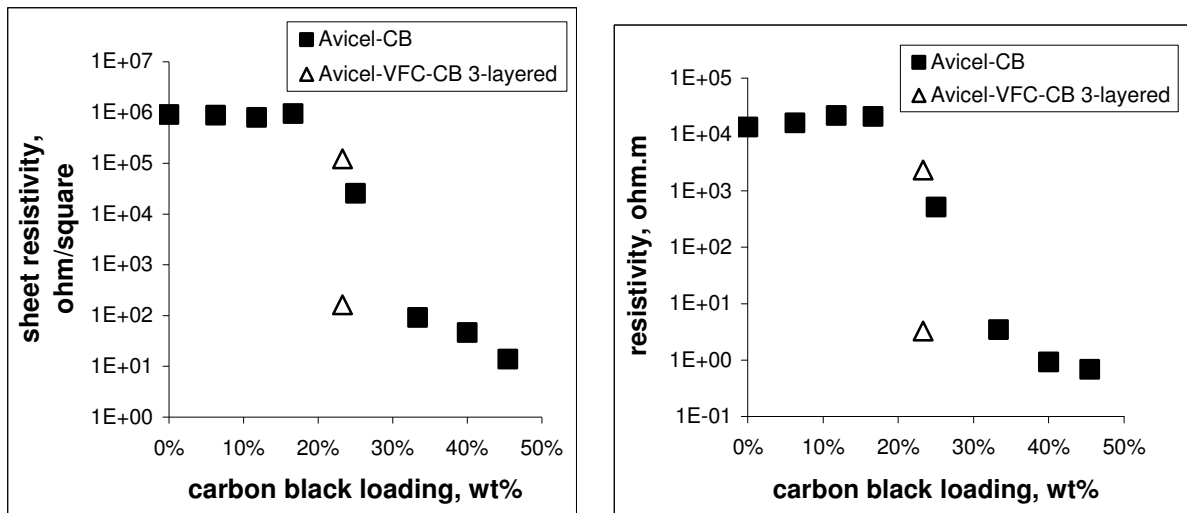


Figure V-15 Sheet resistivity (ohm/square) and resistivity (ohm.m) for three-layered cellulose-CB composite films and one layer cellulose-CB films as a function of total amount of carbon black in the film.

In fact, we obtained two groups of average resistance values on the composite film samples, and the difference is of several orders of magnitude. The discrepancy of the resistance can be explained by the inhomogeneity of the composite films as observed with SEM, since the samples for resistance measurements were films of quite small surface area randomly cut from the initial films. The lower resistance measured was close to the resistance of Avicel-CB blends with 40 wt% carbon black loading, which is the value of CB loading if the coating layer is directly coagulated into films and the concentration is well above the percolation threshold. We assume that it is the resistance value of well-coated samples. It means the conductivity/resistivity of the well-coated composite films is generally determined by the conductive layer, and there is no need to have a migration of carbon black into the center non-conductive layer to achieve a low conductivity. Samples with high resistance, on the other hand, are obtained with the uncoated or “transition” part of the composite films. Thus as long as the composite films can be completely and homogeneously covered with the conductive layers, we are able to prepare a cellulose films with similar conductivity and about half the carbon black loading. This result is very encouraging. It will require a further study of its processing to ensure a better coating, with a more precise control of the solution viscosity, temperature, and speed of spin-coating.

Two-phase “immiscible” celluloses-carbon black composite films (“mix”) route:

The other route was inspired by the research of carbon black mixed with immiscible polymer blends [Sumita 1991]. In our practice, with the same compounder, the carbon black was mixed with 15 wt% Avicel-EMIMAc at first with the Haake Minilab compounder, and then 12% wt VFC-EMIMAc without CB was added into the compounder. The weight ratio of the 15% and 12% solutions was 1.5 to 1. As mentioned in Chapter II, the 15 wt% Avicel-EMIMAc and 12 wt% VFC were simply chosen due to their similar viscosity. Once mixed, the cellulose-cellulose-CB mixtures were spin-coated and coagulated with the same method for preparing films. Figure V-16 shows the surface morphology of the so-called two-phase composite films.

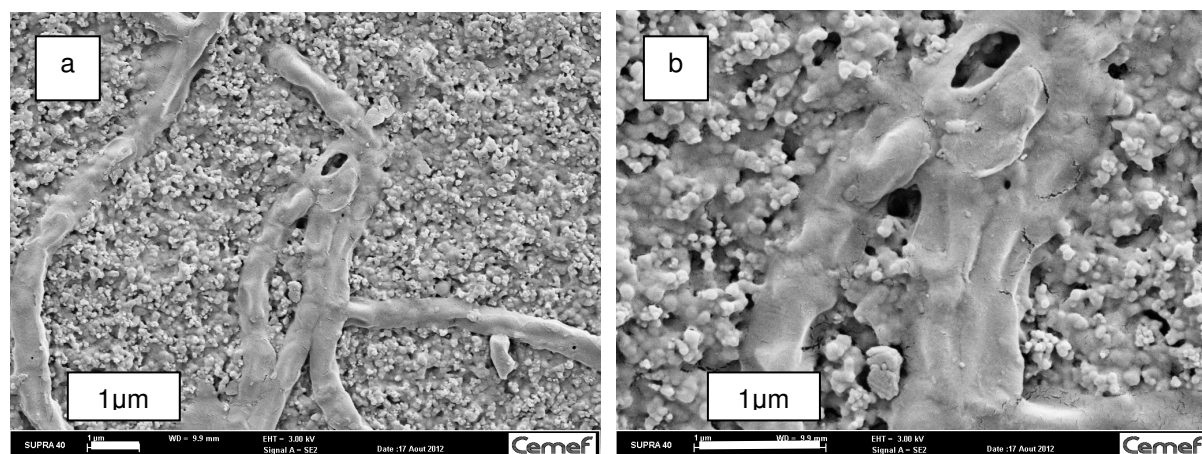


Figure V-16 SEM images of two-phase “immiscible” celluloses-carbon black composite films. Scales are as indicated on the images.

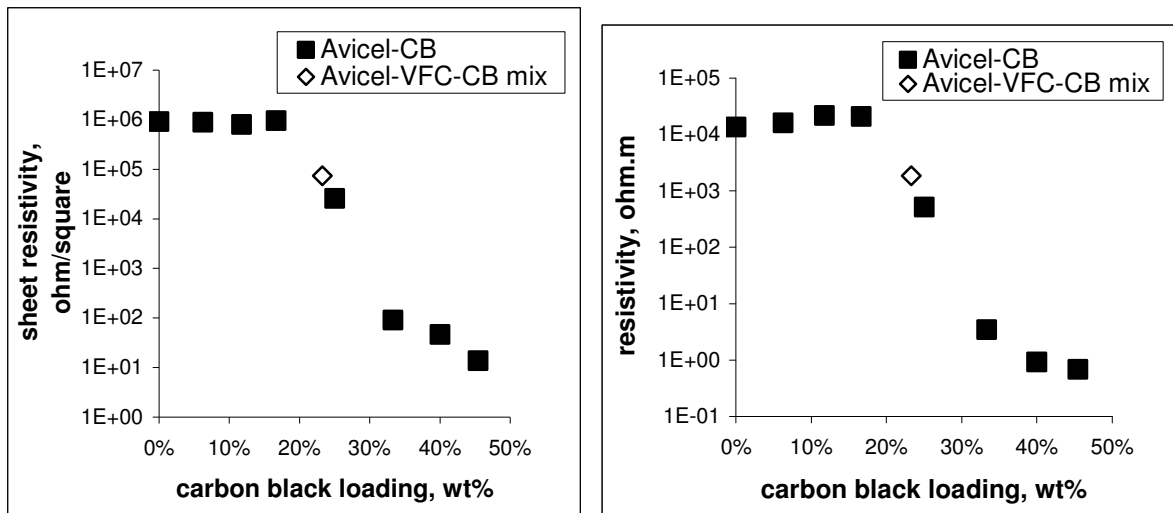


Figure V-17 Sheet resistivity (ohm/square) and resistivity (ohm.m) for two-phase “immiscible” celluloses-carbon black composite films, compared to data of simple cellulose-CB composite films.

We indeed can find two different phases in the composite films prepared with this route. One phase filled with carbon black and the other one more or less interconnected in the composite. We are quite sure that the phase with carbon black is made with Avicel cellulose and the other one with VFC cellulose, but this still requires verification. However, the conductivity measured was not as good as expected, as demonstrated in Figure V-17. We can see that the resistance of the composite films was not different from the Avicel-CB films with similar carbon black loading of 23.3 wt%, which means that here carbon black initially mixed with Avicel was simply diluted by adding VFC cellulose, without having any special synergetic effects such as double percolation. It is not very clear why we obtained this result since the morphology shown in Figure V-16 is percolating. One option is that for some reasons, percolation is interrupted in some region, reducing conductivity. More work is clearly needed to understand our results.

III. Conclusions

The use of a counter-rotating rheo-optical tool enables us to study the dispersion process of carbon black agglomerates in different suspending media, including various types of cellulose dissolved in both ionic liquid and NMMO monohydrate at different concentrations, aqueous hydroxypropylcellulose solutions, and polyisobutylene.

The classical mechanisms of carbon black dispersion, erosion or rupture, were observed. It was possible to measure the values of the critical macroscopic shear stresses for dispersion, which is lower for erosion than for rupture, as usually found.

However, contrary to expectations, the values of the critical macroscopic shear stress were found to strongly depend on the suspending medium. After having eliminated possible effects of agglomerate size and infiltration, it turned out that the reason for the large variation of dispersion critical stress, both for erosion and rupture, was the elasticity of the fluid matrix. Recent numerical simulations of the behavior of a sphere suspended in a visco-elastic fluid shows that when elasticity is increased, there are higher compressive stresses and lower extensional stresses applied to the sphere surface. This is hampering dispersion since it is favoring cohesion of the agglomerate through the compressive forces. The consequence is that it is necessary to apply a higher shear stress to induce dispersion, and it looks as if the hydrodynamic stress necessary for breaking agglomerates is higher. This approach was validated by noticing that there was a linear correlation between elasticity and critical shear stress for dispersion in cellulose solutions, independent of temperature, and that the extrapolation to zero elasticity was giving a critical hydrodynamic stress of the same order of magnitude than that which was found for non-Newtonian thermoplastic polymers, i.e. around 600-800 Pa.

Thus if anyone wishes to study the cohesive forces between the elementary particles in an agglomerate when agglomerate are submitted to dispersion hydrodynamic forces, the study must absolutely be done in a non-elastic fluid. Otherwise, the experimental critical shear stresses are grossly over-estimated and only serve as an indicator for the following processing, but will not correspond to any meaningful cohesion forces inside agglomerate.

Conductive cellulose-CB composite films were prepared. The route of “dissolution-dispersion-coagulation” was chosen; the shear stress within the mixing device was estimated and fixed at values higher than the critical shear stresses. SEM images of the composite films prepared with micro-compounder were compared to industrial samples provided by a partner, and confirmed a satisfying dispersion with this process.

To evaluate the conductivity as a function of the carbon black loadings and to find the percolation threshold, the sheet resistivity of composite films with different concentrations of carbon black was measured with 4-point Van der Pauw method, and the specific resistances were also calculated. We spotted a sharp increase of conductivity indicating that there is a percolation threshold above 20 wt% of carbon black loading. The maximum achieved conductivity was also in line with values reported in literatures. Residual ionic liquid EMIMAc in the coagulated films also is supposed to increase the conductivity, and the effect was more obvious for the cellulose films without carbon black prepared in the same way as control sample, which were clearly much more conductive than they should be.

Two concepts with cellulose of different DP were proposed to reduce the amount of carbon black in the sample while keeping conductivity as it is above the percolation threshold, in order to achieve better processability and mechanical performance of the films. In a “three-layer” route, Avicel cellulose-carbon black-EMIMAc solutions were coated on both side of a VFC cellulose-EMIMAc solution layer and then coagulated. The conductivity measurements and SEM images indicate satisfying results for this concept, but cohesion test and better processing for homogeneity must be done. Two-phase Avicel-VFC-CB composite films were also prepared. Despite of the existence of a two-phase morphology as seen by SEM, were the continuous phase is loaded with CB, the conductivity was not good

It is possible to make cellulose-based conductive films with the more common and economic carbon black agglomerates and easy-to-handle ionic liquid, rather than carbon nanotubes, for examples. The preparation of films, and probably fibres, with low amount of carbon black while keeping a low conductivity seems to be possible by manipulating the morphology of the samples.

References

[Al-Saleh 2008] Al-Saleh, M. H., & Sundararaj, U. (2008). An innovative method to reduce percolation threshold of carbon black filled immiscible polymer blends. *Composites Part a-Applied Science and Manufacturing*, 39(2).

[Astruc 2003] Astruc, M., Vervoort, S., Nouatin, H. O., Coupez, T., De Puydt, Y., Navard, P., & Peuvrel-Disdier, E. (2003). Experimental and numerical study of the rotation and the erosion of fillers suspended in viscoelastic fluids under simple shear flow. *Rheologica Acta*, 42(5), 421-431.

[Bohin 1996] Bohin, F., Manas-Zloczower, I., & Feke, D. L. (1996). Kinetics of dispersion for sparse agglomerates in simple shear flows: Application to silica agglomerates in silicone polymers. *Chemical Engineering Science*, 51 (23), 5193-5204.

[Boudimbou 2011] Boudimbou, I. J. (2011). Mécanismes élémentaires de dispersion de charges de silice dans une matrice élastomère, Thèse de doctorat, Sophia Antipolis : Ecole des Mines de Paris.

[Collin 2004] Collin, V. (2004). Etude rhéo-optique des mécanismes de dispersion du noir de carbone dans des élastomères. Thèse de doctorat. Ecole des Mines de Paris, Sophia-Antipolis.

[Kim 2010] Kim, D.-H., Park, S.-Y., Kim, J., & Park, M. (2010). Preparation and Properties of the Single-Walled Carbon Nanotube/Cellulose Nanocomposites Using N-methylmorpholine-N-oxide Monohydrate. *Journal of Applied Polymer Science*, 117(6).

[Leblanc 1996] Leblanc, J. (1996). Rhéologie des élastomères et leur mise en forme, Artel, Namur (Belgique).

[Rahatekar 2009] Rahatekar, S. S., Rasheed, A., Jain, R., Zammarano, M., Koziol, K. K., Windle, A. H., Gilman, J. W., & Kumar, S. (2009). Solution spinning of cellulose carbon nanotube composites using room temperature ionic liquids. *Polymer*, 50(19), 4577-4583.

[Roux 2008] Roux, C. (2008). Etude rhéo-optique des mécanismes de dispersion de la silice dans des élastomères. Thèse de doctorat. Ecole des Mines de Paris, Sophia-Antipolis.

[Rwei 1990] Rwei, S. P., Manas-Zloczower, I., & Feke, D. L. (1990). Observation of carbon-black agglomerate dispersion in simple shear flows. *Polymer Engineering and Science*, 30(12), 701-706.

[Seyvet 2001] Seyvet, O., & Navard, P. (2001). In situ study of the dynamics of erosion of carbon black agglomerates. *Journal of Applied Polymer Science*, 80 (10), 1627-1629.

[Shiga 1985] Shiga, S., & Furuta, M. (1985). Processability of EPR in an internal mixer. 2. Morphological-changes of carbon-black agglomerates during mixing. *Rubber Chemistry and Technology*, 58(1), 1-22.

[Snick 2011] Snick, M. (2011). The behaviour of a solid body suspended in a viscoelastic fluid, Rapport de stage Master, master dissertation, Ecole des Mines de Paris, Sophia-Antipolis.

[Snijkers 2009] Snijkers, F., D'Avino, G., Maffettone, P. L., Greco, F., Hulsen, M., & Vermant, J. (2009). Rotation of a sphere in a viscoelastic liquid subjected to shear flow. Part II. Experimental results. *Journal of Rheology*, 53 (2), 459-480.

[Snijkers 2011] Snijkers, F., D'Avino, G., Maffettone, P. L., Greco, F., Hulsen, M. A., & Vermant, J. (2011). Effect of viscoelasticity on the rotation of a sphere in shear flow. *Journal of Non-Newtonian Fluid Mechanics*, 166 (7-8), 363-372.

[Sumita 1991] Sumita, M., Sakata, K., Asai, S., Miyasaka, K., & Nakagawa, H. (1991). Dispersion of fillers and the electrical-conductivity of polymer blends filled with carbon black. *Polymer Bulletin*, 25(2).

[Untereker 2009] Untereker, D., Lyu, S., Schley, J., Martinez, G., & Lohstreter, L. (2009). Maximum Conductivity of Packed Nanoparticles and Their Polymer Composites. *Acs*

Applied Materials & Interfaces, 1(1).

[Voigt 2005] Voigt, B., Rouxel, D., McQueen, D. H., & Rychwalski, R. W. (2005). Organization of carbon black in laminates of cellulose and melamine-formaldehyde. *Polymer Composites*, 26(2), 144-151.

[Yu 2005] Yu, J., Zhang, L. Q., Rogunova, M., Summers, J., & Hiltner, A. (2005). Conductivity of polyolefins filled with high-structure carbon black. *Journal of Applied Polymer Science*, 98(4), 1799-1805.

[Yuan 2010] Yuan, Q., & Wu, D. (2010). Low Percolation Threshold and High Conductivity in Carbon Black Filled Polyethylene and Polypropylene Composites. *Journal of Applied Polymer Science*, 115(6).

Conclusions and Perspectives

Conclusions

The overall goal of the present thesis is a better understanding and bringing new functions to an abundant, renewable, biodegradable material – cellulose. Both cellulose solutions and materials prepared from cellulose solutions were studied. The approach of this work was not limited to invent or prepare a given type of new cellulose-based materials, but rather to explore various possibilities with some simple but basic concepts, and to obtain the foundations on which a future research or industrial production could rely on.

We started our work by first reviewing the direct dissolution of cellulose, because the processing of cellulose from solutions can be more environmental-friendly and economic compared to the most common viscose method. Among the various solvents that we considered, aqueous sodium hydroxide (NaOH-water) and ionic liquids (ILs) were selected. Their pros and cons were described in Chapter I. We also reviewed the various forms of materials prepared from cellulose solutions, including fibers, films, membranes, hydrogels and aerogels. Cellulose-based hybrid materials were the major subjects of interest in the review of Chapter I because “blending” cellulose with natural polymers, synthetic polymers, or inorganic fillers offer a nearly unlimited range of options for enhancing the inherent properties of cellulose and/or to create new functions. Conductive cellulose-carbon black (CB) composite is an excellent example for such synergy, combining the conductivity of carbon black and the properties of cellulose fibres.

Following the description of materials and methods in Chapter II, the work of Chapter III focused on the stability of cellulose solutions in NaOH-water. As one of the three most widely used/studied cellulose solvents, the NaOH-water solvent system has a severe problem of gelation, which is hampering its use despite of the advantages that could bring this solvent such as low cost or easy handling. We added zinc oxide as a stabilizer, and confirmed that it efficiently delayed the gelation. In fact, we found two interesting facts:

- Both dissolved and suspended zinc oxide can stabilize the cellulose-NaOH-water solutions, because in both cases they can act as free water “binder”, either via formation of hydrates (in dissolved state) or hydroxides (on suspended particles surface).

- The gelation time (also the delay of gelation) is controlled by temperature, cellulose concentration, and zinc oxide concentration. A semi-empirical equation correlating the three above parameters was proposed to help us predicting the gelation time.

Using relatively small amount of ZnO added, we are able to stabilize cellulose solutions within a desired period, providing an appropriate operating window for either making final materials as aerogels or using the solutions to mix with other components or to modify cellulose matrix.

When we blended cellulose with starch in Chapter IV, ionic liquid (EMIMAc) was chosen as solvent rather than NaOH-water, mainly due to its higher dissolving power, which is essential for preparing the final materials. In that chapter, we firstly studied the properties of starch solutions in EMIMAc, and blended it with cellulose following a simple processing route. Both the solutions and mixtures of each component in EMIMAc, and the obtained blended films were fully characterized, giving the following conclusions:

- Waxy corn starch (amylopectin) can be dissolved in EMIMAc, in which it has a similar compact ellipsoid conformation as in water; and it is less temperature sensitive than cellulose, as suggested by intrinsic viscosity.
- Mixtures of cellulose-EMIMAc solutions with starch-EMIMAc solutions indicate no specific interaction between the two components.
- Porous films can be obtained by blending cellulose with starch through a “dissolution-mixing-coagulation” route, and the porous morphology obtained after coagulation can be tuned by varying solution composition and nature of the coagulation bath.

The above results not only demonstrate the feasibility of mixing the two most abundant polysaccharides with a common solvent, but also, more importantly, open opportunities for making films, separation devices or templates with controlled properties, because we could also replace the two components cellulose and starch with their various functional derivatives.

In Chapter V, a similar processing approach was taken to prepare another group of functional cellulose films – carbon black-filled conductive films. The dispersion of carbon black agglomerates in cellulose-ionic liquid solution was the first phenomenon that we examined, in order to ensure a good and efficient dispersion. Then with the

“dissolution-dispersion-coagulation” route, conductive films were prepared and tested to determine the percolation threshold. Another type of cellulose with different DP was also blended in, aiming at reducing the total amount of carbon black in the composites while keeping the same high electric conductivity. We found that:

- The two classical mechanisms, namely erosion or rupture, have been observed for the carbon black agglomerate dispersion different types of cellulose solutions in EMIMAc.
- In cellulose solutions, the macroscopic critical shear stress for dispersion was found linearly correlated to the elasticity of the fluid matrix, and independent of the agglomerate size or fluid infiltration.
- The influence of elasticity in visco-elastic fluids can be explained by the change of compressive/extensional stresses distribution compared to the cases of Newtonian fluids; and the experimental values of critical cohesion stress for the agglomerate were over-estimated if stresses were calculated macroscopically from shear rate and viscosity of the matrix.
- It is possible to make cellulose-based conductive films from carbon black and cellulose-EMIMAc solutions; and also it might be possible to reduce the carbon black loading in the composites while keeping same level of conductivity, which offers the possibility to keep good processability and properties.

Perspectives

Here we would like to propose some future work to pursue that we could not include in the scope of this thesis mainly due to the lack of time. This could hopefully shed more light on this subject and also inspire further research:

- To replace one or both components in the cellulose-starch blended films with their functional derivatives, in order to take advantages of the porous structure and of the extra functions brought by the derivatives.
- To improve the coating of the three-layered cellulose-carbon black composite films for obtaining a better homogeneity, and to characterize the cohesion between the layers.

- To look into the affinity of carbon black with different types of cellulose, and manage to achieve a “double percolation” morphology in the composite films with controlled localization of carbon black, in order to reduce the carbon black loading without compromising the conductivity.

Annex

The above work lead to the following publications:

Liu, W., Budtova, T., & Navard, P. (2011). Influence of ZnO on the properties of dilute and semi-dilute cellulose-NaOH-water solutions. *Cellulose*, 18(4), 911-920.

Liu, W., Budtova, T. (2012). Dissolution of unmodified waxy starch in ionic liquid and solution rheological properties. *Carbohydrate Polymers*, [10.1016/j.carbpol.2012.01.090](https://doi.org/10.1016/j.carbpol.2012.01.090).

Liu, W., Budtova, T. (2012). Ionic liquid: A powerful solvent for homogeneous starch-cellulose mixing and making films with tuned morphology. *Polymer*, 53(25), 5779-5787.

Solutions de cellulose et matériaux hybrides/composites à base de liquides ioniques et solvants alcalins

RESUME : La cellulose, composé organique le plus courant et polysaccharide le plus abondant sur Terre, est une ressource naturelle très importante. Les initiatives pour remplacer totalement ou partiellement les polymères pétrochimiques conventionnels avec des bio-polymères à base de cellulose ont donc attiré l'intérêt des chercheurs ces dernières décennies, non seulement parce que la cellulose est renouvelable et biodégradable, mais aussi en raison de ses propriétés intéressantes telles que la biocompatibilité et la stabilité chimique. De plus, les propriétés de cellulose peuvent être encore améliorées par des procédés chimiques, des modifications physiques ou en préparant des composites avec des charges fonctionnelles.

Les études concernant d'étudier plusieurs aspects fondamentaux comme la dissolution de la cellulose afin de produire des matériaux et le test de nouveaux concepts autour de la modification de surface ou des revêtements, à l'échelle du laboratoire. Nous présentons dans ce manuscrit nos travaux concernant la caractérisation de solutions de cellulose dans deux solvants différents (hydroxyde de sodium aqueux et un liquide ionique) et la préparation de deux nouveaux types de matériaux à base de cellulose (un matériau hybride cellulose-amidon et un composite cellulose-noir de carbone), qui sont tous les deux préparés à partir de ces solutions de cellulose.

Mots clés : cellulose, amidon, liquides ioniques, hydroxyde de sodium, solutions, gélification, noir de carbone, dispersion, matériaux hybrides

Cellulose solutions and hybrid/composite materials from ionic liquid and alkaline solvents

ABSTRACT : Cellulose, as the most common organic compounds on Earth, and also the most abundant polysaccharide, is definitely an important natural resource. With the initiatives of replacing (partially) the conventional petrochemical polymers by bio-based polymers, cellulose has regained the researchers' interests in the last few decades, not only because it is renewable and biodegradable, but also due to interesting properties such as biocompatibility and chemical stability. Additionally, cellulose properties can be further enhanced by chemical/physical modification or making composites with functional fillers.

This study was to investigate several fundamental scientific aspects as cellulose dissolution, making cellulose-based materials from solutions, and test of new concepts as surface modification or coating at laboratory scale. We studied and will present in this manuscript the characterization and properties of both cellulose solutions in different solvents (aqueous sodium hydroxide and ionic liquid) and two types of cellulose-based hybrid materials (one with starch and the other with carbon black), which were all prepared from dissolved cellulose.

Keywords : cellulose, starch, ionic liquid, sodium hydroxide, solutions, gelation, carbon black, dispersion, hybrid materials